

UNIVERSITÉ DU QUÉBEC À MONTRÉAL

PALYNOSTRATIGRAPHIE DU PLIO-PLÉISTOCÈNE DANS LA MER DU
LABRADOR ET DE LA BAIE DE BAFFIN : CONTRIBUTION À LA
COMPRÉHENSION DES RELATIONS OCÉAN-CLIMAT-VÉGÉTATION LORS
DE L'INTENSIFICATION DES GLACIATIONS DE L'HÉMISPHÈRE NORD

THÈSE
PRÉSENTÉE
COMME EXIGENCE PARTIELLE
DU DOCTORAT EN SCIENCES DE LA TERRE ET DE L'ATMOSPHÈRE

PAR
AURÉLIE AUBRY

FÉVRIER 2020

UNIVERSITÉ DU QUÉBEC À MONTRÉAL
Service des bibliothèques

Avertissement

La diffusion de cette thèse se fait dans le respect des droits de son auteur, qui a signé le formulaire *Autorisation de reproduire et de diffuser un travail de recherche de cycles supérieurs* (SDU-522 – Rév.07-2011). Cette autorisation stipule que «conformément à l'article 11 du Règlement no 8 des études de cycles supérieurs, [l'auteur] concède à l'Université du Québec à Montréal une licence non exclusive d'utilisation et de publication de la totalité ou d'une partie importante de [son] travail de recherche pour des fins pédagogiques et non commerciales. Plus précisément, [l'auteur] autorise l'Université du Québec à Montréal à reproduire, diffuser, prêter, distribuer ou vendre des copies de [son] travail de recherche à des fins non commerciales sur quelque support que ce soit, y compris l'Internet. Cette licence et cette autorisation n'entraînent pas une renonciation de [la] part [de l'auteur] à [ses] droits moraux ni à [ses] droits de propriété intellectuelle. Sauf entente contraire, [l'auteur] conserve la liberté de diffuser et de commercialiser ou non ce travail dont [il] possède un exemplaire.»

REMERCIEMENTS

On m'a un jour dit : « réfléchis bien car le doctorat ce sont les plus belles années de ta vie, mais aussi les pires. » Mon existence n'est certes pas terminée, mais je pense que je donnerai le même conseil à quiconque me le demandera.

Il ne faut pas s'inquiéter, j'ai toujours été un peu pessimiste. Comme le dit ma petite Juliette : « tu vois le verre à moitié vide, mais c'est un verre de paillettes. » Aujourd'hui j'aimerais rajouter que les paillettes c'est un peu vous tous, que vous soyez là depuis longtemps ou que l'on vienne de se rencontrer, vous remplissez ce verre.

Je souhaite donc remercier en premier lieu ma directrice de thèse, Anne de Vernal, pour m'avoir fait découvrir le monde merveilleux des dinokystes mais surtout pour ces années de direction, de discussion et d'apprentissage (surtout à synthétiser mon travail !), ainsi que toutes ces superbes opportunités d'assister à des congrès internationaux. Je remercie également Claude Hillaire-Marcel, mon co-directeur, pour son expertise et ses précieux conseils.

J'aimerais également remercier Martin J. Head pour son expertise et son aide avec l'identification des dinokystes du Pliocène. Un grand merci à Stijn De Schepper pour nos échanges constructifs, l'identification des dinokystes du Pliocène et la rapidité de ses réponses ainsi qu'à Jens Matthiessen pour m'avoir accueilli dans les locaux de l'AWI à Bremerhaven et Michal Kuceras au MARUM à Brême pendant mon stage du programme ArcTain en Allemagne.

À la personne qui de toute cette aventure est la seule qui puisse vraiment comprendre ce que j'ai vécu et ressenti (Coralie tu te reconnaîtras... j'espère !). Tout est possible ! Nous avons eu le même bureau, la même directrice, le même Pliocène, la même cabine dans le *Polarstern*, et partagé tant de chambres dans les congrès, de soirées au microscope.... Finalement je te l'écris, si un jour nous devons retravailler ensemble, ce sera avec joie !!

À Marie-Michèle avec qui nos aventures à San Francisco ont marqué le début de notre amitié, mais aussi à Cynthia qui était une de mes premières étudiantes et à la petite dernière arrivée au labo Marie-Camille, merci pour tous ces supers moments et nos fantastiques soirées VINOUSAURES ! Un petit merci à Sam qui a toujours le mot qui remonte le moral ! Il y a aussi tout ceux avec qui c'était un plaisir de prendre un café ou s'arrêter faire un brin de coquette : David, Kristan, Williams, Marjo, Lucille et même encore André, Bassam, Taoufik. Un merci spécial à Phillippe pour avoir pris le temps de me relire. Thank you to all my new ArcTrain friends Becky, Lera, Misha, Vasco and Valentin for these amazing Arctrain meetings, without you my English would have never improve so fast!

A special thanks to Stefie. I'm very happy to know you and I will never say it enough: thank you for all your support and love (and the K-drama) !

Je souhaite remercier chaleureusement mes coloc' présents : Kevin et Marie, mais également passés : Tamara, Stefie et ma petite Juliette (Dédééééé !!!) chérie, vous avez fait de mon quotidien à la maison un havre de tranquilité et je suis vraiment heureuse d'avoir partagé tous ces bons moments à vos côtés. À mes copines du bollywood, Joanna et Carole, pour toutes ces chorégraphies endiablées et spectacles qu'on a partagés ! Il me tarde de vous revoir avec un petit cocktail et un film de SRK !

À mon amitié la plus ancienne et précieuse : gros bisous à mon coco qui depuis seize ans me supporte et écoute mes plaintes incessantes sans jamais faiblir ! C'est la

malédiction des M. R. Un petit bisou à Bruno aussi parce que bon ça fait longtemps quand même !

Enfin, j'aimerais remercier profondément mes parents qui m'ont encouragée et soutenue depuis toutes ces années malgré le temps et la distance, sans eux rien de tout cela n'aurait été possible. Merci aussi à ma petite sœur même si elle m'a remplacée par un chien, je sais que ce n'était que pour combler mon absence <3 Bisous Fluffy.

À celui qui m'accompagne depuis presque le début de cette aventure sans jamais faillir à son devoir (même s'il n'a pas vraiment le choix) : Sherlock.

Puis, au petit Romain du bureau de Marie-Camille... merci pour ton aide plus que précieuse, ton support et ta présence à mes côtés, sans toi ce doctorat n'aurais pas été possible, je te dois maintenant une vie de dévotion (d'après Juliette).

AVANT-PROPOS

Cette thèse a été rédigée sous forme de trois articles écrits en anglais, chacun correspondant à un chapitre. Au moment de la publication de ce document, un article a été accepté et est en voie d'être publié, un article a été soumis et est en révision par un comité de lecture et un article est en attente des retours des co-auteurs avant soumission à une revue à comité de lecture. La mise en page de ces trois chapitres suit les directives du Guide de présentation des mémoires et des thèses (version 2.0, septembre 2017) du service des bibliothèques de l'Université du Québec à Montréal (UQAM).

Mon travail pour cette thèse a commencé par la sélection et la commande de 158 échantillons de sédiments auprès de l'*International Ocean Discovery Program* (IODP). Deux carottes de forages ont été sous-échantillonées au centre d'archivage de l'IODP à l'Université de Brême en Allemagne (*IODP Bremen Core Repository*). Ces carottes ont été prélevées au cours de deux campagnes de forage du navire de recherche *Joides Resolution* dans le cadre de l'*Ocean Drilling Program* (ODP 105 dans la Mer du Labrador et la Baie de Baffin en 1985) et de l'*Integrated Ocean Drilling Program* (IODP 303 dans l'Atlantique Nord en 2004). J'ai été responsable des traitements physiques et chimiques de ces échantillons dans le laboratoire de micropaléontologie du centre de recherche sur la dynamique du système Terre (Geotop) à l'UQAM et de leurs analyses par microscopie optique au Geotop et à l'*Alfred Wegener Institute for polar research* (AWI) lors d'un stage à Bremerhaven en Allemagne pendant l'été 2017. J'ai co-organisé un atelier sur l'identification des dinokystes du Pliocène au Geotop en janvier 2017 en invitant deux spécialistes des dinokystes du Pliocène : Martin J. Head de l'Université de Brock en Ontario et Stijn De Schepper de l'Université de Bergen, en Norvège.

L'objectif était d'acquérir une expertise pour l'identification des dinokystes et de résoudre des problèmes taxonomiques préalablement nécessaires à l'utilisation des données de comptage. J'ai également réalisé l'ensemble des traitements statistiques, les interprétations des résultats et la rédaction des manuscrits des articles (incluant les figures, les tableaux, les annexes et le corps du texte). Le tout a été réalisé sous la supervision de ma directrice de thèse, Anne de Vernal. Les co-auteurs de mes articles ont contribué à mon travail en fournissant des échantillons et des données complémentaires ainsi que par leurs expertises, conseils, critiques et précieux échanges. Stijn De Schepper a partagé avec moi ses résultats d'analyses palynologiques de 37 échantillons du Site IODP U1307 et a fourni 17 échantillons supplémentaires déjà traités à analyser (cf. Chapitres I et II).

Le premier chapitre est accepté pour publication (janvier 2020) dans la revue *Journal of Micropaleontology* et s'intitule *Dinocyst and Acritarch biostratigraphy of the late Pliocene to early Pleistocene of IODP Site U1307, Labrador Sea*. Cet article est co-écrit avec Stijn De Schepper et Anne de Vernal. Il présente une nouvelle biostratigraphie (dinokystes et acritarches) détaillée de la transition Plio-Pleistocene (3,2 à 2,2 Ma) dans la Mer du Labrador et plus particulièrement au Site IODP U1307, auquel un nouveau modèle d'âge vient d'être établi (Blake-Mizen *et al.* 2019). Cet article apporte donc des informations solides sur la chronologie des apparitions et/ou disparitions d'espèces de dinokystes et acritarches dans le nord-ouest de l'Atlantique Nord. Il permet ainsi d'établir une corrélation entre la Mer du Labrador, le reste de l'Atlantique Nord et les mers nordiques (Mer d'Islande, Mer de Norvège et Mer du Groenland) et discute notamment de la synchronisation ou non des bio-événements durant la transition Plio-Pleistocène.

Le deuxième chapitre sera soumis à la revue *Palaeogeography, Palaeoclimatology, Palaeoecology*. Il a pour titre *Late Pliocene to early Pleistocene dinocyst and acritarch assemblages of the northwest North Atlantic, IODP Site U1307, Labrador Sea*. Cet article est écrit, tout comme le précédent, en collaboration avec Stijn De Schepper et Anne de Vernal

et discute des conditions paleocéanographiques dans la Mer du Labrador ainsi que de l'évolution spatiale et temporelle de la glace sur le sud du Groenland durant la transition Plio-Pléistocène, entre 3,2 et 2,2 Ma. Il se base sur la composition des assemblages de dinokystes et acritarches mais utilise également des indicateurs terrestres tels que les grains de pollen, les spores de ptéridophytes ainsi que les particules transportées par les icebergs (*ice rafted detritus*, IRD).

Le troisième et dernier chapitre de la thèse a été soumis à la *Revue canadienne des sciences de la Terre*. Il est intitulé *Baffin Bay late Neogene palynostratigraphy at ODP Site 645* et a pour co-auteurs Anne de Vernal et Paul Knutz du *Geological Survey of Denmark and Greenland* à Copenhague. Cet article utilise les dinokystes et acritarches afin d'établir une biostratigraphie de la fin du Miocène/début du Pliocène au Pléistocène au Site ODP 645 dans la Baie de Baffin et d'identifier la transition Plio-Pléistocène. Cet article fait référence à la biostratigraphie du premier chapitre et souligne la difficulté et le peu de matériel disponible pour retracer l'histoire paléoclimatique de la Baie de Baffin au cours des temps géologiques.

L'Appendice A correspond à un article publié en 2016 dans la revue *Paleoceanography* se nommant *The « warm » Marine Isotope Stage 31 in the Labrador Sea: Low surface salinities and cold subsurface waters prevented winter convection*. Cet article, dont je suis premier auteur, a été écrit en collaboration avec Anne de Vernal et Claude Hillaire-Marcel au début de ma thèse. Il présente les conditions de surface et de subsurface dans la Mer du Labrador (Site IODP U1305) pendant le stade isotopique marin (*marine isotopic stage*, MIS) 31 reconstruites à partir d'une approche multi-proxy qui combine : des reconstructions basées sur les assemblages de dinokystes (surface) et les foraminifères planctoniques (subsurface), ainsi que des analyses géochimiques sur la composition isotopiques de l'oxygène et du carbone à partir des foraminifères planctoniques et benthiques. Il m'a en particulier permis d'inférer l'absence de convection dans la Mer du Labrador il y a 1 Ma. J'ai réalisé la totalité des analyses palynologiques, micropaléontologiques, géochimiques et statistiques avant de

commencer ma thèse et suis responsable de l'écriture du manuscrit qui a été faite au début de mon doctorat. Cet article constitue un point de départ fondamental qui m'a transmis l'envie l'explorer les temps géologiques dans la Mer du Labrador par le biais d'une approche palynologique.

Enfin, des analyses sur la composition géochimique des IRD provenant des deux sites (ODP 645 et IODP U1307) ont été réalisées dans les laboratoires du département des Sciences de la Terre de l'UQAM avec Michel Preda et l'aide de deux étudiants : Cesar Elies et Tiffany Audet. Les résultats bruts sont présentés dans l'Appendice B. Un quatrième article traitant de l'origine des IRD dans la Mer du Labrador durant la transition du Plio-Pléistocène et de l'englacement du Groenland est en cours d'écriture sous la supervision d'Anne de Vernal et de Claude Hillaire-Marcel, respectivement ma directrice et mon co-directeur de recherche.

TABLE DES MATIÈRES

AVANT-PROPOS	v
LISTE DES FIGURES.....	xiv
LISTE DES TABLEAUX.....	xix
LISTE DES ABBRÉVIATIONS	xxi
RÉSUMÉ.....	xxiii
ABSTRACT	xxv
INTRODUCTION.....	27
0.1 Contexte de l'étude	27
0.1.1 Le Pliocène	27
0.1.2 La transition Plio-Pléistocène.....	29
0.1.3 L'état du Groenland pendant le Pliocène	30
0.1.4 Le rôle de l'Atlantique Nord	33
0.2 Limites des connaissances	36
0.3 Objectifs de la thèse.....	38
0.4 Contexte régional et matériel utilisé pour l'étude.....	39
0.4.1 Contexte régional moderne	39
0.4.2 Sites, échantillons et modèle d'âge	42
0.5 Méthodes.....	43

0.5.1 Les kystes de dinoflagellés ou dinokystes.....	44
0.5.2 Les acritarches.....	46
0.5.3 Les palynomorphes terrestres : les grains de pollen et les spores	47
0.5.4 Les IRD	47
0.6 Organisation de la thèse.....	48
 CHAPITRE I DINOCYST AND ACRITARCH BIOSTRATIGRAPHY OF THE LATE PLIOCENE-EARLY PLEISTOCENE OF IODP SITE U1307, LABRADOR SEA	50
Abstract	51
1.1 Introduction.....	52
1.2 Materials and methods.....	55
1.2.1 Marine sediments	55
1.2.2 Palynological work.....	56
1.2.3 Age model, resolution and uncertainties	59
1.2.4 Origin of particles (dinocysts and acritarchs)	61
1.3 Results.....	62
1.3.1 General	62
1.3.2 Age calibration of selected bioevents.....	63
1.3.3 Biostratigraphy and biozonation	64
1.4 Discussion.....	70
1.4.1 Comparison with previously established zonation at the nearby ODP Hole 646	70
1.4.2 Comparison with the North Atlantic Ocean and the adjacent seas	72
1.4.3 Paleoceanographic and paleoclimatic implications.....	78
1.4.4 The use of the acritarchs in marine palynostratigraphy across the Plio- Pleistocene transition.....	80

1.5 Conclusion	82	
Acknowledgements.....	82	
References.....	83	
Figures.....	93	
Tables	99	
CHAPITRE II LATE PLIOCENE-EARLY PLEISTOCENE PALEOCEANOGRAPHY OF SOUTHERN GREENLAND BASED ON DINOCYST AND ACritARCH ASSEMBLAGES AT IODP SITE U1307, LABRADOR SEA		102
Abstract	103	
2.1 Introduction.....	104	
2.2 Materiel and methods	108	
2.2.1 Stratigraphy of the core	108	
2.2.2 Palynological preparation.....	109	
2.2.3 Palynological analysis	110	
2.3 Results.....	113	
2.3.1 Palynological assemblages.....	114	
2.3.2 Species diversity.....	115	
2.3.3 Dinocyst zones	116	
2.3.4 Close-up on the assemblages of subzone 1c (3.1-3.0 Ma, MIS K2 to MIS G20).....	118	
2.4 Discussion.....	119	
2.4.1 Paleoecological interpretation of dominant dinocyst taxa in Pliocene sediment of IODP Site U1307.....	119	
2.4.2 Paleoceanography of the Mid-Piacenzian Warm Period from MIS KM5 to MIS G20 (3.21–3.00 Ma) in the Labrador Sea	124	

2.4.3 Paleoceanography of the late Pliocene-early Pleistocene Labrador Sea (3.0-2.2 Ma).....	127
2.5 Conclusion	128
Acknowledgements.....	130
References.....	130
Figures.....	143
Tables	151
CHAPITRE III BAFFIN BAY LATE NEogene PALynoSTRATIGRAPHY AT ODP SITE 645	
Abstract	155
3.1 Introduction.....	156
3.2 Stratigraphical context.....	158
3.3 Material and methods	160
3.3.1 Palynological preparation.....	160
3.3.2 Palynological analysis	161
3.4 Results.....	163
3.4.1 Palynological content.....	163
3.4.2 Biostratigraphy	164
3.4.3 Dinocyst assemblages	164
3.4.4 Pollen grains and spores.....	165
3.5 Discussion.....	166
3.5.1 Palynostratigraphy and chronological implication.....	166
3.5.2 Implications for the interpretation of the seismic stratigraphy	170
3.5.3 Paleoclimatic inferences.....	171

3.5.4 Marine paleoenvironments.....	173
3.6 Conclusion	174
Acknowledgements.....	175
References.....	175
Figures.....	187
Tables	198
CONCLUSION	203
ANNEXE A SUPPLEMENTARY INFORMATION A DU CHAPITRE I.....	211
ANNEXE B SUPPLEMENTARY INFORMATION B DU CHAPITRE II.....	215
ANNEXE C SUPPLEMENTARY INFORMATION B DU CHAPITRE I ET A DU CHAPITRE II.....	217
ANNEXE D SUPPLEMENTARY INFORMATION S2 DU CHAPITRE III.....	218
ANNEXE E SUPPLEMENTARY INFORMATION S1 DU CHAPITRE III	221
ANNEXE F SUPPLEMENTARY FIGURE S1 DU CHAPITRE III.....	226
ANNEXE G SUPPLEMENTARY PLATES DU CHAPITRE I.....	228
APPENDICE A <i>THE « WARM » MARINE ISOTOPE STAGE 31 IN THE LABRADOR SEA: LOW SURFACE SALINITIES AND COLD SUBSURFACE WATERS PREVENTED WINTER CONVECTION</i>	233
APPENDICE B RÉSULTATS BRUTS DE LA COMPOSITION MINÉRALOGIQUE DES IRD AU SITE IODP 1307 À PARTIR D'ANALYSES PAR DIFFRACTION À RAYONS X	253
RÉFÉRENCES.....	257

LISTE DES FIGURES

Figure 0.1 Reconstitution PRISM4 (A) des températures de surfaces des océans, (B) de la topographie des continents et de la bathymétrie des océans, (C) des biomes, (D) des sols, (E) de la glace continentale, (F) des grands lacs pendant l'optimum climatique du Pliocène (Dowsett <i>et al.</i> , 2016)	32
Figure 0.2 Localisation des sites mentionnés dans le texte (cercles bleu clair) et positionnement du courant Nord Atlantic (flèches rouges) et du front arctique (ligne pointillée bleu foncée) pendant (a) les périodes chaudes et (b) froides du Pliocène tardifs. Modifié d'après Naafs <i>et al.</i> (2010).....	35
Figure 0.3 Carte de l'Atlantique Nord, présentant les deux sites d'études IODP U1307 et ODP 645 ainsi que la circulation océanique de surface moderne. Le fond de carte provient du logiciel Ocean Data View (Schlitzer, 2018).	40
Figure 0.4 Cycle de vie des dinoflagellés avec l'alternance d'un stade motile (non fossilisable) et d'un stade de dormance (fossilisable) (de Vernal et Marret, 2007)....	45
Figure 1.1 Map of the Labrador Sea showing the location of Site IODP U1307, other sites mentioned in the text, and the modern surface currents (made with Ocean Data View, Schlitzer, 2018).....	93
Figure 1.2 Age models at IODP Site U1307. Magnetostратigraphy and lithology of IODP Site U1307 from Channell <i>et al.</i> , (2004). Stable oxygen isotope data based on the planktic foraminifer <i>Neogloboquadrina atlantica</i> and two proposed age models	

from Sarnthein <i>et al.</i> (2009). Most recent age model based on magnetic reversals and a paleointensity record tuned to IODP Site U1308 (Blake-Mizen <i>et al.</i> , 2019). M = Mammoth subchron, K = Kaena subchron, MIS = Marine Isotope Stage, RPI = Relative Paleo-Intensity.....	94
Figure 1.3 IODP Site U1307 stratigraphic occurrence of selected dinocyst and acritarch taxa and biozones defined in this study, calibrated against Blake-Mizen <i>et al.</i> (2019) age model. All raw data are available in Supplementary Data A.	96
Figure 1.4 Left: Late Pliocene-early Pleistocene dinocyst biozonation schemes from different locations in the North Atlantic. Right: Adapted from De Schepper <i>et al.</i> (2017). Late Pliocene dinocyst extinction events in the Labrador Sea (this study), the western North Atlantic (DSDP Hole 603C, Head and Norris, 2003; M.J. Head, unpublished data), eastern North Atlantic (DSDP Hole 610A, De Schepper and Head, 2008a, 2008b, 2009) and the Norwegian Sea (ODP Hole 642B, De Schepper <i>et al.</i> , 2017).	97
Figure 1.5 Adapted from De Schepper and Head (2014). Selected acritarch stratigraphic ranges from different sites across the North Atlantic (DSDP Sites 603 and 610; ODP Site 646, 642 and 907; IODP Sites U1308, U1313 and U1307) and North Pacific (IODP Site U1314, ODP Site 882). Old = Olduvai Subchron, M= Mammoth Subchron, HCO= Highest Common Occurrence, HPO= Highest Persistent Occurrence	98
Figure 2.1 Map of the Labrador Sea showing the location of the study Site IODP U1307, the other sites mentioned in the text, and the present day surface currents (made with Ocean Data View, Schlitzer, 2018).....	143

Figure 2.2 Concentration of dinocysts, acritarcha, fresh water algae, marine reworked palynomorphs (dinocysts and acritarcha), terrestrial reworked palynomorphs (pollen grains and spores), ice rafted debris $> 150\mu\text{m}$, and pollen grains and spores expressed in number of specimens per g of dry bulk sediment in IODP Site U1307. Pollen assemblage composition (%) of trees (dark green), shrubs (light green) and herbs (yellow), are expressed without Pinus as this genus is usually over-represented in marine sediments, notably in the Labrador Sea (Rochon and de Vernal, 1994). P/G index, P/D index. Shannon-Wiener index is showed with only dinocysts (black) and taking account of dinocysts and acritarcha (grey). Cumulated representation of the number of species of acritarcha (blue), extinct dinocysts (purple) and extant dinocysts (orange). Proportion of extinct species in the dinocysts assemblages in purple 145

Figure 2.3 Results from Principal Component Analysis (PCA) performed on dinocyst percentages in samples from IODP Site U1307 after a logarithmic transformation to increase the weight of accompanying taxa. The first component (PC1) is represented on the vertical axis and the second component (PC2) is represented on the horizontal axis 146

Figure 2.4 Relative abundance (%) of selected dinocysts according to PC scores and associated to variations of the PC1 and PC2 axis in IODP Site U1307 between 3.2 to 2.2 Ma. “Other species” includes all taxa cited in Table 2.2 in regular text and white background. Ecozone boundaries are shown with plain back lines and the subzone boundaries with dashed lines. Samples with less than 10 cysts/sample are not included in the figure. Samples counted by S. De Schepper are shown with purple triangles and samples counted by A. Aubry are shown with black diamonds. The age model is from Blake-Mizen *et al.* (2019) based magnetic inversions (blue stars) and Relative Paleo-Intensity (RPI) correlation with IODP Site U1308 (white rectangles). Planktic foraminifer stable oxygen isotope data are from Sarnthein *et al.* (2009) in black and the

reference stack of benthic foraminifer stable isotope from Lisiecki and Raymo (2005) referred to as LR04 is in grey with marine isotopic stages indicated	148
Figure 2.5 Close-up of terrestrial palynomorph concentration (per g) and the relative abundances (%) of selected dinocyst taxa according to PC scores and associated to variations of the PC1 and PC2 axis in IODP Site U1307 from the mPwP (subzones 1a, 1b and 1c) between 3.2 to 3.0 Ma. Cold Marine Isotope Stage are shaded in light blue	150
Figure 3.1 Map of the northwest North Atlantic Ocean with surface current and sites mentioned in the text. The map was made with Ocean Data View (Schlitzer, 2018)	187
Figure 3.2 Overview of the chronological schemes proposed at ODP Site 645 based on seismic stratigraphy, lithostratigraphical units and palynostratigraphy.....	188
Figure 3.3 Concentrations of marine and detailed terrestrial palynomorphs. Number of dropstones from Korstgård and Nielsen (1989).	189
Figure 3.4 Pollen grains and preservation categories (as in Table 1). Scale bars are 10 µm.	190
Figure 3.5 Biostratigraphical zonation based on dinocysts and acritarchs at ODP Site 645. Results with less than 20 cysts counted per sample (see* in the sample column) were not used.....	192
Figure 3.6 Photographs of the most biostratigraphically important dinocyst and acritarch taxa recovered in sediments from ODP Site n645. Scale bars are 10 µm..	193

Figure 3.7 Relative abundances (percentages) of selected dinocysts. "Other species" includes: *A. zevenboomii*, *Batiacasphaera* spp., *B. hirsuta*, *B.micropapillata* complex, *Bitectatodinium* spp., *Bitectatodinium/Filisphaera* spp., *B. raedwaldii*, *Cordosphaerodinium* spp., *C. labradori*, *Corrudinium* spp., *C. diminutivum*, *Filisphaera* spp., *Habibacysta* of Head 94, *Habibacysta* spp., *Impagidinium* sp. A of De Schepper and Head (2009), *Impagidinium* spp., brown *Impagidinium* spp., *L. machaerophorum*, *Lingulodinium* spp., *Nematosphaeropsis* spp., *O. centrocarpum*, *O.? eirikianum*, *eirikianum*, *O.? eirikianum crebrum*, *O. tegillatum*, *Operculodinium* spp., *Palaeocystidium* spp., *P. tuberculata*, *Pyxidinopsis* spp., indet. Results with less than 20 cysts counted per sample (see * in the sample column) are not presented. 195

Figure 3.8 Revised correlation of the seismic profile of Knutz *et al.* (2015) with the upper part of the ODP Site 645 sequence. The lithological units at ODP Site 645 follow the new stratigraphical interpretation oh horizons and mega-units from this study. The vertical axis shows two-way travel-time (twtt). The vertical blue bar correspond to the interval of the present biostratigraphy study. Mass transport deposit associated to slide scars (black arrows) are highlighted with the pale blue line..... 197

LISTE DES TABLEAUX

Table 1.1 Age model tie point used at IODP Site U1307 from Blake-Mizen <i>et al.</i> , 2019	99
Table 1.2 Dinocyst and acritarch bioevents at IODP Site U1307. The age model error is from Blake-Mizen <i>et al.</i> , (2019) and the age error is based on sampling interval. HO: highest occurrence, HCO: highest common occurrence, HPO: highest persistent occurrence	101
Table 2.1 Age model tie points used in IODP Site U1307 from Blake-Mizen <i>et al.</i> (2019)	151
Table 2.2 List of dinocyst and acritarch taxa recovered in samples from IODP Site U1307 between 3.2 and 2.2 Ma. Indication about their stratigraphic range, extinct or extend to modern, their ecological known affinities (from de Vernal <i>et al.</i> ,2013; Zonneveld <i>et al.</i> 2013 ; De Schepper <i>et al.</i> ,2011; Hennissen <i>et al.</i> , 2017), taxonomical affinities (P: Peridinoid cysts, G: Gonyaulacoid cysts), and neritic (N) to oceanic (O) distribution are given. The grouping of taxa is mentioned. Species used in Figure 4 are in bold with a grey background, all taxa grouped in “Other species” or “Other acritarcha” are in regular text with a white background	153
Table 3.1 Pollen grain preservation state categories	198

Table 3.2 Stratigraphic range of selected dinocyst and acritarch markers. Modified from De Schepper and Mangerud (2017).^a De Schepper *et al.* (2017); ^b De Schepper *et al.* (2015); ^c Schreck *et al.* (2012); ^d Schreck *et al.* (2013); ^e Head and Norris (2003); ^f De Schepper and Head (2008b); ^g De Schepper and Head (2009); ^h Head (1997); ⁱ Dybkjaer and Piasecki (2010); ^j de Vernal and Mudie (1989b); ^k Mudge and Bujak (1996); ^l Head *et al.* (1989); ^m Mattheissen *et al.* (2018); ⁿ Versteegh (1997); ^o Louwye *et al.* (2004); ^p Louwye and De Schepper (2010); ^q De Schepper and Head (2014); ^r Van Ranst (2015); ^s Piasecki *et al.* (2002); ^t Channell *et al.* (1999); ^u Canninga *et al.* (1987). HO: highest occurrence, LO: lowest occurrence, HPO: highest persistent occurrence, HCP: highest common occurrence 200

Table 3.3 Paleoecological affinities of selected Mio-Pliocene and Plio-Pleistocene dinocyst and acritarch taxa based on the literature.^a Schreck *et al.* (2017), ^b de Vernal *et al.* (2013), ^c Zonneveld *et al.* (2013), ^d Limoges *et al.* (2013), ^e De Schepper *et al.* (2011), ^f Hennissen *et al.* (2017), and ^g Rochon *et al.* (1999). Ext: extinct, N: neritic, O: oceanic, Oli: oligotrophic 202

LISTE DES ABBRÉVIATIONS

AMOC : *Atlantic Meridional Overturning/circulation atlantique méridionale*

AWI : *Alfred Wegener Institute for polar research*

BIC : *Baffin Island Current/courant de l'île de Baffin*

DSDP : *Deep Sea Drilling Project*

Geotop : centre de recherche sur la dynamique du système Terre

HO: *Highest Occurrence/disparition d'une espèce*

IPCC : *Intergovernmental Panel on Climate Change/Groupe d'experts intergouvernemental sur l'évolution du climat*

IODP : *Integrated Ocean Drilling Project*

IRD : *Ice Rafted Detritus/Debris*

kyr : millier d'années, 1 000 ans

LC : *Labrador Current/Courant du Labrador*

LO : *Lowest Occurrence/apparition d'une espèce*

LSW : *Labrador Sea Water/Eaux de la Mer du Labrador*

Ma : Million d'années, 10^6 ans

MIS : *Marine Isotopic Stage*

mPwP : *mid Pliocene warm Period/optimum climatique du Pliocène*

NHG : *North Hemisphere glaciation/Englaciation de l'Hémisphère Nord*

ODP : *Ocean Drilling Project*

PCA : Analyses par Composante Principale

RPI : *Relative Paleo-Intensity*

SST : *Sea surface temperatures*

UQAM : Université du Québec à Montréal

WGC : *West Greenland Current/Courant Ouest du Groenland*

RÉSUMÉ

Depuis quelques années, la transition Plio-Pléistocène (2,58 Ma) suscite une attention particulière du point de vue environnemental et climatique. Cette période est en effet marquée par des changements globaux, incluant une diminution importante de la concentration de CO₂ atmosphérique (~400 ppm au Pliocène versus 180-280 ppm au Pléistocène), et par conséquent d'une intensification des grandes glaciations dans l'Hémisphère Nord menant au développement de la calotte groenlandaise. Si la calotte du Groenland est la seule de l'Hémisphère Nord à avoir persisté pendant la plupart des interglaciaires du Pléistocène, contrairement aux inlandsis laurentidien, innuitien et fennoscandinave, elle est présentement menacée par le réchauffement climatique en cours. Un facteur ayant certainement joué un rôle déterminant dans l'intensification des glaciations de l'Hémisphère Nord est la circulation océanique de surface de l'Atlantique Nord, et notamment le courant nord-atlantique (ou en anglais, *North Atlantic Current-NAC*) qui est à l'origine de masses d'air chaudes et humides vers les hautes latitudes. C'est pour cela que mon projet de doctorat s'intéresse à l'interaction entre le climat, la végétation et la circulation océanique de surface dans le nord-ouest de l'Atlantique Nord, afin de documenter l'évolution spatio-temporelle de la glace continentale sur le sud du Groenland pendant la transition Plio-Pléistocène.

Cette étude se base sur le couplage entre les signaux océaniques et terrestres à partir de deux séquences sédimentaires de la Mer du Labrador (site IODP U1307) et de la Baie de Baffin (site ODP 645). Elle s'articule autour de trois thèmes complémentaires :

- La palynologie marine a servi, dans un premier temps, à l'établissement d'une biostratigraphie de référence des bio-événements marqués par des transitions dans les assemblages de palynomorphes marins (dinokystes et acritarches) du Pliocène tardif au début du Pléistocène (3,2-2,2 Ma), incluant l'optimum climatique du Pliocène et la transition Plio-Pléistocène au Site IODP U1307. Cette biostratigraphie a ensuite été comparée avec les schémas biostratigraphiques du reste de l'Atlantique Nord et des mers nordiques afin de discriminer les événements locaux et régionaux.
- Dans un second temps, l'analyse par composante principale a été utilisée pour définir des zones paléoécologiques et extraire le signal des espèces expliquant le mieux les variations observées. Les assemblages de dinokystes ont été interprétés

qualitativement et ont permis de reconstituer les conditions paléocéanographiques entre 3,2 et 2,2 Ma dans la Mer du Labrador. La palynologie terrestre, quant à elle, a été utilisée pour établir des relations avec la végétation sur les terres adjacentes du Groenland. Les débris de vêlage de radeaux de glace et icebergs ont été utilisés comme indices de la croissance des calottes glaciaires jusqu'aux marges continentales.

- Enfin, le dernier aspect thématique traite de l'identification de la transition Plio-Pléistocène dans les sédiments marins de la Baie de Baffin au site ODP 645 à partir des assemblages de dinokystes et acritarches et en exploitant la biostratigraphie de la Mer du Labrador

Les données obtenues suggèrent que, malgré des conditions régionales relativement froides, la Mer du Labrador est fortement connectée avec l'Océan Atlantique Nord, notamment avec le secteur nord-est où est localisé le site DSDP 610. En effet, les sites U1307 (cette étude) et 610 (De Schepper et Head, 2009) partagent des limites biostratigraphiques communes à ~ 2,75 Ma et 2,56 Ma mettant en évidence des événements d'envergure dans les milieux de moyennes et hautes latitudes de l'Atlantique Nord.

L'intervalle chaud du Pliocène moyen est marqué par des changements importants liés à une baisse de l'intensité du courant nord-atlantique vers la Mer du Labrador et à des apports accrus d'eau douce du Groenland vers 3,1 Ma. La transition Plio-Pléistocène fut très importante d'un point de vue paléoclimatique. En effet, au-delà du développement de grands glaciers continentaux dans l'Hémisphère Nord, c'est la réorganisation de la circulation océanique dans l'Atlantique Nord qui se produit. A partir de 2,65 Ma dans la Mer du Labrador, le front arctique et le passage du NAC migrent vers le sud et un peu plus tard, vers 2,60 Ma, dans le nord-est de l'Atlantique Nord. Les conditions terrestres montrent également une diminution du couvert végétal et une augmentation des apports de vêlage témoignant de la progression des glaciers vers les marges continentales groenlandaises à partir de 2,65 Ma.

En ce qui concerne la Baie de Baffin, aucun indice biostratigraphique n'a permis d'identifier clairement la transition Plio-Pléistocène au site ODP 645. Cette étude montre que la transition se situerait dans un hiatus de recouvrement des sédiments et démontre la nécessité de réaliser de nouveaux forages dans la Baie de Baffin.

Mots-clés : Mer du Labrador, Baie de Baffin, dinokystes, acritarches, Pliocène, Pléistocène

ABSTRACT

The Pliocene-Pleistocene transition (2.58 Ma) was marked by global changes, including a significant reduction in the concentration of atmospheric CO₂ (~ 400 ppm during Pliocene vs. 180–280 ppm in Pleistocene), and as a consequence an intensification of the Northern Hemisphere glaciation that led to the growth of the Greenland Ice Sheet. Although the Greenland ice sheet is the only one in the Northern Hemisphere that have persisted during most the Pleistocene interglacials unlike the Laurentide Ice Sheet, Innuitian and Fennoscandian ice sheets, it is currently threatened by the ongoing global warming. An important factor that have played a significant role in the intensification of the North Hemisphere glaciations is the North Atlantic surface circulation and especially the North Atlantic Current (NAC). In this context, my PhD thesis project focused on the interaction between climate, oceanic circulation and the impact on vegetation in the northwest North Atlantic to understand the conditions that prevailed during the initial growth of the Greenland ice sheet in the Plio-Pleistocene.

This study is based on coupling marine and terrestrial signals from the sediments of two drilled sites from the Labrador Sea (IODP Site U1307) and the Baffin Bay (ODP Site 645) and is organized around three major thematics:

- First, we established a detailed marine palynology biostratigraphy based on dinocysts and acritarchs bio-events encompassing the late Pliocene to early Pleistocene (3.2-2.2 Ma) including the mid-Pliocene warm Period (mPwP) and the Plio-Pleistocene transition at IODP Site U1307. This biostratigraphy has been compared with biostratigraphic schemes from the North Atlantic and Nordic Seas to discriminate local and regional events.
- Secondly, principal component analysis was performed to define ecostratigraphic zones from the relative occurrences (percentages) of taxa and to identify which taxa are the most sensitive. We also investigated the pollen and spore records in order to assess the vegetation from Greenland and we examined the ice rafted debris to simultaneously assess the ice cover and glacial expansion of the Greenland Ice Sheet. Finally, analyses of marine and terrestrial palynomorphs at ODP Site 645 in the Baffin Bay led us to refine the biostratigraphy in order to defined better the Plio-Pleistocene transition in this area.

This study suggests that despite relatively cold regional conditions, the Labrador Sea was strongly connected to the North Atlantic during the Plio-Pleistocene especially to the northeast North Atlantic sector where DSDP Site 610 is located. The two sites, U1307 (this study) and 610 (De Schepper and Head, 2009) share common biostratigraphic boundaries at ~3.17, 2.75 Ma and 2.56 Ma, thus highlighting large amplitude changes affecting the mid and high latitudes of the North Atlantic.

The study also shows that the mPwP was affected by high amplitudes changes due to variation in advection of NAC warm and saline water into the Labrador Sea and to cooling/freshening pulses of the surface waters from Greenland. Hence, the late Pliocene was marked by important changes in ocean surface circulation with southward migration of the Arctic front and NAC path at 2.65 Ma in the Labrador Sea, which is slightly earlier than in the northeast North Atlantic, where it is recorded at 2.60 Ma. Reduced warm and saline water penetration into the Labrador Sea possibly fostered the cooling which was accompanied with significant expansion of the Greenland Ice Sheet at about 2.65 Ma.

The pollen assemblages suggest input from humid boreal-type forests located likely in the southwest Greenland. Decrease in abundances of terrestrial palynomorphs and higher IRD suggests a reduce vegetation cover and an increase of ice cover with glacial activity reaching the coast over south Greenland from 2.65 Ma..

Finally, this study permitted to refine the late Miocene to Pleistocene biostratigraphic and seismic stratigraphy schemes at ODP Site 645 in the Baffin Bay. However, the position of the Pliocene to Pleistocene transition at ODP 645 was not identified as it is situated in a sediment recovery gap. Hence, this study demonstrates the need of new drilled holes in the Baffin Bay

Keywords: Labrador Sea, Baffin Bay, dinocysts, acritarcha, Pliocene, Pleistocene

INTRODUCTION

0.1 Contexte de l'étude

0.1.1 Le Pliocène

Le Pliocène (5,33 à 2,58 Ma) est caractérisé par un changement important et global du climat de la planète, et marque le passage progressif du climat relativement chaud du Tertiaire au refroidissement du Quaternaire. Malgré un refroidissement général depuis le début du Cénozoïque (Zachos *et al.*, 2001), le Pliocène était une époque en moyenne plus chaude que l'actuel et, bien qu'il existe quelques indices de glaciers locaux depuis environ 44 Ma (Tripati *et al.*, 2008) et des signes circonstanciés d'englaciations (De Schepper *et al.*, 2014), l'Hémisphère Nord était dépourvu de calottes glaciaires permanentes, contrairement à l'Antarctique. Un des éléments intéressants du système climatique durant la période du Pliocène est sa concentration de CO₂ atmosphérique, qui était élevée et proche des valeurs actuelles de 411,97 ppmv (mars 2019, NOAA/ESRL). En effet, les concentrations de CO₂ atmosphérique sont estimées entre 330 ppmv et 400 ppmv durant le Pliocène (Krüshner *et al.*, 1996 ; Raymo *et al.*, 1996 ; Seki *et al.*, 2010 ; Pagani *et al.*, 2010 ; Martinez-Botí *et al.*, 2015) avec un maximum possible de 425 ppmv (Raymo *et al.*, 1996) voire de 450 ppmv durant l'optimum climatique du Pliocène d'après les compilations réalisées pour le rapport du groupe d'experts intergouvernementaux sur l'évolution du climat (IPCC, 2013).

L'optimum climatique du Pliocène (*mid-Pliocene warm Period*, mPwP), entre ~3,264 et 3,025 Ma, est considéré comme la dernière période géologique significativement plus chaude que l'actuel, avant la mise en place du régime de glaciations du Pléistocène. C'est pourquoi cet intervalle fait l'objet d'une attention particulière, portée par de grands projets internationaux tels que le *Pliocene Model Intercomparison Project* (PlioMIP) et les modélisations du *Pliocene Research, Interpretation and Synoptic Mapping* (PRISM) de l'*US Geological Survey* (voir Dowsett *et al.*, 2016 pour la version la plus récente du projet). Le mPwP peut en effet servir d'analogie ou de référence dans une perspective de réchauffement climatique futur (Schneider et Schneider, 2009 ; IPCC, 2013).

Durant le mPwP, les températures moyennes de l'air étaient 2 à 3,6 °C plus élevées que les valeurs préindustrielles (Dowsett *et al.*, 2009, 2010a, 2016). Il existait un très fort contraste entre les basses et les hautes latitudes, avec un réchauffement accentué aux hautes latitudes de l'Hémisphère Nord, où les valeurs moyennes supérieures sont estimées à 8 °C de plus que celles de l'actuel et allant jusqu'à ~11/12 °C de plus dans l'Arctique canadien (Csank *et al.*, 2013). Le climat global était également plus humide, ce qui a favorisé le développement d'une végétation plus luxuriante, quelle que soit la latitude (Salzmann *et al.*, 2008, Pound *et al.* 2014, Dowsett *et al.*, 2016). Les températures moyennes de surface des océans étaient supérieures à l'actuel de 0 °C à 6 °C (Dowsett *et al.*, 2010a et 2010b ; IPCC 2013) avec une amplification du phénomène aux hautes latitudes de l'Hémisphère Nord (Dowsett *et al.* 2010b). Le niveau moyen des océans était aussi plus élevé de $22 \pm 5\text{--}10$ m par rapport à l'actuel (Miller *et al.*, 2012).

0.1.2 La transition Plio-Pléistocène

À la transition entre le Pliocène et le Pléistocène (2,581 Ma), un refroidissement important (Zachos *et al.*, 2001) a été accompagné par le changement d'un régime de petits glaciers locaux à une glaciation d'abord régionale puis généralisée dans l'Hémisphère Nord (Flesche Kleiven *et al.*, 2002 ; Matthiessen *et al.*, 2009 ; De Schepper *et al.*, 2014). Bien que le Pliocène ait été ponctué par le développement de calottes glaciaires (voir De Schepper *et al.*, 2014), l'englaciation de l'Hémisphère Nord (NHG) semble avoir été progressive (Ravelo *et al.*, 2004). À partir de l'analyse des courbes $\delta^{18}\text{O}$, réalisées sur les tests de foraminifères benthiques, indicatrices de la variation du volume global de glace continentale, Mudelsee et Raymo (2005) proposent une initiation des NHG dès le début du Pliocène supérieur à ~ 3,6 Ma. Les premières évidences directes s'enregistrent vers 3,3 Ma au niveau du Groenland avec un premier pic significatif de particules terrestres transportées par la glace (*Ice Rafted Debris*, IRD), indiquant une augmentation du passage des radeaux de glace (iceberg et/ou glace de mer) transportant des particules provenant du continent (Flesche Kleiven *et al.*, 2002). L'engagement s'intensifie de manière plus générale dans le reste de l'Hémisphère Nord vers 2,7 Ma, comme en atteste l'augmentation synchrone des IRD et de la fraction grossière (> 63 µm) dans les sédiments marins de l'Atlantique Nord (Shackleton *et al.*, 1984 ; Winkler *et al.*, 2002 ; Flesche Kleiven *et al.*, 2002), de la Mer du Labrador (Blake-Mizen *et al.*, 2019), des mers nordiques (Flesche Kleiven *et al.*, 2002 ; Polyak *et al.*, 2010) et du Pacifique Nord (Haug *et al.*, 2005). La récente étude de Clotten *et al.* (2018) dans la Mer d'Islande démontre, à partir de biomarqueurs, une expansion majeure de la calotte groenlandaise à partir de ~2,75 Ma associée à l'établissement d'un couvert de glace de mer permanent proche des côtes est groenlandaises.

Les causes de ces changements sont encore débattues à l'heure actuelle. Il semble cependant que la chute du CO₂ atmosphérique fut indispensable à l'englaciation de l'Hémisphère Nord (Lunt *et al.*, 2008a). En effet, au début du Pléistocène, vers 2,8 Ma, la concentration de CO₂ atmosphérique avoisinait 280 ppmv (DeConto *et al.*, 2008 ; Seki *et al.*, 2010 ; Bartoli *et al.*, 2011) représentant ainsi une diminution d'environ 190 ppmv depuis l'optimum climatique du Pliocène.

0.1.3 L'état du Groenland pendant le Pliocène

Pendant le Pliocène, l'étendue des glaciers sur le Groenland était donc limitée. La présence d'IRD et de dropstones en provenance du Groenland dans la Mer du Groenland (ODP Sites 913 et 985, Thiede *et al.*, 2011), la Mer d'Irminger (ODP Site 918, St. John et Krissek, 2002) et la Mer du Labrador (ODP Site 646, Korstgård et Nielsen, 1989) témoigne du développement de glaciers de montagne ayant atteint la mer à l'est de l'île, et ce depuis au moins le Miocène supérieur (~7 Ma). En ce qui concerne la Baie de Baffin (ODP Site 645), les IRD et dropstones provenant de l'ouest de l'île et des terres environnantes canadiennes suggèrent également la présence de glaciers dès 8 Ma (Cremer et Legigan, 1989; Korstgård et Nielsen, 1989). Durant le mPwP, l'inlandsis groenlandais n'aurait représenté qu'environ 25 % de sa taille actuelle et était majoritairement concentré sur les reliefs situés à l'est et au sud de l'île (Figure 0.1 ; Koenig, *et al.*, 2011 ; Dolan *et al.*, 2015 ; Dowsett *et al.*, 2016).

Les quelques données disponibles et les expériences de modélisation de la végétation durant le mPwP font état d'une végétation mixte avec la présence de forêts tempérées, boréales et de formation arbustives, de prairies et d'une toundra sur le Groenland

(Salzmann *et al.*, 2011 ; Dowsett *et al.*, 2016), plaçant ainsi la limite des arbres à 2500 km plus au Nord que la limite moderne (Figure 0.1, Salzmann *et al.*, 2008). Ces reconstructions s'appuient en partie sur la découverte de macrofossiles et microfossiles, comme par exemple les macrorestes végétaux retrouvés sur l'île de France qui suggèrent la présence d'une forêt boréale ou d'une toundra forestière dans la région nord-est du Groenland, autour de 3,4 à 3 Ma (Bennike *et al.*, 2002). Au nord de l'île, dans la formation du Kap Kobenhavn, des macrorestes végétaux, des insectes et des restes de mammifères confirmé l'absence de calotte glaciaire à cette latitude ainsi que la présence d'une végétation plus abondante de type toundra forestière vers 2,4 Ma (Funder *et al.*, 1985, 2001). L'abondance de plantes et d'organismes d'eau douce laisse supposer la présence de terres humides parsemées de nombreux lacs ou étangs dans la région (Bennike et Bötcher, 1990). De même, dans les sédiments de la Mer du Labrador, un contenu pollinique abondant dans les sédiments pliocènes reflète une végétation de type boréale subarctique au niveau de la région source du Groenland (de Vernal et Mudie, 1989a).

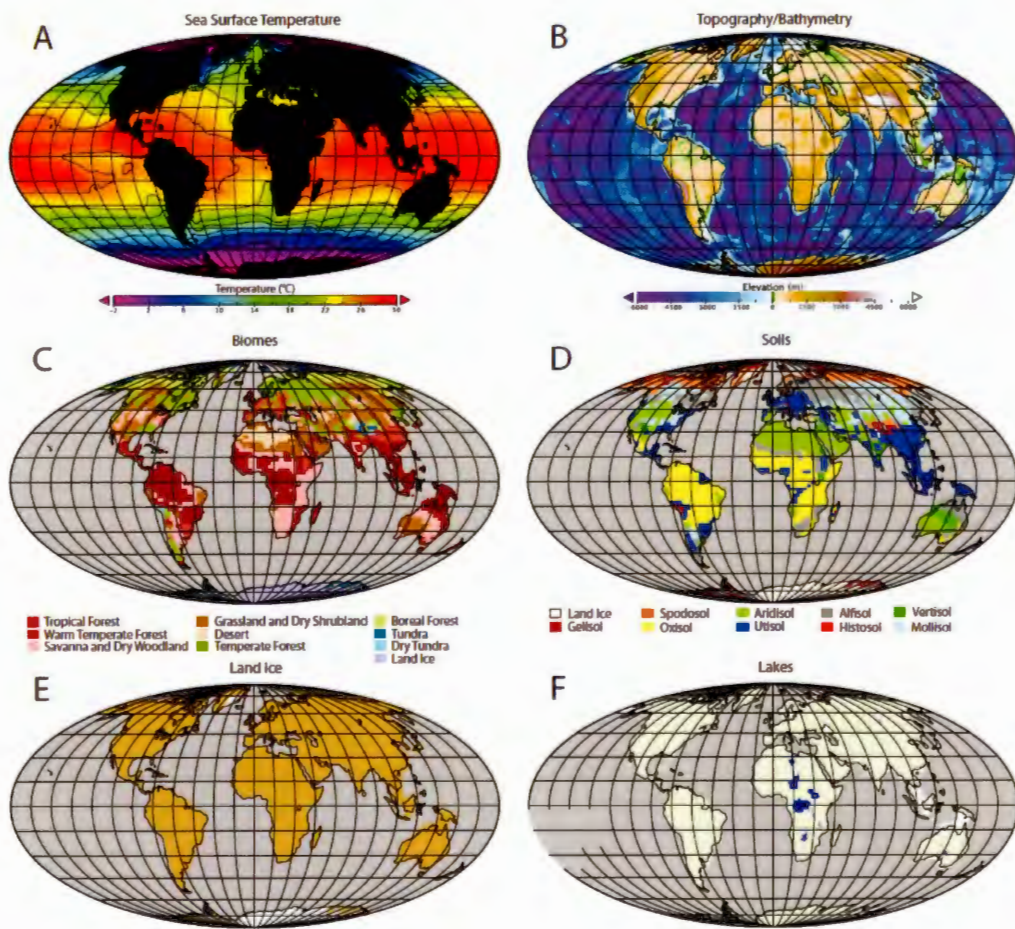


Figure 0.1 Reconstitution PRISM4 (A) des températures de surfaces des océans, (B) de la topographie des continents et de la bathymétrie des océans, (C) des biomes, (D) des sols, (E) de la glace continentale, (F) des grands lacs pendant l'optimum climatique du Pliocène (Dowsett *et al.*, 2016)

0.1.4 Le rôle de l'Atlantique Nord

Dans l'Atlantique Nord, le courant nord-atlantique (*North Atlantic Current*, NAC) semble avoir joué un rôle crucial dans l'établissement des conditions décrites plus haut, en particulier pour l'expansion de la calotte groenlandaise. En effet, suite à la fermeture du passage de l'Amérique centrale (CAS), l'intensification du NAC aurait entraîné une augmentation du transport de chaleur et d'humidité vers les hautes latitudes de l'Atlantique Nord (Klocker, 2005, Lunt *et al.* 2008a, 2008b). Les eaux chaudes et salées des tropiques sont alors transportées vers les hautes latitudes via le NAC (Haug et Tiedman, 1998; Bartoli *et al.*, 2005, Klocker *et al.*, 2005). D'après les modélisations de Driscoll et Haug (1998), la fermeture du CAS est aussi responsable de l'augmentation du transport d'humidité vers les hautes latitudes, nécessaire à l'expansion du couvert de glace sur le Groenland (Lunt *et al.*, 2008a, 2008 b ; Klocker *et al.*, 2005).

Le NAC a ainsi fait l'objet d'une attention particulière quant à son intensité et sa trajectoire durant le Pliocène tardif et la transition Plio-Pléistocène, notamment par l'étude des microfossiles préservés dans les sédiments. Par exemple, les kystes de dinoflagellés (ou dinokystes) permettent de documenter la température, la salinité et la productivité des eaux de surface (de Vernal et Marret, 2007). L'espèce *Operculodinium centrocarpum* sensu Wall and Dale (1966) (dorénavant *Operculodinium centrocarpum* dans le reste de ce document) a été utilisée comme un indicateur du passage et de l'intensité du NAC dans l'Atlantique Nord et les mers nordiques durant la période moderne (Knies *et al.* 2002 ; Van Nieuwenhove *et al.* 2008), mais également au cours du Pliocène (De Schepper *et al.*, 2009a, 2013 ; Hennissen *et al.*, 2014, 2017 ; Panitz *et al.*, 2017).

De Schepper *et al.* (2009a) ont mis en évidence, grâce à l'abondance relative des principales espèces de dinokystes et à partir d'analyses géochimiques, une influence réduite et un changement de trajectoire du NAC aux sites DSDP 610A et IODP 1308C durant l'événement froid du MIS M2 (~ 3,3 Ma, Figure 0.2), rendant possible le développement de glaciers sur le Groenland (De Schepper *et al.*, 2014). De plus, De Schepper *et al.* ont proposé en 2013 qu'une brève réouverture du CAS aurait été responsable de l'intensité du refroidissement du MIS M2. En effet, la pénétration des eaux de surface plus froides et moins salées du Pacifique dans l'Atlantique aurait contribué à la diminution de l'intensité du NAC, limitant ainsi le transport de chaleur vers les hautes latitudes de l'Atlantique Nord (De Schepper *et al.*, 2013).

À partir des alkénones, biomarqueurs produits par des haptophytes, des reconstitutions similaires ont été faites pour les intervalles glaciaires du Pliocène tardif, entre 3,68 et 2,45 Ma, au site IODP U1313 situé dans les moyennes latitudes au niveau de la gyre subtropicale de l'Atlantique Nord (Naafs *et al.*, 2010). En utilisant des reconstructions de température et productivité, les auteurs suggèrent un refroidissement général à partir de 3,1 Ma et proposent que durant les épisodes glaciaires de l'intensification des NHG, le NAC avait une trajectoire ouest-est associée avec une baisse du front polaire jusqu'aux moyennes latitudes (Figure 0.2).

Plus récemment, Hennissen *et al.* (2014) ont utilisé les dinokystes et la géochimie des tests de foraminifères benthiques et planctoniques aux sites DSDP 610 et IODP U1313 pour mettre en évidence une baisse latitudinale du front polaire et un changement de la trajectoire du NAC à 2,61 Ma (MIS 104) qui aurait caractérisé la transition Plio-Pléistocène (Figure 0.2). De même, Panitz *et al.* (2017) ont montré, avec les assemblages de dinokystes, la pénétration d'eaux chaudes et salées de l'Atlantique dans la Mer de Norvège pendant le mPwP (3,320 à 3,137 Ma). Cet événement fut suivi d'une diminution de l'intensité du NAC associée à des températures de surface plus froides

enregistrées par les alkénones, et d'un changement de végétation sur les côtes de la Norvège, tel que démontré par les assemblages polliniques durant les MIS KM4-KM2 (3,184-3,137 Ma, Figure 0.2).

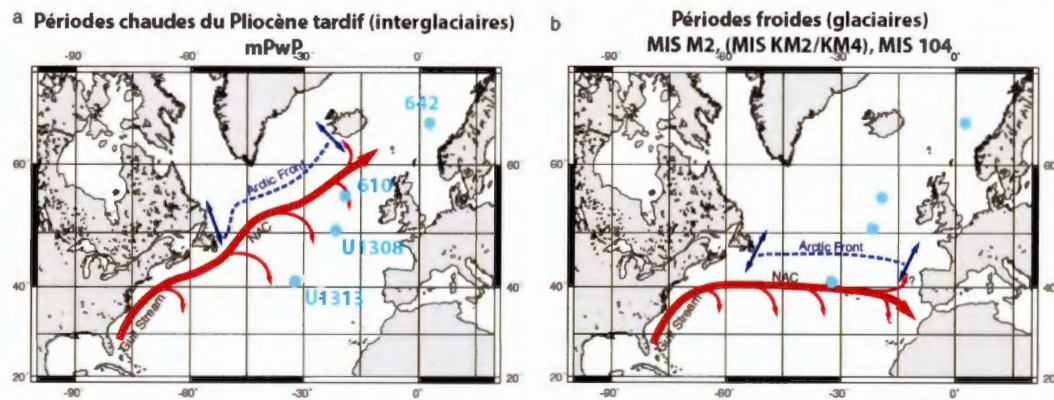


Figure 0.2 Localisation des sites mentionnés dans le texte (cercles bleu clair) et positionnement du courant Nord Atlantic (flèches rouges) et du front arctique (ligne pointillée bleu foncé) pendant (a) les périodes chaudes et (b) froides du Pliocène tardifs. Modifié d'après Naafs *et al.* (2010)

0.2 Limites des connaissances

Les expériences de modélisation du projet PRISM visent à comprendre et à reconstituer la dynamique du climat global pendant l'optimum climatique du Pliocène. Cependant, la robustesse des exercices de modélisation est limitée par le nombre restreint de données disponibles. Par exemple, la première étude qui reconstitue les différents types de sols à l'échelle mondiale pendant l'intervalle PRISM se base sur la modélisation de la végétation (Salzmann *et al.*, 2008) à partir d'extrapolations sur un nombre restreint d'échantillons (54 pour l'ensemble de la planète) dont aucun sur le Groenland ou l'Amérique du Nord (Pound *et al.*, 2014). Par ailleurs, des simulations numériques ont pu reconstituer les biomes à partir de 202 sites mais incluant seulement une dizaine de sites localisés dans l'Arctique (Salzmann *et al.*, 2008). Les reconstitutions de la calotte groenlandaise utilisant les paramètres de PlioMIP sont très diversifiées et dépendent des modèles et des conditions initiales prescrites (Dowsett *et al.*, 2010 a ; Haywood *et al.*, 2010 ; 2011 ; Contoux *et al.*, 2015 ; Dolan *et al.*, 2015 ; Dowsett *et al.*, 2016). Les simulations numériques peuvent varier, rendant compte d'une calotte groenlandaise semblable à celle de l'actuel à une situation caractérisée par le Groenland totalement dénudé de glace (Dolan *et al.*, 2015). Les données fossiles, suggérant une étendue limitée des glaces au nord et à l'est du Groenland, permettent d'orienter les résultats (Salzmann *et al.*, 2008). Généralement, la configuration retenue est celle discutée précédemment, soit une présence réduite de la glace qui est limitée à l'est et au sud du Groenland, où les reliefs sont importants, couplée à une végétation de type boréal subarctique recouvrant une grande partie de l'île (Dowsett *et al.*, 2016).

Sur le Groenland, les archives continentales sont également confrontées à d'importantes limites telles que le faible nombre de sites pliocènes explorés, les

perturbations des affleurements suite à l'érosion glaciaire du Quaternaire ou encore la difficulté d'obtenir un modèle d'âge robuste. En effet, les sites pliocènes du Groenland et de l'Arctique sont en général assez mal datés et ce, notamment dû à l'absence de séquences continues de référence couvrant le Plio-Quaternaire. La biostratigraphie, principalement à partir des organismes marins, permet quant à elle de corrélérer certains affleurements entre eux et en apportant par exemple une précision sur l'âge du sédiment (Funder *et al.*, 1985 ; 2001 ; Bennike *et al.*, 2002 ; Bennike et Böttcher, 1990).

Afin de pallier au problème de hiatus sédimentaire dans les archives continentales, l'étude de carottes sédimentaires marines prélevées près des côtes s'avère être une alternative. Les carottes marines donnent la possibilité d'obtenir un enregistrement quasi continu des variations climatiques au cours du temps ainsi que d'établir des relations entre les conditions terrestres et marines (de Vernal et Hillaire-Marcel, 2008 ; Panitz *et al.*, 2017). Cela permet une meilleure compréhension des relations entre le climat, les conditions terrestres et la circulation océanique dans un monde riche en CO₂ atmosphérique, et ce notamment aux hautes latitudes où s'est développée la calotte groenlandaise (de Vernal et Hillaire-Marcel, 2008 ; Thiede *et al.*, 2011).

Le nord-ouest de l'Atlantique Nord, soit la Mer du Labrador et la Baie de Baffin, qui est directement en contact avec la calotte groenlandaise constitue une région influencée à la fois par une branche du NAC et par des apports de l'Océan Arctique. Toutefois, jusqu'à présent, aucun enregistrement paléocéanographique de haute résolution couvrant tout le Pliocène et la transition Plio-Pléistocène ne fait état des conditions de surface (Figure 0.3).

0.3 Objectifs de la thèse

Mon projet de doctorat se concentre donc sur l'interaction entre le climat, la végétation et la circulation océanique de surface dans le nord-ouest de l'Atlantique Nord, dans le but de documenter l'évolution de la glace continentale sur le sud du Groenland pendant la transition Plio-Pléistocène. Les objectifs spécifiques de cette thèse sont les suivants:

- (1) L'établissement d'une biostratigraphie de référence de la transition Plio-Pléistocène dans la Mer du Labrador, basée sur les bioévénements des palynomorphes marins (dinokystes et acritarches) au site IODP U1307 afin de caractériser le Pliocène tardif et le début du Pléistocène (3,2-2,2 Ma).
- (2) La comparaison de cette biostratigraphie avec les schémas biostratigraphiques existants du reste de l'Atlantique Nord et des mers nordiques afin de discriminer les événements locaux et régionaux (Head and Norris, 2003; De Schepper and Head, 2009; De Schepper *et al.*, 2017).
- (3) L'interprétation des informations écologiques des assemblages de dinokystes et d'acritarches afin de retracer l'influence du NAC dans la Mer du Labrador, ainsi que les conditions océaniques de surface et leurs relations avec le reste de l'Atlantique Nord (De Schepper *et al.*, 2009, 2011, 2013 ; Naafs *et al.*, 2008 ; Hennissen *et al.*, 2014, 2015, 2017) et des mers nordiques (Panitz *et al.*, 2017 ; Clotten *et al.*, 2018) durant le mPwP et la transition Plio-Pléistocène (3,2 et 2,2 Ma).
- (4) La reconstitution des conditions terrestres sur le sud du Groenland à partir des assemblages de grains de pollen et des spores ainsi que des IRD afin d'établir la relation

entre les changement continentaux, les variations paleocéanographiques et l'expansion de la calotte groenlandaise.

(5) L'utilisation des outils biostratigraphiques afin d'identifier la transition Plio-Pléistocène dans la Baie de Baffin au site ODP 645 et par la suite d'évaluer la portée d'études palynologiques dans cette région.

0.4 Contexte régional et matériel utilisé pour l'étude

0.4.1 Contexte régional moderne

La Mer du Labrador est un bassin océanique directement connecté à l'Atlantique Nord au sud et à la Baie de Baffin au nord, par le détroit de Davis. La Baie de Baffin est quant à elle en contact avec l'Océan Arctique au travers de différents détroits tels que les détroits de Jones, de Lancaster et de Nares dans l'archipel arctique canadien (Figure 0.3).

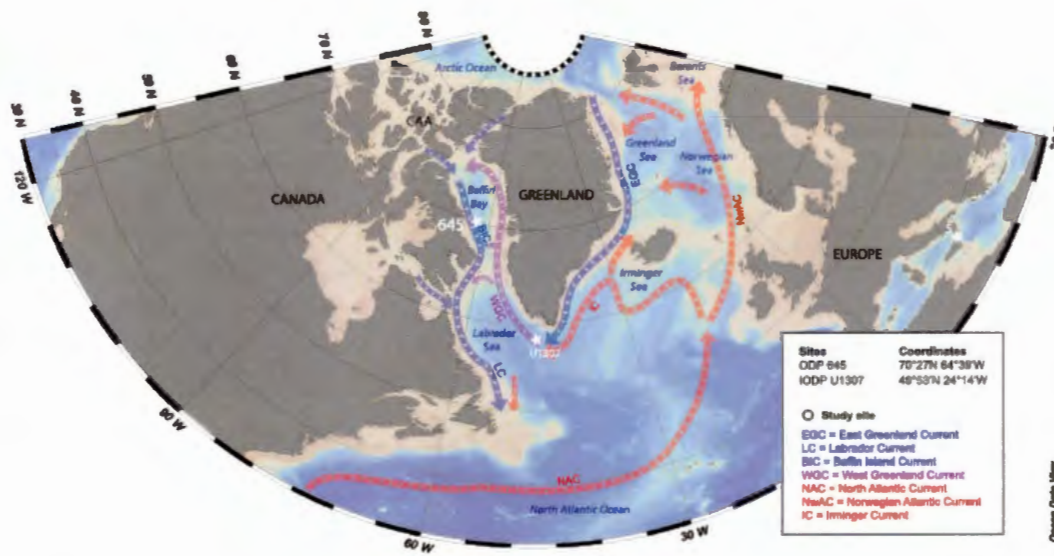


Figure 0.3 Carte de l'Atlantique Nord, présentant les deux sites d'études IODP U1307 et ODP 645 ainsi que la circulation océanique de surface moderne. Le fond de carte provient du logiciel *Ocean Data View* (Schlitzer, 2018).

Les eaux de surface de la Mer du Labrador sont un mélange du NAC, une masse d'eau chaude et salée provenant de l'Atlantique Nord, et de deux courants plus froids : (1) à l'est, le courant Ouest du Groenland (WGC, *West Greenland Current*) qui apporte vers le nord des eaux arctiques réchauffées le long des côtes groenlandaises, et (2) le long des marges canadiennes, le courant du Labrador (LC, *Labrador current*) transportant les eaux froides et peu salées de la Baie de Baffin vers le sud (Figure 0.3). Dans la mer du Labrador, un refroidissement des masses d'eaux superficielles pendant l'hiver donne lieu à une convection verticale et à la formation d'eaux intermédiaires/profondes (LSW, *Labrador Sea Water*). Cette convection prend place entre 150 m et 1000-2000 m de profondeur (Marshall et Schott, 1999 ; Lazier *et al.*, 2002) et joue un rôle clé dans

la circulation atlantique méridionale (AMOC : *Atlantic Meridional Overturning Circulation*) (Weaver *et al.*, 1999 ; Yashayaev, 2007 ; Yashayaev *et al.*, 2007). Or, la convection dans la Mer du Labrador est un élément instable du système climatique, qui semble s'être mis en place il y a seulement ~ 7500 ans au cours du présent interglaciaire (Gibb *et al.*, 2015).

La circulation océanique de surface (0-300 m de profondeur) est dominée par une gyre antihoraire déterminée par les forces de Coriolis rendant compte à l'est du courant chaud et salé du WGC circulant vers le nord, et à l'ouest, des eaux froides et peu salées de l'Arctique s'écoulant vers la Mer du Labrador le long des côtes est canadiennes (BIC, *Baffin Island Current*; Rudels, 1986 ; Tang *et al.*, 2004 ; Zweng et Münchow, 2006, Figure 0.3). De nos jours, la glace de mer recouvre la Baie de Baffin huit mois par année (début en septembre) et son développement suit notamment le BIC et les vents de surface. La majorité des icebergs provient du nord-ouest du Groenland et circule le long de la trajectoire des courants marins, migrant vers le nord le long des marges ouest du Groenland, vers l'ouest et le sud en suivant les côtes canadiennes pour rejoindre la Mer du Labrador (Hanna et Cappelen, 2002).

0.4.2 Sites, échantillons et modèle d'âge

Pour cette étude, 212 échantillons provenant de sédiments marins issus de campagnes de forage de l'ODP et de l'IODP ont été analysés. Le matériel sédimentaire a été récolté durant les expéditions ODP 105 en 1985 et IODP 303 en 2004.

Le site IODP U1307 ($58^{\circ} 30,3'N$; $46^{\circ} 24' W$, Figure 0.3) se situe dans la Mer du Labrador au niveau de la ride d'Eirik au sud du Groenland sous l'influence actuelle des eaux du EGC et du NAC. D'après Rochon et de Vernal (1994) et les modélisations de la vitesse des vents réalisées par Smith *et al.* (2018) durant le mPwP, les apports de grains de pollen et de spores proviendraient du sud du Groenland. Un modèle d'âge du Site IODP U1307 a été récemment établi par Blake-Mizen *et al.* (2019). Il est basé sur les inversions magnétiques et la corrélation des variations de la paléo-intensité relative avec le Site IODP U1308 (Channell *et al.*, 2016).

En ce qui concerne la Baie de Baffin, le site ODP 645 ($70^{\circ} 27,48'N$, $64^{\circ} 39,30'W$, Figure 0.3) est localisé plus proche des côtes canadiennes que groenlandaises. Cependant, il n'existe pour l'instant, aucun autre site remontant jusqu'au Pliocène dans cette région. D'après Hiscott *et al.* (1989), les sédiments récoltés au site ODP 645 enregistrent les apports de matériel terrestre provenant des archipels arctiques canadiennes, de l'île de Baffin et de l'ouest du Groenland. Ainsi, le signal palynologique du Site ODP 645 pourrait provenir de l'île de Baffin (Rochon et de Vernal, 1994) ou peut être du Nord du Groenland (Smith *et al.*, 2018).

Du fait de problèmes techniques lors du forage du site 645, la récupération des sédiments est incomplète (~55 %; Srivastava *et al.*, 1987). L'établissement d'une magnétostratigraphie a été difficile (Clement *et al.*, 1989 ; Baldauf *et al.*, 1989), non

seulement en raison de la discontinuité de la séquence sédimentaire mais aussi à cause de la rareté des microfossiles calcaires et siliceux (Aksu et Kaminski, 1989; Baldauf *et al.*, 1989 ; Knüttle *et al.*, 1989 ; Lazarus et Pallant, 1989; Monjanel et Baldauf, 1989). Cependant, des microfossiles organiques tel que les dinokystes sont régulièrement observés tout au long de la séquence sédimentaire et ont permis d'établir une biostratigraphie de faible résolution (de Vernal et Mudie, 1989b ; Head *et al.*, 1989 ; Anstey 1992). La position de la transition Plio-Pléistocène reste néanmoins incertaine à ce site.

0.5 Méthodes

L'approche principale retenue est le couplage entre la palynologie marine et terrestre et les apports continentaux via les IRD. La palynologie se décrit comme l'étude des microfossiles non minéralisés, c'est-à-dire organiques, qui peuvent être d'origine marine (dinokystes, acritarches, chitinizoaires, etc.) ou terrestre (grains de pollen, spores, fragments de feuilles, de tiges et autres vestiges végétaux).

Le traitement des échantillons a été réalisé selon les procédures du laboratoire de micropaléontologie du Geotop à l'UQAM (de Vernal *et al.*, 1999). Chaque échantillon a été pesé à sec puis, au début du traitement, une tablette de *Lycopodium clavatum* a été ajoutée pour calculer les concentrations (Matthews, 1969; Mertens *et al.*, 2009). Ensuite, les échantillons ont été tamisés entre 106 µm et 10 µm. La fraction supérieure à 106 µm a servi pour l'étude des IRD après avoir été retamisée à 150 µm. Celle comprise entre 106 µm et 10 µm a été traitée à l'acide chlorhydrique (HCl, 10%) et à l'acide fluorhydrique (HF, 49%) afin d'éliminer les particules carbonatées et siliceuses.

La méthode de séparation par liqueur dense (Munsterman et Kerstholt, 1996) a été appliquée afin d'éliminer les dernières particules silicieuses, puis le matériel résiduel a été monté dans de la glycérine gélatinée entre lame et lamelle pour les analyses au microscope optique (objectifs x400 et x1000).

La fraction supérieure à 150 µm a quant à elle été broyée en poudre avant d'être placée sur des porte-échantillons pour analyse dans le diffractomètre à rayons X de l'UQAM sous l'expertise de Mr. Michel Preda du département des Sciences de la Terre.

0.5.1 Les kystes de dinoflagellés ou dinokystes

Les dinoflagellés sont des protistes algaires appartenant à la classe des Dinophycées et constituent, avec les diatomées et les coccolithophores, un des principaux producteurs primaires des océans actuels (de Vernal et Marret, 2007). Ils sont aquatiques (lacs, rivières, océans), ubiquistes (de l'équateur aux pôles) et épipelagiques (0 à 200 m) ainsi qu'hétérotrophes et/ou phototrophes (certaines espèces sont mixotrophes). Leur cycle de vie (Figure 0.4) est complexe alternant entre une phase mobile et une phase de dormance associée à la reproduction (sexuée ou asexuée). Au cours de cette dernière phase, un kyste est produit (Figure 0.4). Dans certains cas ce kyste est constitué de matière organique (dinosporange), lui permettant une certaine résistance et une bonne fossilisation (de Vernal et Marret, 2007 ; Bogus *et al.*, 2014). Il est alors désigné sous l'appellation de dinokyste.

Bien que seulement 10 à 20 % des espèces produisent un kyste fossilisable (Head, 1996, de Vernal et Marret, 2007), les assemblages de dinokystes permettent de documenter quantitativement et qualitativement les propriétés physico-chimiques des

eaux de surface (température, salinité, glace de mer, etc.) ainsi que la circulation de ces dernières (e. g., Rochon *et al.*, 1999; de Vernal et Marret, 2007; de Vernal *et al.*, 2013). Grâce à leur préservation et leurs diversité taxonomique, les dinokystes sont de plus en plus étudiés pour documenter le Néogène par l'établissement de schémas biostratigraphiques de référence (Head, 1993, 1996, 1997; Versteegh et Zevenboom, 1995; Head et Norris, 2003; De Schepper *et al.*, 2004, 2017; De Schepper et Head, 2008a, 2008b, 2009, 2014; Schreck *et al.*, 2012; Verhoeven *et al.*, 2013; Mattingdal *et al.*, 2014; Matthiessen *et al.*, 2018), et des reconstitutions paléocéanographiques et paléoécologiques (de Schepper *et al.*, 2011, 2013 ; Panitz *et al.*, 2017; Hennissen *et al.*, 2017; Schreck *et al.*, 2017) dans l'Atlantique Nord et les mers environnantes.

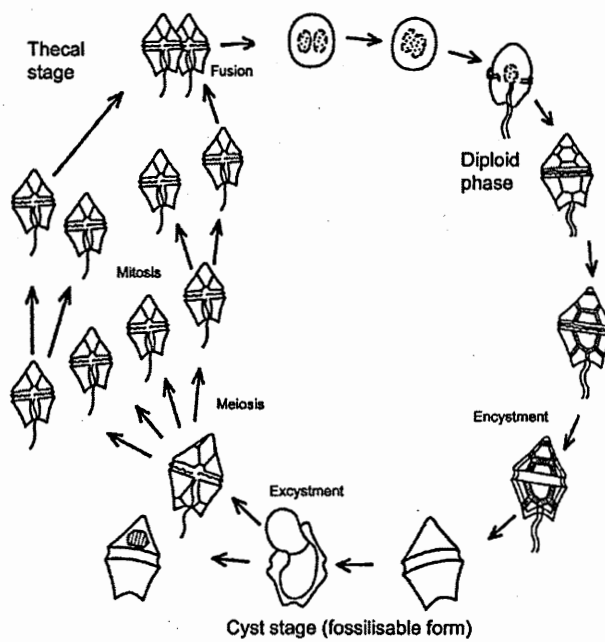


Figure 0.4 Cycle de vie des dinoflagellés avec l'alternance d'un stade motile (non fossilisable) et d'un stade de dormance (fossilisable) (de Vernal et Marret, 2007)

0.5.2 Les acritarches

Les acritarches sont des organismes microscopiques (5-200 µm) fossiles présents depuis le Précambrien, pour lesquels il est impossible d'attribuer une affinité taxonomique. Généralement ils sont décrits comme possédant une cavité centrale entourée par un mur possédant plusieurs couches composées de matière organique (Evitt, 1963). Il s'agit donc de palynomorphes marins, ayant probablement des affinités avec les dinokystes, sinon avec des Prasinophycées (une division des algues vertes). C'est par exemple le cas des genres *Cymatiosphaera* et *Lavradosphaera* qui, malgré leurs attributions au groupe des prasinophycées, restent dans la catégorie des acritarches pour les paléontologues. Récemment, une attention particulière leur a été apportée au vu de leur utilité en biostratigraphie, notamment pour l'étude du Cénozoïque dans l'Atlantique Nord où ils sont présents en très grande quantité (De Schepper *et al.*, 2008; De Schepper et Head, 2009; 2013; Schreck *et al.*, 2013; Schreck et Matthiessen, 2014).

Dans cette thèse, les apparitions (*lowest occurrence, LO*) et disparitions (*highest occurrence, HO*) des espèces de dinokystes et acritarches seront considérées comme des bio-événements qui seront calibrés en fonction du modèle d'âge des sites concernés. Les zones biostratigraphiques seront ainsi définies en fonction de certains bio-événements et comparés à ceux d'autres études dans l'Atlantique Nord. Des analyses par composante principale (PCA) seront utilisées afin de définir des zones paléoécologiques et d'extraire des assemblages les espèces expliquant le mieux les variations observées.

0.5.3 Les palynomorphes terrestres : les grains de pollen et les spores

Les spores et les grains de pollen sont des éléments indispensables du cycle de reproduction des végétaux terrestres. Leur taille microscopique (de l'ordre du μm) leur confère une grande capacité de dispersion par voie aérienne, au point qu'on en retrouve autant dans les sédiments continentaux que marins. Leur préservation à l'état de fossile est, comme celle des dinokystes et acritarches, due à la composition organique extrêmement résistante de leur membrane en sporo-pollinine. Dans les sédiments marins, les grains de pollen et spores permettent de retracer le couvert végétal dominant du continent adjacent (Moore *et al.*, 1991; Sánchez Goñi *et al.*, 2018). La présence de grains de pollen frais peut également être utilisée comme un indicateur de la densité de la végétation indirectement en lien avec la présence ou non de glace sur les terres adjacentes (de Vernal et Hillaire-Marcel, 2008).

0.5.4 Les IRD

Comme mentionné précédemment, les IRD correspondent à des particules minérales ou des fragments de roches terrigènes transportés par des radeaux de glace flottante (iceberg et/ou glace de mer), se déposant ensuite dans les sédiments marins après la fonte de cette dernière. L'abondance des IRD dans les régions polaires et subpolaires est donc considérée comme un indicateur du passage d'iceberg et du développement de glaciers atteignant les marges continentales (Kuijpers *et al.*, 2016). Leur occurrence

est utilisée pour retracer la variabilité de la calotte groenlandaise (voir Thiede *et al.*, 2011; Knutz *et al.*, 2011) au cours du temps et permet de mettre en évidence l'intensification des glaciations de l'Hémisphère Nord (Shackleton *et al.*, 1984; Winkler *et al.*, 2002 ; Flesche Kleiven *et al.*, 2002 ; Haug *et al.*, 2005 ; Polyak *et al.*, 2010).

0.6 Organisation de la thèse

Cette thèse s'articule en trois chapitres écrits en anglais, chacun correspond à un article en préparation pour soumission à une revue scientifique à comité de lecture.

Le chapitre I présente la première biostratigraphie détaillée du Pliocène tardif au début Pléistocène (3,2-2,2 Ma) dans la Mer du Labrador, basée sur les dinokystes et les acritarches. Elle s'inscrit dans un schéma biostratigraphique plus large à l'échelle de l'Atlantique Nord et met en évidence la corrélation entre la Mer du Labrador et le centre-est de l'Atlantique Nord.

Le chapitre II traite des interprétations paléoécologiques et paléocénographiques des assemblages de dinokystes et d'acritarches dans la Mer du Labrador entre 3,2 et 2,2 Ma. Le chapitre couvre une partie du mPwP et la transition Plio-Pléistocène et contribue à documenter l'influence du NAC sur la partie nord-est de l'Atlantique Nord.

Le chapitre III vise à identifier la transition Plio-Pléistocène dans les sédiments marins de la Baie de Baffin au Site ODP 645 à l'aide des dinokystes et acritarches en se basant, entre autre, sur la biostratigraphie élaborée dans la Mer du Labrador dans le chapitre I.

Ce chapitre propose également une révision des corrélations des profils sismiques entre le Site ODP 645 et les transects d'est en ouest de la Baie de Baffin réalisés par Knutz *et al.* (2015).

CHAPITRE I

DINOCYST AND ACRITARCH BIOSTRATIGRAPHY OF THE LATE PLIOCENE-EARLY PLEISTOCENE OF IODP SITE U1307, LABRADOR SEA

A.M.R. Aubry¹, S. De Schepper², A. de Vernal¹

¹ GEOTOP, Université du Québec à Montréal, CP 8888, Montréal, QC, H3C 3P8,
Canada

² NORCE Climate, Norwegian Research Centre, Bjerknes Centre for Climate
Research, Jahnebakken 5, N-5007 Bergen, Norway

Keywords: Labrador Sea; Dinocysts; Acritarcha; Biostratigraphy; Pliocene;
Pleistocene

Article accepté dans *Journal of Micropaleontology*

Abstract

We have analyzed marine palynomorphs (mainly dinocysts and acritarchs) from the Integrated Ocean Drilling Program Site U1307 in the Labrador Sea in order to establish a detailed biostratigraphy for the Late Pliocene to Early Pleistocene. We have defined three magnetostratigraphically-calibrated dinocyst and acritarch biozones in the Late Pliocene to Early Pleistocene. Zone LS1 is defined based on the highest occurrence of *Barssidinium graminosum* and covers the later Pliocene from 3.21 to 2.75 Ma. Zone LS2 is marked by the acme of *Pyxidinopsis braboi* which occurs between 2.75 and 2.57 Ma, thus encompassing the Plio/Pleistocene transition. Finally, zone LS3 extends from 2.57 to 2.23 Ma in the Early Pleistocene.

The palynostratigraphic record of IODP Site U1307 is difficult to correlate to other North Atlantic and Nordic Seas sites mainly because of different temporal resolution and lack of well-defined biostratigraphic marker species at basin scale. The low abundance, discontinuous occurrence and asynchronous events of warm water Pliocene taxa such as *Invertocysta lacrymosa*, *Impagidinium solidum*, *Ataxiodinium confusum*, *Melitasphaerodinium choanophorum* and *Operculodinium? eirikianum* suggest cooler conditions in the Labrador Sea than elsewhere in the North Atlantic, reflecting a strong regionalism. Nevertheless, as recorded at other locations in the North Atlantic, the disappearance of many dinocyst and acritarch taxa around 2.75 Ma at Site U1307 reflects a strong ecological response accompanying the intensification of the Northern Hemisphere glaciation.

1.1 Introduction

The Cenozoic was marked by large tectonic, paleoceanographic, and paleoclimatic events (Zachos *et al.*, 2001) that ultimately led to the initiation and the intensification of the Northern Hemisphere glaciations (iNHG, Shackleton *et al.*, 1985; Mudelsee and Raymo 2005). Well-constrained chronologies are crucial for documenting and better understanding the paleoceanographic conditions and palaeoclimatic changes around the iNHG at the end of the Cenozoic. However, the lack of stratigraphic control in high latitude oceans, due to for example poor carbonate preservation, often prevents to adequately constrain paleoceanographic and climatic events in time. The temporal coverage of existing stratigraphic schemes is often incomplete or the resolution too low (Harrison *et al.*, 1999). Mattingsdal *et al.* (2014) demonstrated the importance of a robust chronology to reconstruct the regional history of the Fram Strait gateway in order to better understand exchange between the Arctic and Atlantic oceans as well as the intensification of glaciation in the Barents Sea and on Svalbard. Unfortunately, uncertainties remain about the relationships between the different ocean gateways, including the Bering Strait, the Canadian Arctic Archipelago, the Fram Strait and Isthmus of Panama and their implication in the intensification of the Northern Hemisphere glaciation (iNHG, Sarnthein *et al.*, 2009; Matthiessen *et al.*, 2009).

The Labrador Sea is well located to document past climate and ocean circulation in relation with the Northern Hemisphere glaciation because of its proximity to Greenland and northeast North America, and permits to identify important phases of glacial activity of the Greenland and Laurentide ice sheets through its sedimentary input (Thiede *et al.*, 2011; Andrews and Tedesco, 1992). The Labrador Sea is also a transitional basin between the Baffin Bay and the western North Atlantic (Figure 1),

where winter convection presently accounts for a part in the Atlantic Meridional Overturning Circulation (AMOC, Weaver, 1999, Yashayahev, 2007, Yashayahev *et al.*, 2007). Two main surface currents characterize the Labrador Sea. Along the Greenland margins, the West Greenland Current (WGC) is composed of the warm waters from the North Atlantic Drift (NAD) mixing with cold and arctic waters of the East Greenland Current (ECG). Along the Canadian margins, the Labrador Current (LC) flows southward carrying cold waters from the Arctic via Baffin Bay and the Hudson Strait. Hence, the paleoceanography of the Labrador Sea should permit to document exchanges between the Arctic and the North Atlantic. However, in the Labrador Sea as in many high latitude settings, biostratigraphy and paleoceanographic reconstructions from deep-sea sediments are challenging because of low preservation of biosiliceous and calcareous microfossils (e. g. Baldauf *et al.*, 1989). Hence, in the Neogene sediments of subpolar North Atlantic and North Pacific oceans, organic-walled microfossils such as dinoflagellate cysts (hereafter dinocysts) and acritarchs are very useful to establish biostratigraphical schemes (Louwye *et al.*, 2004; De Schepper and Head, 2008a, 2008b, 2009; De Schepper *et al.*, 2009, 2014, 2017; Dybkjaer and Piasecki, 2010; Verhoeven *et al.*, 2011; Schreck *et al.*, 2012; Zorzi *et al.*, 2019). Since the 1980s, several regional studies across the North Atlantic and the Nordic Seas (Iceland Sea, Norwegian Sea) led to improve the taxonomy of dinocysts and acritarchs (Head, 1993, 1996, 1997; Versteegh and Zevenboom, 1995; Head and Norris, 2003; De Schepper *et al.*, 2004; De Schepper and Head, 2008a, 2014; Schreck *et al.*, 2012; Verhoeven *et al.*, 2014) and to develop well calibrated biozonations that may allow correlations (De Schepper and Head, 2009; Schreck *et al.*, 2012; De Schepper *et al.*, 2017). Moreover, the palaeoecological affinities of extinct Neogene taxa were also explored to better understand the significance of bioevents (De Schepper *et al.*, 2009, 2011; Hennissen *et al.*, 2015, 2017; Schreck *et al.*, 2017).

The number of studies dealing with Neogene dinocysts and acritarchs in the western part of the subpolar North Atlantic remains, however, very low and their spatial coverage is still incomplete. Only a few sites drilled in the northwestern North Atlantic cover the Pliocene. They include the Ocean Drilling Program (ODP) Site 646 off southwest Greenland, Site 647 in the south central Labrador Sea, Site 645 in Baffin Bay and the Integrated Ocean Drilling Program (IODP) sites U1306 and U1307 both located at the southern tip of Greenland on the Eirik Drift in the Labrador Sea (Figure 1) (Baldauf *et al.*, 1989; Channel *et al.*, 2010, Blake-Mizen *et al.*, 2019). In the Labrador Sea, marine palynological studies at the above mentioned ODP sites have led to coarse resolution biostratigraphy of dinocysts and acritarchs encompassing from upper Miocene to Pleistocene (de Vernal and Mudie, 1989; Head *et al.*, 1989). At ODP Site 646, de Vernal and Mudie (1989) defined 5 biostratigraphic zones encompassing the Early Pliocene (~5.4 Ma) to Holocene (0 Ma) based on acmes and the common occurrence of dinocyst and acritarch taxa. The age model was based on calcareous nannofossil biostratigraphy (Knüttel *et al.*, 1989) and magnetostratigraphy (Clement *et al.*, 1989). The dinocyst biostratigraphy of de Vernal and Mudie (1989) deserves to be revisited in the light of the new dinocyst descriptions (cf. above) and because of the low resolution of the initial stratigraphic study. Here, we focus on the nearby and more recently drilled IODP Site U1307 (58°30.3'N; 46°24'W, Figure 1), where a continuously spliced sedimentary sequence has been recovered and a detailed age model was established (Blake-Mizen *et al.*, 2019). The present study has been undertaken to establish a detailed palynostratigraphy covering the Late Pliocene to Early Pleistocene in the Labrador Sea with the double objective of (i) identifying bioevents that may be used for biostratigraphic purpose at large scale and (ii) to pinpoint dinocyst and acritarch assemblage transitions that rather represent regional ecological responses to ocean changes related to the ice sheet growth over Greenland. To do so, we have defined biozones and bioevents which we compare to calibrated

dinocyst and acritarch biostratigraphic schemes from the North Atlantic and Nordic Seas (Head and Norris, 2003; De Schepper and Head, 2008a, 2008b, 2009, 2014; De Schepper *et al.*, 2017).

1.2 Materials and methods

1.2.1 Marine sediments

IODP Site U1307 is located near the southern tip of Greenland ($58^{\circ}30.3'N$; $46^{\circ}24'W$) at a water depth of 2575 meters on the Eirik Drift (Figure 1.1). Two holes (U1307A and U1307B) were drilled, reaching a maximum depth of 162.6 meters below sea floor (mbsf). The composite sequence from the 2 holes yields a complete and an almost continuous section of ~175 meters of Late Pliocene through Holocene sediments.

The lithology has been divided into three units from the top to the bottom (Expedition 303 Scientists, 2006). Unit I (49.55-0 mcd-meters composite depth) consists of predominant silty clay with foraminifers and foraminifer and nannofossil oozes. Unit II (49.55 to 133.86 mcd) consists of almost exclusively silty clay. Unit III (133.86 to 173.6 mcd) consists mainly of silty clay and silty clay with nannofossils oozes and occasional diatom mats. All samples for this study were collected from the lower part of Unit II and Unit III between 116.43 and 172.99 mcd.

1.2.2 Palynological work

Palynological preparation

The 180 samples were prepared in two different laboratories. A total of 126 samples were treated with the standard palynological preparation method of de Vernal *et al.* 1999 and processed at the micropaleontological laboratory of Geotop at UQAM. Samples were first dried and weighed prior to be wet sieved on 10 and 106 µm mesh sieves. One *Lycopodium clavatum* spore tablet (Batch no. 177745, n = 18584 ± 829 spores; no. 124961, n = 12542 ± 931 spores; no. 483216, n = 18583 ± 1708 spores; no. 3862, n = 9666 ± 671 spores per tablet) was added to the remaining 10–106 µm fraction and digested in warm hydrochloric acid (HCl, 10%) to remove carbonate particles. This was followed by a hydrofluoric acid (HF, 49%) treatment to dissolve silicates. Between each step samples were washed with water. Finally, the residues were sieved again on 10 µm mesh sieve. In addition, heavy liquid separation in a solution of sodium polytungstate calibrated for a specific density of 2 was used (Munsterman *et al.*, 1996) was done for the removal of the remaining silicates and heavy minerals. According to Mertens *et al.* (2009), heavy liquid separation does not bias the results. Residues were mounted on microscope slides with glycerin jelly.

The 54 remaining samples were prepared at Palynological Laboratory Services Ltd (Holyhead, UK) and followed the palynological preparation described in De Schepper *et al.* (2017). The samples were dried, weighed and put in a beaker. One *Lycopodium clavatum* spore tablet (Batch no. 483216, n = 18583 ± 1708 spores and no. 124961, n = 12542 ± 931 spores per tablet) was added prior to chemical degradation with cold acids. First HCl (50%) was added followed by adding water and sieving using a 10-µm sieve cloth. The collected residue was returned to the beaker and 100 ml HF (60%) was

added. After dilution with water, the residue was again sieved using a 10- μm sieve cloth. Oxidation or ultrasound was not used. Polyvinyl alcohol (1%) was added to the residue to prevent clumping and some samples were stained with Safranin-O. Residues were mounted on microscope slides with glycerin jelly.

Microscopic analysis and counts

The microscope analyses of 143 samples were done by A. Aubry using a Leica DMR microscope, while 37 samples were counted by S. De Schepper using a Zeiss AxioImager A2 microscope. All counts were done using transmitted light at 400X and 1000X magnification. Dinocyst and acritarch assemblages were the focus of this study but spores, pollen grains, benthic foraminifer linings, freshwater algae and reworked palynomorphs were also enumerated. Reworked palynomorphs were distinguished based on the preservation state and/or their known extinct range. The concentrations of palynomorphs were calculated using the marker grain method of Stockmarr (1971) and are reported as specimens per gram (g) of dry sediment with an approximate error of \pm 10% for a confidence interval of 0.95 (de Vernal *et al.*, 1987; Mertens *et al.*, 2009). The stratigraphic occurrence of selected dinocyst and acritarch taxa is reported in Figure 1.3 with reference to absolute abundance as follows: occasional (< 10 cysts/g), few (10–100 cysts/g), common (100–1000 cysts/g), abundant (> 1000 cysts/g).

The list of taxonomic names and their full authorial citations of taxa encountered in this study is presented in the Supplementary material A. Raw data are available in Supplementary material B.

Taxonomy and nomenclatures

The taxonomic nomenclature follows DINOFLAJ3 database of Williams *et al.* (2017). Some taxa were grouped only into generic categories when identification at species level was equivocal: *Spiniferites/Achomosphaera* spp., *Impagidinium* spp., *Lejeuneocystsa* spp. and *Operculodinium* spp.

The identification of the “round hairy” cysts was not always easy and sometimes it was not possible to distinguish the crucial morphological features of *Filisphaera filifera*, *Filisphaera microornata*, and *Bitectatodinium tepikiense*. This led us to group some specimens as *Filisphaera* spp. or *Filisphaera/Bitectatodinium* indet. when classification to species level was not possible. The subspecies *Filisphaera filifera filifera* and *Filisphaera filifera pilosa* (Head *et al.*, 1993) were grouped as *Filisphaera filifera*. The vermiculate and columellate forms of *Bitectatodinium tepikiense* were identified but grouped as *Bitectatodinium tepikiense*.

1.2.3 Age model, resolution and uncertainties

The age model established in the initial report of the expedition was mainly based on nannofossil and magnetostatigraphic datums (Figure 1.2; Expedition 303 Scientists, 2006; Channell *et al.*, 2010). Later measurements in planktonic foraminifera (*Neogloboquadrina atlantica*) from 117.64 to 173.32 mcd and correlation with the LR04 benthic foraminiferal $\delta^{18}\text{O}$ stack of Lisiecki and Raymo (2005) led Sarnthein *et al.* (2009) to propose another age model. Hence, there were two different age models for the interval spanning from 2.6 to 3.6 Ma, both relying on the shipboard magnetostratigraphy and biostratigraphy (Expedition 303 Scientists, 2006; Channell *et al.*, 2010). The age models differed in the identification of the Kaena and Mammoth magnetic events and in the position of the pronounced cold Marine Isotopic Stage (MIS) M2 in the $\delta^{18}\text{O}$ record (Figure 1.2). Sarnthein *et al.* (2009) also used the highest occurrence (HO) of two dinocyst species, *Operculodinium? eirikianum* and *Barssidinium pliocenicum*, as tie points for the isotopic stratigraphy at \sim 3.3 Ma. However, the HOs of these species have been shown to be asynchronous in the North Atlantic and the Nordic Seas (De Schepper *et al.*, 2015, 2017) and the age of 3.3 Ma based on correlation with the discontinuous ODP Hole 646B sequence (de Vernal and Mudie, 1989; Clement *et al.*, 1989) was not warranted. Further uncertainty about using these dinocyst events is the resolution of the shipboard palynological analyses for Site U1307. As the onboard analyses were done in core catcher sediments, the intervals between samples was at least 10 m (Expedition 303 Scientists, 2006; Channell *et al.*, 2010).

Recently, Blake-Mizen *et al.* (2019) published a new high-resolution magnetic susceptibility record and proposed a revised chronostratigraphy for IODP Site U1307.

Their age model spans the last ~3.2 Myrs and is based on magnetostratigraphic reversals and the relative paleointensity (RPI), which was tuned to the RPI of IODP Site U1308 (Channell *et al.*, 2016). The lowest paleomagnetic reversal is identified to be the top the Mammoth subchron (3.20 Ma) and not the Gauss/Gilbert reversal (3.58 Ma) as previously thought (Expedition 303 Scientists, 2006; Sarnthein *et al.*, 2009; Channell *et al.*, 2010). The revised chronostratigraphy for Site U1307 permits a better correlation of the $\delta^{18}\text{O}$ record by Sarnthein *et al.* (2009) with LR04 (Figure 1.2).

For this study, we used the new IODP U1307 splice and age model (Table 1.1) established by Blake-Mizen *et al.* (2019), which is continuous for an interval encompassing the Late Pliocene to Holocene. For each of our samples, we converted meters below sea floor (mbsf) in Holes U1307A and U1307B to revised meters composite depth (rmcd) according to the splice of Blake-Mizen *et al.* (2019). We calculated the age for each sample based on linear interpolations between their age model tie points (Table 1.1).

The error of paleomagnetic reversal age corresponds to half the age difference between the two samples that record the reversal (Weaver and Clement, 1987). In IODP Site U1307 cores, the extent of the reversals varied from 32 to 77 cm with an average of 48 cm. Considering an average sedimentation rate of ~6 cm/kyr (Blake-Mizen *et al.*, 2019) the error ranges from 5.3 to 12.8 kyr. The sampling resolution also affects the accuracy of the highest occurrence (HO) and lowest occurrence (LO) because the real disappearances and appearances may occur anywhere between the analyzed samples (see Versteegh, 1997). We analyzed a total of 180 sediment samples between 116.43 and 175.11 rmcd, with a sample spacing varying between 1 to 400 cm (average 33 cm). This corresponds to a time resolution of 0.1 to 30 kyr (average 5.5 kyr), which thus applies to the error in the timing of HO and LO.

I.1.4 Origin of particles (dinocysts and acritarchs)

Lateral particle transport can be relatively high in the Labrador Sea due to the surface currents (EGC) and deep circulation (Western Boundary Under Current -WBUC; Nootenboom *et al.*, 2019). Based on high-resolution sedimentological records, Blake-Mizen *et al.* (2019) inferred that bottom current dominated depositional processes at IODP Site U1307 before ~2.9 Ma. A sedimentary change recorded between 2.9 and 2.7 Ma was interpreted as a change in the depth of the flow path of the WBUC relative to the site (Blake-Mizen *et al.*, 2019). Although assessment on the strength of the WBUC remains equivocal, the change in sedimentary regime implies possibly variation in lateral transport from ~2.9-2.7 Ma. Hence, taphonomical processes cannot be discarded as an important factor of the palynological signal at our study site as elsewhere in the ocean (Nootenboom *et al.*, 2019). As lateral transport would follow the route of the EGC and WBUC, upstream origin of small size particles is possible and our record could represent fluxes from along the southern or southeastern Greenland margins (see also planktondrift.org).

1.3 Results

1.3.1 General

In the 180 analyzed samples, organic palynomorphs are well preserved. Dinocysts and acritarchs dominate the palynomorph assemblages but freshwater algae, pollen grains and spores, and reworked marine and terrestrial palynomorphs are also common. Dinocysts occur in all samples and only 3 samples contain less than 10 cysts per slide. Two samples have been discarded because of mislabeling (#13C316 and #13C317). Concentrations range from 27 to 3126 cysts/g dry sediment with an average of 442 cysts/g dry sediment. Acritarch concentrations are higher with an average of 1352 acritarchs/g dry sediment and maximum value of 8975 acritarchs/g dry sediment. Terrestrial palynomorphs (pollen and spores) are less abundant. Among samples analyzed, 10 yielded less than 10 terrestrial palynomorphs per slides. They are nevertheless common with concentrations ranging up to 1209 palynomorphs/g dry sediment (average of 262 palynomorphs/g dry sediment). Freshwater algae occur occasionally, with maximum value of 106 algae/g dry sediment and an average of 11 algae/g dry sediment.

The number of dinocyst species is high with 115 taxa identified, among which 43 are extinct. The number of taxa ranges from 4 to 26 per sample with an average of 14. The two most dominant taxa are *Operculodinium centrocarpum* sensu Wall and Dale (1966) (*Operculodinium centrocarpum* hereafter) and the round brown cysts group. Round brown cysts combine all sub-spherical brown protoperidinoid cysts without processes and with or without a visible archeopyle (for example they include all cysts

of *Brigantedinium*). In addition, the other dominant taxa are *Nematosphaeropsis labyrinthus*, *Impagidinium aculeatum*, *Habibacysta tectata*, *Filisphaera filifera*, *Impagidinium pallidum*, *Filisphaera microornata*, cysts of *Pentapharsodinium dalei*, *Spiniferites/Achromosphaera* spp., *Bitectatodinium tepikiense* and *Impagidinium paradoxum*.

Acritarchs dominate the marine assemblages with up to 96 percent and an average of 63%. A total of 24 taxa were recorded. Common to abundant species include *Cymatiosphaera? invaginata*, *Cymatiosphaera? fensomei*, *Cymatiosphaera? aegirii*, *Cymatiosphaera? icenorum*, *Lavradosphaera crista* and *Lavradosphaera canalis*. Sphaeromorph acritarchs are also abundant and globally correspond to discoidal to spherical forms as illustrated in Schreck *et al.* (2013).

1.3.2 Age calibration of selected bioevents

We have identified biostratigraphic events as described in De Schepper and Head (2008b). The highest occurrence (HO) is the last sample with the presence of a given taxon and, conversely, the lowest occurrence (LO) is the first sample with the occurrence of a taxa. The highest persistent occurrence (HPO) is the highest successive occurrence of a species, even in low abundance, and sporadic occurrence after the HPO might be reworked specimens. The highest common occurrence (HCO) is the highest notable and abundant occurrence of a taxon, which can still occur higher up in the record but then in lower numbers.

Calibrated ages for dinocyst and acritarch HO, LO, HPO and HCO are summarized in Table 1.2. Standard zonations of calcareous nannofossils (Martini, 1971), planktonic foraminifers (Berggren *et al.* 1985, 1995) and diatoms (Baldauf 1987, Baldauf *et al.*, 1989) are used for correlation (see also Hilgen *et al.*, 2012), as well as the ATNTS2012 for polarity and chron (Ogg, 2012).

1.3.3 Biostratigraphy and biozonation

Our Labrador Sea biozonation is the first high resolution biostratigraphy of the Neogene to Quaternary for the Labrador Sea. It has been made to better document the biostratigraphy of the Plio-Pleistocene transition in this region in order to lay foundations for future regional and supra-regional correlations with other records from the North Atlantic and Arctic oceans. It has been suggested that bioevents recorded during the Neogene-Quaternary primarily represent a response to ecological stresses due to climatic changes rather than being evolutionary features (De Schepper and Head, 2008b; 2013 Schreck *et al.*, 2012; De Schepper *et al.* 2015). However, some dinocysts and acritarchs have stratigraphically well-defined ranges. This is the case for *Habibacysta tectata* and *Filisphaera filifera*, which have been used for supra-regional stratigraphic correlation between the Arctic Ocean and adjacent basins (Matthiessen *et al.*, 2018), and the acritarch genus *Lavradosphaera* and *Cymatiosphaera* that also seems to have a stratigraphical range allowing correlations at mid- to high latitudes of the Northern Hemisphere (De Schepper and Head, 2004; this study).

The biozonation we developed here follows the nomenclature of the “International Stratigraphic Guide” (abridge version of Murphy and Salvador, 1999). Accordingly, the zones are defined as assemblage (LS1, LS3) and abundance (acme) biozones (LS2).

Zone boundaries are defined from bioevents, which occur almost synchronously across the high latitude North Atlantic including the Labrador Sea. These bioevents include the HO of *Barssidinium graminosum* and the acme of *Pyxidinopsis braboi* (Figure 1.3, 1.4; Table 1.2). Most dinocyst and acritarch taxa used as stratigraphic markers in the study are illustrated in the Supplementary Plate 1 and Plate 2. The biozones have been given informal names (LS1 to LS3) in reference to the location of IODP Site U1307 in the Labrador Sea. Dinocyst and acritarch taxa in each zone are described based on their relative abundances: rare (1-3%), frequent (3-10%), common (10-30%), abundant (30-50%) and dominant (>50%).

LS 1 *Barssidinium graminosum* Assemblage Zone

Definition: This zone is characterized by the association of almost continuous occurrence of *Barssidinium graminosum*, *Lavradosphaera crista* and *Corrudinium harlandii*. It spans from the base of the studied interval to the HO of *Barssidinium graminosum*.

Other bioevents: *Operculodinium?* *eirikianum eirikianum* and *Operculodinium?* *eirikianum crebrum* have limited occurrences restricted from the base of the zone to 167.61 rmcd and 169.63 rmcd respectively.

At the top of zone LS1, the HPO of *Lavradosphaera crista* occurs at 130.00 rmcd. Near the top of zone LS1, the HPO of *Lejeuneacysta hatterasensis* occurs between 134.15

and 130.80 rmcd, an acme of the acritarch *Cymatiosphaera? fensomei* occurs at 136.80–130.80 rmcd and the HCO of *Lavradosphaera canalis* occurs at ~130.00 rmcd. The lowest common occurrence of *Lavradosphaera canalis* occurs at 136.50 rmcd.

Reference section: Samples U1307A-19H07-28-30 cm to U1307B-14H03-30-32 cm or 175.11 to 130.00 rmcd.

Age: Late Pliocene, from >3.21 to 2.75 Ma.

Calibration: calcareous nannofossil zone NN16, planktonic foraminifer zone N20-21, *Nitzschia jouseae* diatom zone and correspond to subchron C2An.2n, C2An.1r and C2An.1n.

Correlation: The top zone LS1 coincides with the top of *Invertocysta lacrymosa* Interval Zone or RT5 zone at DSDP 610A placed at 2.74 Ma (De Schepper *et al.*, 2008b).

Dinocyst association: Dominant to rare round brown cysts, *Operculodinium centrocarpum*, *Filisphaera filifera* and *Nematosphaeropsis labyrinthus*. Abundant to rare *Impagidinium aculeatum* and *Habibacysta tectata*. Common to rare *Impagidinium paradoxum*, *Spiniferites/Achomosphaera* spp., *Bitectatodinium tepikiense/Filisphaera microornata*, *Impagidinium pallidum*, *Pyxidinopsis braboi* and cysts of *Pentapharsodinium dalei*. Rare *Impagidinium* sp. 2 of De Schepper and Head, 2009 and *Corrudinium? labradori*.

Acritharch association: Dominant to abundant *Cymatiosphaera? invaginata*. Dominant to common *Lavradosphaera crista*. Abundant to rare *Cymatiosphaera? fensomei*. Common to rare *Cymatiosphaera? aegirii*. Frequent to rare *Cymatiosphaera? icernorum*. Rare *Cymatiosphaera latisepta*.

LS 2 *Pyxidinopsis braboi* Abundance Zone

Definition: The body of strata from the HO of *Barssidinium graminosum* to the top of the acme of *Pyxidinopsis braboi*.

Other events: The HPO of *Lavradosphaera canalis* (124.71 rmcd) occurs near the top of the zone.

Reference section: Samples U1307B-14H03-28-30 cm to U1307A 14H03-120-122 cm, or from 130.00 to 124.51 rmcd.

Age: Late Pliocene to early Pleistocene, from 2.75 to 2.57 Ma.

Calibration: upper calcareous nannofossil zone NN16, planktonic foraminifer zone N20-21, upper *Nitzschia jouseae* diatom zone and uppermost part of subchron C2An.1n to C2r.2r. The top of the zone broadly corresponds to the Matuyama/Gauss reversal and the Plio/Pleistocene boundary.

Correlation: Zone LS2 correlates well with zone RT6 at DSDP Hole 610A of De Schepper and Head (2009) in eastern North Atlantic. The HO of *Barssidinium graminosum* defines the base of zone RT6, which is placed at 2.74–2.69 Ma. The *Pyxidinopsis braboi* acme was missed by De Schepper and Head (2009) probably because of a 2.1 m sample gap between 126.37 and 128.47 mbsf. Hennissen *et al.* (2014) covered this interval in more detail and recorded the *Pyxidinopsis braboi* acme between 127.55 and 128.21 mbsf (2.59–2.61 Ma, corresponding to MIS 104), at the boundary between zones RT6 and RT7 as defined by De Schepper and Head (2009).

Dinocyst association: Dominant to rare round brown cysts, *Operculodinium centrocarpum*. Abundant to rare *Impagidinium aculeatum* and *Habibacysta tectata*. Common to rare *Impagidinium pallidum*, *Nematosphaeropsis labyrinthus*, *Impagidinium paradoxum*, *Spiniferites/Achomosphaera*, *Bitectatodinium tepikiense* and *Filisphaera microornata*. Rare *Corrudinium?*

labradori and *Impagidinium* sp. 2 of De Schepper and Head, 2009.

Aceritarch association: Dominant to frequent *Cymatiosphaera? invaginata*. Dominant to rare *Cymatiosphaera? aegirii*. Frequent to rare *Lavradosphaera canalis*. Rare and sporadic *Cymatiosphaera? fensomei* and *Cymatiosphaera? icenorum*.

LS 3 *Habibacysta tectata* Assemblage Zone

Definition: The body strata from the acme of *Pyxidinopsis braboi* to the top of the studied interval. The zone is characterized by the association of *Habibacysta tectata*, *Filisphaera filifera* and *Filisphaera microornata* and *Bitectatodinium tepikiense*.

Other events: HPOs of *Cymatiosphaera? aegirii* (120.85 rmcd) and *Impagidinium* sp. 2 of De Schepper and Head 2009 (122.41 rmcd).

Reference section: Samples U1307A 14H03-120-122 cm to U1307B-13H01-60-62 cm, or from 124.51 to 116.43 rmcd.

Age: early Pleistocene, from 2.57 to 2.23 Ma.

Calibration: calcareous nannofossil zone NN17 and NN18, planktonic foraminifer zone N20-21, latest *Nitzschia jouseae* and *Nitzschia marina* diatom zone and subchron C2r.2r. The base of the zone broadly corresponds to the Matuyama/Gauss reversal and the Plio/Pleistocene boundary.

Correlation: Precise correlation with the eastern North Atlantic zonation is difficult, but the dinocyst association of zone LS3 shows great similarities with zone RT7 characterized by *Habibacysta tectata* (De Schepper and Head, 2009; Hennissen *et al.* 2014).

Dinocyst association: Dominant to rare round brown cysts. Sporadic occurrence peaks of *Pyxidinopsis braboi*. Abundant to rare *Impagidinium aculeatum*, *Spiniferites/Achomosphaera*, *Bitectatodinium tepikiense*, *Habibacysta tectata*, *Nematosphaeropsis labyrinthus* and *Filisphaera microornata*. Common to rare *Impagidinium paradoxum*, *Impagidinium pallidum*, *Filisphaera filifera*. Frequent to rare *Operculodinium centrocarpum*.

Aceritarch association: Dominant to frequent *Cymatiosphaera? invaginata*. Dominant to rare *Cymatiosphaera? aegirii*. Rare and sporadic *Cymatiosphaera? fensomei*. Rare *Cymatiosphaera? icenorum*

1.4 Discussion

1.4.1 Comparison with previously established zonation at the nearby ODP Hole 646

We analyzed 180 samples from Late Pliocene to Early Pleistocene at intervals ranging between 1 and 400 cm (0.1 and 30 kyr). Our study focused on the Plio/Pleistocene transition and was made with considerably higher temporal resolution than that of de Vernal and Mudie (1989), who investigated 155 samples at 1.5 m interval in the Pliocene to Holocene sediments recovered at ODP Hole 646B. The pioneering work of de Vernal and Mudie (1989) identified a rich palynological assemblage, including several new taxa characteristic of the Pliocene that were left in open nomenclature. The knowledge of the North Atlantic Neogene dinocyst and acritarchs has improved considerably over the last two decades as several new taxa were described (Head, 1993, 1996, 1997; Versteegh and Zevenboom, 1995; Head and Norris, 2003; De Schepper *et al.*, 2004; De Schepper and Head, 2008a, 2014; Schreck *et al.*, 2012; Verhoeven *et al.*, 2014). Using the state-of-the-art taxonomy, we identified 115 dinocyst and 24 acritarch taxa at Site U1307, which represents a much higher species diversity than the one reported by de Vernal and Mudie (1989) who reported ~51 dinocyst and ~8 acritarch taxa at ODP Hole 646B.

De Vernal and Mudie (1989) defined 5 intervals: The interval V (~5.4-4.8 Ma) is based on the occurrence of the dominant taxa: *Brigantedinium* spp., *Nematosphaeropsis labyrinthus* (as *Nematosphaeropsis labyrinthea*), *Filisphaera filifera*, *Cymatiosphaera? invaginata* (as *Cymatiosphaera* sp. I) and *Batiacasphaera sphaerica*; Interval IV (~4.8-4.0 Ma) is defined by the stratigraphic range and abundance of cyst

type 1; Intervall III (4-2.3 Ma) is distinguished by the common-to-abundant occurrence of *Lavradosphaera crista* (as Incertae sedis I). The base of Interval II (~2.36~1.23 Ma) corresponds to the common occurrence of *Cymatiosphaera latisepta* (as *Nematosphaeropsis* sp. I) and *Pyxidinopsis braboi* (as *Tectatodinium* sp. II), and the top corresponds to the HOs of *Filisphaera filifera* and *Cymatiosphaera? invaginata*. Finally, Interval I (~1.2-0 Ma) is characterized by modern dinocyst species common in the Labrador Sea such as *Operculodinium centrocarpum*, *Nematosphaeropsis labyrinthus* and *Brigantedinium* spp.

The comparison of the biostratigraphical schemes is hampered by the temporal resolution and the definition of the biozones and their boundaries in the different studies. While de Vernal and Mudie (1989) defined biozones using abundances of dinocyst and acritarch, we used bioevents such as HOs and acme to define our biozone limits. Nevertheless, our zones LS1, LS2 and most part of LS3 correspond generally to Interval III of de Vernal and Mudie (1989) (Figure 1.4). Their Interval III is characterized by common to abundant occurrence of *Lavradosphaera crista* and the top of this interval correspond to the last record of this acritarch in IODP Site U1307 at 2.38 Ma. Interval III is also defined by the dominance of the acritarchs *Cymatiosphaera? invaginata* and *Lavradosphaera crista* accompanied with the dinocysts *Brigantedinium* spp., *Filisphaera filifera*, *Nematosphaeropsis labyrinthus* and *Operculodinium centrocarpum*. We also identified these species throughout our study interval at IODP Site U1307 as an important part in the dinocyst assemblage. However, the lower part of Interval III does not have overlap with our biozonation. It is characterized by the last common occurrence of *Operculodinium? eirikianum* (as *Operculodinium longispinigerum* in de Vernal and Mudie, 1989). At IODP Site U1307, both subspecies *Operculodinium? eirikianum* var. *crebrum* and *Operculodinium? eirikianum* var. *eirikianum* occur at the base of zone LS1, which thus extend their stratigraphic range in the Labrador Sea.

The uppermost part of zone LS3 corresponds to the lowest part of Interval II (Figure 1.4). The base of Interval II was defined based on common occurrence of *Cymatiosphaera latisepa* (as *Nematosphaeropsis* sp. I in de Vernal and Mudie, 1989) and *Pyxidinopsis braboi* of which the end of the acme marked the base of zone LS3.

1.4.2 Comparison with the North Atlantic Ocean and the adjacent seas

Restricted time resolution

The comparison of our new dinocyst and acritarch zonation for the Labrador Sea with the palynostratigraphy of other regions is difficult. The time interval and resolution of the biostratigraphic record differs from site to site and our study interval (3.2-2.2 Ma) is often poorly represented in previously published zonations (see Figure 1.4). Our study interval is situated in the *Melitasphaeridium choanophorum* zone of William and Bujak (1977) from offshore eastern Canada, Zone III of Harland (1979) defined from DSDP 400 in Bay of Biscay, Zone II of Mudie (1987) at DSDP Sites 607 and 611 in the North Atlantic, and in the PMS *Filisphaera filifera* acme zone at ODP Sites 642/643/644 in the Norwegian Sea (Mudie, 1989). Only two studies reporting data with a temporal resolution highlighting boundaries within our studied time interval allow a comparison with our record: one is from the Danish North Sea onshore-offshore well section compilation of Dybkjaer and Piasecki (2010) and the other is from the North Atlantic DSDP Hole 610A (De Schepper and Head, 2009) (Figure &4).

Absence of Pliocene stratigraphic marker species in the Labrador Sea

Despite the relatively high temporal resolution of our analyses, the occurrence of indicator taxa used in the Neogene biostratigraphy of the North Atlantic is rare and discontinuous. The indicator taxa include *Impagidinium solidum*, *Ataxiodinium confusum* and *Invertocysta lacrymosa*, which occur occasionally making them unsuitable for robust biostratigraphic assessment at IODP Site U1307 (see Figure 1.4).

The top of zone RT4 in the North Atlantic DSDP Hole 610A is defined by the HO of *Impagidinium solidum* at 3.25 Ma (De Schepper *et al.*, 2009). This species, which has not been recorded in the Labrador Sea by de Vernal and Mudie (1989), is identified only in two samples as single occurrences in our study (Figure 1.3, 1.4). *Ataxiodinium confusum* seems to disappear at the end of the Pliocene around 2.6 Ma across the North Atlantic (De Schepper and Head, 2008b, 2009; Hennissen *et al.*, 2014). In our Labrador Sea record, *Ataxiodinium confusum* has three single occurrences before 2.75 Ma (Figure & 4). The HO of *Invertocysta lacrymosa* that characterizes the top of zone RT5 at DSDP Hole 610A (2.72 Ma; De Schepper *et al.*, 2009) seems to be a widespread bioevent during the iNHG across the mid latitudes in the North Atlantic Ocean: in the Gulf of Biscay it occurred at 2.84 Ma (Harland, 1979), in the central north Atlantic site DSDP 607/607A and the Singa section southern Italy at 2.74 Ma (Versteegh, 1997), in the western North Atlantic DSDP Hole 603C at 2.81 Ma (M.J. Head unpublished data in De Schepper and Head, 2008b), in Hole U1313C at 2.74 Ma (Hennissen *et al.*, 2014). Its HO occurs around 2.79 Ma at IODP Site U1307, which is consistent with other North Atlantic records, but a single specimen was only found in three samples.

Other taxa that could be used as stratigraphical markers are conspicuously present in our study interval and have a continuous range of occurrence with marked HOs. These taxa include *Barssidinium graminosum*, *Lavradosphaera crista* and *Lavradosphaera*

canalis (Figure 1.3, 1.4 and 1.5). *Barssidinium* species are used in both biostratigraphical schemes of the Danish North Sea onshore-offshore well section compilation of Dybkjaer and Piasecki (2010) and of the North Atlantic DSDP Hole 610A of De Schepper and Head (2009). In the scheme of Dybkjaer and Piasecki (2010) the boundary between the *Barssidinium pliocenicum* zone and the *Impletosphaerodinium multiplexum* zone, defined at 2.4–2.6 Ma, encompasses our LS2/LS3 limit at 2.57 Ma (Figure 1.4). This boundary is based on the HO of *Barssidinium pliocenicum*, and the LO of *Impletosphaerodinium multiplexum* followed by the LO of *Bitectatodinium tepikiense*. At IODP Site U1307, *Impletosphaerodinium multiplexum* is not recorded; *Bitectatodinium tepikiense* is common throughout the interval studied (3.2–2.2 Ma) but *Barssidinium pliocenicum* is found until 2.66 Ma (Figure 1.3). Specimens of *Barssidinium pliocenicum* were identified in younger sediments of southwest England (~ 2.1–1.95 Ma; Head, 1993), the North Sea (2.4–1.8 Ma; Head *et al.*, 2004), ODP Site 986 on the Svalbard-Barents shelf (up to 2.17 Ma; Smelror, 1999; Knies *et al.*, 2009) and northern Iceland (>2 Ma; Verhoeven *et al.*, 2011 and references therein). At other North Atlantic sites, the HO of *Barssidinium pliocenicum* is older. It occurs around 2.75 Ma in ODP Hole 603C (M.J. Head unpublished) and around 2.72 Ma at DSDP Hole 610A (De Schepper, 2006). The HO of *Barssidinium pliocenicum* seems therefore diachronous across the North Atlantic. On the contrary, the HO of *Barssidinium graminosum* that we use to define the top of zone LS1 seems to occur simultaneously in the Labrador Sea (2.75 Ma), the western North Atlantic (DSDP Hole 603C, ~2.76–2.77, M.J. Head unpublished) and the eastern North Atlantic (DSDP Hole 610A, 2.74 Ma, De Schepper *et al.*, 2008b) (Figure 1.4).

Regional paleoceanographic conditions overprinting the biostratigraphy

While most sites used to establish a late Neogene stratigraphical schemes are under the influence of warm North Atlantic waters, IODP Site U1307 is situated in the path of the East Greenland Current, which carries relatively fresh and cool waters (Figure 1.1). Hence, the ocean circulation and distribution of water masses may have played an important role in the geographical occurrences of Neogene species such as *Impagidinium solidum*, *Ataxiodinium confusum*, *Invertocysta lacrymosa* and *Melitasphaeridinium choanophorum*, thus causing asynchronous events and hampering the biostratigraphic correlations throughout the Labrador Sea and North Atlantic.

Impagidinium solidum and *Ataxiodinium confusum* have preference for warmer waters (De Schepper *et al.*, 2011; Hennissen *et al.*, 2017) and their low abundance during the Late Pliocene in the Labrador Sea may indicate cooler waters than those in the eastern North Atlantic, where they persisted longer. In the Norwegian Sea, De Schepper *et al.* (2017) also found rare occurrences of *Impagidinium solidum* but restricted to the early Pliocene until 3.59 Ma. We may thus suggest a strong diachronism between the Norwegian Sea, the North Atlantic and the Labrador Sea. Hennissen *et al.* (2017) interpreted *Invertocysta lacrymosa* as a warm water species typical of open oceanic condition. Again, the low occurrences of *Invertocysta lacrymosa* in the Labrador Sea and its earlier HOs in the Norwegian Sea (3.27 Ma, De Schepper *et al.*, 2017) and Iceland Sea (4.45 Ma, Schreck *et al.*, 2012) during early Pliocene are concordant with conditions in the northern part of the North Atlantic Ocean cooler than at middle latitudes.

The low occurrence of *Melitasphaeridinium choanophorum* in only two samples before 2.29 Ma at our study site contrasts with the persistent, rare to common record in DSDP Hole 610A until 2.98 Ma (De Schepper, 2006). The occurrence of *Melitasphaeridinium*

choanophorum in the western North Atlantic in DSDP Hole 603C through the Pliocene and early Pleistocene (M.J. Head unpublished in De Schepper *et al.*, 2017), on the Scotian Shelf-Grand Banks in the Pliocene and the late Gelasian (Williams and Bujak, 1977) and even in recent sediments of the Gulf of Mexico (Limoges *et al.*, 2013, 2014; Price *et al.*, 2017) indicate a more extended range than previously thought and affinities for subtropical conditions. This species is considered typical of the Pliocene across the North Atlantic Ocean (Williams and Bujak, 1977; De Schepper and Head 2009; Dybkjaer and Piasecki, 2010; De Schepper *et al.*, 2017). Its diachronous disappearance from the North Atlantic and persistence in the Gulf of Mexico may reflect southward migration associated with cooling and the intensification of glaciation during the Quaternary.

At DSDP 610A, the top of zone RT6 dated at 2.62 Ma corresponds to the HO of *Operculodinium?* *eirikianum* var. *eirikianum*. However, at IODP Site U1307 both subspecies *Operculodinium?* *eirikianum* var. *eirikianum* and *Operculodinium?* *eirikianum* var. *crebrum* are restricted to the beginning of zone LS1 with HOs around 3.18-3.16 Ma. *Operculodinium?* *eirikianum* is a cool-intolerant species that prefers warmer waters (De Schepper *et al.*, 2015; Hennissen *et al.*, 2017). During the early Pliocene, this taxon disappeared from the Iceland Sea records, which is interpreted to result from regional cooling due to changes in oceanic gateway configuration at the onset of the modern circulation in the Nordics Seas and deep ocean circulation in the North Atlantic (De Schepper *et al.*, 2015). Thus, the *Operculodium?* *eirikianum* HOs highlight an asynchronous disappearance across the North Atlantic, the Nordic Seas and the Labrador Sea, possible due to regional changes and reorganization of ocean circulation.

At IODP Site U1307, we noticed low abundance but recurring occurrence of *Corrudinium harlandii* until 2.76 Ma. This species is considered extinct, but it shares

morphological similarities with the modern taxon *Pyxidinopsis reticulata*, notably in the expression of crests. A morphological gradation between the two taxa was reported to occur in DSDP Hole 610A (De Schepper and Head, 2009) with typical *Corrudinium harlandii* being more frequent during the Pliocene and typical *Pyxidinopsis reticulata* extending to the Pleistocene. It is thus possible that *Corrudinium harlandii* and *Pyxidinopsis reticulata* represent a morphological gradation of a same genotype that evolved naturally or in response to changing environmental conditions. In modern sediments, *Pyxidinopsis reticulata* is found from equatorial to subpolar waters but with a preference for temperate conditions in the Pacific Ocean (de Vernal and Marret, 2007; de Vernal *et al.*, 2019). The rare and low occurrence of this taxa in the Labrador Sea is consistent with cool conditions. Although no paleoecological affinity is known for *Corrudinium harlandii*, the rare and low occurrence of transitional morphotypes suggests distinct conditions in the Labrador Sea compared to the eastern North Atlantic.

Finally, in the Labrador Sea, we defined the top of zone LS2 at 2.57 Ma based on the end of the acme of *Pyxidinopsis braboi*, which is recorded in DSDP Hole 610A at ~2.58 Ma, during MIS 104 (Hennissen *et al.*, 2014). *Pyxidinopsis braboi* is also found in low numbers in sediment of MIS 104 at IODP Hole U1313C (~2.61-2.59 Ma; Hennissen *et al.*, 2014). This species is interpreted as a cold-polar, opportunistic taxa (Warny *et al.*, 2009; Hennissen *et al.*, 2014, 2017) and its acme is suggested to result from the Arctic Front moving south, close to the DSDP Hole 610A position in the North Atlantic at the Plio/Pleistocene boundary (Hennissen *et al.*, 2014, 2017). Thus, its acme at IODP Site U1307 may provide evidence for increasingly cool and freshwater transport via the EGC into the Labrador Sea at the Plio/Pleistocene transition. However, there are several samples above the Plio-Pleistocene transition that record very few dinocysts, clearly indicating changes in environmental conditions, which may have blurred the stratigraphic range of the different taxa (see Supplement B).

1.4.3 Paleoceanographic and paleoclimatic implications

In general, the transitions in the dinocyst and acritarch records, which led us to define stratigraphic zones and bioevents at IODP Site U1307, seem to reflect regional cooling phases. These could be related to the EGC strengthening and the development of the Greenland ice sheet during the Plio-Pleistocene transition.

Among common taxa recorded at IODP Site U1307, *Operculodinium centrocarpum* sensu Wall and Dale 1966 is a cosmopolitan modern species particularly abundant in the path of the North Atlantic Current (NAC) (Rochon *et al.*, 1999). In the Plio-Pleistocene sediments of the North Atlantic and the Nordic Seas, this species was interpreted to indicate (warmer) Atlantic waters (De Schepper *et al.*, 2009, 2013; Hennissen, 2013; Hennissen *et al.*, 2014, 2017). The dominance of this species in zone LS1 and the lower half of zone LS2 (Figure 1.4) suggest Atlantic water inflow into the Labrador Sea possibly through the Irminger Current until about 2.65 Ma. At the base of zone LS1, the common occurrence of both *Operculodinium?* *eirikianum* var. *eirikianum* and *Operculodinium?* *eirikianum* var. *crebrum* suggest warm conditions. *Operculodinium?* *eirikianum* was reported as a cool-intolerant species by Hennissen *et al.* (2017). In the Iceland Sea the disappearance of this species in the Early Pliocene was associated with the establishment of the proto-EGC, whereas its continued presence in the Late Pliocene (< 3 Ma) Norwegian Sea reflects the continued influence of Atlantic water there (De Schepper *et al.* 2015). *Operculodinium?* *eirikianum* var. *crebrum* has also been linked to warm, stable conditions following MIS M2 (De Schepper *et al.* 2014). Hence, at IODP Site U1307, the occurrence of both subspecies of *Operculodinium?* *eirikianum* at the base of LS1 (Figure 1.4, Table 1.2) suggest relatively warm, Atlantic water influenced sea surface conditions before 3.1 Ma.

At about 2.75 Ma, several dinocyst and acritarch taxa have HO, HPO or HCOs at IODP Site U1307 (Figure 1.4, Table 1.2). Among the taxa, *Impagidinium solidum*, *Ataxiodinium confusum* and *Invertocysta lacrymosa* are Pliocene markers. Their disappearance suggests a regional cooling contemporaneous with the onset of persistent ice-rafted deposition at ~ 2.72 Ma in response to major expansion of the Greenland ice sheet (Blake-Mizen *et al.*, 2019). Subsequently, between 2.65 and 2.57 Ma, we record the acme of *Pyxidinopsis braboi* at Site U1307 as well as at the eastern North Atlantic DSDP Hole 610A (Hennissen *et al.*, 2014). *Pyxidinopsis braboi* is interpreted as a cold-polar, opportunistic taxa and its acme suggests the proximity of the Arctic Front (Warny *et al.*, 2009; Hennissen *et al.*, 2014, 2017). After 2.57 Ma, zone LS3 is characterized by the occurrence of typical late Neogene cool-water species such as *Habibacysta tectata*, *Filisphaera microornata* and *Filisphaera filifera*. These disappeared from the North Atlantic, the Nordic Seas, the Arctic and the North Pacific oceans during the early Pleistocene after 2.0 Ma (Matthiessen *et al.*, 2018). *Filisphaera filifera*, *Filisphaera microornata* and *Habibacysta tectata* are considered cool-tolerant (De Schepper *et al.*, 2011; Hennissen *et al.*, 2017; Schreck *et al.*, 2017). In the Arctic Ocean, their acme has been associated with inflow of North Atlantic waters (Matthiessen *et al.*, 2018). However, at North Atlantic DSDP Site 610, high abundance of *Filisphaera filifera* characterized the cold MIS M2 (3.26–3.31 Ma; De Schepper *et al.*, 2009), whereas *Habibacysta tectata* dominated the Early Pleistocene (2.57–2.20 Ma) assemblages and was associated with reduced influence of Atlantic waters and a southward shift of the NAC (De Schepper *et al.* 2009; Hennissen *et al.*, 2014). At IODP Site U1307, the increased occurrence of *Habibacysta tectata* is concomitant with minima of *Operculodinium centrocarpum* percentages after 2.65 Ma, which could be attributed to further surface water cooling.

1.4.4 The use of the acritarchs in marine palynostratigraphy across the Plio-Pleistocene transition

Compared to dinocysts, acritarchs are extremely abundant and have a continuous range of occurrence in the Labrador Sea throughout the entire study interval (Figures 1.3 and 5). Common taxa from IODP Site U1307 also occurred at other sites from the North Atlantic (De Schepper and Head, 2014) making potential correlation possible between the North Atlantic and the Labrador Sea during the Late Pliocene.

De Vernal and Mudie (1989) defined biostratigraphic Interval II in ODP Hole 646B based on the common to abundant occurrence of *Lavradosphaera crista* (as *Incertae sedis* I) until ~2.3 Ma, which broadly corresponds to the last appearance of this species at IODP Site U1307, where it is dated of 2.38 Ma. The three single occurrences above the HPO at 2.75 Ma may represent reworking (Figure 1.5). *Lavradosphaera crista* is extremely abundant in middle Late Pliocene of the North Atlantic with an HPO between 3.05 and 2.91 Ma at DSDP Sites 603, 610 and IODP Site U1308 (De Schepper and Head, 2014). The record of *Lavradosphaera crista* in the Labrador Sea is also restricted to the Late Pliocene with very abundant specimens between 3.05 and 3.00 Ma. De Schepper and Head (2014) found specimens in the Bering Sea (IODP Site U1314) making the species a potential marker for correlation between the North Pacific and the North Atlantic. However, its stratigraphic distribution in the Bering sea appears to be restricted to 3.66 to 3.40 Ma. Zorzi and de Vernal (in prep.) extended its geographic distribution to the western North Pacific (ODP Site 882), where specimens are common between ~3.8 to ~2.9 Ma. Hence, *Lavradosphaera crista* could be a good indicator of the middle and late Late Pliocene, mostly across the mid and high latitude of the North Atlantic, but also in the North Pacific.

Cymatiosphaera? fensomei encompasses the entire study interval, from 3.21 to 2.33 Ma, thus making it impossible to assess its specific range at IODP Site U1307. Across the North Atlantic, this species has a total range spanning from 3.38 Ma to 2.57 Ma (De Schepper and Head, 2014) making it a good marker for the latest Pliocene. *Cymatiosphaera? fensomei* in the Labrador Sea is more abundant from 3.08 to 2.76 Ma and the HCO at 2.76 Ma is useful, thus adding another Late Pliocene bioevent around 2.75 Ma in the Labrador Sea (Figure 1.5). Similarly, *Lavradosphaera canalis* is found mainly between 2.8 and 2.58 Ma in the Labrador Sea with maximum abundance recorded between 2.8 and 2.75 Ma. Other sporadic and single occurrences after the Plio-Pleistocene transition might be related to reworking (Figure 1.5) as this species has a very narrow stratigraphic range from 2.8 to 2.6 Ma at IODP Site U1308 and DSDP Site 610A (De Schepper and Head, 2014), suggesting that this taxon is a good marker at mid and high latitudes of the North Atlantic (Figure 1.5).

On the contrary, *Cymatiosphaera? icenorum* does not seem to have any stratigraphic significance. This species is present throughout our study interval and its total stratigraphic range spans from 5.7 Ma to 1.71 Ma (this study and DSDP 603C, M.J. Head unpublished in De Schepper *et al.*, 2017). It has its HCO at 2.72 at IODP Site U1308 (De Schepper *et al.*, 2014) and at 2.74 Ma in DSDP Hole 610A (De Schepper and Head, 2009) (Figure 1.5).

1.5 Conclusion

We have established a new marine Late Pliocene to Early Pleistocene palynostratigraphic scheme based on the analyses of 180 samples, spanning from 3.2 to 2.2 Ma at the Labrador Sea Site U1307. The succession of three distinct biozones (LS1, LS2 and L3) is based on the HO of *Barssidinium graminosum* (LS1/LS2) at 2.75 Ma and the end of the acme of *Pyxidinopsis braboi* (LS2/LS3) at 2.57 Ma. Most sites with comparable biostratigraphical schemes are from the North Atlantic and have been influenced by warm waters from the North Atlantic Current. In contrast, IODP Site U1307 is situated in the path of the East Greenland Current marked by cold and low saline waters of Arctic origin. As a result, a strong regionalism marks the Labrador Sea dinoflagellate cyst and acritarch assemblage, which is reflected in asynchronous bioevents between the North Atlantic, Nordic Seas and Labrador Sea. Nevertheless, despite diachronous stratigraphic ranges for several taxa, our Labrador Sea zone boundaries were constructed with bioevents that are in large part contemporaneous with those of the eastern North Atlantic DSDP Hole 610A (RT5, RT6 and RT7; De Schepper and Head, 2009).

Acknowledgements

This is an ArcTrain contribution. We acknowledge support from the Natural sciences and Engineering Research Council of Canada (NSERC) and the Fonds de Recherche du Québec Nature et Technology (FRQNT) (Grants to AdV). SDS was funded by Research Council of Norway project # 229819. The authors thank the scientific party, technical staff and crews of the Integrated Ocean Drilling Program 303 for their efforts

in providing data and samples used in this study. We like to thank Malcolm Jones at Palynological Laboratory Services Ltd. (Holyhead, UK) for aid with preparing palynological slides. We are grateful to M.J. Head for allowing us to use unpublished data of DSDP 603C. We also thank Peter Bijl, an anonymous reviewer and the editor of the Journal for constructive comments, which helped to improve the manuscript.

References

- Andrews, J. T., and Tedesco, K. (1992). Detrital carbonate-rich sediments, northwestern Labrador Sea: Implications for ice-sheet dynamics and iceberg rafting (Heinrich) events in the North Atlantic. *Geology*, 20(12), 1087-1090. 10.1130/0091-7613(1992)020<1087:DCRSNL>2.3.CO;2
- Baldauf, J. G. (1987). Diatom biostratigraphy of the middle-and high latitude North Atlantic Ocean, Deep Sea Drilling Project Leg 94. *Init. Repts. DSDP*, 94, 729-762.
- Baldauf, J. G., Clement, B. G., Aksu, A. E., de Vernal, A., Firth, J. V., Hall, F., Head, M. J., Jarrad, R. D., Kaminski, M. A., Lazarus, D., Monjanel, A. L., Berggren, W. A., Gradstein, F. E., Knüttel, S., Mudie, P. J., and Russel, M. D. (1989). Magnetostratigraphic and biostratigraphic synthesis of ocean drilling program leg 105: Labrador Sea and Baffin Bay. In *Proceedings of the Ocean Drilling Program: Scientific Results* (Vol. 105, pp. 935-956). doi:10.2973/odp.proc.sr.105.165.1989
- Berggren, W.A., Kent, D.V., and Van Couvering, J.A. (1985). Neogene geochronology and chronostratigraphy, In Snelling, N J . (Ed.). Geochronology and the Geologic Time Scale. Geol. Soc. (London) Mem., 10:211-250.
- Berggren, W.A., Kent, D.V., Swisher III, C.C., and Aubry, M.P. (1995). A revised Cenozoic geochronology and chronostratigraphy. Geochronology Times Scales and global Stratigraphic Correlation, SEPM Special Publication, 54, 129-212.
- Blake-Mizen, K., Hatfield, R., Stoner, J., Carlson, A., Xuan, C., Walczak, M., Lawrence, K.T., Channell, J.E.T, and Bailey, I. (2019). Southern Greenland glaciation and Western Boundary Undercurrent evolution recorded on Eirik Drift during the late Pliocene intensification of Northern Hemisphere glaciation. *Quaternary Science Reviews*, 209, 40-51. <https://doi.org/10.1016/j.quascirev.2019.01.015>

Expedition 303 Scientists (2006). Site U1307. In Channell, J.E.T., Kanamatsu, T., Sato, T., Stein, R., Alvarez Zarikian, C.A., Malone, M.J., and the Expedition 303/306 Scientists. Proc. IODP, 303/306: College Station TX (Integrated Ocean Drilling Program Management International, Inc.). doi:10.2204/iodp.proc.303306.107.2006

Channell, J.E.T., Sato, T., Kanamatsu, T., Stein, R., and Alvarez Zarikian, C. (2010). Expedition 303/306 synthesis: North Atlantic climate. In Channell, J.E.T., Kanamatsu, T., Sato, T., Stein, R., Alvarez Zarikian, C.A., Malone, M.J., and the Expedition 303/306 Scientists, Proc. IODP, 303/306: College Station, TX (Integrated Ocean Drilling Program Management International, Inc.). doi:10.2204/iodp.proc.303306.214.2010

Channell, J. E. T., Hodell, D. A., and Curtis, J. H. (2016). Relative paleointensity (RPI) and oxygen isotope stratigraphy at IODP Site U1308: North Atlantic RPI stack for 1.2–2.2 Ma (NARPI-2200) and age of the Olduvai Subchron. *Quaternary Science Reviews*, 131, 1-19.

Clement, B.M., Hall, F.J., and Jarrad, R.D. (1989): The magnetostratigraphy of Ocean Drilling Program Leg 105 sediments. In: Srivastava, SP; Arthur, M; Clement, B; et al., (eds.), *Proceedings of the Ocean Drilling Program, Scientific Results, College Station, TX (Ocean Drilling Program)*, 105, 583-596, <https://doi.org/10.2973/odp.proc.sr.105.147.1989>

De Schepper, S. (2006). Plio-Pleistocene dinoflagellate cyst biostratigraphy and palaeoecology of the eastern North Atlantic and southern North Sea Basin. PhD Thesis, Wolfson College, University of Cambridge.

De Schepper, S., and Head, M. J. (2008a). New dinoflagellate cyst and acritarch taxa from the Pliocene and Pleistocene of the eastern North Atlantic (DSDP Site 610). *Journal of Systematic Palaeontology*, 6(1), 101-117. doi:10.1017/S1477201907002167

De Schepper, S., and Head, M. J. (2008b). Age calibration of dinoflagellate cyst and acritarch events in the Pliocene–Pleistocene of the eastern North Atlantic (DSDP Hole 610A). *Stratigraphy*, 5(2), 137-161.

De Schepper, S., and Head, M. J. (2014). New late Cenozoic acritarchs: evolution, palaeoecology and correlation potential in high latitude oceans. *Journal of Systematic Palaeontology*, 12(4), 493-519. DOI: 10.1080/14772019.2013.783883

De Schepper, S., Head, M. J., and Louwye, S. (2004). New dinoflagellate cyst and incertae sedis taxa from the Pliocene of northern Belgium, southern North Sea Basin. *Journal*

- of Paleontology*, 78(4), 625-644. [https://doi.org/10.1666/0022-3360\(2004\)078<0625:NDCAIS>2.0.CO;2](https://doi.org/10.1666/0022-3360(2004)078<0625:NDCAIS>2.0.CO;2)
- De Schepper, S., and Head, M. J. (2009). Pliocene and Pleistocene dinoflagellate cyst and acritarch zonation of DSDP Hole 610A, eastern North Atlantic. *Palynology*, 33(1), 179-218. DOI: 10.1080/01916122.2009.9989673
- De Schepper, S., and M. J. Head, M. J. (2014) New late Cenozoic acritarchs: evolution, palaeoecology and correlation potential in high latitude oceans, *Journal of Systematic Palaeontology*, 12(4), 493-519, DOI: 10.1080/14772019.2013.783883
- De Schepper, S., Head, M. J., and Groeneveld, J. (2009). North Atlantic Current variability through marine isotope stage M2 (circa 3.3 Ma) during the mid-Pliocene. *Paleoceanography and Paleoceanography*, 24(4). doi:10.1029/2008PA001725
- De Schepper, S., Fischer, E. I., Groeneveld, J., Head, M. J., and Matthiessen, J. (2011). Deciphering the palaeoecology of Late Pliocene and Early Pleistocene dinoflagellate cysts. *Palaeogeography, Palaeoclimatology, Palaeoecology*, 309(1-2), 17-32. <https://doi.org/10.1016/j.palaeo.2011.04.020>
- De Schepper, S., Schreck, M., Beck, K. M., Matthiessen, J., Fahl, K., and Mangerud, G. (2015). Early Pliocene onset of modern Nordic Seas circulation related to ocean gateway changes, *Nature Communications*, 6, 8659. DOI: 10.1038/ncomms9659.
- De Schepper, S., Beck, K. M., and Mangerud, G. (2017). Late Neogene dinoflagellate cyst and acritarch biostratigraphy for Ocean Drilling Program Hole 642B, Norwegian Sea. *Review of Palaeobotany and Palynology*, 236, 12-32. <https://doi.org/10.1016/j.revpalbo.2016.08.005>
- de Vernal, A., and Mudie, P. J. (1989). Pliocene and Pleistocene palynostratigraphy at ODP Sites 646 and 647, eastern and southern Labrador Sea. In *Proceedings of the Ocean Drilling Program, Scientific Results* (Vol. 105, pp. 401-422). Ocean Drilling Program Texas A & M University, College Station, Texas. doi:10.2973/odp.proc.sr.105.134.1989
- de Vernal, A., and Marret, F. (2007). Organic-walled dinoflagellate cysts: tracers of sea-surface conditions. In *Developments in marine geology*, 1, 371-408. [https://doi.org/10.1016/S1572-5480\(07\)01014-7](https://doi.org/10.1016/S1572-5480(07)01014-7)

- de Vernal, A., Larouche, A., and Richard, P. J. H. (1987). Evaluation of palynomorph concentrations: do the aliquot and the marker-grain methods yield comparable results?. *Pollen et spores*.
- de Vernal, A., Henry, M., and Bilodeau, G. (1999). Techniques de préparation et d'analyse en micropaléontologie. *Les cahiers du GEOTOP*, 3, 41.
- de Vernal, A., Radi, T., Zaragozi, S., Van Nieuwenhove, N., Rochon, A., Allan, E., Eynaud, F., Head, M., Limoges, A., Londeix, L., Marret, F., Matthiessen, J., Penaud, A., Pospelova, V., Price, A., Richerol, T. (2019). Distribution of common modern dinocyst taxa in surface sediment of the Northern Hemisphere in relation to environmental parameters: the updated n=1968 database. *Marine Micropaleontology*, 101796. <https://doi.org/10.1016/j.marmicro.2019.101796>
- Dybkjær, K., and Piasecki, S. (2010). Neogene dinocyst zonation for the eastern North Sea Basin, Denmark. *Review of Palaeobotany and Palynology*, 161(1-2), 1-29. <https://doi.org/10.1016/j.revpalbo.2010.02.005>
- Gibbard, P. L., Head, M. J., Walker, M. J., and Subcommission on Quaternary Stratigraphy. (2010). Formal ratification of the Quaternary System/Period and the Pleistocene Series/Epoch with a base at 2.58 Ma. *Journal of Quaternary Science*, 25(2), 96-102.
- Gibb, O. T., Hillaire-Marcel, C., and de Vernal, A. (2014). Oceanographic regimes in the northwest Labrador Sea since Marine Isotope Stage 3 based on dinocyst and stable isotope proxy records. *Quaternary Science Reviews*, 92, 269-279. DOI: 10.1016/j.quascirev.2013.12.010
- Gibb, O. T., Steinhauer, S., Fréchette, B., de Vernal, A., and Hillaire-Marcel, C. (2015). Diachronous evolution of sea surface conditions in the Labrador Sea and Baffin Bay since the last deglaciation. *The Holocene*, 25(12), 1882-1897. <https://doi.org/10.1177/0959683615591352>
- Harland, R. (1979). Dinoflagellate biostratigraphy of Neogene and Quaternary sediments at holes 400/400A in the Bay of Biscay (Deep Sea Drilling Project Leg 48). *Initial Reports of the Deep Sea Drilling Project*, 48, 531-545.
- Harrison, J. C., Mayr, U., McNeil, D. H., Sweet, A. R., McIntyre, D. J., Eberle, J. J., Harrington, C.R., Chalmers, J.A., Dam, G., and Nohr-Hansen, H. (1999). Correlation of Cenozoic sequences of the Canadian Arctic region and Greenland; implications for

- the tectonic history of northern North America, *Bulletin of Canadian Petroleum Geology*, 47(3), 223-254.
- Head, M. J. (1993). Dinoflagellates, sporomorphs, and other palynomorphs from the Upper Pliocene St. Erth Beds of Cornwall, southwestern England. *Memoir (The Paleontological Society)*, 1-62.
- Head, M. J., (1996). Late Cenozoic dinoflagellates from the Royal Society borehole at Ludham, Norfolk, eastern England. *Journal of Paleontology*, 70(4), 543-570.
- Head, M. J., (1997). Thermophilic dinoflagellate assemblages from the mid Pliocene of eastern England. *Journal of Paleontology* 165-193.
- Head, M. J., and Norris, G. (2003). New species of dinoflagellate cysts and other palynomorphs from the latest Miocene and Pliocene of DSDP Hole 603C, western North Atlantic. *Journal of Paleontology*, 77(1), 1-15. [https://doi.org/10.1666/0022-3360\(2003\)077<0001:NSODCA>2.0.CO;2](https://doi.org/10.1666/0022-3360(2003)077<0001:NSODCA>2.0.CO;2)
- Head, M. J., Norris, G., and Mudie, P. J. (1989). Palynology and dinocyst stratigraphy of the upper Miocene and lowermost Pliocene, ODP Leg 105, Site 646, Labrador Sea. In *Proceedings of the Ocean Drilling Program, Scientific Results* (Vol. 105, pp. 423-451). Ocean Drilling Program Texas A & M University, College Station, Texas. Palynology and dinocyst stratigraphy of the upper Miocene and lowermost Pliocene, ODP. DOI: 10.2973/odp.proc.sr.105.135.1989
- Hennissen, J. A., Head, M. J., De Schepper, S., and Groeneveld, J. (2014). Palynological evidence for a southward shift of the North Atlantic Current at~ 2.6 Ma during the intensification of late Cenozoic Northern Hemisphere glaciation. *Paleoceanography and Paleoclimatology*, 29(6), 564-580. 10.1002/2013PA002543
- Hennissen, J. A., Head, M. J., De Schepper, S., and Groeneveld, J. (2015). Increased seasonality during the intensification of Northern Hemisphere glaciation at the Pliocene–Pleistocene boundary~ 2.6 Ma. *Quaternary Science Reviews*, 129, 321-332. <https://doi.org/10.1016/j.quascirev.2015.10.010>
- Hennissen, J. A., Head, M. J., De Schepper, S., and Groeneveld, J. (2017). Dinoflagellate cyst paleoecology during the Pliocene–Pleistocene climatic transition in the North Atlantic. *Palaeogeography, palaeoclimatology, palaeoecology*, 470, 81-108. <http://dx.doi.org/10.1016/j.palaeo.2016.12.023>

- Hilgen, F.J., Lourens, L.J., and Van Dam, J.A. (2012). Chapter 29 – The Neogene Period. In: Gradstein, F. M., Ogg, J.G., Schmitz, M. D., Ogg, G. M. (Eds.), *The Geologic Time Scale*, Elsevier, Boston, 923–978.
- Hillaire-Marcel, C., A. de Vernal, G. Bilodeau, and A. J. Weaver (2001), Absence of deep-water formation in the Labrador Sea during the last interglacial period, *Nature*, 410(6832), 1073–1077, doi:10.1038/35074059.
- Knüttel, S., Russell, M.D., Jr., and Firth, J.V. (1989). Neogene calcareous nannofossils from ODP Leg 105: implications for Pleistocene paleoceanographic trends. In Srivastava, S.P., Arthur, M.A., Clement, B., *et al.*, Proc. ODP, Sci. Results, 105: College Station, TX (Ocean Drilling Program), 245–262. doi:10.2973/odp.proc.sr.105.130.1989
- Limoges, A., Londeix, L., and de Vernal, A. (2013). Organic-walled dinoflagellate cyst distribution in the Gulf of Mexico. *Marine Micropaleontology*, 102, 51–68. <http://dx.doi.org/10.1016/j.marmicro.2013.06.002>
- Lisiecki, L. E., and Raymo, M. E. (2005). A Pliocene-Pleistocene stack of 57 globally distributed benthic $\delta^{18}\text{O}$ records. *Paleoceanography*, 20(1). DOI: 10.1029/2004PA001071
- Louwye, S., Head, M. J., and de Schepper, S. (2004). Dinoflagellate cyst stratigraphy and palaeoecology of the Pliocene in northern Belgium, southern North Sea Basin. *Geological Magazine*, 141(3), 353–378. DOI: 10.1017/S0016756804009136
- Martini, E. (1971). Standard Tertiary and Quaternary calcareous nannoplankton zonation. In *Proc. II Planktonic Conference, Roma 1970, Roma, Tecnoscienza* (Vol. 2, pp. 739–785).
- Matthews, J. (1969). The assessment of a method for the determination of absolute pollen frequencies. *New Phytologist*, 68(1), 161–166.
- Mertens, K. N., Verhoeven, K., Verleye, T., Louwye, S., Amorim, A., Ribeiro, S., Deaf, A.S., Harding, I.C., De Schepper, S., Gonzalez, C., Kodrans-Nsiah, M., de Vernal, A., Henry, M., Radi, T., Dybkjaer, K., Poulsen, N.E., Feist-Burkhardt, S., Chitolie, J., Heilmann-Clausen, C., Londeix, L., Turon, J-L., Marret, F., Matthiessen, J., McCarthy, F.M.G., Prasad, V., Pospelova, V., Kyffin Highes, J.E., Riding, J.B., Rochon, A., Sangiorgio, F., Welters, N., Sinclair, N., Thun, C., Soliman, A., Van Nieuwenhove, N., Vink, Annemiek, and Young, M. (2009). Determining the absolute abundance of dinoflagellate cysts in recent marine sediments: the

- Lycopodium marker-grain method put to the test. *Review of Palaeobotany and Palynology*, 157(3-4), 238-252. <https://doi.org/10.1016/j.revpalbo.2009.05.004>
- Mudie, P. J. (1987). Palynology and dinoflagellate biostratigraphy of Deep-Sea Drilling Project Leg 94, Sites 607 and 611, North-Atlantic Ocean. *Initial Reports of the Deep Sea Drilling Project*, 94, 785. DOI: 10.2973/dsdp.proc.94.118.1987
- Mudie, P. J. (1989). Palynology and dinocyst biostratigraphy of the late Miocene to Pleistocene, Norwegian Sea: ODP Leg 104, Sites 642 to 644. In *Proceedings of the Ocean Drilling Program, Scientific Results* (Vol. 104, pp. 587-610). <https://doi.org/10.2973/odp.proc.sr.104.174.1989>
- Munsterman, D., and Kerstholt, S. (1996). Sodium polytungstate, a new non-toxic alternative to bromoform in heavy liquid separation. *Review of Palaeobotany and Palynology*, 91(1-4), 417-422. [https://doi.org/10.1016/0034-6667\(95\)00093-3](https://doi.org/10.1016/0034-6667(95)00093-3)
- Murphy, M.A., and Salvador, A.(1999). International Stratigraphic Guide-an abridged version, *Episodes*, 22(4),255.
- Nooteboom, P.D., Bijn, P.K., van Sebille, I., von der Heydt, A.S., and Dijkstra, H.A. (2019). Transport bias by ocean currents in sedimentary microplankton assemblages: implications for paleoceanographic reconstructions, *Paleoceanography and paleoclimatology*, 34, 1178-1194. doi: <https://doi.org/10.1029/2019PA003606>.
- Ogg, J. G. (2012). Chapter 5 – Geomagnetic Polarity Time Scale, In: Gradstein, F. M., Ogg, J.G., Schmitz, M. D., Ogg, G. M. (Eds.), *The Geologic Time Scale*, Elsevier, Boston, 85–113.
- Price, A.M., Baustian, M.M., Turner, R.E., Rabalais, N.N., and Chmura, G.L. (2017). Melitasphaeridium choanophorum – a living fossil dinoflagellate cyst in the Gulf of Mexico, *Palynology*, 41, 351-358.
- Rochon, A., Vernal, A. D., Turon, J. L., Matthießen, J., and Head, M. J. (1999). Distribution of recent dinoflagellate cysts in surface sediments from the North Atlantic Ocean and adjacent seas in relation to sea-surface parameters. *American Association of Stratigraphic Palynologists Contribution Series*, 35, 1-146.
- Sarnthein, M., Bartoli, G., Prange, M., Schmittner, A., Schneider, B., Weinelt, M., Andersen, N., and Garbe-Schönberg, D. (2009). Mid-Pliocene shifts in ocean overturning circulation and the onset of Quaternary-style climates. *Climate of the Past*, 5(2), 269-283. DOI: 10.5194/cpd-5-251-2009

- Shackleton, N. J., Backman, J., Zimmerman, H. T., Kent, D. V., Hall, M. A., Roberts, D. G., Scnitker, D., Baldauf, J.G, Desprairies, A., Homrighausen, R., Huddleston, P., Keene, J.B., Kaltenback, A.J., Krumsiek, K.A.O., Morton, A.C., Murray, J.W., and Westberg-Smith, J. (1984). Oxygen isotope calibration of the onset of ice-rafting and history of glaciation in the North Atlantic region, *Nature*, 307(5952), 620.
- Schreck, M., Matthiessen, J., and Head, M. J. (2012). A magnetostratigraphic calibration of Middle Miocene through Pliocene dinoflagellate cyst and acritarch events in the Iceland Sea (Ocean Drilling Program Hole 907A). *Review of Palaeobotany and Palynology*, 187, 66-94. <http://dx.doi.org/10.1016/j.revpalbo.2012.08.006>
- Schreck, M., Meheust, M., Stein, R., and Matthiessen, J. (2013). Response of marine palynomorphs to Neogene climate cooling in the Iceland Sea (ODP Hole 907A). *Marine Micropaleontology*, 101, 49-67.
- Schreck, M., Nam, S. I., Clotten, C., Fahl, K., De Schepper, S., Forwick, M., and Matthiessen, J. (2017). Neogene dinoflagellate cysts and acritarchs from the high northern latitudes and their relation to sea surface temperature. *Marine Micropaleontology*, 136, 51-65. <https://doi.org/10.1016/j.marmicro.2017.09.003>
- Schlitzer, R. (2018). Ocean Data View, <https://odv.awi.de>
- Stockmarr, J. (1971). Tablets with spores used in absolute pollen analysis, *Pollen et Spores* 13, 615-621.
- Thiede, J., Jessen, C., Knutz, P., Kuijpers, A., Mikkelsen, N., Nørgaard-Pedersen, N., and Spielhagen, R. F. (2011). Millions of years of Greenland Ice Sheet history recorded in ocean sediments. *Polarforschung*, 80(3), 141-159.
- Verhoeven, K., Louwye, S., Eiríksson, J., and De Schepper, S. (2011). A new age model for the Pliocene–Pleistocene Tjörnes section on Iceland: its implication for the timing of North Atlantic–Pacific palaeoceanographic pathways. *Palaeogeography, Palaeoclimatology, Palaeoecology*, 309(1-2), 33-52. <https://doi.org/10.1016/j.palaeo.2011.04.001>
- Verhoeven, K., and Louwye, S. (2013). Palaeoenvironmental reconstruction and biostratigraphy with marine palynomorphs of the Plio–Pleistocene in Tjörnes, Northern Iceland. *Palaeogeography, Palaeoclimatology, Palaeoecology*, 376, 224-243. <https://doi.org/10.1016/j.palaeo.2013.03.002>

- Versteegh, G. J. (1997). The onset of major Northern Hemisphere glaciations and their impact on dinoflagellate cysts and acritarchs from the Singa section, Calabria (southern Italy) and DSDP Holes 607/607A (North Atlantic). *Marine Micropaleontology*, 30(4), 319-343. DOI: 10.1016/S0377-8398(96)00052-7
- Versteegh, G. J. M., and Zevenboom, D. (1995). New genera and species of dinoflagellate cysts from the Mediterranean Neogene. *Review of Palaeobotany and Palynology*, 85(3-4), 213-229. DOI: 10.1016/0034-6667(94)00127-6
- Wall, D., and Dale, B. (1966). "Living fossils" in western Atlantic plankton. *Nature*, 211(5053), 1025.
- Warny, S., Askin, R.A., Hannah, M.J., Mohr, B.A.R., Raine, J.I., Harwood, D.M., Florindo, F., and SMS Science Team. (2009). Palynomorphs from a sediment core reveal a sudden remarkably warm Antarctica during the middle Miocene. *Geology*, 37(10), 955-958. <http://dx.doi.org/10.1130/G30139A.1>.
- Weaver, P.E. and Clement, B. (1987). Magnetobiostratigraphy of planktonic foraminiferal datums: Deep Sea Drilling Project Leg 94, North Atlantic. In: Ruddiman, W.F., Kidd, R.B., Thomas, E., et al. (Eds.), Initial Reports of the Deep Sea Drilling Project, 94. U.S. Government Printing Office, Washington, D.C., pp. 815–829.
- Weaver, A. J., Bitz, C. M., Fanning, A. F., and Holland, M. M. (1999). Thermohaline circulation: High-latitude phenomena and the difference between the Pacific and Atlantic. *Annual Review of Earth and Planetary Sciences*, 27(1), 231-285. <https://doi.org/10.1146/annurev.earth.27.1.231>
- Williams, G. L., and Bujak, J. P. (1977). Cenozoic palynostratigraphy of offshore eastern Canada. *American Association of Stratigraphic Palynologists, Contribution Series*, 5, 14-47.
- Williams, G.L., Fensome, R.A., and MacRae, R.A. (2017). DINOFLAJ3. American Association of Stratigraphic Palynologists, Data Series no. 2. <http://dinoflaj.smu.ca/dinoflaj3>
- Yashayaev, I. (2007). Hydrographic changes in the Labrador Sea, 1960–2005. *Progress in Oceanography*, 73(3-4), 242-276. <https://doi.org/10.1016/j.pocean.2007.04.015>
- Yashayaev, I., Bersch, M., and van Aken, H. M. (2007). Spreading of the Labrador Sea Water to the Irminger and Iceland basins. *Geophysical Research Letters*, 34(10). DOI: 10.1029/2006GL028999

Zorzi, C., Head, M. J., Matthiessen, J., and de Vernal, A. (2019). *Impagidinium detroitense* and *I.? diaphanum*: Two new dinoflagellate cyst species from the Pliocene of the North Pacific Ocean, and their biostratigraphic significance. *Review of Palaeobotany and Palynology*, 264, 24-37. <https://doi.org/10.1016/j.revpalbo.2019.02.005>

Zorzi, C., and de Vernal, A., (in prep.). Plio-Pleistocene palynostratigraphy at ODP Site 882, northwest Pacific: biostratigraphy and paleoceanography.

Figures

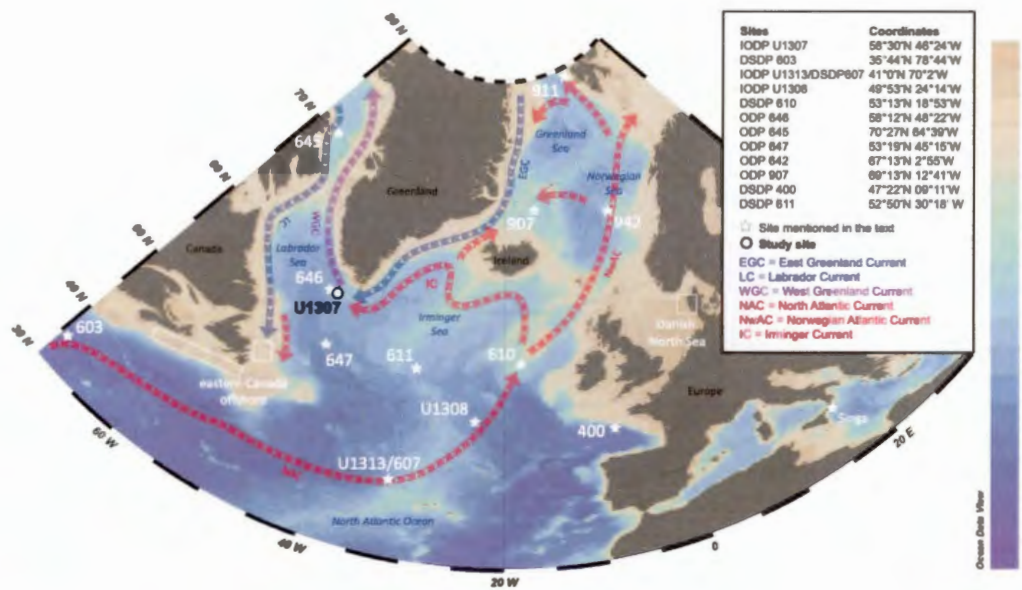


Figure 1.1 Map of the Labrador Sea showing the location of Site IODP U1307, other sites mentioned in the text, and the modern surface currents (made with Ocean Data View, Schlitzer, 2018)

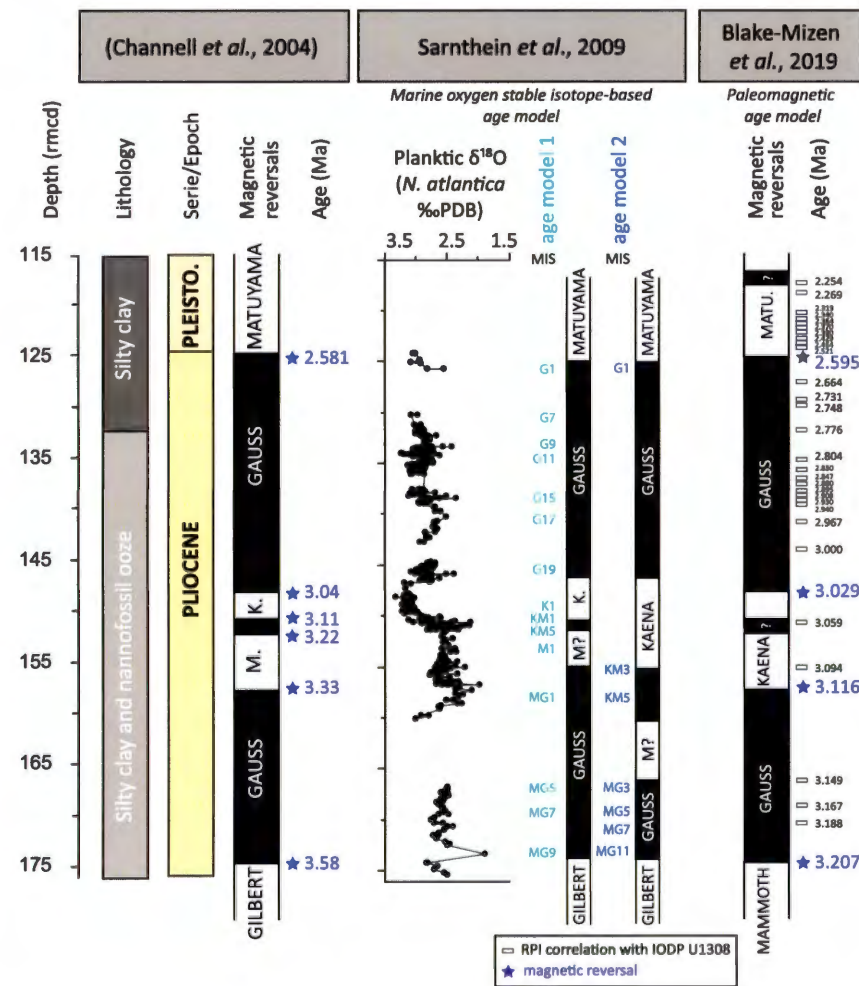


Figure 1.2 Age models at IODP Site U1307. Magnetostratigraphy and lithology of IODP Site U1307 from Channell *et al.*, (2004). Stable oxygen isotope data based on the planktic foraminifer *Neogloboquadrina atlantica* and two proposed age models from Sarnthein *et al.* (2009). Most recent age model based on magnetic reversals and a paleointensity record tuned to IODP Site U1308 (Blake-Mizen *et al.*, 2019). M = Mammoth subchron, K = Kaena subchron, MIS = Marine Isotope Stage, RPI = Relative Paleo-Intensity.

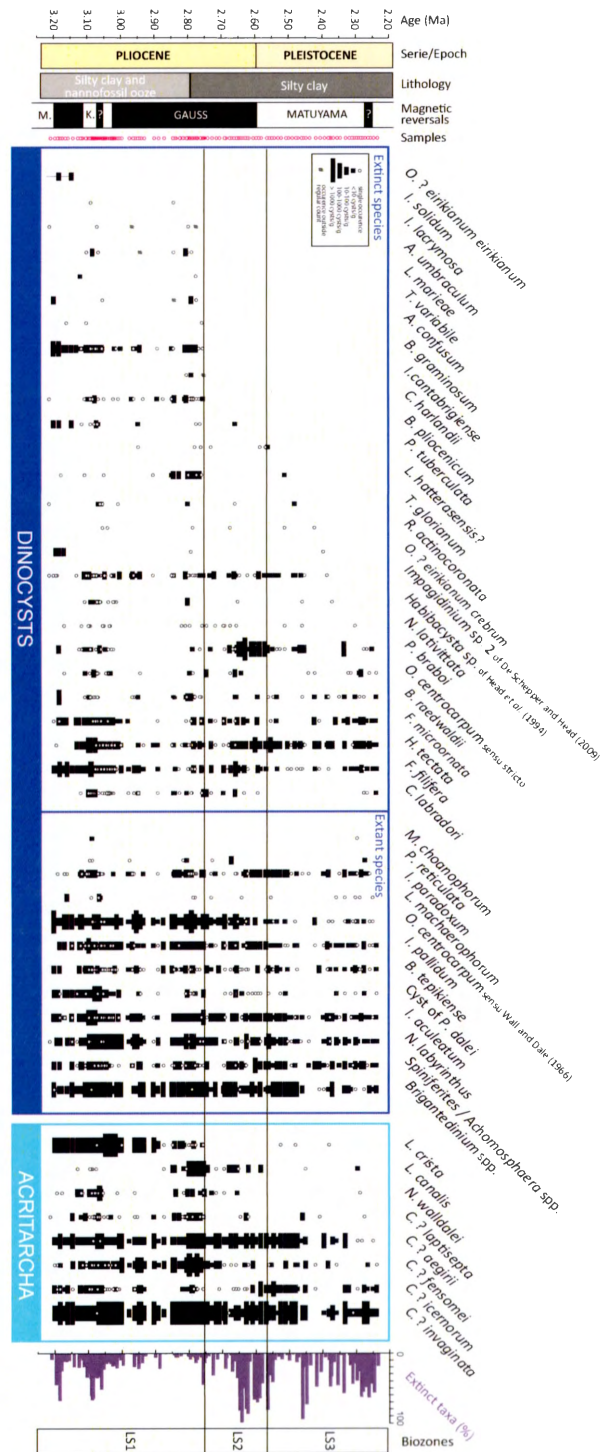


Figure 1.3 IODP Site U1307 stratigraphic occurrence of selected dinocyst and acritarch taxa and biozones defined in this study, calibrated against Blake-Mizen *et al.* (2019) age model. All raw data are available in Supplementary Data A.

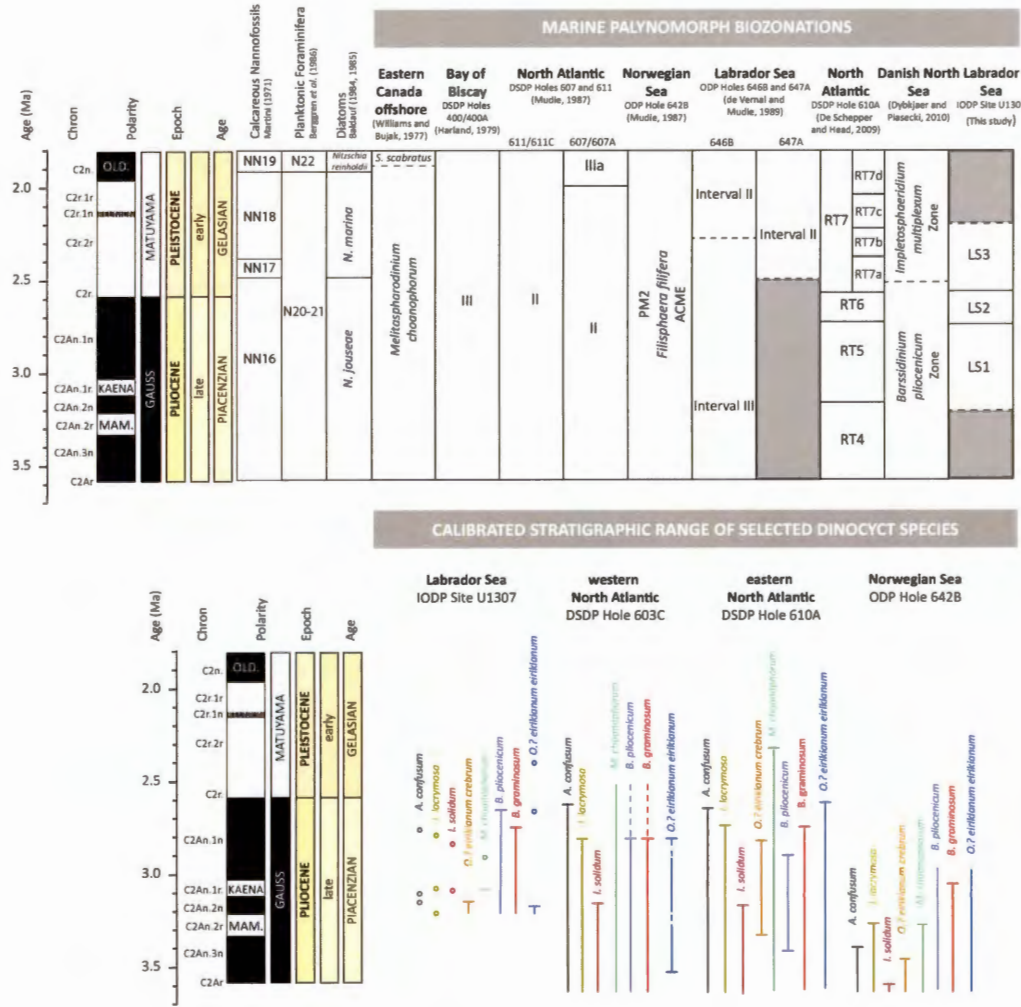


Figure 1.4 Left: Late Pliocene-early Pleistocene dinocyst biozonation schemes from different locations in the North Atlantic. Right: Adapted from De Schepper *et al.* (2017). Late Pliocene dinocyst extinction events in the Labrador Sea (this study), the western North Atlantic (DSDP Hole 603C, Head and Norris, 2003; M.J. Head, unpublished data), eastern North Atlantic (DSDP Hole 610A, De Schepper and Head, 2008a, 2008b, 2009) and the Norwegian Sea (ODP Hole 642B, De Schepper *et al.*, 2017).

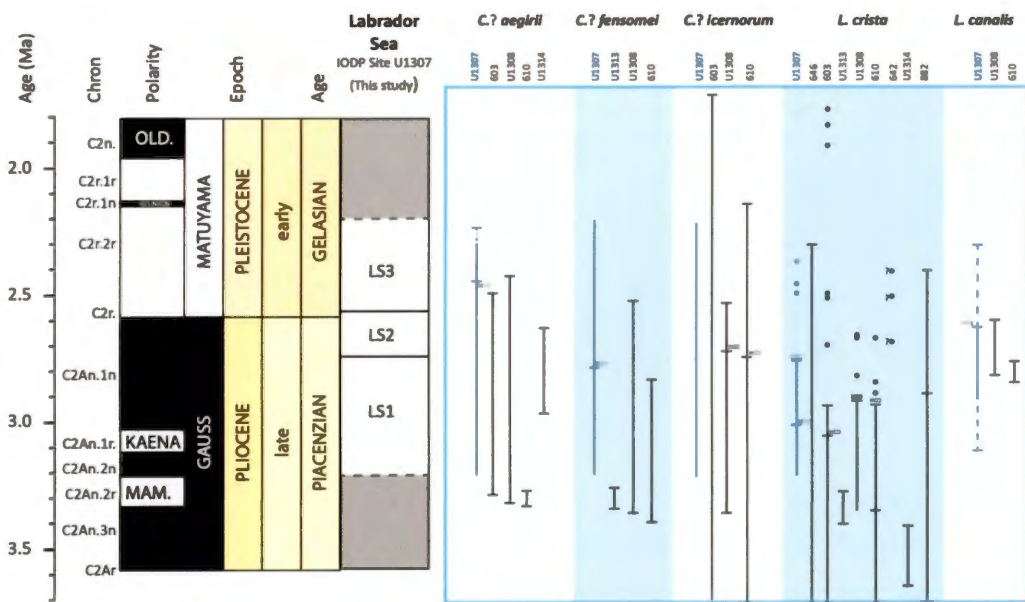


Figure 1.5 Adapted from De Schepper and Head (2014). Selected acritarch stratigraphic ranges from different sites across the North Atlantic (DSDP Sites 603 and 610; ODP Site 646, 642 and 907; IODP Sites U1308, U1313 and U1307) and North Pacific (IODP Site U1314, ODP Site 882). Old = Olduvai Subchron, M= Mammoth Subchron, HCO= Highest Common Occurrence, HPO= Highest Persistent Occurrence

Tables

Depth (rmcd)	Age (Ma)	Type	Chronology	Upper boundary		Lower Boundary	
				sample	depth (rmcd)	sample	depth (rmcd)
117.63	2.25384	RPI	U1308				
118.51	2.2687	RPI	U1308				
120.52	2.31938	RPI	U1308				
121.3	2.34027	RPI	U1308				
121.86	2.3642	RPI	U1308				
122.05	2.37048	RPI	U1308				
122.4	2.38028	RPI	U1308				
123.11	2.42918	RPI	U1308				
123.53	2.46437	RPI	U1308				
123.96	2.52141	RPI	U1308				
124.88	2.595	Reversal	Gauss/Matuyama	U1307A-14H-3 143 cm	124.74	U1307A-14H-4 25 cm	125.06
127.32	2.66445	RPI	U1308				
129.1	2.73077	RPI	U1308				
129.73	2.74782	RPI	U1308				
132	2.77611	RPI	U1308				
135	2.80408	RPI	U1308				
136.03	2.82958	RPI	U1308				
136.86	2.84671	RPI	U1308				
137.47	2.88009	RPI	U1308				
138.13	2.89464	RPI	U1308				
138.54	2.90858	RPI	U1308				
138.8	2.93008	RPI	U1308				
139.31	2.94014	RPI	U1308				
141.12	2.96667	RPI	U1308				
143.76	3.00041	RPI	U1308				
147.97	3.029	Reversal	Kaena (t)	U1307A-17H-2 61 cm	147.81	U1307A-17H-2 97 cm	148.17
151.01	3.05942	RPI	U1308				
155.41	3.09399	RPI	U1308				
157.33	3.116	Reversal	Kaena (b)	U1307A-18H-2 31 cm	157.06	U1307A-18H-2 82 cm	157.57
166.48	3.14918	RPI	U1308				
168.96	3.16734	RPI	U1308				
170.7	3.18776	RPI	U1308				
174.48	3.207	Reversal	Mammoth (t)	U1307A-19H-6 60 cm	173.93	U1307A-19H-6 120 cm	174.53

Table 1.1 Age model tie point used at IODP Site U1307 from Blake-Mizen *et al.*, 2019

Event	Species	Sample	Depth (rmcd)	Age (Ma)	Error (Ma)
Dinocysts					
HO	<i>Melitaspharodinium choanophorum</i>	U1307B-13H03, 57.5-59.5 cm	119.4	2.291	0.0068
HO	<i>Impagidinium</i> sp.2 of De Schepper and Head (2009)	U1307A-14H02, 60-62 cm	122.41	2.381	0.0041
HO	<i>Lejeuneacysta hatterasensis</i>	U1307A-14H03, 54-56cm	123.85	2.5068	0.0079
HO	<i>Pyxidinopsis tuberculata</i>	U1307A-14H03, 110-112 cm	124.41	2.5574	0.008
Acme (top)	<i>Pyxidinopsis braboi</i>	U1307A-14H03, 120-122 cm	124.5	2.5654	0.008
Acme (bottom)	<i>Pyxidinopsis braboi</i>	U1307B-13H07, 55-57 cm	126.75	2.6482	0.0057
HO	<i>Barssidinium pliocenicum</i>	U1307B-14H01, 30-32 cm	127.0	2.6553	0.0028
HO	<i>Corrudinium harlandii</i>	U1307B-14H03, 28-33 cm	129.98	2.7509	0.0093
HO	<i>Barssidinium graminosum</i>	U1307B-14H03, 30-32 cm	130.0	2.7512	0.0003
HO	<i>Ataxiodinium confusum</i>	U1307B-14H03, 50-52 cm	130.2	2.7537	0.0025
HPO	<i>Lejeuneacysta hatterasensis</i>	U1307B-14H03, 110-112 cm	130.8	2.7612	0.0038
HO	<i>Invertocysta lacrymosa</i>	U1307B-14H05, 130-132 cm	134.01	2.7948	0.0046
HO	<i>Impagidinium solidum</i>	U1307B-15H01, 50-52 cm	136.5	2.8393	0.0041
HO	<i>Operculodinium? eirikianum eirikianum</i>	U1307A-19H02, 28-30 cm	167.61	3.1575	0.014
HPO	<i>Operculodinium? eirikianum crebrum</i>	U1307A-19H03, 80-82 cm	170.63	3.1899	0.0103
Acritarchs					
HPO	<i>Cymatiosphaera? aegirii</i>	U1307B-13H04, 52-54 cm	120.85	2.3282	0.0067

HPO	<i>Lavradosphaera canalis</i>	U1307B-14H03, 140-142 cm	124.71	2.5814	0.0043
HCO	<i>Lavradosphaera canalis</i>	U1307B-14H03, 30-32 cm	130.0	2.7512	0.0003
HPO	<i>Lavradosphaera crista</i>	U1307B-14H03, 50-52 cm	130.2	2.7537	0.0253
Acme (top)	<i>Cymatiosphaera? fensomei</i>	U1307B-14H03, 110-112 cm	130.8	2.7612	0.0038
Acme (bottom)	<i>Cymatiosphaera? fensomei</i>	U1307B-15H01, 80-82 cm	136.8	2.8455	0.0062
HCO	<i>Lavradosphaera crista</i>	U1307B-15H02, 80-82 cm	138.3	2.9004	0.0078

Table 1.2 Dinocyst and acritarch bioevents at IODP Site U1307. The age model error is from Blake-Mizen *et al.*, (2019) and the age error is based on sampling interval. HO: highest occurrence, HCO: highest common occurrence, HPO: highest persistent occurrence

CHAPITRE II
LATE PLIOCENE-EARLY PLEISTOCENE PALEOCEANOGRAPHY OF
SOUTHERN GREENLAND BASED ON DINOCYST AND ACRITARCH
ASSEMBLAGES AT IODP SITE U1307, LABRADOR SEA

A.M.R. Aubry¹, S. De Schepper², A. de Vernal¹

¹GEOTOP, Université du Québec à Montréal, CP 8888, Montréal, QC, H3C 3P8,
Canada

²NORCE Climate, Norwegian Research Centre, Bjerknes Centre for Climate Research,
Jahnebakken 5, N-5007 Bergen, Norway

Keywords: iNHG; Pliocene; Pleistocene; MIS KM2; Dinocysts; Acritarcha;
Palynology; North Atlantic; Labrador Sea

Article soumis prochainement dans *Palaeogeography, Palaeoclimatology, Palaeoecology*

Abstract

In this study we report about a new record of dinoflagellate cysts and acritarcha spanning 3.2-2.2 Ma from the Integrated Ocean Drilling Program Site U1307, Labrador Sea. Dinocyst assemblage dominated by *Operculodinium centrocarpum* sensu Wall and Dale (1966) reflects an important penetration of the warm and saline surface waters of the North Atlantic current (NAC) into the Labrador Sea during part of the late Pliocene. The latest part of the Pliocene, at ~ 2.65 Ma was marked by a very sharp increase of ice rafted debris (IRD), the decline of *Operculodinium centrocarpum* and the acme of *Pyxidinopsis braboi* in dinocyst assemblages, which indicates the onset of polar influence and southward shift of the NAC. Above this transition and during the early Pleistocene low occurrence of NAC taxa and the dominance of subpolar taxa such as *Habibacysta tectata*, *Filisphaera filifera*, *Filisphaera microornata* and *Bitectatodinium tepikiense* characterized the dinocyst assemblages. Together, the composition of assemblages, low concentrations and low species diversity of both marine and terrestrial palynomorphs associated with high abundance of IRD reflect the onset of harsh condition likely related with significant expansion of the Greenland ice sheet at about 2.65 Ma. Beyond this main transition, important variations occurred as exemplified by high resolution analyses of dinocyst assemblages in the interval spanning 3.2 to 3.0 Ma (marine isotope stages -MIS- KM5 to G20). The result suggest advection of NAC warm and saline water into the Labrador Sea until the end of MIS KM2 (~ 3.12 Ma) followed by cooling/freshening pulses of the surface waters as shown from successive abundance peaks of *Habibacysta tectata*, *Filisphaera filifera*, cysts of *Pentaspharodinium dalei* and *Operculodinium centrocarpum*-short processes form until MIS G22 (~ 3.05 Ma).

2.1 Introduction

The Plio-Pleistocene boundary, dated at 2.58 Ma and corresponding to the Matuyama/Gauss magnetic reversal (Gibbard *et al.*, 2010), is associated with major climatic changes in the Northern Hemisphere, notably marked by the transition from relatively stable and warm climate to glacial-interglacial oscillations with recurring ice sheets (Zachos *et al.*, 2001; Flesche Kleiven *et al.*, 2002; Tripati *et al.*, 2008; Matthiessen *et al.*, 2009; De Schepper *et al.*, 2014). However, the timing of the onset of the North Hemisphere Glaciations (NHG) is unclear. Whereas marine data such as ice-rafted debris (IRD) in the Greenland Sea suggest episodic glacier or ice sheet advance in the circum-Arctic regions as early as ~44-30 Ma (Tripati *et al.*, 2008), most marine and terrestrial data from the Northern Hemisphere rather evidence glacial events without development of large ice sheet during the Pliocene as highlighted by the compilation of De Schepper *et al.* (2014). Based on the oxygen isotope ($\delta^{18}\text{O}$) data in benthic foraminifera, which record both the changes in deep water temperatures and global continental ice volumes (Mudelsee and Raymo, 2005), it is generally accepted that the onset of NHG occurred progressively during the Pliocene. The $\delta^{18}\text{O}$ data indicate an increase in the amplitude of glacial cycles after 3.6 Ma and a general intensification of North Hemisphere Glaciations (iNHG) at approximately 2.7 Ma, during the Marine Isotopic Stage (MIS) G6 (Mudelsee and Raymo, 2005).

The NHG may have started on Greenland as documented by an important IRD pulse at 3.3 Ma in the Greenland Sea (Flesche Kleiven *et al.*, 2002). The synchronous increase of IRD around 2.7 Ma in the North Atlantic (Shackleton *et al.*, 1984; Winkler *et al.*, 2002; Flesche Kleiven *et al.*, 2002; Bailey *et al.*, 2010), the Nordic seas (Flesche Kleiven *et al.*, 2002; Polyak *et al.*, 2010), the Svalbards-Barents sea region (Knies *et*

al., 2009) and the North Pacific (Haug *et al.*, 2005), suggests ice sheet development in Greenland as well as Northern Eurasia at the end of the Late Pliocene (see also De Schepper *et al.*, 2014). On the contrary, there is no evidence that the North American ice sheet expanded before 2.64 Ma (Bailey *et al.*, 2013).

Poor preservation - or absence - of biosiliceous and calcareous microfossils in the late Neogene-early Quaternary sediments of subpolar North Atlantic and North Pacific have been a limitation for paleoceanographic studies (Matthiessen *et al.*, 2018). Hence, organic-walled microfossils including dinoflagellate cysts and acritarcha has revealed very useful for biostratigraphical and paleoceanographical investigations in the subarctic North Atlantic (Hennissen, 2013; Hennissen *et al.*, 2014, 2015; De Schepper and Head, 2008a, 2009), the Yermark Plateau area (Matthiessen and Brenner, 1996), the Iceland Sea (Schreck *et al.*, 2012, 2013), the Norwegian Sea (Mudie, 1989; De Schepper *et al.*, 2017), the Labrador Sea (de Vernal and Mudie, 1989a; Head *et al.*, 1989, Aubry *et al.*, in prep), the Baffin Bay (de Vernal and Mudie, 1989b; Aubry *et al.*, sub.), the subarctic North Pacific (Zorzi *et al.*, 2019, in prep.) and the Bering Sea (De Clercq, 2015).

Dinoflagellate cysts (hereafter dinocysts) were widely used to reconstruct sea surface parameters from the analyses of their assemblages in late Quaternary sediments (e.g., Radi and de Vernal, 2008; de Vernal *et al.*, 2005, 2013). However, because of species evolution with appearance and disappearance of taxa, the Pliocene and early Pleistocene assemblages are not fully comparable to those of the surface sediment and late Quaternary. Recent attempts to compare the relative abundances of dinocyst and acritarch taxa with sea-surface temperatures were made by confronting the Pliocene and/or Neogene palynological data with temperatures estimates from Mg/Ca in the epipelagic planktonic foraminifera *Globigerina bulloides* (De Schepper *et al.*, 2011; Hennissen *et al.*, 2017) and alkenones (Schreck *et al.*, 2017). The above-mentioned

studies revealed useful to explore the ecological affinities of extinct taxa including acritarcha that are also very useful biostratigraphical indicators (De Schepper and Head, 2014).

In this study, we have paid special attention to the southern Greenland margins in the Labrador Sea, northwest North Atlantic (Figure 2.1) as it may help to establish linkages between the Greenland onshore climate history and paleoceanographical conditions. The present day oceanography of the Labrador Sea is characterized by northward flow of warm waters from the North Atlantic Current (NAC) and the West Greenland Current (WGC), in addition to cold and fresh polar waters of the East Greenland Current (ECG) and the Labrador Current (LC), which flows southward and carry cold and low saline waters originating from the Arctic ocean through Baffin Bay and the Canadian Arctic Archipelago (Figure 2.1). Vertical convection in the Labrador Sea that leads to the formation of the Labrador Sea Water (LSW), which presently constitutes one of the main sources of the North Atlantic Deep Water (e.g. Yashayaev, 2007), is not a permanent feature of the Quaternary (cf. Hillaire-Marcel *et al.*, 2001) and apparently developed lately, at about 7.5 ka during the present interglacial (Gibb *et al.*, 2015). Hence the Labrador Sea is a highly sensitive region with regard to ocean circulation and appears strategically located to document past ocean circulation and the Atlantic meridional overturning. Moreover, because of the proximity of Greenland and northeast North America, the Labrador Sea basin contains the geological archives of the growth and decay of the Greenland and Laurentide ice sheets (de Vernal and Hillaire-Marcel, 1987, 2008; Andrews and Tedesco, 1997; Thiede *et al.*, 2011). A few sites were drilled in this area. They include the Ocean Drilling Program (ODP) Sites 646 and 647 (Figure 2.1; Srivastava *et al.*, 1989) and Integrated Ocean Drilling Program (IODP) Sites U1306 and U1307 (Figure 2.1; Channell *et al.*, 2010) that reached the mid-Pliocene (~3.6 Ma). Palynological studies in ODP cores collected in 1985 (Srivastava *et al.*, 1989) resulted in the establishment of biostratigraphical

schemes of dinocysts and acritarcha from Late Pliocene to Pleistocene at ODP Sites 647 (de Vernal and Mudie, 1989a) and from upper Miocene to lowermost Pleistocene at ODP 646 (de Vernal and Mudie, 1989a; Head *et al.*, 1989), but with a coarse temporal resolution and a taxonomy now deserving to be updated.

The Site U1307 is located off southwest Greenland, 180 km from the coastline, where the ECG flows westward (Figure 2.1). It is thus ideally situated to make linkages between ocean and terrestrial conditions based on paleoceanographical proxies and pollen and spores (e.g. de Vernal and Hillaire-Marcel, 2008). The interval of interest here encompasses the Pliocene to Pleistocene transition from 3.2 to 2.2 Ma, which is comprised between 175.11 and 116.43 rmcd, thus allowing analyses with a relatively high temporal resolution. Here we present palynological data with special attention paid to dinocysts and acritarcha with the aim to document the sea surface conditions of the Labrador Sea during the iNHG.

2.2 Materiel and methods

2.2.1 Stratigraphy of the core

The IODP Site U1307 was collected at a water depth of 2575 meters on the Eirik Drift ($58^{\circ}30.3'N$; $46^{\circ}24'W$; Figure 2.1). Two holes were drilled, reaching a maximum depth of 162.6 meters below sea floor (mbsf). The composite sequence made from the 2 holes, yields to a complete and an almost continuous record (Expedition 303 Scientists, 2006). The lithology has been divided into three units (Expedition 303 Scientists, 2006). Unit I (49.55-0 mcd) consists in hemipelagic mud composed of foraminifera, silty clay and nannofossils, with some layers of foraminifer oozes. Unit II (49.55 to 133.86 mcd) consists of silty clay with little biogenic contents. Unit III (133.86 to 173.6 mcd) consists of silty clay, silty clay with nannofossils and nannofossils silty clay. The samples examined for this study were collected from the Unit III and the lower part of Unit II.

We used the new paleomagnetostratigraphy age model of Blake-Mizen *et al.* (2019), which is based on the combination of reversal and relative paleointensity (RPI) tuned to IODP Site U1308 (Channell *et al.*, 2016). Blake-Mizen *et al.* (2019) identified the last paleomagnetic reversal as the top the Mammoth subchron (3.201 Ma) rather than in Gauss/Gilbert reversal (3.581 Ma) as previously defined (Expedition 303 Scientists, 2006; Sarnthein *et al.*, 2009; Channell *et al.*, 2010). Hence, the new age model reveals a complete recovery of a sequence spanning the last ~3.2 Myrs in which the oxygen isotope ($\delta^{18}\text{O}$) stratigraphy in planktonic foraminifera (*Neogloboquadrina atlantica*) established by Sarnthein *et al.* (2009) correlates well with the benthic foraminiferal

$\delta^{18}\text{O}$ stack reference of Lisiecki and Raymo (2005) referred to as LR04 (Figure 2.2). We converted all mbsf of Holes A and B in revisited meter composite depth (rmcd) according to Blake-Mizen *et al.* (2019) and calculated numerical ages for each sample and bio-event based on linear interpolation between tie points (Table 2.1).

2.2.2 Palynological preparation

We collected 180 sediment samples between 116.43 and 175.11 rmcd, which represents an average time resolution of 5.5 kyr from 2.2336 to 3.2102 Ma.

For this study the samples were prepared and analyzed in 2 different laboratories. In the Palynological Laboratory Services Ltd. (Holyhead, UK), 54 samples were prepared following the technique described in De Schepper *et al.* (2017). In brief, weighted samples were wet-sieve on 63 and 150 μm mesh sieves and *Lycopodium clavatum* spores were added in the remaining $< 63\mu\text{m}$ fraction for calculating concentration of palynomorphs (Matthews, 1969; Mertens *et al.*, 2009). Hydrochloric acid (HCl-50%) was added until reaction stopped to dissolve carbonates. The samples were rinsed with water and sieved at 10 μm . Hydrofluoridric acid (HF-60%) was added to the residue and left for 2 days while stirring to remove silicate. After the chemical treatments, the samples were rinsed with water and sieved at 10 μm . Finally, a short ultrasonic treatment was made prior to sieving at 10 μm . Polyvinyl alcohol (1%) was added to prevent clumping and samples were stained with Safranin-O.

In the micropaleontological laboratory of Geotop at UQAM (Montréal, QC) A.M.R. Aubry prepared 126 samples following the procedures of de Vernal *et al.* (1999). Samples were first weighted wet and dried. *Lycopodium clavatum* tablets were added to the samples, which were wet-sieved to eliminate the coarse fraction ($> 106 \mu\text{m}$) and fine silts and clays ($< 10 \mu\text{m}$). Ice rafted debris (IRD) were counted in the $> 150 \mu\text{m}$ fraction after dry sieving. The remaining fraction between 106 and 10 μm was treated with warm HCL (10%) during 20 min, rinsed with distilled water and treated with warm HF (48%) during 20 min. These chemical treatments were repeated three times, one with HF for 12 hours. Finally, the samples were sieved at 10 μm to remove remaining fine particles. In some samples containing abundant mineral particles, we also used heavy liquid separation to remove the remaining silicates and heavy minerals with a solution of sodium polytungstate calibrated for a specific gravity of 2 (Munsterman and Kerstholt, 1996). Such a treatment should not yield different results (cf. Mertens *et al.*, 2009).

The residues of samples prepared in both laboratories were mounted between glass slides and cover glass in glycerin jelly.

2.2.3 Palynological analysis

Dinocyst and acritarch counts were performed with optical microscope by A.M.R. Aubry (Leica DMR) and S. De Schepper (Zeiss Axiophot and Zeiss Axio imager A2) using transmitted light and at 400X and 1000X magnification. The nomenclature followed Rochon *et al.* (1999), De Schepper and Head (2008b, 2014), De Schepper *et*

al. (2004, 2017), and Williams *et al.*, (2017). The dinocyst and acritarch taxa identified here are listed in Table 2.2.

Spores of pteridophytes and *Sphagnum*, pollen grains, benthic foraminifer linings, fresh water algae (*Pediastrum*, *Botryococcus*, etc.) and reworked palynomorphs were also counted. Spores and pollen grains were identified following the nomenclature of McAndrews *et al.* (1973), Bassett *et al.* (1978) and Kapp *et al.* (2000). Terrestrial reworked palynomorphs were distinguished based on the preservation state often characterized by flattening and alteration of the exine and sporoderm. The reworked dinocysts were distinguished based on and their known stratigraphical range. All palynomorph counts are presented in Supplementary Table A.

The concentrations of palynomorphs (Figure .22) are reported as specimens per gram (g) of dry sediment. It was calculated using the marker grain method (Stockmarr, 1971; Mertens *et al.*, 2009). IRD are expressed in number of grains >150µm per g of dry sediment. Pollen percentages were calculated excluding *Pinus* sp. due to over-representation in marine sediments, and notably in the Labrador Sea (e.g., Rochon and de Vernal, 1994).

The Shannon-Wiener index (Figure 2.2) and Principal Component Analysis (PCA, Figure 2.3) were performed with the Paleontological Statistics Software (PAST, Hammer *et al.*, 2001). The Shannon-Wiener index is used to measure the species diversity taking into consideration the number of species and the number of specimens counted in each sample. PCA were performed to better define ecostratigraphic zones from the relative occurrences (percentages) of taxa, which were log-transformed in order to increase the weight of accompanying taxa.

The ratio of peridinioid (P) and gonyaulacoid (G) was used to calculate the P/G index (Figure 2.2). Peridinioid cysts (P) include *Barssidinium* spp., *Brigantedinium* spp.,

Lejeuneacysta spp., *Selenopemphix* spp., *Trinovantedinium* spp and the round brown cysts which combine all sub-spherical brown peridinioid cysts. The P/G index could be used as proxy of productivity (cf. Radi and de Vernal, 2008).

The proportion of pollen and spores (P) and dinocysts (D) led to calculate the P/D index, which can be used as indicator of continentality (cf. de Vernal and Giroux, 1991).

Although results were obtained after sample preparation and microscope analyses in distinct laboratories, the data are comparable for what concern the relative abundance of taxa and species diversity (cf. also Mertens *et al.*, 2009). However, some differences are recorded in absolute concentrations, which can be due in part to the loss of marker grains during the preparation (Mertens *et al.*, 2009) thus, authors decided to not put too much weight in a directed comparison and focus of the trends of concentration variations (see supplementary Table B). Reproducibility tests by de Vernal *et al.* (1987) and Mertens *et al.* (2009) suggest an error of +/- 10% for a confidence interval of 0.95. The standard deviation of the number of *Lycopodium* spores per tablet calculated following Stockmarr (1971) and Maher (1981) is reported in the Supplementary Table A.

Both observers worked together in order to standardize their taxonomy and compare their results. Nevertheless, some taxa were grouped into generic categories to avoid biases. This is the case of *Spiniferites/Achomosphaera* spp., *Impagidinium* spp., *Lejeuneacysts* spp. or *Operculodinium* spp. The two subspecies *Filisphaera filifera filifera* and *Filisphaera filifera pilosa* (Head *et al.*, 1993) are grouped as *Filisphaera filifera*. Moreover, identification of “round hairy” cysts is not always simple and uncertainties to distinguish the characteristic morphological features between *Filisphaera filifera*, *Filisphaera microornata*, *Bitectatodinium tepikiense* vermiculate and columellate forms, lead us to group several specimens as *Filisphaera* spp.,

Bitectatodinium tepikiense and *Filisphaera/Bitectatodinium* indet. in case of equivocal identification. We also grouped *Bitectatodinium tepikiense* columellate form and *Filisphaera microornata*, which share morphological similarities and ecological affinities (Hennissen *et al.*, 2017).

Operculodinium centrocarpum cysts bearing small processes (<2µm; cf. Rochon *et al.*, 1999) were counted separately as the process length may be related with salinity as it was shown from the morphometry of cysts in the Baltic Sea (cf. Mertens *et al.*, 2011).

The relative abundance of selected dinocyst taxa is reported Figure 2.3 as follows: rare = 1-3%; frequent = 3-10%; common = 10-30%; abundant = 30-50%; dominant = > 50%.

2.3 Results

Organic palynomorphs are generally well preserved. Among the 180 samples analyzed, 177 contained enough dinocysts and acritarcha for the calculation of concentrations and percentages. The good preservation of palynomorphs is also indicated by the high and common occurrence of peridinioid cysts, which are more sensitive to oxidation (Zonneveld *et al.*, 2008) and by high values of the P/G index (Figure 2.2). Three samples with low dinocyst counts (< 10 cysts per slide) were discarded for dinocyst percentage calculation. The detailed counts including those of discarded samples are reported in Supplementary Table A.

2.3.1 Palynological assemblages

Dinocysts occur in all samples with concentrations ranging 27 to 3126 cysts/g and averaging 448 cysts/g. Acritarcha are generally more abundant than dinocysts with up to 8975 acritarcha/g and mean concentrations of 1317 acritarcha/g (Figure 2.2).

The identified fresh water palynomorphs that include *Pediastrum*, *Botryococcus* and *Gelasinicysta vangeelii* in low number through the study sequence with concentrations averaging 11 specimens/g, except between ~2.7 and ~2.4 Ma, where an abundance peak of about 100 specimen/g is recorded (Figure 2.2).

Reworked palynomorphs are rare, especially in Pliocene sediments. Their concentration average 29 specimens/g. Three concentration peaks occurred at 2.68, 2.42 and 2.37 Ma with values of 922, 269 and 342 specimens/g respectively. Among reworked palynomorphs, pollen and spores are more abundant with concentrations averaging 768/g (Figure 2.2). The IRD content of the sediment is very low in the late Pliocene with an average of 487 grains/g but it drastically increased after 2.66 Ma with an average of 14593 grains/g in the early Pleistocene (Figure 2.2).

Pollen grains are abundant with concentrations averaging 178 pollen grains/g and ranging up to 996 pollen grains/g. Assemblages are largely dominated by tree pollen grains such as *Pinus*, *Picea*, *Tsuga*, and *Abies* which together average about 73% of the pollen sum. Shrubs pollen of *Betula*, *Alnus*, Ericaceae and *Salix* are common averaging about 20% of the assemblages. The proportion of herb pollen is low (~ 7% on the average), the most common taxa being Poaceae, Caryophyllaceae, Asteraceae, *Ambrosia*, *Artemisia*. Spores reach up to 465 spores/g with an average of 84 spores/g. There is a high dominance of *Sphagnum*, which is accompanied by *Lycopodium*,

Selluginella, and *Osmunda*. There is no major change in the composition of pollen and spore assemblages throughout the study sequence, except a slight decrease in pollen abundance from the Pliocene to the early Pleistocene. Detail terrestrial palynomorph identification and count are reported in Supplementary Table A.

2.3.2 Species diversity

The number of dinocyst species is high with 112 taxa identified, among which at least 43 are extinct (see Figure 2.2 and Table 2.2). The number of taxa averages 14 per sample, with maximum of 26 taxa at 2.79 Ma. The taxonomic diversity of acritarcha is relatively high with 24 taxa, including the genera *Leiosphaera*, *Cymatiosphaera* and *Lavradosphaera*. Among those, the most common taxa are *Cymatiosphaera?* *invaginata*, *Cymatiosphaera?* *fensomei*, *Cymatiosphaera?* *aegirii*, and *Lavradosphaera crista*, which is restricted to the late Pliocene. The number of dinocyst and acritarch species is generally higher during the Pliocene than during the Pleistocene (Figure 2.2).

The Shannon-Wiener index shows slight variations in diversity, with maximum in the samples from the upper part of the sequence, after 2.41 Ma and during the mid-Pliocene warm Period (mPwP, 3.26-3.00 Ma), when considering dinocyst. The index yields similar values when the acritarch are included (Figure 2.2).

2.3.3 Dinocyst zones

The PCA analyses performed on all dinocyst taxa led to distinguish two main ecozones and 7 subzones (Figures 2.3-2.4). The first axis (PC1) on the vertical that explains 16% of the variance shows the opposition between *Operculodinium centrocarpum* and *Impagidinium* taxa (*Impagidinium aculeatum*, *paradoxum* and *pallidum*) on the negative side and *Filisphaera microornata*, *Filisphaera filifera*, *Habibacysta tectata*, *Pyxidinopsis braboi* and the cyst of *Pentaspharodinium dalei* on the positive side. The known distribution of the second axis (PC2) on the horizontal helped to define the subzones and accounts for 12% of the variance. It shows an opposition between round brown cysts and *Operculodinium centrocarpum* on the negative side and *Habibacysta tectata*, *Impagidinium aculeatum*, *Impagidinium* taxa, *Pyxidinopsis braboi* and *Spiniferites/Achomosphaera* spp. on the positive side (Figure 2.3).

Hence the PCA distribution (Figure 2.3) suggests that some taxa record significant changes throughout the sequences likely in response to ecological stress. In Figure 2.4, we reported the relative abundances (%) of these taxa, which include *Operculodinium centrocarpum* sensu Wall and Dale (1966) (*Operculodinium centrocarpum* hereafter), round brown cysts, *Habibacysta tectata*, *Nematosphaeropsis labyrinthus*, *Impagidinium aculeatum*, *pallidum* and *paradoxum*, *Filisphaera filifera*, *Filisphaera microornata*, cysts of *Pentaspharodinium dalei*, *Spiniferites/Achomosphaera* spp., *Bitectatodinium tepikiense* and *Pyxidinopsis braboi*. In addition, we also represent *Spiniferites mirabilis/hyperacanthus* despite its rather neutral position according to its PCA scores because of its temperate to tropical waters affinities in the modern oceans (e.g., Zonneveld *et al.*, 2013). The “Other species” group include taxa with neutral scores from PCA analyses (Figure 2.4-2.5; Table 2.2).

The Ecozone 1 (3.21-2.65 Ma) corresponds to the Late Pliocene. It is characterized by abundant *Operculodinium centrocarpum* leading to negative PC1 scores. The first subzone (1a), spanning from 3.21 to 3.18 Ma (MIS KM5 – KM4), is characterized by *Operculodinium centrocarpum* in addition to *Filisphaera filifera*. A decrease of *Filisphaera filifera* and an increase of round brow cysts (up to 55%) marked the transition that corresponds to the subzone 1b (3.176-3.10 Ma, MIS KM4-KM2). In Sub-ecozone 1c (3.099-3.004 Ma, MIS K2 to MIS G20), the round brown cysts are the most common and abundant taxa with maximum values up to 82% and *Nematosphaeropsis labyrinthus* records high percentages at the end of the subzone. The abundance of *Habibacysta tectata*, *Filisphaera filifera*, the cyst of *Pentapharsodinium dalei*, and *Operculodinium centrocarpum* bearing short processes record maximum peaks at the beginning of subzone 1c (Figure 2.4). The successive abundance peaks of subzone 1c suggest very important changes, which we illustrate with more details in Figure 2.5. Subzone 1d (3.004-2.65 Ma) is characterized by the dominance of round brown cysts and *Operculodinium centrocarpum* and by very low percentages of extinct dinocyst taxa (Figures 2.2 and 2.4).

The transition from Ecozone 1 to Ecozone 2 at ~2.65 Ma is marked by a sharp decrease in *Operculodinium centrocarpum* (Figure 2.4) concomitant with increase of IRD (Figure 2.2). The Ecozone 2 (2.65 -2.045 Ma) is characterized by positive PC1 scores and abundant *Habibacysta tectata*. In subzone 2a (2.65-2.39 Ma) the abrupt replacement of *Operculodinium centrocarpum* by *Pyxidinopsis braboi*, which largely dominates the assemblages from MIS G2 to MIS 102 (2.65-2.565 Ma), is followed by the dominance of round brown cysts until MIS 97 (2.45 Ma). In Subzone 2b (2.39 to 2.29 Ma), *Impagidinium* taxa are relatively abundant together with *Spiniferites/Achromosphaera* spp. Subzone 2c (MIS 88 to 85; 2.29-2.24 Ma) is marked by the decrease of *Impagidinium* taxa and the dominance of *Habibacysta tectata* in association with *Filisphaera* taxa (Figure 2.4).

2.3.4 Close-up on the assemblages of subzone 1c (3.1-3.0 Ma, MIS K2 to MIS G20)

In the interval from 175.11 to 144.24 rmcd (3.1-3.0 Ma), the analyses of 80 samples yield an average temporal resolution of 2 400 years (Figure 2.5). The assemblages show successive abundance peaks of several taxa. At the base, the MIS K2 is characterized by *Habibacysta tectata* (up to 37%) and *Filisphaera filifera*. *Spiniferites mirabilis/hyperacanthus*, which is otherwise practically absent of the entire study interval, also records an abundance peak (up to 6%) centered at 3.088 Ma. At, the transition from MIS K2 to MIS K1, *Filisphaera filifera* increases to a maximum (53%) which is followed by increase of *Impagidinium* taxa, *Habibacysta tectata* and the cysts of *Pentaspharodinium dalei*. The MIS K2 corresponds to a high percentages of *Operculodinium centrocarpum* bearing short processes, which reach maximum between 3.076 and 3.065 Ma. The top of MIS K2 is characterized by abundant cysts of *Pentaspharodinium dalei* and the MIS G22-G20 record dominant *Nematosphaeropsis labyrinthus* and round brown cysts.

2.4 Discussion

2.4.1 Paleoecological interpretation of dominant dinocyst taxa in Pliocene sediment of IODP Site U1307

One of the most abundant dinocyst taxon, *Operculodinium centrocarpum*, is a cosmopolitan species which tolerates a large amplitude of temperatures and salinities (e.g., Rochon *et al.*, 1999; Mertens *et al.*, 2011; de Vernal *et al.*, 2001, 2013; Zonneveld *et al.*, 2013). In the surface sediments, it is particularly abundant in the temperate to subpolar North Atlantic Ocean, notably in the path of the North Atlantic Current (NAC) (Rochon *et al.*, 1999). In the Plio-Pleistocene sediments of the North Atlantic and the Nordic Seas, this species was interpreted as a proxy for the NAC influence (De Schepper *et al.*, 2009, 2013; Hennissen, 2013; Hennissen *et al.*, 2014, 2017). The IODP U1307 zone 1 characterized by *Operculodinium centrocarpum* abundances could reflect NAC inflow into the Labrador Sea possibly through warm and saline waters from Irminger Current until about 2.65 Ma (Figure 2.4).

The round brown cysts that are often associated with neritic conditions and lower salinities in the recent Labrador Sea records (Rochon *et al.*, 1999; de Vernal *et al.*, 2013; Gibb *et al.*, 2015) may correspond also to high nutrient availability and primary productivity (e.g., Rochon *et al.*, 1999; Radi and de Vernal, 2008). In the Pliocene sediments of the northern North Atlantic, round brown taxa are not a dominant part of the assemblages (De Schepper *et al.*, 2013; Hennissen *et al.*, 2014, Clotten *et al.*, 2018; Schreck *et al.*, 2017), except at ODP Hole 999A, situated in the Caribbean Sea, where it was associated with high productivity related to the inflows of Pacific waters (De

Schepper *et al.*, 2013), and at ODP Site 911 situated off Svalbard, where it might indicate cold conditions and seasonal sea-ice cover (Matthiessen and Brenner, 1996). In our record, the round brown cysts are recurrent throughout the study interval (Figure 2.4). In the context of the study area and taking into consideration the diversity of accompanying taxa, abundant round brown cysts suggest high productivity with possibility of seasonal sea ice cover. This would be compatible with the biogenic opal data from ODP Site 646, which led to suggest seasonal sea ice cover in the Labrador Sea since 4 Ma in association with the onset of the modern EGC (Bohrmann *et al.*, 1990). High abundance of round brown cysts and high P/G index generally concomitant with high P/D index values together suggest high nutrient inputs from surrounding areas of the Greenland (Figure 2.2) during the late Pliocene and early Pleistocene, at least until ~2.45 Ma. A decrease of terrestrial and marine palynomorph concentrations including the acritarcha *Cymatiosphaera* and *Lavradosphaera* (Figure 2.2), strongly suggest reduced productivity after 2.45 Ma.

Filisphaera filifera, *Filisphaera microornata* and *Habibacysta tectata* occurred almost continuously in our study interval. They are extinct species, which disappeared from the North Atlantic, the Nordic Seas, the Arctic and the North Pacific oceans during the Pleistocene after 2.0 Ma (Matthiessen *et al.*, 2018). *Filisphaera filifera* and *Habibacysta tectata* are both considered cool-tolerant water species (De Schepper *et al.*, 2011; Hennissen *et al.*, 2017; Schreck *et al.*, 2017). *Filisphaera microornata* is also considered as a cool-tolerant species in the Pliocene of the North Atlantic (Hennissen *et al.*, 2017) and was grouped with the extant species *Bitectatodinium tepikiense* vermiculate var. as they share similar morphological and paleoecologic affinities (Hennissen *et al.*, 2017). According to Matthiessen *et al.* (2018), the acme of *Filisphaera filifera*, *Filisphaera microornata* and *Habibacysta tectata* in the Arctic Ocean could be associated to inflow from the North Atlantic. At the North Atlantic

DSDP Site 610, high abundance of *Filisphaera filifera* characterized the cold MIS M2 between 3.264 and 3.312 Ma (De Schepper *et al.*, 2009) whereas *Habibacysta tectata* dominated the assemblages during MIS 103 (2.595-2.575 Ma) and was associated with reduced influence of Atlantic waters and a southern shift of the NAC path (Hennissen *et al.*, 2014, 2017). At IODP Site U1307, the increased abundance of *Habibacysta tectata* is concomitant with minimum percentages of *Operculodinium centrocarpum* in Ecozone 2 after 2.65 Ma and during a brief interval around 3.1 Ma can be attributed to significant cooling.

One of the major species of the Plio-Pleistocene transition at IODP U1307 is *Pyxidinopsis braboi* which records an acme from MIS G2 to 102 (2.65-2.565 Ma). This extinct species was described from Pliocene of Belgium where it occurred in low number (De Schepper *et al.*, 2004) as in the North Atlantic at IODP Hole 1313C (Hennissen, 2013; Hennissen *et al.*, 2014). A peak in abundance is found in the Ross Sea, Antarctica, during the middle Miocene climatic optimum (Warny *et al.*, 2009). At DSDP Site 610 the acme of this species occurred during the Plio-Pleistocene transition but is restricted to the MIS 104 (Hennissen, 2013; Hennissen *et al.*, 2014). *Pyxidinopsis braboi* is considered as a cold-polar opportunistic species (Warny *et al.*, 2009; Hennissen *et al.*, 2014, 2017; De Schepper *et al.*, 2004) and its acme at DSDP Site 610A was associated with a southward shift of the Arctic Front in the North Atlantic (Hennissen, 2013; Hennissen *et al.*, 2014, 2017). This is consistent with our results at IODP Site U1307 where this taxon characterized the base of the Ecozone 2 at about 2.65 Ma.

Other cool water indicators in the dinocyst assemblages are extant species including the cysts of *Pentaspharodinium dalei* and *Impagidinium pallidum* (e.g., Rochon *et al.*, 1999; de Vernal *et al.*, 2001, 2013, subm.; Zonneveld *et al.*, 2013). In recent sediments of the Northern Hemisphere, the cysts of *Pentaspharodinium dalei* occurs in high

percentages (> 40%) at many sites from the Arctic and subarctic seas in addition to temperate continental margin areas and appear to characterize a wide range of sea-surface temperature and salinity in summer, from -1 to 16°C and from 20 to 35 psu (de Vernal *et al.*, subm.). It can thus be considered as a highly tolerant taxon in neritic settings of high latitudes. From the study of Plio-Pliocene sediments the cysts of *Pentaspharodinium dalei* was also considered as a cool water species (Hennissen *et al.*, 2017). The recent distribution of *Impagidinium pallidum* shows a relatively narrow range in offshore setting of Arctic and subarctic seas, with percentages > 10% where summer sea-surface temperature is lower than 7°C and summer salinity higher than 31 psu (de Vernal *et al.*, subm.). From Plio-Pleistocene studies this species is associated to warmer conditions than the modern ones (De Schepper *et al.*, 2011; Hennissen *et al.*, 2017).

Among dinocyst taxa, *Operculodinium centrocarpum* bearing small processes records a significant abundance peak in MIS K1 sediments. This peak could relate to a low salinity pulse as the average process length variation of *Operculodinium centrocarpum* was shown to be correlated with sea surface salinity in the Baltic Sea (Mertens *et al.*, 2011). A similar peak in abundance (up to 20%) has been observed earlier in the Norwegian Sea during MIS KM4 and KM3 interpreted as a freshening of the water masses (Panitz *et al.*, 2017). However, such an interpretation is not unequivocal as the relationship between the process lengths of *Operculodinium centrocarpum* and the salinity is reverse in the North Pacific, rather pointing to different cryptic species (Mertens *et al.*, 2012).

In surface sediments, *Nematopshaeropsis labyrinthus* is a cosmopolitan species with a wide temperature tolerance (e.g. Rochon *et al.*, 1999; de Vernal *et al.*, 2001, 2013; Zonneveld *et al.*, 2013). In recent sediments of the Northern Hemisphere, it is dominant with percentages > 40% at sites where summer sea-surface temperature and salinity

range 2-14°C and 30-35.5 psu respectively (de Vernal *et al.*, subm.). In the northern North Atlantic and subpolar seas, it dominates the postglacial sediment together with *Opercudolinium centrocarpum* (e.g., Solignac *et al.*, 2004; Van Nieuwenhove *et al.*, 2016) and characterized most interglacial stages of the last million years in the Labrador Sea (de Vernal and Mudie, 1992) which were likely characterized by subpolar conditions not unlike those of the present interglacial. The occurrence of *Nematosphaeropsis labyrinthus* in Mio-Pliocene sediments of the Iceland Sea seems to correspond to the higher temperature range of the species according to alkenone paleothermometry (Schreck *et al.*, 2017). High abundance of *Nematosphaeropsis labyrinthus* in Pliocene was also linked to transitional climatic conditions and oligotrophic conditions (Hennissen *et al.*, 2017). However, in subzone 1C where *Nematosphaeropsis labyrinthus* is particularly abundant, such conditions are not compatible with the high proportion of heterotrophic dinocyst taxa and the high acritarch concentration, especially those belonging to *Cymatiosphaera* and *Lavradosphaera* (Figures 2.2, 2.4 and 2.5), which are often associated with cool surface waters and high productivity (Schreck *et al.*, 2017, De Schepper and Head, 2014).

Low to moderate abundance of *Impagidinium aculeatum* and *Impagidinium paradoxum* indicated that cold or polar conditions could not have characterized the study interval (e.g., Rochon *et al.*, 1999; Zonneveld *et al.*, 2013; De Schepper *et al.*, 2011; Hennissen *et al.*, 2017). *Impagidinium aculeatum* is a temperate-warm water, oligotrophic species in the modern ocean (e.g., Zonneveld *et al.*, 2013). The dominance of *Impagidinium aculeatum* and *Impagidinium paradoxum* instead of round brown cysts at ODP Site 999 during MIS M2 was interpreted as the result of diminishing inflow of nutrients from the Pacific via the American Seaway (De Schepper *et al.*, 2013). At IODP Site U1307, the opposition between abundant heterotrophic round brown cysts and the oligotrophic *Impagidinium* taxa throughout the study interval also

suggests variations in productivity. Accordingly, more oligotrophic conditions apparently prevailed during the Pleistocene after ~2.45 Ma in the Labrador Sea (Figure 2.3).

2.4.2 Paleoceanography of the Mid-Piacenzian Warm Period from MIS KM5 to MIS G20 (3.21–3.00 Ma) in the Labrador Sea

According to the new age model of Blake-Mizen *et al.* (2019), the palynological analyses performed in samples from IODP Site U1307 provide a very high temporal resolution dinocyst and acritarch records of most of the mid-Piacenzian warm Period (mPwP) that extend from 3.264 to 3.025 Ma and corresponds to the time target of the Pliocene Research, Interpretation and Synoptic Mapping (PRISM) project (Dowsett *et al.*, 2010, 2016). At IODP Site U1307, the mPwP is represented by our subzones 1a to 1c encompassing from 3.21 to 3.00 Ma (MIS KM5-G20; Figure 2.5). The early mPwP including the cold glacial MIS M2, M1 and KM6 were not recovered (Blake-Mizen *et al.*, 2019).

The mPwP is described as the last geological period significantly warmer than present (e.g., Dowsett *et al.*, 2010, 2016). Global air temperatures were estimated ~2–3 °C higher than preindustrial ones (Salzmann *et al.*, 2011, Dowsett *et al.*, 2016). Similar reconstructions were made for the mean oceanic temperatures, which are evaluated to range between 0 and 6 °C higher than at present (Dowsett *et al.*, 2016). This interval is widely studied and used for numerical climate simulation in order to understand the

response to global warming as the one expected during the 21st century (Dowsett *et al.*, 2016).

From the MIS KM5 to the beginning of MIS KM1 (3.21-3.117 Ma), the surface ocean conditions in the North Atlantic were apparently influenced by a strong NAC (De Schepper *et al.*, 2009, 2011, 2013; Hennissen *et al.*, 2017, Panitz *et al.*, 2017). Our data showing high percentages of *Operculodinium centrocarpum* suggest that warm and saline waters penetrated into the Labrador Sea during this interval. However, the increase of *Filisphaera* at the end of MIS KM5 and during MIS KM2 suggest cooling pulses (Figure 2.5). Such cooling pulses as also recorded at ODP Sites 642 and 982 from the Norwegian Sea and northeast North Atlantic where the alkenone based sea-surface temperatures and IRD were associated to an eastward shift of the subpolar gyre into the Nordic Seas (Bachem *et al.*, 2016). The MIS KM2 is one of the cold phase of the mPwP also identified from increase IRD at ODP Hole 907A (Jansen *et al.*, 2000) and 610A (Flesche Kleiven *et al.*, 2002). Although we have no IRD data characterizing the event, the dinocysts assemblages clearly show a cooling in the surface waters based on a marked decrease in the diversity of species.

From MIS KM1 to MIS K1, the decrease in abundance of *Operculodinium centrocarpum*, the increase of percentages of *Habibacysta tectata* and round brown cysts may reflect a reduced influence of Atlantic waters in the Labrador Sea and higher productivity from MIS KM1 through the end of subzone 1c (MIS G20). The overall assemblages characterized by *Filisphaera*, *Bitectatodinium* and *Impagidinium pallidum* are consistent with relative cool surface waters, while the abundance peaks of the cysts of *Pentapharsodinium dalei* may suggest some freshening and stronger stratifications in the upper water masses.

In the MIS K2, the dinocyst assemblages are dominated by *Habibacysta tectata*, *Filisphaera filifera* and cysts of *Pentasphaerodinium dalei*, which indicate cool surface water. In contrast, the significant occurrence of *Spiniferites mirabilis* and *Impagidinium aculeatum* at the base of MIS K1 together suggest relatively warm and saline conditions (e.g., Zonneveld *et al.*, 2013; de Vernal *et al.*, subm.), at least episodically. In the upper part of MIS K1 the most striking feature in the abundance of *Operculodinium centrocarpum* bearing short processes. This taxon may lead to infer a freshening of surface waters in the Labrador Sea (cf. Mertens *et al.*, 2011) possibly related to freshwater flux from the Greenland or freshwater supply from the Arctic via the EGC. According to Clotten *et al.* (2018) strengthening of the EGC only occurs after 2.9 Ma, which makes it unlikely inputs through the EGC. Actually, the increase concentration of terrestrial palynomorphs at IODP Site U1307 during MIS K1 (Figure 2.5) indicates larger vegetation cover over south Greenland and inputs from wind pattern (Smith *et al.*, 2018) and/or runoff from Greenland.

After MIS K1, the mid-MIS G22 characterized by increased $\delta^{18}\text{O}$ (Sarnthein *et al.*, 2009) probably corresponds to ice volume increase in addition to regional cooling. The transition is marked by an important increase of *Nematosphaeropsis labyrinthus* percentages, which likely relate to a major change in surface ocean conditions. In this interval spanning MIS G22-G20, acritarcha are far more abundant than dinocysts. At IODP U1308 and DSDP 610A, acritarcha outnumbering the dinocysts are associated to less oligotrophic conditions and temperatures estimated between 10°C and 17°C (De Schepper and Head, 2014).

2.4.3 Paleoceanography of the late Pliocene-early Pleistocene Labrador Sea (3.0-2.2 Ma)

From MIS G19 to G3 (3 Ma to 2.65 Ma; see Figures 2.2 and 2.4), the dinocysts assemblages are composed of dominant round brown cysts alternating with abundant *Operculodinium centrocarpum*. Such changes in assemblages likely reflect variations in productivity and inflow from the NAC in the Labrador Sea. The occurrence of *Impagidinium paradoxum* and *Impagidinium aculeatum* also indicates relatively warm environments.

The MIS G3 upper boundary at ca. 2.65 Ma is marked by an important IRD peak, which is contemporaneous with that of other records in the North Atlantic and marks the initial development of the ice sheet over the Northern Hemisphere (see De Schepper *et al.*, 2014 and ref. therein). A drop in dinocyst species diversity and increase in reworked palynomorphs also reflect massive cooling in the Labrador Sea and input from erosion of sedimentary formations along the Greenland during the iNHG.

From MIS G2 to 102 including the Plio-Pleistocene transition, the most important feature is the turnover in the dinocyst assemblages with the replacement of *Operculodinium centrocarpum* by *Pyxidinopsis braboi*. Such a change is also recorded at the ODP Hole 610A but mostly during MIS 104, where it is interpreted as being the result of southward shift of the Polar Front and the NAC (Naafs *et al.*, 2010; Hennissen, 2013; Hennissen *et al.*, 2014, 2017). The earlier transition at IODP Site U1307 could be explained by the northern and closer position of IODP Site U1307 to the Arctic Front compared to DSDP Site 610.

Hennissen *et al.* (2014) hypothesized a change in the atmospheric pattern and NAC path due to ice sheet growth and topography changes near the Plio-Pleistocene transition. Such a change is concomitant with increased IRD in the North Atlantic (Flesche Kleiven *et al.*, 2002) and at IODP Site U1307, where it is also marked by a decrease of palynomorph concentrations associated with decreased primary productivity and diversity in marine waters, together with reduced inputs from vegetation of surrounding land. These features are consistent with extensive growth of continental ice sheet and fundamental reorganization of the ocean circulation leading to cool-cold conditions in the Labrador Sea during the early Pleistocene.

From MIS 102 to MIS 97, the palynological assemblages are marked by high P/G values, high freshwater algae concentrations, but low dinocyst concentration and species diversity whereas acritarcha are still a major component of the assemblages (Figure 2.2). Such assemblages reflect neritic conditions. After MIS 97 at about 2.45 Ma, the drop in concentrations of both acritarcha and dinocysts suggests very low productivity, whereas abundant IRD inputs indicate ice calving and iceberg transport along the EGC (Clotten *et al.*, 2018) likely as the result of major expansion of the Greenland ice Sheet.

2.5 Conclusion

This study presents a new Plio-Pleistocene transition (~3.2-2.2 Ma) record of dinocyst and acritarch assemblages from IODP Site U1307 in the Labrador Sea. Our results highlight two major dinocysts ecozones, which we tentatively associate with the

strength of NAC inflow into the Labrador Sea. During the late Pliocene, generally warm and saline surface waters from the North Atlantic penetrated in the Labrador Sea, whereas this was apparently restricted to interglacial stages of the Pleistocene (cf. de Vernal and Mudie, 1992). The Plio-Pleistocene transition was also marked by a turnover of the assemblage, which occurred mostly from MISG2 to MIS 102, with the acme of the *Pyxidinopsis braboi*, indicating a southern position of the Arctic front and a shift of the NAC at the iNHG.

Our study also provided high temporal resolution records of palynological assemblages during the mPwP, which was characterized by large amplitude changes related to variable advection of NAC and cooling/freshening of the surface waters due to freshwater discharges from Greenland.

Acknowledgements

This study is an ArcTrain contribution. We acknowledge support provided by the Natural Sciences and Engineering Research Council (NSERC) of Canada through the Collaborative Research and Training Experience (CREATE) program and the Discovery Grant to A. de Vernal. The authors thank the scientific party, technical staff and crews of the Integrated Ocean Drilling Program 303 for their efforts in providing the data and samples used in this research. We are grateful to Martin Head from Brock University, Canada, for his help with dinocyst identification, to Michal Kucera from the University of Bremen, Germany, and Jens Matthiessen from the Alfred Wegener Institute for their advices and hospitality in Germany. Special thanks to Cesare Elies and Tiffany Audet for their precious help with IRD counting.

References

- Aubry, A.M.R., Knütz, P., and de Vernal, A. (subm.). *Baffin Bay late Neogene palynostratigraphy at ODP Site 645. Revue Canadienne des sciences de la Terre.*
- Aubry, A.M.R., De Schepper, S., and de Vernal, A. (accepted). Dinocyst and acritarch biostratigraphy of the late Pliocene-early Pleistocene of IODP site U1307, Labrador Sea. *Journal of Micropaleontology*
- Andrews, J. T., and Tedesco, K. (1992). Detrital carbonate-rich sediments, northwestern Labrador Sea: Implications for ice-sheet dynamics and iceberg rafting (Heinrich) events in the North Atlantic. *Geology*, 20(12), 1087-1090. 10.1130/0091-7613(1992)020<1087:DCRSNL>2.3.CO;2
- Bachem, P. E., Risebrobakken, B., and McClymont, E. L. (2016). Sea surface temperature variability in the Norwegian Sea during the late Pliocene linked to subpolar gyre strength and radiative forcing. *Earth and Planetary Science Letters*, 446, 113-122. DOI: 10.1016/j.epsl.2016.04.024

- Bailey, I., Hole, G. M., Foster, G. L., Wilson, P. A., Storey, C. D., Trueman, C. N., and Raymo, M. E. (2013). An alternative suggestion for the Pliocene onset of major Northern Hemisphere glaciation based on the geochemical provenance of North Atlantic Ocean ice-raftered debris. *Quaternary Science Reviews*, 75, 181-194.
- Bassett, I. J., Crompton, C. W., and Parmelee, J. A. (1978). An atlas of airborne pollen grains and common fungus spores of Canada. Printing and Publishing Supply and Services Canada. 320 pp.
- Baumann, K. H., and Matthiessen, J. (1992). Variations in surface water mass conditions in the Norwegian Sea: evidence from Holocene coccolith and dinoflagellate cyst assemblages. *Marine Micropaleontology*, 20(2), 129-146.
[https://doi.org/10.1016/0377-8398\(92\)90003-3](https://doi.org/10.1016/0377-8398(92)90003-3)
- Blake-Mizen, K., Hatfield, R., Stoner, J., Carlson, A., Xuan, C., Walczak, M., Lawrence, K.T., Channell, J.E.T, and Bailey, I. (2019). Southern Greenland glaciation and Western Boundary Undercurrent evolution recorded on Eirik Drift during the late Pliocene intensification of Northern Hemisphere glaciation. *Quaternary Science Reviews*, 209, 40-51. doi: <https://doi.org/10.1016/j.quascirev.2019.01.015>, 2019
- Bohrmann, G., Henrich, R., and Thiede, J. (1990). Miocene to Quaternary paleoceanography in the northern North Atlantic: Variability in carbonate and biogenic opal accumulation. In *Geological history of the polar oceans: Arctic versus Antarctic*(pp. 647-675). Springer, Dordrecht.
- Channell, J.E.T., Sato, T., Kanamatsu, T., Stein, R., and Alvarez Zarikian, C. (2010). Expedition 303/306 synthesis: North Atlantic climate. In Channell, J.E.T., Kanamatsu, T., Sato, T., Stein, R., Alvarez Zarikian, C.A., Malone, M.J., and the Expedition 303/306 Scientists, Proc. IODP, 303/306: College Station, TX (Integrated Ocean Drilling Program Management International, Inc.).
doi:[10.2204/iodp.proc.303306.214.2010](https://doi.org/10.2204/iodp.proc.303306.214.2010)
- Clotten, C., Stein, R., Fahl, K., and De Schepper, S. (2018). Seasonal sea ice cover during the warm Pliocene: Evidence from the Iceland Sea (ODP Site 907). *Earth and Planetary Science Letters*, 481, 61-72. <https://doi.org/10.1016/j.epsl.2017.10.011>
- Channell, J. E. T., Hodell, D. A., and Curtis, J. H. (2016). Relative paleointensity (RPI) and oxygen isotope stratigraphy at IODP Site U1308: North Atlantic RPI stack for 1.2–2.2 Ma (NARPI-2200) and age of the Olduvai Subchron. *Quaternary Science Reviews*, 131, 1-19.<https://doi.org/10.1016/j.quascirev.2015.10.011>

- De Clercq, J. (2015). Marine palynomorphs from the Pliocene and Lower Quaternary of the Bering Sea (IODP U1341): a biostratigraphical analysis and paleoenvironmental reconstruction. Unpubl. MSc Thesis Univ. Ghent 116 P.
- De Schepper, S., and Head, M. J. (2008a). Age calibration of dinoflagellate cyst and acritarch events in the Pliocene–Pleistocene of the eastern North Atlantic (DSDP Hole 610A). *Stratigraphy*, 5(2), 137-161.
- De Schepper, S., and Head, M. J. (2008b). New dinoflagellate cyst and acritarch taxa from the Pliocene and Pleistocene of the eastern North Atlantic (DSDP Site 610). *Journal of Systematic Palaeontology*, 6(1), 101-117. doi:10.1017/S1477201907002167
- De Schepper, S., and Head, M. J. (2009). Pliocene and Pleistocene dinoflagellate cyst and acritarch zonation of DSDP Hole 610A, eastern North Atlantic. *Palynology*, 33(1), 179-218. DOI: 10.1080/01916122.2009.9989673
- De Schepper, S., and M. J. Head, M. J. (2014) New late Cenozoic acritarchs: evolution, palaeoecology and correlation potential in high latitude oceans, *Journal of Systematic Palaeontology*, 12:4, 493-519, DOI: 10.1080/14772019.2013.783883
- De Schepper, S., Head, M. J., and Louwye, S. (2004). New dinoflagellate cyst and incertae sedis taxa from the Pliocene of northern Belgium, southern North Sea Basin. *Journal of Paleontology*, 78(4), 625-644. [https://doi.org/10.1666/0022-3360\(2004\)078<0625:NDCAIS>2.0.CO;2](https://doi.org/10.1666/0022-3360(2004)078<0625:NDCAIS>2.0.CO;2)
- De Schepper, S., Head, M. J., and Groeneveld, J. (2009). North Atlantic Current variability through marine isotope stage M2 (circa 3.3 Ma) during the mid-Pliocene. *Paleoceanography and Paleoceanography*, 24(4). doi:10.1029/2008PA001725
- De Schepper, S., Fischer, E. I., Groeneveld, J., Head, M. J., and Matthiessen, J. (2011). Deciphering the palaeoecology of Late Pliocene and Early Pleistocene dinoflagellate cysts. *Palaeogeography, Palaeoclimatology, Palaeoecology*, 309(1-2), 17-32. doi:10.1016/j.palaeo.2011.04.020.
- De Schepper, S., Groeneveld, J., Naafs, B. D. A., Van Renterghem, C., Hennissen, J., Head, M. J., Louwye, S., and Fabian, K. (2013). Northern Hemisphere glaciation during the globally warm early late Pliocene. *PloS one*, 8(12), e81508. <https://doi.org/10.1371/journal.pone.0081508>

- De Schepper, S., Gibbard, P. L., Salzmann, U., and Ehlers, J. (2014). A global synthesis of the marine and terrestrial evidence for glaciation during the Pliocene Epoch. *Earth-Science Reviews*, 135, 83-102. DOI: 10.1016/j.earscirev.2014.04.003
- De Schepper, S., Beck, K. M., and Mangerud, G. (2017). Late Neogene dinoflagellate cyst and acritarch biostratigraphy for Ocean Drilling Program Hole 642B, Norwegian Sea. *Review of Palaeobotany and Palynology*, 236, 12-32.
<https://doi.org/10.1016/j.revpalbo.2016.08.005>
- de Vernal, A., and Giroux, L. (1991). Distribution of organic walled microfossils in recent sediments from the Estuary and Gulf of St. Lawrence: some aspects of the organic matter fluxes. *Canadian Journal of Fisheries and Aquatic Sciences*, 113(189), e199.
- de Vernal, A., and Hillaire-Marcel, C. (1987). Paleoenvironments along the eastern Laurentide ice sheet margin and timing of the last ice maximum and retreat. *Géographie physique et Quaternaire*, 41(2), 265-277. DOI: 10.7202/032682ar
- de Vernal, A., and Hillaire-Marcel, C. (2008). Natural variability of Greenland climate, vegetation, and ice volume during the past million years. *Science*, 320(5883), 1622-1625. DOI: 10.1126/science.1153929
- de Vernal, A., and Mudie, P. J. (1989a). Pliocene and Pleistocene palynostratigraphy at ODP Sites 646 and 647, eastern and southern Labrador Sea. In *Proceedings of the Ocean Drilling Program, Scientific Results* (Vol. 105, pp. 401-422). Ocean Drilling Program Texas A & M University, College Station, Texas. doi:10.2973/odp.proc.sr.105.134.1989
- de Vernal, A., and Mudie, P.J. (1989b). Late Pliocene to Holocene palynostratigraphy at ODP Site 645, Baffin Bay. In *Proceedings of the Ocean Drilling Program, Scientific Results* (Vol. 105, pp. 387-399). Ocean Drilling Program Texas A & M University, College Station, Texas. doi:10.2973/odp.proc.sr.105.133.1989
- de Vernal, A., and Mudie, P.J. (1992) Pliocene and Quaternary dinoflagellate cyst stratigraphy in Labrador Sea: paleoecological implications, In: M.J. Head and J.H. Wrenn (eds.), *Neogene and Quaternary dinoflagellate cysts and acritarchs*, American Association of Stratigraphic Palynologists Foundation: 329-346
- de Vernal, A., Henry, M., and Bilodeau, G. (1999). Techniques de préparation et d'analyse en micropaléontologie. *Les cahiers du GEOTOP*, 3, 41.

- de Vernal, A., Larouche, A., and Richard, P. J. H. (1987). Evaluation of palynomorph concentrations: do the aliquot and the marker-grain methods yield comparable results?. *Pollen et spores*.
- de Vernal, A., Henry, M., Matthiessen, J., Mudie, P.J., Rochon, A., Boessenkool, K., Eynaud, F., Grøsfjeld, K., Guiot, J., Hamel, D., Harland, R., Head, M.J., Kunz-Pirrung, M., Levac, E., Loucheur, V., Peyron, O., Pospelova, V., Radi, T., Turon, J.-L., and Voronina, E. (2001). Dinoflagellate cyst assemblages as tracers of sea-surface conditions in the northern North Atlantic, Arctic and sub-Arctic seas: the new "n = 677" database and application for quantitative paleoceanographical reconstruction. *Journal of Quaternary Science*, 16(7), 681-699. DOI: 10.1002/jqs.659
- de Vernal, A., Eynaud, F., Henry, M., Hillaire-Marcel, C., Londeix, L., Mangin, S., Matthiessen, J., Marret, F., Radi, T., Rochon, A., Solignac, S., and Turon, J-L. (2005). Reconstruction of sea-surface conditions at middle to high latitudes of the Northern Hemisphere during the Last Glacial Maximum (LGM) based on dinoflagellate cyst assemblages. *Quaternary Science Reviews*, 24(7-9), 897-924. doi:10.1016/j.quascirev.2004.06.014
- de Vernal, A., Rochon, A., Fréchette, B., Henry, M., Radi, T., and Solignac, S. (2013). Reconstructing past sea ice cover of the Northern Hemisphere from dinocyst assemblages: status of the approach. *Quaternary Science Reviews*, 79, 122-134. <https://doi.org/10.1016/j.quascirev.2013.06.022>
- de Vernal, A., Radi, T., Zaragosi, S., Van Nieuwenhove, N., Rochon, Allan, E., De Schepper, S., Eynaud, F., Head, M., Limoges, A., Londeix, L., Marret, F., Matthiessen, J., Penaud, A., Pospelova, V., Price, A., and Richerol, T. (2019). Distribution of common modern dinocyst taxa in surface sediments of the Northern Hemisphere in relation to environmental parameters: the updated n=1968 database. *Marine Micropaleontology*, 101796. <https://doi.org/10.1016/j.marmicro.2019.101796>
- Dowsett, H., Robinson, M., Haywood, A. M., Salzmann, U., Hill, D., Sohl, L. E., Chandler, M., Williams, M., Foley, K., and Stoll, D. K. (2010). The PRISM3D paleoenvironmental reconstruction. *Stratigraphy*, 7(2-3), 123-139.
- Dowsett, H., Dolan, A., Rowley, D., Pound, M., Salzmann, U., Robinson, M., Chandler, M., Foley, M., and Haywood, A. (2016). The PRISM4 (mid-Piacenzian) palaeoenvironmental reconstruction. *Climate of the Past Discussions*, 12, 1519-1538. <http://dx.doi.org/10.5194/cp-2016-33>

Expedition 303 Scientists. (2006). Site U1307. In Channell, J.E.T., Kanamatsu, T., Sato, T., Stein, R., Alvarez Zarikian, C.A., Malone, M.J., and the Expedition 303/306 Scientists. Proc. IODP, 303/306: College Station TX (Integrated Ocean Drilling Program Management International, Inc.). doi:10.2204/iodp.proc.303306.107.2006

Eynaud, F., Turon, J. L., and Duprat, J. (2004). Comparison of the Holocene and Eemian palaeoenvironments in the South Icelandic Basin: dinoflagellate cysts as proxies for the North Atlantic surface circulation. *Review of Palaeobotany and Palynology*, 128(1-2), 55-79. [https://doi.org/10.1016/S0034-6667\(03\)00112-X](https://doi.org/10.1016/S0034-6667(03)00112-X)

Gibb, O. T., Steinhauer, S., Fréchette, B., de Vernal, A., and Hillaire-Marcel, C. (2015). Diachronous evolution of sea surface conditions in the Labrador Sea and Baffin Bay since the last deglaciation. *The Holocene*, 25(12), 1882-1897. <https://doi.org/10.1177/0959683615591352>

Gibbard, P. L., Head, M. J., Walker, M. J., and Subcommission on Quaternary Stratigraphy. (2010). Formal ratification of the Quaternary System/Period and the Pleistocene Series/Epoch with a base at 2.58 Ma. *Journal of Quaternary Science*, 25(2), 96-102.

Hammer, Ø., Harper, D. A., and Ryan, P. D. (2001). PAST: paleontological statistics software package for education and data analysis. *Palaeontologia electronica*, 4(1), 9.

Haug, G. H., Ganopolski, A., Sigman, D. M., Rosell-Mele, A., Swann, G. E., Tiedemann, R., Jaccard, S.L., Bollmann, J., Maslin, M.A., Leng, M.J. and Eglington, G. (2005). North Pacific seasonality and the glaciation of North America 2.7 million years ago. *Nature*, 433(7028): 821-825.

Head, M. J., Norris, G., and Mudie, P. J. (1989). Palynology and dinocyst stratigraphy of the upper Miocene and lowermost Pliocene, ODP Leg 105, Site 646, Labrador Sea. In *Proceedings of the Ocean Drilling Program, Scientific Results* (Vol. 105, pp. 423-451). Ocean Drilling Program Texas A & M University, College Station, Texas. Palynology and dinocyst stratigraphy of the upper Miocene and lowermost Pliocene, ODP DOI: 10.2973/odp.proc.sr.105.135.1989

Hennissen, J.A. (2013) Late Pliocene-Early Pleistocene North Atlantic circulation: integrating dinocyst assemblages and foraminiferal geochemistry. PhD Dissertation thesis, University of Toronto, 243 p.

Hennissen, J. A., Head, M. J., De Schepper, S., and Groeneveld, J. (2014). Palynological evidence for a southward shift of the North Atlantic Current at~ 2.6 Ma during the

- intensification of late Cenozoic Northern Hemisphere glaciation. *Paleoceanography and Paleoclimatology*, 29(6), 564-580. 10.1002/2013PA002543
- Hennissen, J. A., Head, M. J., De Schepper, S., and Groeneveld, J. (2015). Increased seasonality during the intensification of Northern Hemisphere glaciation at the Pliocene–Pleistocene boundary~ 2.6 Ma. *Quaternary Science Reviews*, 129, 321-332.<https://doi.org/10.1016/j.quascirev.2015.10.010>
- Hennissen, J. A., Head, M. J., De Schepper, S., and Groeneveld, J. (2017). Dinoflagellate cyst paleoecology during the Pliocene–Pleistocene climatic transition in the North Atlantic. *Palaeogeography, palaeoclimatology, palaeoecology*, 470, 81-108. <http://dx.doi.org/10.1016/j.palaeo.2016.12.023>
- Hillaire-Marcel, C., A. de Vernal, G. Bilodeau, and A. J. Weaver (2001), Absence of deep-water formation in the Labrador Sea during the last interglacial period, *Nature*, 410(6832), 1073–1077, doi:10.1038/35074059
- IPCC: Climate Change 2013: The Physical Science Basis (2013). Contribution of Working Group I to the Fifth Assessment Report of the Intergovernmental Panel on Climate Change, in, Cambridge University Press, Cambridge, United Kingdom, New York, NY, USA, 1535.
- Jansen, E., Fronval, T., Rack, F., and Channell, J. E. (2000). Pliocene-Pleistocene ice rafting history and cyclicity in the Nordic Seas during the last 3.5 Myr. *Paleoceanography*, 15(6), 709-721 DOI: 10.1029/1999PA000435
- Kapp, R. O., Davis, O. K., and King, J. E. (2000). Pollen and Spores. The American Association of Stratigraphic Palynologists. Texas A&M University, College Station, TX.
- Kuhlmann, G., Langereis, C. G., Munsterman, D., Van Leeuwen, R. J., Verreussel, R., Meulenkamp, J. E., and Wong, T. E. (2006). Integrated chronostratigraphy of the Pliocene–Pleistocene interval and its relation to the regional stratigraphical stages in the southern North Sea region. *Netherlands Journal of Geosciences*, 85(1), 19-35.
- Flesche Kleiven, H., Jansen, E., Fronval, T., and Smith, T. M. (2002). Intensification of Northern Hemisphere glaciations in the circum Atlantic region (3.5–2.4 Ma)–ice rafted detritus evidence. *Palaeogeography, Palaeoclimatology, Palaeoecology*, 184(3-4), 213-223.doi:10.1016/S0031-0182(01)00407-2
- Knies, J., Mattingdal, R., Fabian, K., Grøsfjeld, K., Baranwal, S., Husum, K., De Schepper, S., Vogt, Christoph, Andersen, N., Matthiessen, J., Andreassen, K., Jokat,

- W., Nam, S-II and Gaina, C. (2014). Effect of early Pliocene uplift on late Pliocene cooling in the Arctic–Atlantic gateway. *Earth and Planetary Science Letters*, 387:132-144
- Lisiecki, L. E., and Raymo, M. E. (2005). A Pliocene-Pleistocene stack of 57 globally distributed benthic $\delta^{18}\text{O}$ records. *Paleoceanography*, 20(1). doi:10.1029/2004PA001071
- Maher Jr, L. J. (1981). Statistics for microfossil concentration measurements employing samples spiked with marker grains. *Review of Palaeobotany and Palynology*, 32(2-3), 153-191.
- Marret, F., and Zonneveld, K. A. (2003). Atlas of modern organic-walled dinoflagellate cyst distribution. *Review of Palaeobotany and Palynology*, 125(1-2), 1-200. [https://doi.org/10.1016/S0034-6667\(02\)00229-4](https://doi.org/10.1016/S0034-6667(02)00229-4)
- Matthews, J. (1969). The assessment of a method for the determination of absolute pollen frequencies. *New Phytologist*, 68(1), 161-166.
- Matthiessen, J., and Brenner, W. W. (1996): Dinoflagellate Cyst Ecostratigraphy of Pliocene-Pleistocene Sediments from the Yermak Plateau (Arctic Ocean, Hole 911A). In: Thiede, J; Myhre, AM; Firth, JV; Johns, GL & Ruddiman, WF (eds.) Proceedings of the Ocean Drilling Program, Scientific Results; College Station, Texas (Ocean Drilling Program), 151, 243-253 DOI: 10.1594/PANGAEA.761371
- Matthiessen, J., Knies, J., Vogt, C., and Stein, R. (2008). Pliocene palaeoceanography of the Arctic Ocean and subarctic seas. *Philosophical Transactions of the Royal Society A: Mathematical, Physical and Engineering Sciences*, 367(1886), 21-48. doi:10.1098/rsta.2008.0203
- Matthiessen, J., Schreck, M., De Schepper, S., Zorzi, C., and de Vernal, A. (2018). Quaternary dinoflagellate cysts in the Arctic Ocean: Potential and limitations for stratigraphy and paleoenvironmental reconstructions. *Quaternary Science Reviews*, 192, 1-26. <https://doi.org/10.1016/j.quascirev.2017.12.020>
- McAndrews, J. H., Berti, A. A., and Norris, G. (1973). Key to the Quaternary pollen and spores of the Great Lakes region.
- Mertens, K. N., Verhoeven, K., Verleye, T., Louwye, S., Amorim, A., Ribeiro, S., Deaf, A.S., Harding, I.C., De Schepper, S., Gonzalez, C., Kodrans-Nsiah, M., de Vernal, A., Henry, M., Radi, T., Dybkjaer, K., Poulsen, N.E., Feist-Burkhardt, S., Chitolie, J.,

- Heilmann-Clausen, C., Londeix, L., Turon, J-L., Marret, F., Matthiessen, J., McCarthy, F.M.G., Prasad, V., Pospelova, V., Kyffin Highes, J.E., Riding, J.B., Rochon, A., Sangiorgo, F., Welters, N., Sinclair, N., Thun, C., Soliman, A., Van Nieuwenhove, N., Vink, Annemiek, and Young, M. (2009). Determining the absolute abundance of dinoflagellate cysts in recent marine sediments: the *Lycopodium* marker-grain method put to the test. *Review of Palaeobotany and Palynology*, 157(3-4), 238-252. <https://doi.org/10.1016/j.revpalbo.2009.05.004>
- Mertens, K. N., Dale, B., Ellegaard, M., Jansson, I.-M., Godhe, A., Kremp, A. and Louwey, S. (2011): Process length variation in cysts of the dinoflagellate *Protoceratium reticulatum*, from surface sediments of the Baltic–Kattegat–Skagerrak estuarine system: a regional salinity proxy. *Boreas*, Vol. 40, pp. 242–255. DOI: 10.1111/j.1502-3885.2010.00193.x. ISSN 0300-9483.
- Mertens, K.N., Bringué, M., Van Nieuwenhove, N., Takano, Y., Pospelova, V., Rochon, A., de Vernal, A., Radi, T., Dale, B., Patterson, R.T., Weckström, K., Andrén, E., Louwey, S., and Matsuoka, K. (2012) Process length variation of the cyst of the dinoflagellate *Protoceratium reticulatum* in the North Pacific and Baltic-Skagerrak region: calibration as annual density proxy and first evidence of pseudo-cryptic speciation. *Journal of Quaternary Science* 27: 734-744. DOI: 10.1002/jqs.2564
- Mudelsee, M., and Raymo, M. E. (2005). Slow dynamics of the Northern Hemisphere glaciation. *Paleoceanography*, 20(4). <https://doi.org/10.1029/2005PA001153>
- Mudie, P. J. (1989). Palynology and dinocyst biostratigraphy of the late Miocene to Pleistocene, Norwegian Sea: ODP Leg 104, Sites 642 to 644. In *Proceedings of the Ocean Drilling Program, Scientific Results* (Vol. 104, pp. 587-610). <https://doi.org/10.2973/odp.proc.sr.104.174.1989>
- Munsterman, D., and Kerstholt, S. (1996). Sodium polytungstate, a new non-toxic alternative to bromoform in heavy liquid separation. *Review of Palaeobotany and Palynology*, 91(1-4), 417-422. [https://doi.org/10.1016/0034-6667\(95\)00093-3](https://doi.org/10.1016/0034-6667(95)00093-3)
- Naafs, B. D. A., Stein, R., Heftet, J., Khélifi, N., De Schepper, S., and Haug, G. H. (2010). Late Pliocene changes in the North Atlantic current. *Earth and Planetary Science Letters*, 298(3-4), 434-442.
- Panitz, S., De Schepper, S., Salzmann, U., Bachem, P. E., Risebrobakken, B., Clotten, C., and Hocking, E. P. (2017). Mid-Piacenzian Variability of Nordic Seas Surface Circulation Linked to Terrestrial Climatic Change in Norway. *Paleoceanography*, 32(12), 1336-1351. DOI: 10.1002/2017PA003166

- Penaud, A., Eynaud, F., Turon, J. L., Zaragosi, S., Marret, F., and Bourillet, J. F. (2008). Interglacial variability (MIS 5 and MIS 7) and dinoflagellate cyst assemblages in the Bay of Biscay (North Atlantic). *Marine Micropaleontology*, 68(1-2), 136-155. <https://doi.org/10.1016/j.marmicro.2008.01.007>
- Polyak, L., Alley, R. B., Andrews, J. T., Brigham-Grette, J., Cronin, T. M., Darby, D. A., Dyke, A.S., Fitzpatrick, J.J., Funder, S., Holland, M., Jennings, A.E., Miller, G.H., O'Regan, M., Savelle, J., Serreze, M., St. John, K., White, J.C.W.C and Wolff, E.. (2010). History of sea ice in the Arctic. *Quaternary Science Reviews*, 29(15): 1757-1778. doi:10.1016/j.quascirev.2010.02.010
- Radi, T., and de Vernal, A. (2008). Dinocysts as proxy of primary productivity in mid-high latitudes of the Northern Hemisphere. *Marine Micropaleontology*, 68(1-2), 84-114. DOI: 10.1016/j.marmicro.2008.01.012
- Rochon, A., and Vernal, A. D. (1994). Palynomorph distribution in recent sediments from the Labrador Sea. *Canadian Journal of Earth Sciences*. 31(1), 115-127. <https://doi.org/10.1139/e94-010>
- Rochon, A., Vernal, A. D., Turon, J. L., Matthießen, J., and Head, M. J. (1999). Distribution of recent dinoflagellate cysts in surface sediments from the North Atlantic Ocean and adjacent seas in relation to sea-surface parameters. *American Association of Stratigraphic Palynologists Contribution Series*, 35, 1-146.
- Salzmann, U., Haywood, A. M., Lunt, D. J., Valdes, P. J., and Hill, D. J. (2008). A new global biome reconstruction and data-model comparison for the middle Pliocene. *Global Ecology and Biogeography*, 17(3), 432-447. 10.1111/j.1466-8238.2008.00381.x
- Salzmann, U., Williams, M., Haywood, A. M., Johnson, A. L., Kender, S., and Zalasiewicz, J. (2011). Climate and environment of a Pliocene warm world. *Palaeogeography, Palaeoclimatology, Palaeoecology*, 309(1-2), 1-8.<https://doi.org/10.1016/j.palaeo.2011.05.044>
- Sarnthein, M., Bartoli, G., Prange, M., Schmittner, A., Schneider, B., Weinelt, M., Andersen, N., and Garbe-Schönberg, D. (2009). Mid-Pliocene shifts in ocean overturning circulation and the onset of Quaternary-style climates. *Climate of the Past*, 5(2), 269-283. doi:10.5194/cp-5-269-2009.
- Shackleton, N. J., Backman, J., Zimmerman, H. T., Kent, D. V., Hall, M. A., Roberts, D. G., Scnitker, D., Baldauf, J.G, Desprairies, A., Homrighausen, R., Huddleston, P.,

- Keene, J.B., Kaltenback, A.J., Krumsiek, K.A.O., Morton, A.C., Murray, J.W., and Westberg-Smith, J. (1984). Oxygen isotope calibration of the onset of ice-raftering and history of glaciation in the North Atlantic region. *Nature*, 307(5952), 620.
- Schlitzer, R. (2018). Ocean Data View, <https://odv.awi.de>
- Schreck, M., Matthiessen, J., and Head, M. J. (2012). A magnetostratigraphic calibration of Middle Miocene through Pliocene dinoflagellate cyst and acritarch events in the Iceland Sea (Ocean Drilling Program Hole 907A). *Review of Palaeobotany and Palynology*, 187, 66-94. <http://dx.doi.org/10.1016/j.revpalbo.2012.08.006>
- Schreck, M., Meheust, M., Stein, R., and Matthiessen, J. (2013). Response of marine palynomorphs to Neogene climate cooling in the Iceland Sea (ODP Hole 907A). *Marine Micropaleontology*, 101, 49-67. <https://doi.org/10.1016/j.marmicro.2013.03.003>
- Schreck, M., Nam, S. I., Clotten, C., Fahl, K., De Schepper, S., Forwick, M., and Matthiessen, J. (2017). Neogene dinoflagellate cysts and acritarchs from the high northern latitudes and their relation to sea surface temperature. *Marine Micropaleontology*, 136, 51-65. <https://doi.org/10.1016/j.marmicro.2017.09.003>
- Smith, Y. M., Hill, D. J., Dolan, A. M., Haywood, A. M., Dowsett, H. J., and Risebrobakken, B. (2018). Icebergs in the Nordic seas throughout the Late Pliocene. *Paleoceanography and Paleoceanography*, 33(3), 318-335. <https://doi.org/10.1002/2017PA003240>
- Solignac, S., de Vernal, A., and Hillaire-Marcel, C. (2004) Holocene sea-surface conditions in the North Atlantic - contrasted trends and regimes in the western and eastern sectors (Labrador Sea vs. Iceland Basin). *Quaternary Sci. Rev.* 23: 319-334.
- Srivastava, S.P., Arthur, M., Clement, B., Aksu, A., Baldauf, J., Bohtmann, G., Busch, W., Cederberg, T., Cremer, M., Dadey, K., de Vernal, A., Firth, J., Hall, F., Head, M., Hiscott, R., Jarrard, R., Kaminski, M., Lazarus, D., Monjanel, A-L., Nielsen, O.B., Ruediger, S., Thiebault, F., Zachos, J., and Zimmerman, H. (1989). Proceedings of the Ocean Drilling Program, Scientific Results, College Station, TX (Ocean Drilling Program), 105, doi:10.2973/odp.proc.sr.105.1989
- Stockmarr, J. (1971). Tablets with spores used in absolute pollen analysis, *Pollen et Spores* 13, 615-621.
- Tripathi, A. K., Eagle, R. A., Morton, A., Dowdeswell, J. A., Atkinson, K. L., Bahé, Y., Dawber, C.F., Khadun, E., Shaw, R.M.H., Shorttle, O., and Thanabalasundaram, L.

- (2008). Evidence for glaciation in the Northern Hemisphere back to 44 Ma from ice rafted debris in the Greenland Sea. *Earth and Planetary Science Letters*, 265(1-2), 112-122. doi:10.1016/j.epsl.2007.09.045
- Van Nieuwenhove, N., Baumann, A., Matthiessen, J., Bonnet, S., and de Vernal, A. (2016) Sea surface conditions in the southern Nordic Seas during the Holocene based on dinoflagellate cyst assemblages. *The Holocene*, 26, 722-735.
- Wall, D., and Dale, B. (1966). "Living fossils" in western Atlantic plankton. *Nature*, 211(5053), 1025.
- Warny, S., Askin, R. A., Hannah, M. J., Mohr, B. A., Raine, J. I., Harwood, D. M. Florindo, F., and SMS Science Team. (2009). Palynomorphs from a sediment core reveal a sudden remarkably warm Antarctica during the middle Miocene. *Geology*, 37(10), 955-958. <https://doi.org/10.1130/G30139A.1>
- Williams, G.L., Fensome, R.A., and MacRae, R.A. (2017). DINOFLAJ3. American Association of Stratigraphic Palynologists, Data Series no. 2. <http://dinoflaj.smu.ca/dinoflaj3>
- Winkler, A., Wolf-Welling, T., Stattegger, K., and Thiede, J. (2002). Clay mineral sedimentation in high northern latitude deep-sea basins since the Middle Miocene (ODP Leg 151, NAAG). *International Journal of Earth Sciences*, 91(1), 133-148. doi: 10.1007/s005310100199
- Zachos, J., Pagani, M., Sloan, L., Thomas, E., and Billups, K. (2001). Trends, rhythms, and aberrations in global climate 65 Ma to present. *science*, 292(5517), 686-693. doi:10.1126/science.1059412.
- Zonneveld, K.A.F., Versteegh, G.J.M., and Kodrans-Nsiah, M. (2008). Preservation and organic chemistry of Late Cenozoic organic-walled dinoflagellate cysts: A review. *Marine Micropaleontology*, 86, 179–197. <https://doi.org/10.1016/j.marmicro.2008.01.015>
- Zonneveld, K. A., and Pospelova, V. (2015). A determination key for modern dinoflagellate cysts. *Palynology*, 39(3), 387-409. <https://www.marum.de/Karin-Zonneveld/dinocystkey.html>
- Zonneveld, K. A., Marret, F., Versteegh, G. J., Bogus, K., Bonnet, S., Bouimetarhan, I., Crouch, E., de Vernal, A., Elshanawany, R., Edwards, L., Esper, I., Forke, S., Grosfeld, K., Henry, M., Holzwarth, U., Kielt, J-F., Kim, S-Y., Ladouceur, S., Ledu, D., Chen, L., Limoges, A., Londeix, L., Lu, S-H., Mahmoud, M.S., Marino, G.,

- Matsuoka, Matthiessen, J., Mildenhall, D.C., Mudie, P., Neil, H.L., Pospelova, V., Qi, Y., Radi, T., Richerol, T., Rochon, A., Sangiorgi, F., Solignac, S., Turon, J-L., Verleye, T., Wang, Y., Wang, Z., and Young, M. (2013). Atlas of modern dinoflagellate cyst distribution based on 2405 data points. *Review of Palaeobotany and Palynology*, 191, 1-197. <https://doi.org/10.1016/j.revpalbo.2012.08.003>
- Zorzi, C., Head, M. J., Matthiessen, J., and de Vernal, A. (2019). *Impagidinium detroitense* and *I.? diaphanum*: Two new dinoflagellate cyst species from the Pliocene of the North Pacific Ocean, and their biostratigraphic significance. *Review of Palaeobotany and Palynology*, 264, 24-37. <https://doi.org/10.1016/j.revpalbo.2019.02.005>
- Zorzi, C., and de Vernal, A., (in prep.). Plio-Pleistocene palynostratigraphy at ODP Site 882, northwest Pacific: biostratigraphy and paleoceanography.

Figures

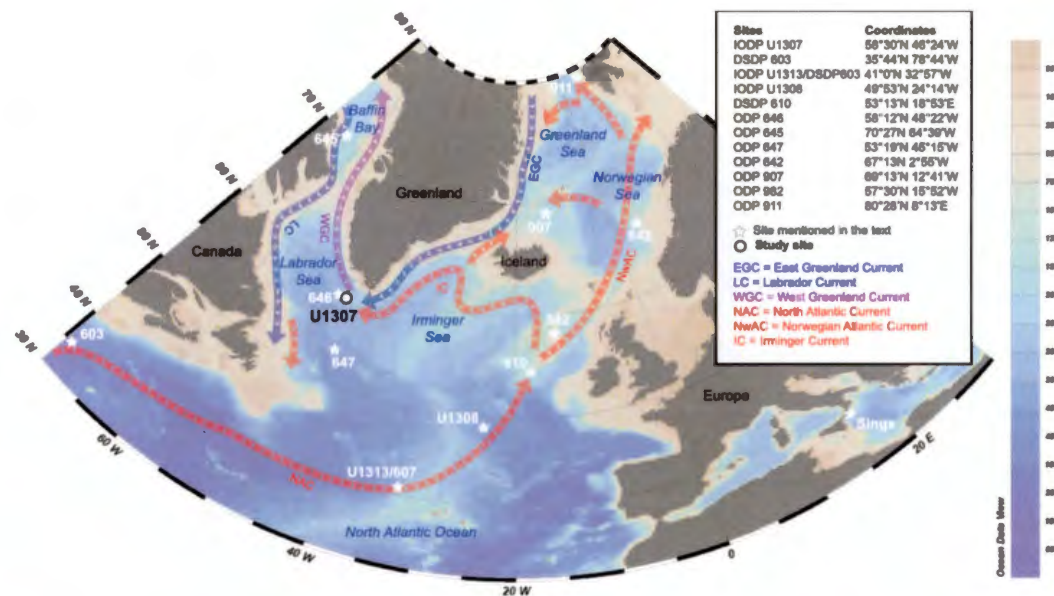


Figure 2.1 Map of the Labrador Sea showing the location of the study Site IODP U1307, the other sites mentioned in the text, and the present day surface currents (made with Ocean Data View, Schlitzer, 2018)

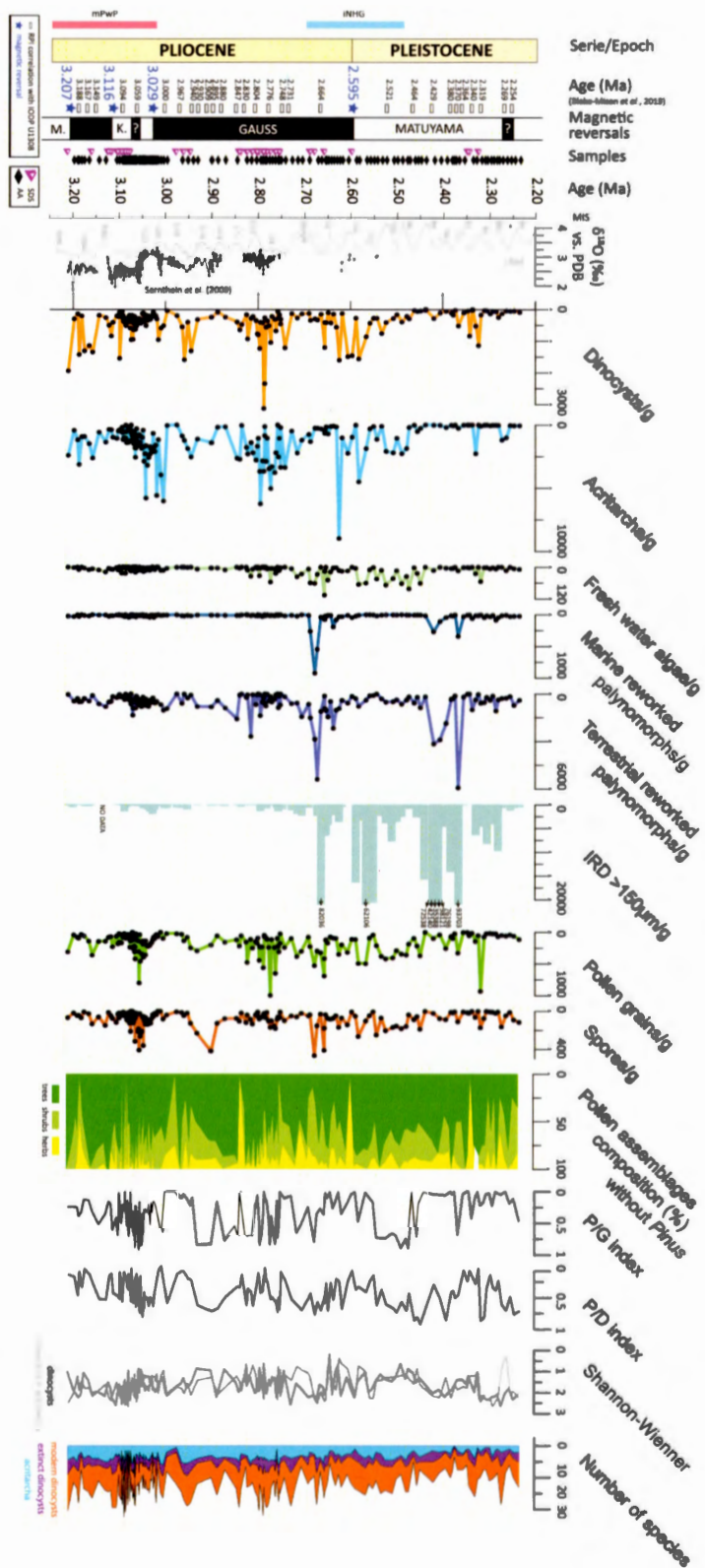


Figure 2.2 Concentration of dinocysts, acritarcha, fresh water algae, marine reworked palynomorphs (dinocysts and acritarcha), terrestrial reworked palynomorphs (pollen grains and spores), ice rafted debris $> 150\mu\text{m}$, and pollen grains and spores expressed in number of specimens per g of dry bulk sediment in IODP Site U1307. Pollen assemblage composition (%) of trees (dark green), shrubs (light green) and herbs (yellow), are expressed without *Pinus* as this genus is usually over-represented in marine sediments, notably in the Labrador Sea (Rochon and de Vernal, 1994). P/G index, P/D index. Shannon-Wiener index is showed with only dinocysts (black) and taking account of dinocysts and acritarcha (grey). Cumulated representation of the number of species of acritarcha (blue), extinct dinocysts (purple) and extand dinocysts (orange). Proportion of extinct species in the dinocysts assemblages in purple

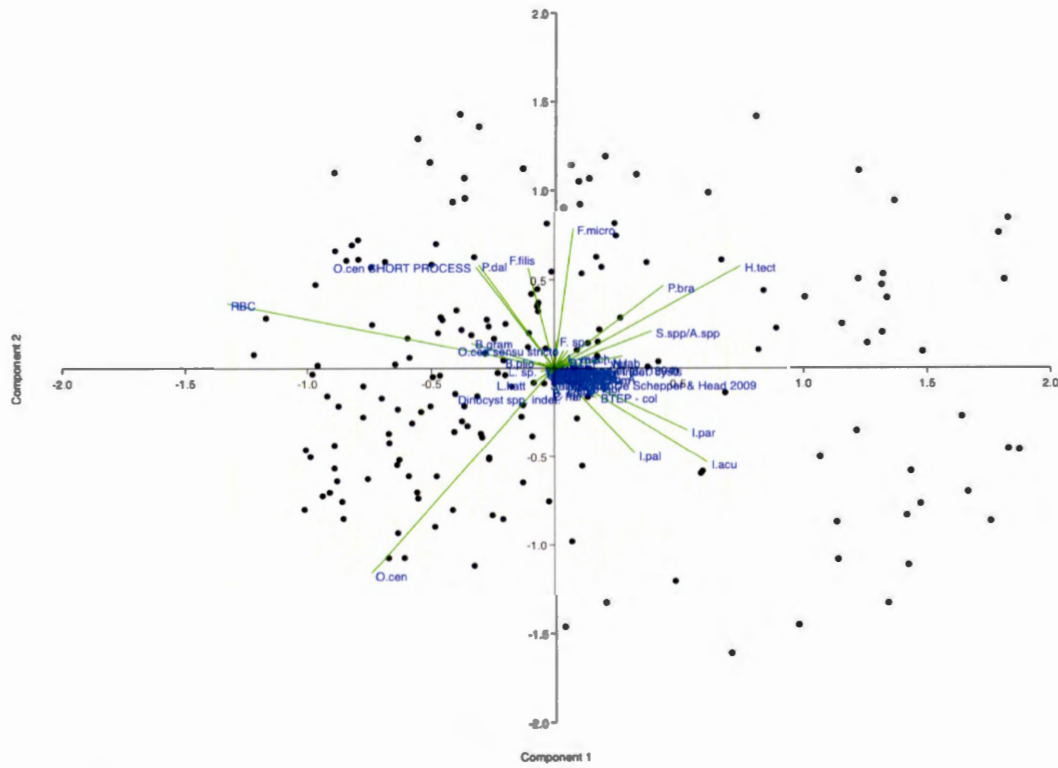


Figure 2.3 Results from Principal Component Analysis (PCA) performed on dinocyst percentages in samples from IODP Site U1307 after a logarithmic transformation to increase the weight of accompanying taxa. The first component (PC1) is represented on the vertical axis and the second component (PC2) is represented on the horizontal axis

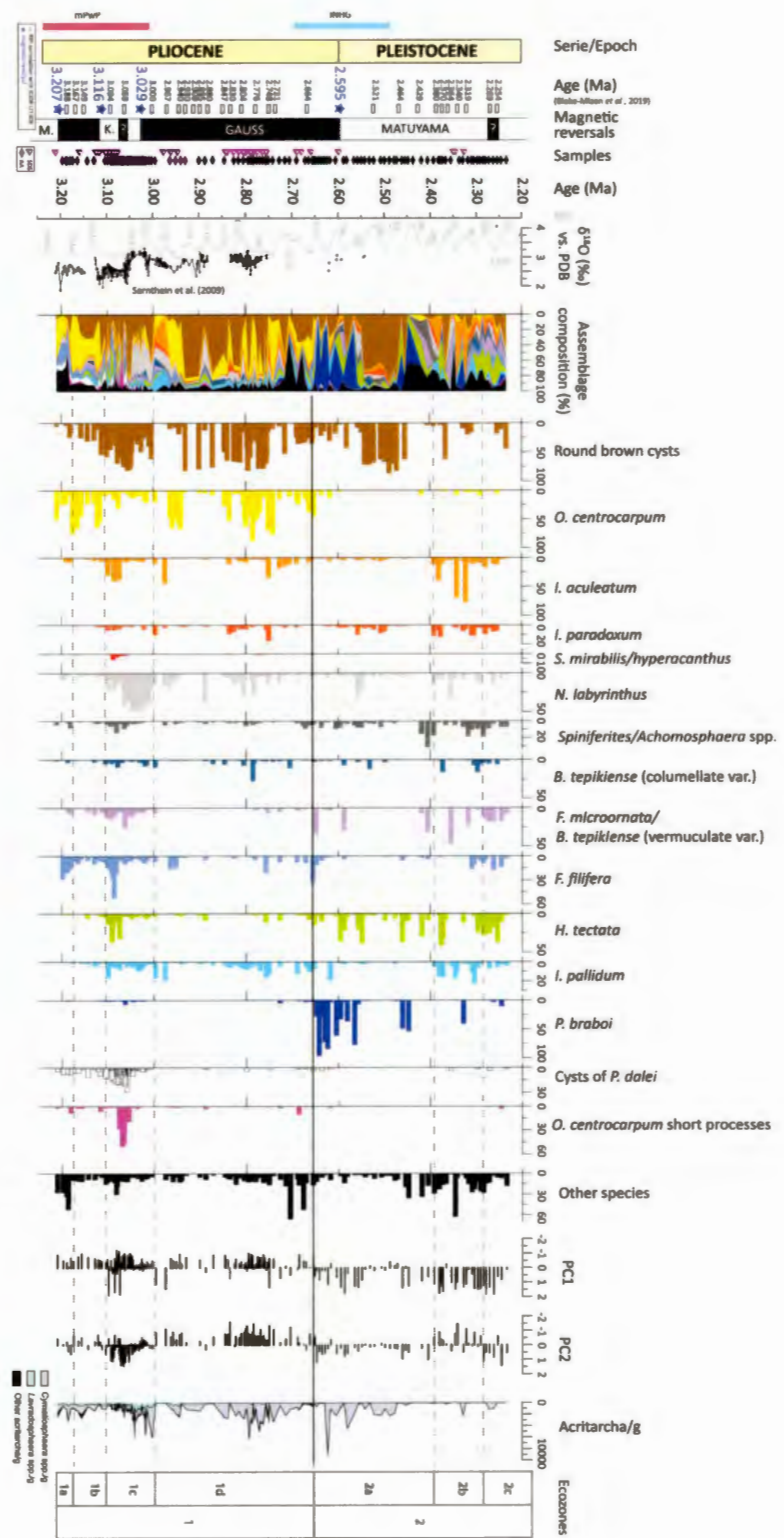


Figure 2.4 Relative abundance (%) of selected dinocysts according to PC scores and associated to variations of the PC1 and PC2 axis in IODP Site U1307 between 3.2 to 2.2 Ma. “Other species” includes all taxa cited in Table 2.2 in regular text and white background. Ecozone boundaries are shown with plain back lines and the subzone boundaries with dashed lines. Samples with less than 10 cysts/sample are not included in the figure. Samples counted by S. De Schepper are shown with purple triangles and samples counted by A. Aubry are shown with black diamonds. The age model is from Blake-Mizen *et al.* (2019) based magnetic inversions (blue stars) and Relative Paleo-Intensity (RPI) correlation with IODP Site U1308 (white rectangles). Planktic foraminifer stable oxygen isotope data are from Sarnthein *et al.* (2009) in black and the reference stack of benthic foraminifer stable isotope from Lisiecki and Raymo (2005) referred to as LR04 is in grey with marine isotopic stages indicated

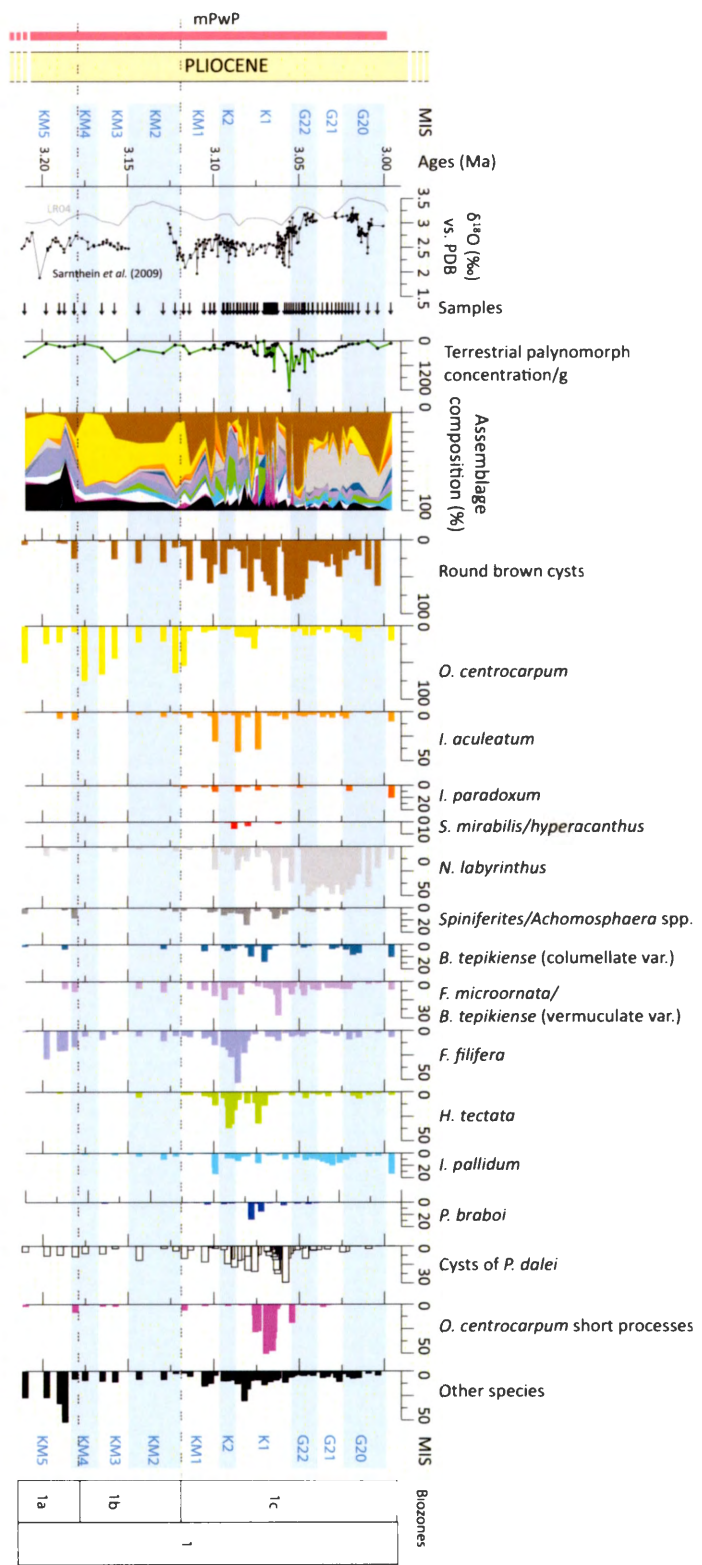


Figure 2.5 Close-up of terrestrial palynomorph concentration (per g) and the relative abundances (%) of selected dinocyst taxa according to PC scores and associated to variations of the PC1 and PC2 axis in IODP Site U1307 from the mPwP (subzones 1a, 1b and 1c) between 3.2 to 3.0 Ma. Cold Marine Isotope Stage are shaded in light blue

Tables

Depth (rmcd)	Age (Ma)	Type	Chronology	Upper boundary		Lower Boundary	
				sample	depth (rmcd)	sample	depth (rmcd)
117.63	2.25384	RPI	U1308				
118.51	2.2687	RPI	U1308				
120.52	2.31938	RPI	U1308				
121.3	2.34027	RPI	U1308				
121.86	2.3642	RPI	U1308				
122.05	2.37048	RPI	U1308				
122.4	2.38028	RPI	U1308				
123.11	2.42918	RPI	U1308				
123.53	2.46437	RPI	U1308				
123.96	2.52141	RPI	U1308				
124.88	2.595	Reversal	Gauss/Matuyama	U1307A-14H-3 143 cm	124.74	U1307A-14H-4 25 cm	125.06
127.32	2.66445	RPI	U1308				
129.1	2.73077	RPI	U1308				
129.73	2.74782	RPI	U1308				
132	2.77611	RPI	U1308				
135	2.80408	RPI	U1308				
136.03	2.82958	RPI	U1308				
136.86	2.84671	RPI	U1308				
137.47	2.88009	RPI	U1308				
138.13	2.89464	RPI	U1308				
138.54	2.90858	RPI	U1308				
138.8	2.93008	RPI	U1308				
139.31	2.94014	RPI	U1308				
141.12	2.96667	RPI	U1308				
143.76	3.00041	RPI	U1308				
147.97	3.029	Reversal	Kaena (t)	U1307A-17H-2 61 cm	147.81	U1307A-17H-2 97 cm	148.17
151.01	3.05942	RPI	U1308				
155.41	3.09399	RPI	U1308				
157.33	3.116	Reversal	Kaena (b)	U1307A-18H-2 31 cm	157.06	U1307A-18H-2 82 cm	157.57
166.48	3.14918	RPI	U1308				
168.96	3.16734	RPI	U1308				
170.7	3.18776	RPI	U1308				
174.48	3.207	Reversal	Mammoth (t)	U1307A-19H-6 60 cm	173.93	U1307A-19H-6 120 cm	174.53

Table 2.1 Age model tie points used in IODP Site U1307 from Blake-Mizen *et al.* (2019)

Dinocysts	extinct	extant	G	P	O	N
<i>Amiculosphaera umbraculum</i>	x	x				
<i>Ataxiodinium choone</i>		x	x			
<i>Ataxiodinium confusum</i>	x		x		x	
<i>Ataxiodinium ? sp.</i>	x	x				
cf. <i>Alexandrium?</i>						
<i>Barssidinium graminosum</i>	x		x		x	
<i>Barssidinium plicenicum</i>	x		x	x		
<i>Barssidinium sp.</i>	x		x	x		
<i>Baticasphaera minuta</i>	x	x				
<i>Baticasphaera sp. ?</i>	x					
<i>Bitectatodinium readwaldii</i>	x	x				
<i>Bitectatodinium tepikiense</i>	x	x	x			
<i>Bitectatodinium tepikiense - columnate</i>	x	x	x			
<i>Bitectatodinium tepikiense - vermiculate</i>	x	x	[x]			
<i>Bitectatodinium sp. A De Schepper et al. (2017)</i>		x				
<i>Bitectatodinium spp.</i>	x	x				
<i>Cerebrocysta? namencensis</i>	x	x				
cf. <i>Cerebrocyta</i>	x	x				
<i>Cordospharodium minimum</i>	x	x				
<i>Corrudinium harlandii</i>	x	x				
<i>Corrudinium harlandii / Pyxidinopsis reticulata</i>	x					
<i>Corrudinium labradori</i>	x	x				
<i>Corrudinium sp.</i>	x					
<i>Dubridinium spp.</i>		x	x			
<i>Echinidium zonneveldeae</i>	x		x	x		
<i>Echinidium spp.</i>	x		x	x		
<i>Filisphaera spp.</i>	x	x				
<i>Filisphaera filifera</i>	x	x				
<i>Filisphaera microornata</i>	x	x				
<i>Habibacysta tectata</i>	x	x				
<i>Habibacysta sp. A</i>	x	x				
<i>Habibacysta sp. Head et al., 1994</i>	x	x				
<i>Heteraulacocysta sp. Costa & Downie 1979</i>	x					
<i>Impagidinium aculeatum</i>	x	x	x			
<i>Impagidinium cantabrigiense</i>	x	x	x			
<i>Impagidinium cf. cantabrigiense</i>	x	x	x			
<i>Impagidinium pallidum</i>	x	x	x			
<i>Impagidinium paradoxum</i>	x	x	x			
<i>Impagidinium sp. cf. paradoxum</i>	x	x	x			
<i>Impagidinium patulum</i>	x	x	x			
<i>Impagidinium plicatum</i>	x	x	x			
<i>Impagidinium sphaeritum</i>	x	x	x			
<i>Impagidinium solidum</i>	x	x	x			
<i>Impagidinium striatum</i>	x	x	x			
<i>Impagidinium cf. velorum</i>	x	x	x			
<i>Impagidinium sp. granular form</i>	x	x	x			
<i>Impagidinium spp. Indet.</i>	x	x				
<i>Impagidinium sp. 2 of De Schepper & Head 2009</i>	x					
<i>Invertocysta spp.</i>	x					
<i>Invertocysta lacrymosa</i>	x	x				
<i>Invertocysta tabulata</i>	x					
<i>Icelandium brevispinosa</i>		x	x			
<i>Icelandium ? cesare</i>	x	x	x			
<i>Icelandium minutum</i>	x	x	x			
<i>Lejeuneocysta spp.</i>	x	x				
<i>Lejeuneocysta catomus</i>	x		x	x		
<i>Lejeuneocysta hattersensis?</i>	x		x	x		
<i>Lejeuneocysta mariae</i>	x		x	x		
<i>Lejeuneocysta sp. A</i>	x		x	x		
<i>Lingulodinium machaeorophorum</i>	x	x				
<i>Melitasphaeridium choanophorum</i>	x		x			
<i>Nematosphaeropsis labyrinthus</i>	x	x	x			
<i>Nematosphaeropsis lativittata</i>	x		x			
<i>Operculodinium spp.</i>		x				
<i>Operculodinium centrocarpum sensu Wall & Dale (1966)</i>		x	x			
<i>Operculodinium centrocarpum sensu stricto</i>	x		x			
<i>Operculodinium centrocarpum sensu Wall & Dale (1966) short process form</i>		x	x			
<i>Operculodinium piaseckii</i> (Schreck, 2012)	x		x			
<i>Operculodinium ? elrikianum elrikianum</i>	x		x			
<i>Operculodinium ? elrikianum crebrum</i>	x		x			
<i>Operculodinium centrocarpum/israelianum</i>		x				
Dinocysts	extinct	extant	G	P	O	N
Cyst of <i>Pentaspharodinium dalei</i>						
<i>Piccolodinium sp. ??</i>			x	x	x	
<i>Polykrikos sp.?</i>			x		x	
<i>Pyxidinopsis brabot</i>	x		x			
<i>Pyxidinopsis psilata</i>			x			
<i>Pyxidinopsis reticulata</i>			x			
<i>Pyxidinopsis tuberculata</i>	x		x			
<i>Pyxidinopsis spp.</i>			x			
<i>Reticulatosphaera actinocoronata</i>	x		x			
<i>Selenopemphix brevispinosa</i>	x		x	x		
<i>Selenopemphix diaeocysta</i>	x		x	x		
cf. <i>Selenopemphix quanta</i>			x	x	x	
<i>Selenopemphix nephoides</i>	x		x	x		
<i>Selenopemphix spp.</i>			x	x		
<i>Spiniferites elongatus</i>	x	x				
<i>Spiniferites membranaceus</i>	x	x				
<i>Spiniferites mirabilis/hyperacanthus</i>	x	x				
<i>Spiniferites ramosus?</i>	x					
<i>Spiniferites rubinus</i>						
<i>Spiniferites granular form</i>						
<i>Spiniferites sp. A</i>						
<i>Spiniferites/Achomosphaera spp. Indet.</i>			x	x		
<i>Tectatodinium sp. A</i>						
<i>Tectatodinium pellitum</i>	x		x			
<i>Trinovantedinium variable</i>	x		x	x		
<i>Trinovantedinium glorianum</i>	x		x	x		
<i>Trinovantedinium spp.</i>	x		x	x		
<i>Brigantedinium auranteum</i>	x		x	x		
<i>Brigantedinium carioceps</i>	x		x	x		
<i>Brigantedinium majusculum</i>	x		x	x		
<i>Brigantedinium simplex</i>	x		x	x		
<i>Brigantedinium sp.</i>	x		x	x		
round brown cysts	x		x	x		
Brown Indet. cysts	x		x	x		
Brown cysts spp.						
Cyst of <i>Scrippsiella trifida</i>					x	
Cysts type I of de Vernal & Mudie 1989	x		x			
Dinocyst sp. A						
Dinocyst sp. B						
Dinocyst spp. Indet.						
Acritarcha	extinct	extant	G	P	O	N
<i>Cymatosphaera ? aegirii</i>	x					
<i>Cymatosphaera ? fensomei</i>	x					
<i>Cymatosphaera ? icernorum</i>	x					
<i>Cymatosphaera ? invaginata</i>	x					
<i>Cymatosphaera ? laptisepa</i>	x					
<i>Cymatosphaera sp.2 of Schreck 2013</i>						
<i>Cymatosphaera sp.1 of Schreck 2013</i>						
<i>Cymatosphaera spp.</i>	x					
<i>Lavradosphaera canalis</i>	x					
<i>Lavradosphaera crista</i>	x					
<i>Lavradosphaera lucifer</i>	x					
<i>Lavradosphaera spp.</i>	x					
<i>Leiosphaeridia rockhallensis</i>	x					
<i>Leiosphere spp.</i>						
Ornamented leiosphere						
* Leiosphere large folded *						
* Leiosphere, small spherical thick wall *						
* Leiosphere 'ornamented', angular pyrme *						
<i>Mycristridium spp.</i>	x					
<i>Cystidiopsis certa</i>	x					
<i>Nanoborpha walldalei</i>	x					
<i>Pterospermella sp.</i>	x					
Cyst 1 of de Vernal & Mudie 1989	x					
Acritarch sp. 1 of Hennissen 2013						
Acritarch sp. 6 of Hennissen 2013						
Acritarch sp. 9 of Hennissen 2013						
Acritarch spp. indet.						

Table 2.2 List of dinocyst and acritarch taxa recovered in samples from IODP Site U1307 between 3.2 and 2.2 Ma. Indication about their stratigraphic range, extinct or extend to modern, their ecological known affinities (from de Vernal *et al.*, 2013; Zonneveld *et al.* 2013 ; De Schepper *et al.*, 2011; Hennissen *et al.*, 2017), taxonomical affinities (P: Peridinoid cysts, G: Gonyaulacoid cysts), and neritic (N) to oceanic (O) distribution are given. The grouping of taxa is mentioned. Species used in Figure 4 are in bold with a grey background, all taxa grouped in “Other species” or “Other acritarcha” are in regular text with a white background

CHAPITRE III
BAFFIN BAY LATE NEOGENE PALYNOSTRATIGRAPHY AT ODP SITE 645

A. M. R. Aubry¹, A. de Vernal¹, P. Knutz²

¹GEOTOP, Université du Québec à Montréal, CP 8888, Montréal, QC, H3C 3P8,
Canada

²Geological Survey of Denmark and Greenland, Øster Voldgade 10, 1350 København,
Denmark

Keywords: Baffin Bay; Dinocysts; Palynology; Pliocene; Pleistocene; Biostratigraphy

Article soumis dans *la Revue Canadienne des sciences de la Terre*

Abstract

Analyses of marine and terrestrial palynomorphs of ODP Site 645 in Baffin Bay led us to define a biostratigraphical scheme covering the late Miocene to Pleistocene based on dinocyst and acritarch assemblages. Four biozones were defined. The first one, from 438.6 mbsf (meters below sea floor) to 388 mbsf, can be assigned a late Miocene to early Pliocene age (>4.5 Ma), based on the common occurrence of *Cristadinium diminutivum* and *Selenopemphix brevispinosa*. Biozone 2, spanning from an erosional unconformity to a recovery hiatus, is marked by the highest occurrences (HO) of *Veriplicidium franklinii* and *C. diminutivum*, which suggest an early Pliocene age (>3.6 Ma). Biozone 3, above the recovery hiatus and up to 220.94 mbsf, corresponds to late Pliocene or early Pleistocene based on occurrences of *Bitectatodinium readwaldii*, *Cymatiosphaera? icenorum* and *Lavradosphaera canalis*. Finally, between 266.4 and 120.56 mbsf, biozone 4, marked by the HO of *Filisphaera filifera*, *Filisphaera microornata* and *Habibacysta tectata*, has an early Pleistocene age.

Our biostratigraphy implies that horizon b1 of the Baffin Bay seismic stratigraphy by Knutz *et al.* (2015) corresponds to the recovery hiatus at ODP Site 645, which suggests a very thick Pliocene sequence along the Baffin Island slope. Dinocyst assemblages and terrestrial palynomorphs indicate that the late Miocene-early Pliocene were characterized by relatively warm coastal surface waters and boreal forest-forest tundra vegetation over surrounding lands. In contrast, the early Pleistocene dinocyst assemblages above the recovery hiatus indicate cool surface waters, while pollen data suggest reduced vegetation on surrounding lands.

3.1 Introduction

Baffin Bay is an important transitional basin for heat and salt exchanges between the Arctic and North Atlantic (NA) (Figure 3.1); it receives more than one third of the freshwater discharge from the drainage of the western Greenland ice sheet (e.g. Rignot and Mouginot 2012; Rignot *et al.* 2016). In the west, the Baffin Island Current (BIC), which feeds the Labrador Current (LC), carries large amounts of freshwater from the Arctic (Aksenov *et al.* 2010), impacting the surface water salinity and density in the Labrador Sea, thus the formation of intermediate/deep water mass (Cheng and Rhines 2004) and the Atlantic meridional overturning circulation (AMOC) (Lozier 2012; Rhein *et al.* 2015). In eastern Baffin Bay, the West Greenland Current (WGC) carries relatively warm and saline Atlantic waters northward (Tang *et al.* 2004; Zweng and Münchow 2006; Figure 3.1).

The Late Neogene ocean circulation in Baffin Bay may have been different from the modern pattern but large uncertainties about the paleo-configurations of through-flow remain. Regional plate tectonic reconstructions suggest that the channels of the Canadian Arctic Archipelago (CAA) were closed (Torsvik *et al.* 2002; Matthiessen *et al.* 2008), thus limiting regional inflow of Arctic waters. Moreover, the seismic profiles and sediment structures at Ocean Drilling Program (ODP) Site 645, situated in central Baffin Bay (Figure 3.1), led to suggest that local production of deep waters may have occurred after the middle Miocene, with strong contour currents in western Baffin Bay carrying dense water southward into the Labrador Sea (Cremer and Legigan 1989; Arthur *et al.* 1989; Hiscott *et al.* 1989). More recently, high-quality seismic reflection data from Baffin Bay provided evidence of contourite drift accumulations along the margins, which would correspond to an interval spanning the middle Miocene to late

Pliocene (Knutz *et al.* 2015). According to Knutz *et al.* (2015), the sedimentation was controlled by transport of North Atlantic water masses from the Labrador Sea/Irminger Sea across the Davis Strait and into eastern Baffin Bay. Northward flow of Atlantic waters is compatible with a mild regional climate over northeastern Canada, as inferred from boreal forest and peatland remains of Pliocene and early Pleistocene age on Ellesmere Island (Matthews and Ovenden 1990; Tedford and Harington 2003; Elias *et al.* 2006; Ballantyne *et al.* 2010) and Bylot Island (Csank *et al.* 2011; Guertin-Pasquier 2012). Hence, northward transport of warm and humid air masses toward high latitudes in the Labrador Sea-Baffin Bay corridor during the Pliocene likely played a role in the climate over Greenland and eastern Canada (Knutz *et al.* 2015). By the end of the Pliocene, the intensification of the Northern Hemisphere glaciation (iNHG) was followed by a general cooling, marking the transition from relatively warm conditions with atmospheric pCO₂ around 400 ppmv (Raymo *et al.* 1996; Seki *et al.* 2010; Bartoli *et al.* 2011) to the onset of the Quaternary glacial-interglacial oscillations (Zachos *et al.* 2001; Flesche Kleiven *et al.* 2002; Tripati *et al.* 2008; Matthiessen *et al.* 2008; De Schepper *et al.* 2014). In northwest Greenland, this transition was marked by westward expansion of the Greenland Ice Sheet on the shelves after ~2.7 Ma (Knutz *et al.* 2019).

The Ocean Drilling Program (ODP) Site 645 in central Baffin Bay (70°27.48'N, 64°39.30'W, 2018 m; Figure 3.1), drilled in 1985, provided a stratigraphic anchoring point to understand the Baffin Bay oceanographic gateway and its role in the iNHG (Srivastava *et al.* 1987). However, the sedimentary sequence recovered provided a limited paleoclimatological record due to poor recovery (~55%), sedimentary discontinuities, mass-transport deposits and rare microfossil content (Srivastava *et al.* 1987). Consequently, it was not possible to generate a robust paleomagnetic record from the correlation of geomagnetic polarity time scale with biostratigraphic data (Clement *et al.* 1989; Baldauf *et al.* 1989). Dinoflagellate cysts (hereafter dinocysts) and acritarchs, composed of resistant organic matter, were the only microfossils to be

regularly recovered in sediments from ODP Site 645 (de Vernal and Mudie 1989a; Head *et al.* 1989; Anstey 1992). However, the lack of a well-established reference Plio-Pleistocene dinocyst biostratigraphical scheme in the 1980s prevented precise dating inferences from dinocysts. Since then, major progress has been made concerning the Neogene dinocyst and acritarch taxonomy (Head 1993, 1996, 1997; Versteegh and Zevenboom 1995; Head and Norris 2003; De Schepper *et al.* 2004; De Schepper and Head 2008a, 2014; Schreck *et al.* 2012; Verhoeven *et al.* 2014) and the biostratigraphic scheme for the North Atlantic and Arctic Ocean has been completely revised (De Schepper and Head 2009; De Schepper *et al.* 2015, 2017; Schreck *et al.* 2012; Mattingdal *et al.* 2014; Matthiessen *et al.* 2018). The above-mentioned studies yield relatively well documented regional palynostratigraphy and provide us with the opportunity to improve the biostratigraphic scheme of ODP Site 645 and to document paleoenvironmental conditions in the light of a better constrained stratigraphical context. In the present paper, we revisit the palynostratigraphy of ODP Site 645 with the aim to optimize the definition of the Pliocene-Pleistocene transition in relation with the iNHG. Additionally, we revise the paleoenvironmental interpretation of the Pliocene to early Pleistocene interval and improve the chronology of a regional seismic marker horizon.

3.2 Stratigraphical context

The sedimentary sequence at ODP Site 645 covers the last ~16-24 Ma. It is characterized by terrigenous silty clay and muds and sandy silts, with three major lithological units (cf. Srivastava *et al.* 1987; Figure 3.2). Unit I (0-168.1 meters below

sea floor – mbsf) is composed of alternating beds of calcareous muddy sands and silts with gravel associated with ice rafted debris (IRD). Unit II (168.1–335 mbsf) comprises silty mud, clayey silt and silty clays with some dropstones and other IRD. Unit III (335–1147.1 mbsf) consists of homogeneous, poorly sorted muddy sand with IRD associated with turbiditic currents (subunit IIIA) and bottom currents (subunits IIIB and IIIC) (Srivastava *et al.* 1987; Arthur *et al.* 1989; Busch 1989; Hall and King 1989).

Four seismic sequences have been defined based on their uniformity and seismic characteristics (Figure 3.2, Srivastava *et al.* 1987). Sequence 1 from the seafloor to the top of reflector R1 (388 mbsf) corresponds to lithologic units I and II. It is subdivided in subsequence 1A (0–167 mbsf), which is composed of horizontal and uniform interbedded deposits, subsequence 1B (167–388 mbsf), which has chaotic internal reflectors suggesting multiple episodes of sediment redeposition or mass transport deposit (cf. Knutz *et al.* 2015), and subsequence 1C. Subsequence 1C is relatively thin at Site 645 and nearly absent westward but reaches thickness of 900 meters in the eastern basin. At Site 645, subsequence 1C consists of interbedded sediments between 330 and 388 mbsf, just above reflector R1 that marks an erosional unconformity (Srivastava *et al.* 1987; Arthur *et al.* 1989). Seismic sequence 2 encompasses lithologic units IIIA and IIIB and comprises flat layers from below reflector R1 down to ~546 mbsf. The high-resolution seismic profiles of Knutz *et al.* (2015) show disorganized structures in the lower part of unit IIIA, which was interpreted as the result of mass transport deposition. The base of seismic sequence 3 corresponds to the strong reflector R2, expressing an unconformity at 913 mbsf. Sequence 3 is composed of relatively continuous reflectors and corresponds to lithologic subunit IIIC.

The detailed seismic survey of the northwest Greenland margin by Knutz *et al.* (2015) includes long-distance, cross-basin correlations with the ODP Site 645 stratigraphy, which led to propose a middle Miocene to late Pliocene age for Unit III and a

Pleistocene age for Unit II and Unit I (Figure 3.2). However, the seismic profile does not precisely cross ODP Site 645 as the nearest point of the line is located 17 km south of the drilling site and the exact well-tie is complicated by a series of submarine slides that back-step from the deep basin across the rise and lower part of the slope. Moreover, because of a ~40 m recovery hiatus between Unit III and Unit II at ODP Site 645, the location of the Pliocene to Pleistocene transition at ODP 645 remains uncertain.

3.3 Material and methods

3.3.1 Palynological preparation

A total of 32 samples collected at about ~10 m intervals were analyzed. Samples were taken in cores from 2 different holes: 12 samples were collected below the recovery hiatus in Hole 645D between 438.6 mbsf and 340.6 mbsf in the lithological Unit IIIA; 20 samples were collected above the hiatus in Hole 645B between 302.05 mbsf and 120.56 mbsf in Units II (n=14) and IB (n=6).

Samples were prepared and analyzed at the Geotop Micropaleontology Laboratory in Montreal. Standard laboratory procedures of de Vernal *et al.* (1999) were used for 22 of the samples. *Lycopodium clavatum* spore markers were added to each sample before chemical treatment for quantitative estimation of palynomorph concentrations (Matthews 1969; Mertens *et al.* 2009). Sample preparation includes wet sieving at 10 and 106 µm to remove the fine fraction including fine silts and clays and the coarse fraction (IRD, foraminifera, radiolaria, etc.), chemical treatment of the remaining

fraction (10-106 µm) with warm hydrochloric acid (HCl, 10%) and warm hydrofluoric acid (HF, 48%) to dissolve calcium carbonate and silicate particles respectively (cf. de Vernal *et al.* 1999). In addition, to remove remaining silicates, we used sodium polytungstate in a solution calibrated at a specific gravity of 2 (Munsterman and Kerstholt 1996). According to Mertens *et al.* (2009), this technique does not change dinocyst results. In order to enhance the sampling resolution between 130 mbsf and 326 mbsf and above the recovery hiatus, we also used the residue of 10 samples from the previous study by de Vernal and Mudie (1989a), which were archived at Geotop. For these samples, a *Eucalyptus globulus* suspension was used for concentration calculations instead of *Lycopodium* tablets. Samples were wet sieved between 10 and 125 µm and the 10-125 µm fraction was successively treated with cold HCl (10%), warm HF (48%) and warm HCl (10%) prior to wet sieving with distilled water at 10 µm.

The residual organic matter of all 34 samples was mounted between slide and cover slide in glycerin jelly. All samples are stored at the Geotop Micropaleontology Laboratory.

3.3.2 Palynological analysis

Identification and count of palynomorphs were performed on a Leica DMR at a magnification of x400 or x1000, using transmitted light. Concentrations (Figure 3.3) were calculated with the marker grain method (Matthews 1969; Mertens *et al.* 2009). This approach yields results with an accuracy of ± 10% for a confidence interval of

95% (de Vernal *et al.* 1987; Mertens *et al.* 2009). When possible, 2 or 3 slides were analyzed to achieve a statistically representative number of specimens per sample. Despite our efforts, some samples remain poorly defined because of low material availability and/or low content of dinocysts (Table S1). Samples with less than 20 dinocysts per sample were not taken into consideration for paleoecological interpretations. Dinocyst and acritarch identification follow the nomenclature of Williams *et al.* (2017). Reworked dinocysts were identified according to their known stratigraphic range (extinct in the Mesozoic and/or Tertiary) and/or preservation state (Figure 3.4). Stratigraphic occurrence of selected dinocysts and acritarchs is illustrated in Figure 3.5 based on concentrations as follows: occasional (<10 cysts/g), few (10-100 cysts/g), common (100-1000 cysts/g), abundant (> 1000 cysts/g).

Spores and pollen grains were identified based on the nomenclature of McAndrews *et al.* (1973), Bassett *et al.* (1978) and Kapp *et al.* (2000). The preservation state of terrestrial specimens was used to distinguish 3 categories (Table 3.1, Figure 3.4). For clarity purposes and to avoid interpretation bias, we discarded intermediate forms (category 2); we show only the results from well-preserved pollen and spores (category 1) and unquestionably reworked palynomorphs (category 3) in Figure 3.3.

All raw data and the list of all dinocyst and acritarch taxa encountered are available in Supplementary Tables S1 and S2.

3.4 Results

3.4.1 Palynological content

In the 32 analyzed samples, palynomorphs were moderately to well preserved but folding or orientation prevented identification of some specimens. The palynological assemblages include dinocysts, acritarchs, freshwater algae, *Halodinium*, pollen grains and spores in addition to reworked palynomorphs. In general, palynomorph concentrations are high in lithologic units IIIA and II, between 220.94 and 438.6 mbsf, and very low in lithologic unit IB, between 209.89 and 120.56 mbsf (Figure 3.3, Table S1).

Dinocysts occur in all samples between 120.56 mbsf and 438.6 mbsf except for one at 302.05 mbsf (Figure 3.3), and concentrations range from 5 to 2969 cysts/g with an average of 472 cysts/g. The concentration of acritarchs is lower than that of dinocysts with an average of 237 acritarchs/g and a maximum of 2239 acritarchs/g (Figure 3.3). Two intervals are characterized by particularly high concentration of pollen grains and spores: one between 220.94 and 276 mbsf (average 765/g) and the other between 353.4 and 392 mbsf (average of 1372/g) (Figure 3.3).

Marine and terrestrial reworked palynomorph concentrations are higher in the lower part of the study interval between 353.4 and 438.6 mbsf with a maximum of 2131 marine reworked palynomorphs/g at 421.94 mbsf and 1733 terrestrial older reworked palynomorphs/g at 399.2 mbsf (Figure 3.3). In the upper part of the study sequence, above the recovery hiatus, concentrations of reworked palynomorphs are very low (Figure 3.3).

3.4.2 Biostratigraphy

Four dinocyst and acritarch biozones were defined based on species distribution and assemblages using Lowest (LO) and Highest Occurrence (HO) of taxa (Figure 3.5, Figure 3.6) in addition to species diversity and abundances. We used bio-events and stratigraphical range of marker species (Table 3.2) as defined from the eastern North Atlantic Ocean (DSDP Site 610, De Schepper and Head 2008a, 2008b, 2009), the Norwegian Sea (ODP Site 642, De Schepper *et al.* 2015, 2017) and the Iceland Sea (ODP Site 907, Schreck *et al.* 2012, 2013).

3.4.3 Dinocyst assemblages

The dinocysts assemblages include a total of 58 taxa (Table S2) among them 16 taxa were used for paleoecological interpretations (Figure 3.7, Table 3.3). Assemblages are commonly dominated by Protoperidinale cysts (100% at 130 mbsf), which include all brown cysts and brown spiny cysts, *Echinidinium* spp., *Selenopemphix brevispinosa*, *Selenopemphix nephroides*, *Selenopemphix dionaceacysta*, *Lejeunecysta cinctoria*, *Lejeunecysta fallax*, *Lejeunecysta mariae* (Table S1). The second most abundant dinocyst taxa include *Filisphaera filifera* and *Filisphaera microornata/Bitectatodinium tepikiense* (vermiculate var.) group with up to 42% and 55% at 372.6 and 286.42 mbsf,

respectively (Figure 3.7; Table S1). The remaining part of the assemblages is composed of *Operculodinium centrocarpum*, *Reticulatosphaera actinocoronata*, *Melitaspharodinium choanophorum*, *Impagidinium aculeatum*, *Impagidinium paradoxum*, *Nematosphaeropsis labyrinthus*, *Spiniferites/Achomosphaera* spp., *Bitectatodinium tepikiense* (columellate var.), *Habibacysta tectata*, *Impagidinium pallidum*, *Spiniferites elongatus/frigidus*, *Pyxidinopsis braboi* and the cyst of *Pentapharsodinium dalei* (Figure 3.7).

3.4.4 Pollen grains and spores

We report only the well-preserved terrestrial palynomorphs in Fig. 3 (Table 3.1). They record concentrations ranging from 12 to 3219 pollen grains/g (Table S1, Figure 3.3). Pollen and spore assemblages are relatively uniform in the study interval. They are dominated by tree pollen, recording an average of 70% (Figure 3.3, Table S1). Shrubs percentages (~26%) are higher in the lower part of our study interval below the recovery hiatus with mean values of 82 grains/g, while an average of 22 grains/g is recorded above. Herb pollen grains are present in low concentration and represent only 4% of the assemblages (Figure 3.3, Table S1).

Spore concentrations are high between 392 and 353.4 mbsf (up to 996 spores/g). The dominant spore type is *Sphagnum*, which is a bryophyte typical of peatbogs that accounts roughly for 70% of the assemblages (Figure 3.3, Table S1).

3.5 Discussion

3.5.1 Palynostratigraphy and chronological implication

The age determinations from biostratigraphical markers made below assume that dinocysts and acritarchs have similar stratigraphic ranges at the study site compared with other northern North Atlantic Ocean sites (DSDP Site 610: De Schepper and Head 2008a, 2008b, 2009; ODP Site 642: De Schepper *et al.* 2015, 2017; ODP Site 907: Schreck *et al.* 2012, 2013; Table 3.2; Figure 3.1). The recent studies of De Schepper *et al.* (2015, 2017) and Matthiessen *et al.* (2018), however, highlighted diachronism in stratigraphical ranges of bio-events (acme), HO and LO of dinocysts and acritarchs across the North Atlantic Ocean, the Nordic Seas and the Arctic Ocean. Nevertheless, we defined biozones (Figure 3.5) and made attempts to provide age estimates based on the dinocyst and acritarch occurrences at ODP 645 using biostratigraphical information from the literature (Table 3.2).

Biozone 1 (> 4.5 Ma)

Biozone 1 (438.6 - 392 mbsf) is consistent with a late Miocene to early Pliocene age, older than ~ 4.5 Ma based on common occurrences of *Cristadinium diminutivum* and *S. brevispinosa* (Figure 3.5, Figure 3.6), which both range up in the early Pliocene (~4.6 Ma) in the Norwegian and Iceland seas and characterize the Miocene in the Labrador Sea (Table 3.2). Moreover, the acritarch *Veriplicidium franklinii* (Figure 3.6) has a known range extending from late Miocene to early Pliocene (8.2- 4.5 Ma) in the

northern North Atlantic (Table 3.2), and the HO of *Reticulosphaera actinocoronata* (Figure 3.6) occurred between 4.8 and 4.4 Ma at several sites of the North Atlantic (Table 3.2). Other species restricted to Biozone 1 and suggesting a late Miocene to early Pliocene age include *Batiacasphaera hirsuta*, *Lejeunecysta cintoria* and *Operculodinium? eirikianum eirikianum* (Table 3.2). These taxa, however, occur in low numbers.

The base of Biozone 1 corresponds to undisturbed sediments (Srivastava *et al.* 1987; Arthur *et al.* 1989) likely representing in situ deposition of pelagic microfossils, such as dinocysts and acritarchs. The seismic reflector R1 at 388 mbsf, which is interpreted as an erosional unconformity (Srivastava *et al.* 1987; Arthur *et al.* 1989), marks the top of Biozone 1.

Biozone 2 (> 3.6 Ma)

In Biozone 2 (380.65-340.6 mbsf) the HOs of *V. franklinii*, *C. diminutivum*, the *Batiacasphaera micropapillata* complex and *S. brevispinosa* indicate an early Pliocene age, necessarily older than 3.6 Ma (Figure 3.5, Table 3.2). Biozone 2 is also marked by the first continuous occurrence of *F. filifera*, which is also consistent with a Pliocene age assignment (see Matthiessen *et al.* 2018).

Biozone 2 ranges from the sedimentary hiatus (reflector R1) at 388 mbsf to the recovery hiatus (Srivastava *et al.* 1987; Arthur *et al.* 1989). It corresponds to ODP Site 645 seismic unit 1C that consists of a thin layer (~50 m) of interbedded muddy sand and silt (Srivastava *et al.* 1987; Arthur *et al.* 1989).

Biozone 3: Late Pliocene or early Pleistocene? (302.05-220.94 mbsf)

The top of Biozone 3 (302.05 - 276 mbsf) is defined based on the highest significant occurrence of *R. actinocoronata*, *Operculodinium cf. tegillatum* and *Bitectatodinium readwaldii* (Figure 3.5). The dinocyst and acritarch assemblages in Biozone 3 are difficult to interpret. The occurrence of *R. actinocoronata* may suggest an early Pliocene age, but acritarchs *Cymatiosphaera? icenorum* and *Lavradosphaera canalis* rather point to a late Pliocene-early Pleistocene age (Table 3.2). This interval is also marked by relatively high number of dropstones (Figure 3.3) as reported by Korstgård and Nielsen (1989), thus suggesting a significant expansion of marine-based ice margins around Baffin Bay at the time. A supporting argument for a late Pliocene age is the strong IRD pulse around 300 mbsf with the onset of trough-mouth fan progradation (Knutz *et al.* 2019; Hofmann *et al.* 2016). The HO of *R. actinocoronata* was used as a synchronous bio-event for early Pliocene (~4.4 Ma) correlation throughout the North Atlantic including the Nordic Seas (Table 3.2). Specimens of this species were found in low number in late Pliocene sediments of Belgium and the Norwegian Sea and were interpreted to be reworked (Louwye and De Schepper 2010; De Schepper *et al.* 2017). At ODP site 645, the sample at 276 mbsf in Biozone 3 contains high number of *R. actinocoronata* (~228 cysts/g; Figure 3.5), challenging the reworking interpretation. In Biozone 3, the co-occurrence of *Cymatiosphaera? fensomei*, *Lavradosphaera canalis* and *Lavradosphaera crista* in addition to *Invertocystsa lacrymosa* up to 278.9 mbsf indicates an age not younger than 2.3 Ma (Anstey 1992), which is also compatible with a late Pliocene-early Pleistocene age.

Biozone 3 corresponds to seismic subsequence 1B, which is composed of chaotic internal reflectors that may be interpreted as mass-transport disturbance (Srivastava *et al.* 1987; Arthur *et al.* 1989; Knutz *et al.* 2015; Figure 3.8 and Figure S1). Hence, although we should be cautious with the biostratigraphical interpretation of

microfossils, our results indicate that mass transport in this interval dates back to the Pliocene/ early Pleistocene.

Biozone 4 (early Pleistocene)

The dinocyst and acritarch assemblage of Biozone 4 (266.4 to 120.56 mbsf) suggests an early Pleistocene age based on HO of *F. filifera*, *F. microornata* and *H. tectata* (Figure 3.5, Table 3.2, see Matthiessen *et al.* 2018). Sediments below 170 mbsf are older than ~1.4 Ma according to the highest persistent occurrence (HPO) of *H. tectata* and the top of the acme of *F. filifera*, which are considered as super bio-events across the North Atlantic and Arctic oceans (cf. Matthiessen *et al.* 2018). Furthermore, the common occurrence of *C.? invaginata* up to 220.94 mbsf at ODP 645 may suggest an age of 2.3 Ma, perhaps slightly younger, based on a comparison with the IODP Site 1307 record in the Labrador Sea (Aubry *et al.* accepted).

Biozone 4 corresponds to the lithologic units II and IB, which contain abundant IRD (Srivastava *et al.* 1987, Arthur *et al.* 1989). It also corresponds to early Pleistocene unit mu-a of Knutz *et al.* (2015).

3.5.2 Implications for the interpretation of the seismic stratigraphy

The transition between biozones 1 and 2 has an early Pliocene age (~4.5 Ma) according to our study. It is located above horizon b1 in the seismic profile of Knutz *et al.* (2015), which was assigned to the late Pliocene in the original interpretation (Knutz *et al.*, 2015). Consequently, our biostratigraphy and the recognition of back-stepping slide scars in the upper part of the seismic profile led us to revise the seismic stratigraphic interpretation in the vicinity of ODP Site 645 (Figure 3.8). According to our biostratigraphy, horizon b1 transgresses now across two slide scars and intersects ODP Site 645 at its nearest point at a level corresponding to the recovery hiatus (~340-300 mbsf), thus indicating higher sediment thickness of unit mu-b. This interpretation of the seismic stratigraphy implies that the contourite features on the middle to upper slope influenced by mass-wasting are part of unit mu-b. Despite remaining uncertainties due to disrupted package and distance from the borehole, this interpretation is in better harmony with the observation of similar upslope climbing contourite features on the northwest Greenland margin (Knutz *et al.* 2015). Moreover, it implies a late Pliocene age for horizon b1, which also agrees with stratigraphical correlation with West Greenland wells (Knutz *et al.* 2019).

According to our biostratigraphy, the study interval encompasses the stratified interval of late Miocene/early Pliocene age below horizon b1 and early Pleistocene above the recovery hiatus. Horizon b1 now corresponds to the base of the recovery hiatus with a late Pliocene age (Figure 3.8).

3.5.3 Paleoclimatic inferences

Abundant pollen grain and spores (1000-3000 grains/g) in samples older than 2.3 Ma (Figure 3.3) suggest close location of the vegetation source area. The concentrations of terrestrial palynomorphs and fresh algae exceed those of marine palynomorphs, including dinocysts and acritarchs (Figure 3.3), which indicates a nearshore environment with inputs from runoff and hydrodynamical transport (e.g., Rochon and de Vernal 1994) from the late Miocene/early Pliocene to early Pleistocene.

The variable preservation state of terrestrial palynomorphs may result from multiphase grain transport and deposition with wet-dry cycles (rivers-subaerial weathering) and/or chemical-mechanical damaging environmental conditions such as oxidation, turbid transport, bacterial degradation, etc. (see Campbell 1999; Tweddle and Edwards 2010 and references therein). Considering the epicontinental context of Baffin Bay, inputs from washed soils through runoff and river flow are compatible with our observations. For example, similar concentrations of palynomorphs, including dinocysts, pollen grains, spores and reworked material, have been reported in postglacial sediment from Hudson Bay (Bilodeau *et al.* 1990).

Pollen and spore assemblages of the study interval reflect inputs from boreal forest and/or forest tundra. Conifer tree taxa such as spruce (*Picea*), pine (*Pinus*) and fir (*Abies*) are common, together with shrub taxa such as willow (*Salix*), birch (*Betula*), alder (*Alnus*) and Ericaceae. Assemblages contain abundant *Pinus*. However, this genus is usually over-represented in marine sediment cores because of high pollen production and long-distance atmospheric and hydrodynamic transport (Rochon and de Vernal, 1994). Hence, despite the dominance of *Pinus* pollen, the overall assemblages may indicate open coniferous woodland. High concentration of spores,

especially pteridophytes (*Lycopodium*, *Selaginella*) and *Sphagnum*, implies humid land conditions and extensive peatlands (Figure 3.3). Such assemblages are concordant with those of other high latitude Pliocene records, such as those from the Beaufort formation and reflect humid, cool-temperate to subarctic vegetation over the landmasses surrounding Baffin Bay (Matthews *et al.* 1986; Matthews and Ovenden 1990; Vincent 1990; Fyles *et al.* 1994; Matthews and Fyles 2000; Tedfort and Harington 2003; Elias *et al.* 2006; Ballantyne *et al.* 2010; Csank *et al.* 2011; Guertin-Pasquier 2012).

The decrease in pollen and spore concentrations above the recovery hiatus implies changes in the density of the vegetation cover. It corresponds to a slight increase in herb percentages, probably due to more open vegetation linked to a cooling climate during the Pleistocene at the time of the iNHG, prior to about 2.3 Ma according to our biostratigraphical scheme.

3.5.4 Marine paleoenvironments

The abundance of Protoperidinale cysts suggest inputs from nearshore environments (Figure 3.7; Table 3.3). Moreover, the much lower diversity of dinocyst and acritarch species in Baffin Bay compared to the Labrador Sea suggests limited penetration of North Atlantic waters, notably during the late Pliocene and early Pleistocene (de Vernal and Mudie 1989a, 1989b; Aubry *et al.* accepted).

In the late Miocene to early Pliocene interval of Biozone 1, the dominance of *R. actinocoronata* and *H. tectata* suggests warm surface water conditions (Figure 3.7, Table 3.3). In Miocene sediments from the Iceland Sea, the significant occurrence (> 2.5%) of *R. actinocoronata* is associated with sea surface temperatures greater than 18°C (Schreck *et al.* 2017; Table 3.3). *H. tectata* has been associated with a broader temperature range, with a preference for warm temperate waters during the Miocene (8-26°C; Schreck *et al.* 2017; Table 3.3) but slightly cooler during the Plio/Pleistocene (11-17°C; De Schepper *et al.* 2011; Hennissen *et al.* 2017; Table 3.3). The presence of other warm water taxa such as *Batiacasphaera* spp., *O.? erikianum* and *Lingulodinium machaerophorum* confirms relatively warm conditions in Baffin Bay during the late Miocene-early Pliocene. However, the cyst of *P. dalei*, which is presently a high latitude taxon (e.g. de Vernal *et al.* 2001; Matthiessen *et al.* 2005), may suggest episodic cool and low saline surface water events (Figure 3.7; Table 3.3).

In the interval covering the early Pliocene to early Pleistocene (biozones 2-4), the assemblages are characterized by *F. filifera*, *F. microornata* and *B. tepikiense* (Figure 3.7). Given the distribution of these taxa in the Pliocene and early Pleistocene sediments of the North Atlantic and Arctic oceans, their common occurrence likely relates to cool conditions (Table 3.3; De Schepper *et al.* 2011; Hennissen *et al.* 2017;

Matthiessen *et al.* 2018). The extant taxon *B. tepikiense* is presently found in coastal areas with low sea surface salinities and large winter to summer temperature contrasts (e.g. Rochon *et al.* 1999; de Vernal *et al.* 2001, 2005, 2013). It was a dominant taxon in dinocyst assemblages throughout the northern North Atlantic during the last glacial maximum (de Vernal *et al.* 2005). At the end of the study interval, the increase in *O. centrocarpum* may also suggest more open ocean conditions (Figure 3.7, Table 3.3). The very low concentration would point to low productivity, possibly due to harsh sea-surface conditions, as it is presently the case in central Baffin Bay (e.g. Gibb *et al.* 2015).

3.6 Conclusion

This study has allowed us to refine the biostratigraphical scheme, the chronostratigraphy and the environmental interpretation of the late Neogene sequence at ODP Site 645. Our results indicate that the late Miocene to early Pliocene interval (Biozones 1 and 2) at this site was characterized by nearshore environments, with very limited open ocean water inflow but strong fluvial and terrigenous inputs. Warm surface waters apparently prevailed, while the surrounding lands were covered by boreal forest or tundra forest with extensive peatlands. In the early/late? Pliocene to early Pleistocene interval (Biozone 3 and 4), cool stratified surface waters and reduced vegetation cover with southward migration of the tree line are inferred. The position of the Pliocene to Pleistocene transition is ambiguous due to poor chronological control and a recovery hiatus, but it was likely associated with a major IRD pulse linked to ice sheet growth.

This study also made it possible to improve the correlation between the seismic stratigraphy of Baffin Bay and the West Greenland margins. However, it highlights the need for new drilling sites in Baffin Bay to better define the regional stratigraphy and reconstruct past ocean conditions at the time of the intensification of the North Hemisphere Glaciation and opening of the Canadian Arctic Archipelago gateway.

Acknowledgements

This is a contribution to the ArcTrain program, which was supported by the Natural Sciences and Engineering Research Council (NSERC) of Canada. The authors also acknowledge support from the *Fonds de recherche du Québec – Nature et Technologie* (FRQNT).

References

- Aksenov, Y., Bacon, S., Coward, A. C., and Holliday, N. P. (2010). Polar outflow from the Arctic Ocean: A high resolution model study. *Journal of Marine Systems*, 83(1-2), 14-37. <https://doi.org/10.1016/j.jmarsys.2010.06.007>
- Aksu, A. E., and Kaminski, M. A. (1989). Neogene and Quaternary planktonic foraminifer biostratigraphy and biochronology in Baffin Bay and the Labrador Sea. In Srivastava, S.P., Arthur, M.A., Clement, B., *et al.*, Proc. ODP, Sci. Results, 105: College Station, TX (Ocean Drilling Program), pp. 287-304. doi:10.2973/odp.proc.sr.105.122.1989
- Anstey, C.E. (1992). Biostratigraphic and paleoenvironmental interpretation of upper middle Miocene through lower Pleistocene dinoflagellate cyst, acritarch, and other algal palynomorph assemblages from Ocean Drilling Program Leg 105, Site 645, Baffin Bay. Master thesis, University of Toronto. 271 pp

- Arthur, M.A., Dean, W.E., Zachos, J.C., Kaminski, M., Hagerty Reig, S., and Elmstrom, K. (1989). Geochemical expression of early diagenesis in middle Eocene–lower Oligocene pelagic sediments in the southern Labrador Sea, Site 647, ODP Leg 105. In Srivastava, S.P., Arthur, M.A., Clement, B., *et al.*, Proc. ODP, Sci. Results, 105: College Station, TX (Ocean Drilling Program), 111–135. doi:10.2973/odp.proc.sr.105.157.1989
- Aubry A. M. R., De Schepper S., and de Vernal A. (accepted). Dinocyst and acritarch biostratigraphy of the Late Pliocene to early Pleistocene of IODP Site U1307, Labrador Sea. *Journal of Micropaleontology*, 101796. <https://doi.org/10.1016/j.marmicro.2019.101796>
- Baldauf, J.G., Clement, B.G., Aksu, A.E., de Vernal, A., Firth, J.V., Hall, F., Head, M.J., Jarrard, R.D., Kaminski, M.A., Lazarus, D., Monjanel, A.-L., Berggren, W.A., Gradstein, F.E., Knüttel, S., Mudie, P.J., and Russell, M.D. (1989). Magnetostratigraphic and biostratigraphic synthesis of Ocean Drilling Program Leg 105: Labrador Sea and Baffin Bay. In Srivastava, S.P., Arthur, M.A., Clement, B., *et al.*, Proc. ODP, Sci. Results, 105: College Station, TX (Ocean Drilling Program), 935–956. doi:10.2973/odp.proc.sr.105.165.1989
- Ballantyne, A. P., Greenwood, D. R., Sinninghe Damsté, J. S., Csank, A. Z., Eberle, J. J., and Rybczynski, N. (2010). Significantly warmer Arctic surface temperatures during the Pliocene indicated by multiple independent proxies. *Geology*, 38(7), 603–606. <https://doi.org/10.1130/G30815.1>
- Bartoli, G., Hönisch, B., and Zeebe, R. E. (2011). Atmospheric CO₂ decline during the Pliocene intensification of Northern Hemisphere glaciations. *Paleoceanography*, 26(4). doi:10.1029/2010PA002055.
- Bassett, I. J., Crompton, C. W., and Parmelee, J. A. (1978). An atlas of airborne pollen grains and common fungus spores of Canada. *Printing and Publishing Supply and Services Canada*. 320 pp.
- Bilodeau, G., Vernal, A. D., Hillaire-Marcel, C., and Josenhans, H. (1990). Postglacial paleoceanography of Hudson Bay: stratigraphic, microfaunal, and palynological evidence. *Canadian Journal of Earth Sciences*, 27(7): 946–963. <https://doi.org/10.1139/e90-098>.
- Busch, W.H. (1989). The origin of small-scale bulk density anomalies in Miocene sediments at ODP Site 645, Baffin Bay. In Srivastava, S.P., Arthur, M.A., Clement,

- B., *et al.*, Proc. ODP, Sci. Results, 105: College Station, TX (Ocean Drilling Program), 775–779. doi:10.2973/odp.proc.sr.105.142.1989
- Campbell, I. D. (1999). Quaternary pollen taphonomy: examples of differential redeposition and differential preservation. *Palaeogeography, Palaeoclimatology, Palaeoecology*, 149(1-4), 245-256. [https://doi.org/10.1016/S0031-0182\(98\)00204-1](https://doi.org/10.1016/S0031-0182(98)00204-1)
- Canninga, G., Zijderveld, J.D.A., and van Hinte, J. (1987). Late Cenozoic magnetostratigraphy of Deep Sea Drilling Project Hole 603C, Leg 93, on the North American continental rise off Cape Hatteras. In: van Hinte, J., Wise, S.W.J., *et al.* (Eds.), Initial Reports of the Deep Sea Drilling. doi:10.2973/dsdp.proc.93.130.1987
- Channell, J.E.T., Smelror, M., Jansen, E., Higgins, S.M., Lehman, B., Eidvin, T., and Solheim, A. (1999). Age models for glacial fan deposits off East Greenland and Svalbard (Sites 986 and 987). In Raymo, M.E., Jansen, E., Blum, P., and Herbert, T.D. (Eds.), Proc. ODP, Sci. Results, 162: College Station, TX (Ocean Drilling Program), 149–166. doi:10.2973/odp.proc.sr.162.008.1999
- Cheng, W., and Rhines, P. B. (2004). Response of the overturning circulation to high-latitude fresh-water perturbations in the North Atlantic. *Climate dynamics*, 22(4), 359-372. DOI: 10.1007/s00382-003-0385-6
- Clement, B.M., Hall, F.J., and Jarrard, R.D. (1989). The magnetostratigraphy of Ocean Drilling Program Leg 105 sediments. In Srivastava, S.P., Arthur, M.A., Clement, B., *et al.*, Proc. ODP, Sci. Results, 105: College Station, TX (Ocean Drilling Program). 583–595. doi:10.2973/odp.proc.sr.105.147.1989
- Cremer, M., and Legigan, P. (1989). Morphology and surface texture of quartz grains from ODP Site 645, Baffin Bay. In Srivastava, S.P., Arthur, M.A., Clement, B., *et al.*, Proc. ODP, Sci. Results, 105: College Station, TX (Ocean Drilling Program). 21–30. doi:10.2973/odp.proc.sr.105.112.1989
- Csank, A. Z., Tripati, A. K., Patterson, W. P., Eagle, R. A., Rybczynski, N., Ballantyne, A. P., and Eiler, J. M. (2011). Estimates of Arctic land surface temperatures during the early Pliocene from two novel proxies. *Earth and Planetary Science Letters*, 304(3-4), 291-299. <https://doi.org/10.1016/j.epsl.2011.02.030>
- De Schepper, S., and Head, M. J. (2008a). New dinoflagellate cyst and acritarch taxa from the Pliocene and Pleistocene of the eastern North Atlantic (DSDP Site 610). *Journal of Systematic Palaeontology*, 6(1). 101-117. doi:10.1017/S1477201907002167

- De Schepper, S., and Head, M. J. (2008b). Age calibration of dinoflagellate cyst and acritarch events in the Pliocene–Pleistocene of the eastern North Atlantic (DSDP Hole 610A). *Stratigraphy*, 5(2), 137-161.
- De Schepper, S., and Head, M. J. (2009). Pliocene and Pleistocene dinoflagellate cyst and acritarch zonation of DSDP Hole 610A, eastern North Atlantic. *Palynology*, 33(1), 179-218.
- De Schepper, S., and Head, M. J. (2014). New late Cenozoic acritarchs: evolution, palaeoecology and correlation potential in high latitude oceans. *Journal of Systematic Palaeontology*, 12(4), 493-519. DOI: 10.1080/14772019.2013.783883.
- De Schepper, S., Head, M. J., and Louwye, S. (2004). New dinoflagellate cyst and incertae sedis taxa from the Pliocene of northern Belgium, southern North Sea Basin. *Journal of Paleontology*, 78(4), 625-644. [https://doi.org/10.1666/0022-3360\(2004\)078<0625:NDCAIS>2.0.CO;2](https://doi.org/10.1666/0022-3360(2004)078<0625:NDCAIS>2.0.CO;2)
- De Schepper, S., Head, M. J., and Groeneveld, J. (2009). North Atlantic Current variability through marine isotope stage M2 (circa 3.3 Ma) during the mid-Pliocene. *Paleoceanography and Paleoceanography*, 24(4). doi:10.1029/2008PA001725
- De Schepper, S., Fischer, E. I., Groeneveld, J., Head, M. J., and Matthiessen, J. (2011). Deciphering the palaeoecology of Late Pliocene and Early Pleistocene dinoflagellate cysts. *Palaeogeography, Palaeoclimatology, Palaeoecology*, 309(1), 17-32. doi:10.1016/j.palaeo.2011.04.020
- De Schepper, S., Gibbard, P. L., Salzmann, U., and Ehlers, J. (2014). A global synthesis of the marine and terrestrial evidence for glaciation during the Pliocene Epoch. *Earth-Science Reviews*, 135, 83-102. <http://dx.doi.org/10.1016/j.earscirev.2014.04.003>
- De Schepper, S., Schreck, M., Beck, K. M., Matthiessen, J., Fahl, K., and Mangerud, G. (2015). Early Pliocene onset of modern Nordic Seas circulation related to ocean gateway changes. *Nature communications*, 6, 8659. DOI: 10.1038/ncomms9659
- De Schepper, S., Beck, K. M., and Mangerud, G. (2017). Late Neogene dinoflagellate cyst and acritarch biostratigraphy for Ocean Drilling Program Hole 642B, Norwegian Sea. *Review of Palaeobotany and Palynology*, 236, 12-32. <https://doi.org/10.1016/j.revpalbo.2016.08.005>
- de Vernal, A., and Mudie, P.J. (1989a). Late Pliocene to Holocene palynostratigraphy at ODP Site 645, Baffin Bay. In Srivastava, S.P., Arthur, M.A., Clement, B., *et al.*, Proc.

- ODP, Sci. Results, 105: College Station, TX (Ocean Drilling Program), 387–399. doi:10.2973/odp.proc.sr.105.133.1989
- de Vernal, A., and Mudie, P.J. (1989b). Pliocene and Pleistocene palynostratigraphy at ODP Sites 646 and 647, eastern and southern Labrador Sea. In Srivastava, S.P., Arthur, M.A., Clement, B., *et al.*, Proc. ODP, Sci. Results, 105: College Station, TX (Ocean Drilling Program), 401–422. doi:10.2973/odp.proc.sr.105.134.1989
- de Vernal, A., Larouche, A., and Richard, P. J. H. (1987). Evaluation of palynomorph concentrations: do the aliquot and the marker-grain methods yield comparable results?. *Pollen et spores*.
- de Vernal, A., Henry, M., and Bilodeau, G. (1999). Techniques de préparation et d'analyse en micropaléontologie, *Les cahiers du GEOTOP*, 3, 41.
- de Vernal, A., Eynaud, F., Henry, M., Hillaire-Marcel, C., Londeix, L., Mangin, S., Matthiessen, J., Marret, F., Radi, T., Rochon, A., Solignac, S., and Turin, J-L. (2005). Reconstruction of sea-surface conditions at middle to high latitudes of the Northern Hemisphere during the Last Glacial Maximum (LGM) based on dinoflagellate cyst assemblages. *Quaternary Science Reviews*, 24(7), 897–924. <https://doi.org/10.1016/j.quascirev.2004.06.014>
- de Vernal, A., Hillaire-Marcel, C., Rochon, A., Fréchette, B., Henry, M., Solignac, S., and Bonnet, S. (2013). Dinocyst-based reconstructions of sea ice cover concentration during the Holocene in the Arctic Ocean, the northern North Atlantic Ocean and its adjacent seas. *Quaternary Science Reviews*, 79, 111–121. <https://doi.org/10.1016/j.quascirev.2013.07.006>
- Dybkjær, K., and Piasecki, S. (2010). Neogene dinocyst zonation for the eastern North Sea Basin, Denmark. *Review of Palaeobotany and Palynology*, 161(1-2), 1–29. <https://doi.org/10.1016/j.revpalbo.2010.02.005>
- Elias, S. A., Kuzmina, S., and Kiselyov, S. (2006). Late Tertiary origins of the Arctic beetle fauna. *Palaeogeography, Palaeoclimatology, Palaeoecology*, 241(3-4), 373–392. <http://dx.doi.org/10.1016/j.palaeo.2006.04.002>
- Flesche Kleiven, H., Jansen, E., Fronval, T., and Smith, T. M. (2002). Intensification of Northern Hemisphere glaciations in the circum Atlantic region (3.5–2.4 Ma)—ice rafted detritus evidence. *Palaeogeography, Palaeoclimatology, Palaeoecology*, 184(3-4), 213–223. [https://doi.org/10.1016/S0031-0182\(01\)00407-2](https://doi.org/10.1016/S0031-0182(01)00407-2)

- Fyles, J. G., Hills, L. V., Matthews Jr, J. V., Barendregt, R., Baker, J., Irving, E., and Jette, H. (1994). Ballast Brook and Beaufort formations (Late Tertiary) on northern Banks Island, Arctic Canada. *Quaternary International*, 22, 141-171.
[https://doi.org/10.1016/1040-6182\(94\)90010-8](https://doi.org/10.1016/1040-6182(94)90010-8)
- Gibb, O. T., Steinhauer, S., Fréchette, B., de Vernal, A., and Hillaire-Marcel, C. (2015). Diachronous evolution of sea surface conditions in the Labrador Sea and Baffin Bay since the last deglaciation. *The Holocene*, 25(12), 1882-1897.
<https://doi.org/10.1177/0959683615591352>.
- Guertin-Pasquier, A. (2012). Reconstitution paléo-écologique et contexte magnéto-stratigraphique de la forêt fossile de l'île Bylot (Nunavut). Master thesis. Université de Montréal.
- Hall, F.R., and King, J.W. (1989). Rock-magnetic stratigraphy of Site 645 (Baffin Bay) from ODP Leg 105. In Srivastava, S.P., Arthur, M.A., Clement, B., *et al.*, Proc. ODP, Sci. Results, 105: College Station, TX (Ocean Drilling Program), 843–859. doi:10.2973/odp.proc.sr.105.150.1989
- Head, M. J. (1993). Dinoflagellates, sporomorphs, and other palynomorphs from the Upper Pliocene St. Erth Beds of Cornwall, southwestern England. *Memoire (The Paleontological Society)*, 1-62.
- Head, M. J. (1996). Late Cenozoic dinoflagellates from the Royal Society borehole at Ludham, Norfolk, eastern England. *Journal of Paleontology*, 70(4), 543-570.
- Head, M. J. (1997). Thermophilic dinoflagellate assemblages from the mid Pliocene of eastern England. *Journal of Paleontology*, 165-193.
- Head, M. J., and Norris, G. (2003). New species of dinoflagellate cysts and other palynomorphs from the latest Miocene and Pliocene of DSDP Hole 603C, western North Atlantic. *Journal of Paleontology*, 77(1), 1-15.
<https://doi.org/10.1017/S0022336000043377>
- Head, M.J., Norris, G., and Mudie, P.J. (1989a). Palynology and dinocyst stratigraphy of the Miocene in ODP Leg 105, Hole 645E, Baffin Bay. In Srivastava, S.P., Arthur, M.A., Clement, B., *et al.*, Proc. ODP, Sci. Results, 105: College Station, TX (Ocean Drilling Program), 467–514. doi:10.2973/odp.proc.sr.105.137.1989

- Head, M. J., Edwards, L. E., Garrett, J. K., Head, M. J., Lentin, J. K., Marret, F., Matsuoka, K., Matthiessen, J., O'Mahony, J., Sun, X., and de Verteuil, L. (1993). A forum on Neogene and Quaternary dinoflagellate cysts: the edited transcript of a round table discussion held at the Third Workshop on Neogene and Quaternary Dinoflagellates; with taxonomic appendix. *Palynology*, 17(1), 201-239.
<https://doi.org/10.1080/01916122.1993.9989428>
- Hennissen, J. A., Head, M. J., De Schepper, S., and Groeneveld, J. (2017). Dinoflagellate cyst paleoecology during the Pliocene–Pleistocene climatic transition in the North Atlantic. *Palaeogeography, palaeoclimatology, palaeoecology*, 470, 81-108.
<https://doi.org/10.1016/j.palaeo.2016.12.023>
- Hiscott, R.N., Cremer, M., and Aksu, A.E. (1989). Evidence from sedimentary structures for processes of sediment transport and deposition during post-Miocene time at Sites 645, 646, and 647, Baffin Bay and the Labrador Sea. In Srivastava, S.P., Arthur, M.A., Clement, B., *et al.*, Proc. ODP, Sci. Results, 105: College Station, TX (Ocean Drilling Program), 53–63. doi:10.2973/odp.proc.sr.105.119.1989
- Hofmann, J. C., Knutz, P. C., Nielsen, T. and Kuijpers, A. (2016). Seismic architecture and evolution of the Disko Bay trough-mouth fan, central West Greenland margin. *Quaternary Science Review*, 147, 69-90. DOI: 10.1016/j.quascirev.2016.05.019.
- Kapp, R. O., Davis, O. K., and King, J. E. (2000). Pollen and Spores. The American Association of Stratigraphic Palynologists. Texas A&M University, College Station, TX.
- Knüttel, S., Russell, M.D., Jr., and Firth, J.V. (1989). Neogene calcareous nannofossils from ODP Leg 105: implications for Pleistocene paleoceanographic trends. In Srivastava, S.P., Arthur, M.A., Clement, B., *et al.*, Proc. ODP, Sci. Results, 105: College Station, TX (Ocean Drilling Program), 245–262. doi:10.2973/odp.proc.sr.105.130.1989
- Knutz, P. C., Hopper, J. R., Gregersen, U., Nielsen, T., and Japsen, P. (2015). A contourite drift system on the Baffin Bay–West Greenland margin linking Pliocene Arctic warming to poleward ocean circulation. *Geology*, 43(10), 907-910.
<https://doi.org/10.1130/G36927.1>
- Knutz, P. C., Newton, A. M., Hopper, J. R., Huuse, M., Gregersen, U., Sheldon, E., and Dybkjær, K. (2019). Eleven phases of Greenland Ice Sheet shelf-edge advance over the past 2.7 million years. *Nature Geoscience*, 1. <https://doi.org/10.1038/s41561-019-0340-8>

- Korstgård J.A., and Nielsen, O.B. (1989). Provenance of Dropstones in Baffin Bay and Labrador Sea, Leg 105. In Proceedings of the Ocean Drilling Program: Scientific Results 105. Edited by Srivastava, S.P., Arthur, M.A., Clement, B., *et al.*. College Station (Ocean Drilling Program), Texas State. pp. 65-69.
doi:10.2973/odp.proc.sr.105.200
- Lazarus, D., and Pallant, A. (1989). Oligocene and Neogene radiolarians from the Labrador Sea: ODP Leg 105. In Srivastava, S.P., Arthur, M.A., Clement, B., *et al.*, Proc. ODP, Sci. Results, 105: College Station, TX (Ocean Drilling Program), 349–380. doi:10.2973/odp.proc.sr.105.125.1989
- Limoges, A., Londeix, L., and de Vernal, A. (2013). Organic-walled dinoflagellate cyst distribution in the Gulf of Mexico. *Marine Micropaleontology*, 102, 51-68.
<https://doi.org/10.1016/j.marmicro.2013.06.002>
- Louwye, S., and De Schepper, S. (2010). The Miocene–Pliocene hiatus in the southern North Sea Basin (northern Belgium) revealed by dinoflagellate cysts. *Geological Magazine*, 147(5), 760-776. <https://doi.org/10.1017/S0016756810000191>
- Louwye, S., Head, M. J., and de Schepper, S. (2004). Dinoflagellate cyst stratigraphy and palaeoecology of the Pliocene in northern Belgium, southern North Sea Basin. *Geological Magazine*, 141(3), 353-378.
- Lozier, M.S. (2012). Overturning in the North Atlantic. *Annual Review of Marine Science*, 4, 291-315, doi:10.1146/annurev-marine-120710-100740
- Matthews, J. V., and Fyles, J. G. (2000). Late Tertiary plant and arthropod fossils from the High Terrace Sediments on the Fosheim Peninsula of Ellesmere Island (Northwest Territories, District of Franklin). *Geological Survey of Canada Bulletin*, 529, 295-317.
- Matthews Jr, J. V., and Ovenden, L. E. (1990). Late Tertiary plant macrofossils from localities in Arctic/Subarctic North America: a review of the data. *Arctic*, 364-392.
DOI:10.14430/arctic1631
- Matthews Jr, J., Mott, R., and Vincent, J. S. (1986). Preglacial and interglacial environments of Banks Island: pollen and macrofossils from Duck Hawk Bluffs and related sites. *Géographie physique et Quaternaire*, 40(3), 279-298.
<https://doi.org/10.7202/032649ar>
- Matthiessen, J., de Vernal, A., Head, M., Okolodkov, Y., Zonneveld, K., and Harland, R. (2005). Modern organic-walled dinoflagellate cysts in arctic marine environments and

their (paleo-) environmental significance. *Paläontologische Zeitschrift*, 79(1), 3-51.
 DOI: 10.1007/BF03021752

Matthiessen, J., Knies, J., Vogt, C., and Stein, R. (2008). Pliocene palaeoceanography of the Arctic Ocean and subarctic seas. *Philosophical Transactions of the Royal Society A: Mathematical, Physical and Engineering Sciences*, 367(1886), 21-48.
<https://doi.org/10.1098/rsta.2008.0203>

Matthiessen, J., Schreck, M., De Schepper, S., Zorzi, C., and de Vernal, A. (2018). Quaternary dinoflagellate cysts in the Arctic Ocean: Potential and limitations for stratigraphy and paleoenvironmental reconstructions. *Quaternary Science Reviews*, 192, 1-26. <https://doi.org/10.1016/j.quascirev.2017.12.020>

Mattingsdal, R., Knies, J., Andreassen, K., Fabian, K., Husum, K., Grøsfjeld, K., and De Schepper, S. (2014). A new 6 Myr stratigraphic framework for the Atlantic–Arctic Gateway. *Quaternary Science Reviews*, 92, 170-178.
<https://doi.org/10.1016/j.quascirev.2013.08.022>

McAndrews, J. H., Berti, A. A., and Norris, G. (1973). Key to the Quaternary pollen and spores of the Great Lakes region.

Mertens, K. N., Verhoeven, K., Verleye, T., Louwye, S., Amorim, A., Ribeiro, S., Deaf, A.S., Harding, I.C., De Schepper, S., Gonzalez, C., Kodrans-Nsiah, M., de Vernal, A., Henry, M., Radi, T., Dybkjaer, K., Poulsen, N.E., Feist-Burkhardt, S., Chitolie, J., Heilmann-Clausen, C., Londeix, L., Turon, J-L., Marret, F., Matthiessen, J., McCarthy, F.M.G., Prasad, V., Pospelova, V., Kyffin Highes, J.E., Riding, J.B., Rochon, A., Sangiorgio, F., Welters, N., Sinclair, N., Thun, C., Soliman, A., Van Nieuwenhove, N., Vink, Annemiek, and Young, M. (2009). Determining the absolute abundance of dinoflagellate cysts in recent marine sediments: the Lycopodium marker-grain method put to the test. *Review of Palaeobotany and Palynology*, 157(3), 238-252. <https://doi.org/10.1016/j.revpalbo.2009.05.004>

Monjanel, A.-L., and Baldauf, J.G. (1989). Miocene to Holocene diatom biostratigraphy from Baffin Bay and Labrador Sea, Ocean Drilling Program Sites 645 and 646. In Srivastava, S.P., Arthur, M.A., Clement, B., *et al.*, Proc. ODP, Sci. Results, 105: College Station, TX (Ocean Drilling Program), 305–322. doi:10.2973/odp.proc.sr.105.127.1989

Mudge, D. C., and Bujak, J. P. (1996). Palaeocene biostratigraphy and sequence stratigraphy of the UK central North Sea. *Marine and Petroleum Geology*, 13(3), 295-312. DOI: 10.1016/0264-8172(95)00066-6

- Munsterman, D., and Kerstholt, S. (1996). Sodium polytungstate, a new non-toxic alternative to bromoform in heavy liquid separation. *Review of Palaeobotany and Palynology*, 91(1-4), 417-422. [https://doi.org/10.1016/0034-6667\(95\)00093-3](https://doi.org/10.1016/0034-6667(95)00093-3)
- Piasecki, S., Gregersen, U., and Johannessen, P. N. (2002). Lower Pliocene dinoflagellate cysts from cored Utsira Formation in the Viking Graben, northern North Sea. *Marine and Petroleum Geology*, 19(1), 55-67. [https://doi.org/10.1016/S0264-8172\(01\)00053-8](https://doi.org/10.1016/S0264-8172(01)00053-8)
- Raymo, M. E., Grant, B., Horowitz, M., and Rau, G. H. (1996). Mid-Pliocene warmth: stronger greenhouse and stronger conveyor. *Marine Micropaleontology*, 27(1-4), 313-326. [https://doi.org/10.1016/0377-8398\(95\)00048-8](https://doi.org/10.1016/0377-8398(95)00048-8)
- Rhein, M., Kieke, D., and Steinfeldt, R. (2015). Advection of North Atlantic Deep Water from the Labrador Sea to the southern hemisphere. *Journal of Geophysical Research Oceans*, 120, 2471-2487. doi:10.1002/2014JC010605
- Rignot, E., and Mouginot, J. (2012). Ice flow in Greenland for the international polar year 2008-2009. *Geophysical Research Letters*, 39(11): L11501. <https://doi.org/10.1029/2012GL051634>
- Rignot, E., Xu, Y., Menemenlis, D., Mouginot, J., Scheuchl, B., Li, X., Morlighem, M., Seroussi, H., van den Broeke, M., Fenty, I., Cai, C., An, L., and de Fleurian, B. (2016). Modeling of ocean-induced ice melt rates of five west Greenland glaciers over the past two decades. *Geophysical Research Letters*, 43(12), 6374-6382. doi:10.1002/2016GL068784
- Rochon, A., and Vernal, A. D. (1994). Palynomorph distribution in recent sediments from the Labrador Sea. *Canadian Journal of Earth Sciences*, 31(1), 115-127. <https://doi.org/10.1139/e94-010>
- Rochon, A., Vernal, A. D., Turon, J. L., Matthiessen, J., and Head, M. J. (1999). Distribution of recent dinoflagellate cysts in surface sediments from the North Atlantic Ocean and adjacent seas in relation to sea-surface parameters. *American Association of Stratigraphic Palynologists Contribution Series*, 35, 1-146.
- Schlitzer, R. (2018). Ocean Data View, <https://odv.awi.de>
- Schreck, M., Matthiessen, J., and Head, M. J. (2012). A magnetostratigraphic calibration of Middle Miocene through Pliocene dinoflagellate cyst and acritarch events in the

- Iceland Sea (Ocean Drilling Program Hole 907A). *Review of Palaeobotany and Palynology*, 187, 66-94. <https://doi.org/10.1016/j.revpalbo.2012.08.006>
- Schreck, M., Meheust, M., Stein, R., and Matthiessen, J. (2013). Response of marine palynomorphs to Neogene climate cooling in the Iceland Sea (ODP Hole 907A). *Marine Micropaleontology*, 101, 49-67. <https://doi.org/10.1016/j.marmicro.2013.03.003>
- Schreck, M., Nam, S. I., Clotten, C., Fahl, K., De Schepper, S., Forwick, M., and Matthiessen, J. (2017). Neogene dinoflagellate cysts and acritarchs from the high northern latitudes and their relation to sea surface temperature. *Marine Micropaleontology*, 136, 51-65. <https://doi.org/10.1016/j.marmicro.2017.09.003>
- Seki, O., Foster, G. L., Schmidt, D. N., Mackensen, A., Kawamura, K., and Pancost, R. D. (2010). Alkenone and boron-based Pliocene pCO₂ records, *Earth and Planetary Science Letters*, 292, 201–211. <https://doi.org/10.1016/j.epsl.2010.01.037>
- Srivastava, S.P., Arthur, M., Clement, B., et al. (1987). Proc. ODP, Init. Repts., 105: College Station, TX (Ocean Drilling Program). doi:10.2973/odp.proc.ir.105.1987
- Tang, C. C., Ross, C. K., Yao, T., Petrie, B., DeTracey, B. M., and Dunlap, E. (2004). The circulation, water masses and sea-ice of Baffin Bay. *Progress in Oceanography*, 63(4), 183-228. <https://doi.org/10.1016/j.pocean.2004.09.005>
- Tedford, R. H., and Harington, C. R. (2003). An Arctic mammal fauna from the early Pliocene of North America. *Nature*, 425(6956), 388. DOI:10.1038/nature01892
- Torsvik, T. H., Carlos, D., Mosar, J., Cocks, L. R. M., and Malme, T. (2002). Global reconstructions and North Atlantic paleogeography 440 Ma to recent. BATLAS–Mid Norway plate reconstruction atlas with global and Atlantic perspectives. *Geological Survey of Norway*, Trondheim, 18, 39.
- Tripathi, A. K., Eagle, R. A., Morton, A., Dowdeswell, J. A., Atkinson, K. L., Bahé, Y., Dawber, C.F., Khadun, E., Shaw, R.M.H., Shorthle, O., and hanabalasundaram, L. (2008). Evidence for glaciation in the Northern Hemisphere back to 44 Ma from ice rafted debris in the Greenland Sea. *Earth and Planetary Science Letters*, 265(1), 112-122. <https://doi.org/10.1016/j.epsl.2007.09.045>
- Tweddle, J. C., and Edwards, K. J. (2010). Pollen preservation zones as an interpretative tool in Holocene palynology. *Review of Palaeobotany and Palynology*, 161(1-2), 59-76. <https://doi.org/10.1016/j.revpalbo.2010.03.004>

- Van Ranst, G. (2015). The Miocene–Pliocene boundary in the eastern North Atlantic (ODP Site 982): dinoflagellate cyst biostratigraphy and paleoenvironmental reconstruction. Master thesis, Universiteit Gent, 145 pp. <http://lib.ugent.be/catalog/rug01:002213965>
- Verhoeven, K., Louwye, S., Paez-Reyes, M., Mertens, K. N., and Vercauteren, D. (2014). New acritarchs from the late Cenozoic of the southern North Sea Basin and the North Atlantic realm. *Palynology*, 38(1), 38-50.
- Versteegh, G. J. M., and Zevenboom, D. (1995). New genera and species of dinoflagellate cysts from the Mediterranean Neogene. *Review of Palaeobotany and Palynology*, 85(3-4), 213-229. [https://doi.org/10.1016/0034-6667\(94\)00127-6](https://doi.org/10.1016/0034-6667(94)00127-6)
- Versteegh, G. J. (1997). The onset of major Northern Hemisphere glaciations and their impact on dinoflagellate cysts and acritarchs from the Singa section, Calabria (southern Italy) and DSDP Holes 607/607A (North Atlantic). *Marine Micropaleontology*, 30(4), 319-343. [https://doi.org/10.1016/S0377-8398\(96\)00052-7](https://doi.org/10.1016/S0377-8398(96)00052-7)
- Vincent, J. S. (1990). Late Tertiary and early Pleistocene deposits and history of Banks island, southwestern Canadian arctic Archipelago. *Arctic*, 339-363.
- Williams, G.L., Fensome, R.A., and MacRae, R.A. (2017). DINOFLAJ3. American Association of Stratigraphic Palynologists, Data Series no.2. <http://dinoflaj.smu.ca/dinoflaj3>
- Zachos, J., Pagani, M., Sloan, L., Thomas, E., and Billups, K. (2001). Trends, rhythms, and aberrations in global climate 65 Ma to present. *Science*, 292(5517), 686-693.
- Zonneveld, K. A. , Marret, F. , Versteegh, G. J. , Bogus, K. , Bonnet, S. , Bouimetarhan, I. , Crouch, E. , de Vernal, A. , Elshanawany, R. , Edwards, L. , Esper, O. , Forke, S. , Grøsfjeld, K. , Henry, M. , Holzwarth, U. , Kielt, J. F. , Kim, S. Y. , Ladouceur, S. , Ledu, D. , Chen, L. , Limoges, A. , Londeix, L. , Lu, S. H. , Mahmoud, M. S. , Marino, G. , Matsouka, K. , Matthiessen, J. , Mildenhall, D. , Mudie, P. , Neil, H. , Pospelova, V. , Qi, Y. , Radi, T. , Richerol, T. , Rochon, A. , Sangiorgi, F. , Solignac, S. , Turon, J. L. , Verleye, T. , Wang, Y. , Wang, Z. and Young, M. (2013). Atlas of modern dinoflagellate cyst distribution based on 2405 data points , *Review of Palaeobotany and Palynology*. 191 , pp. 1-197. doi: 10.1016/j.revpalbo.2012.08.003
- Zweng, M. M., and Münchow, A. (2006). Warming and freshening of Baffin Bay, 1916–(2003). *Journal of Geophysical Research: Oceans*, 111(C7). doi:10.1029/2005JC003093

Figures

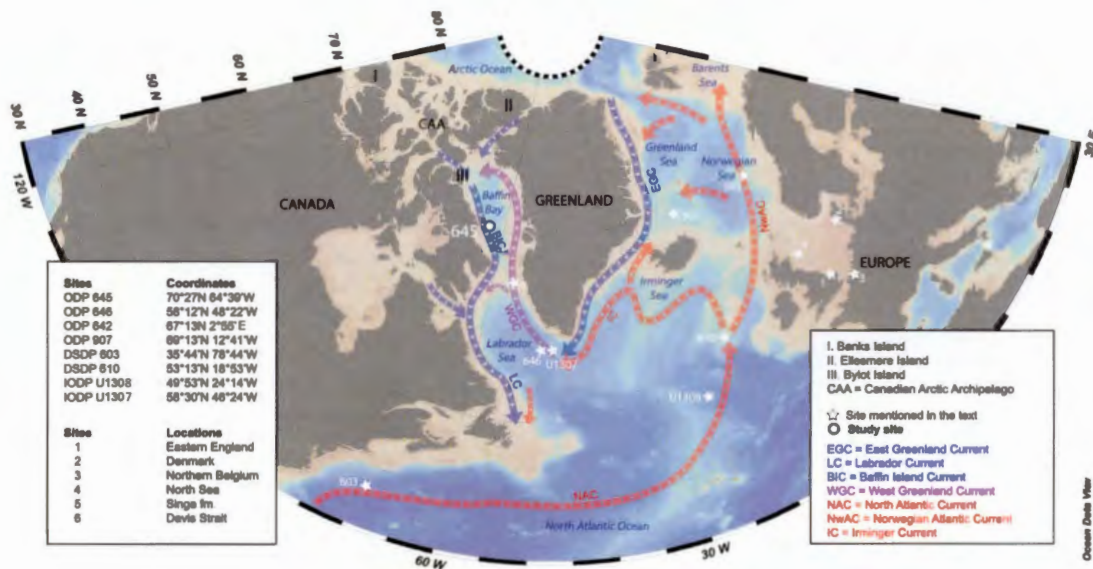


Figure 3.1 Map of the northwest North Atlantic Ocean with surface current and sites mentioned in the text. The map was made with Ocean Data View (Schlitzer, 2018)

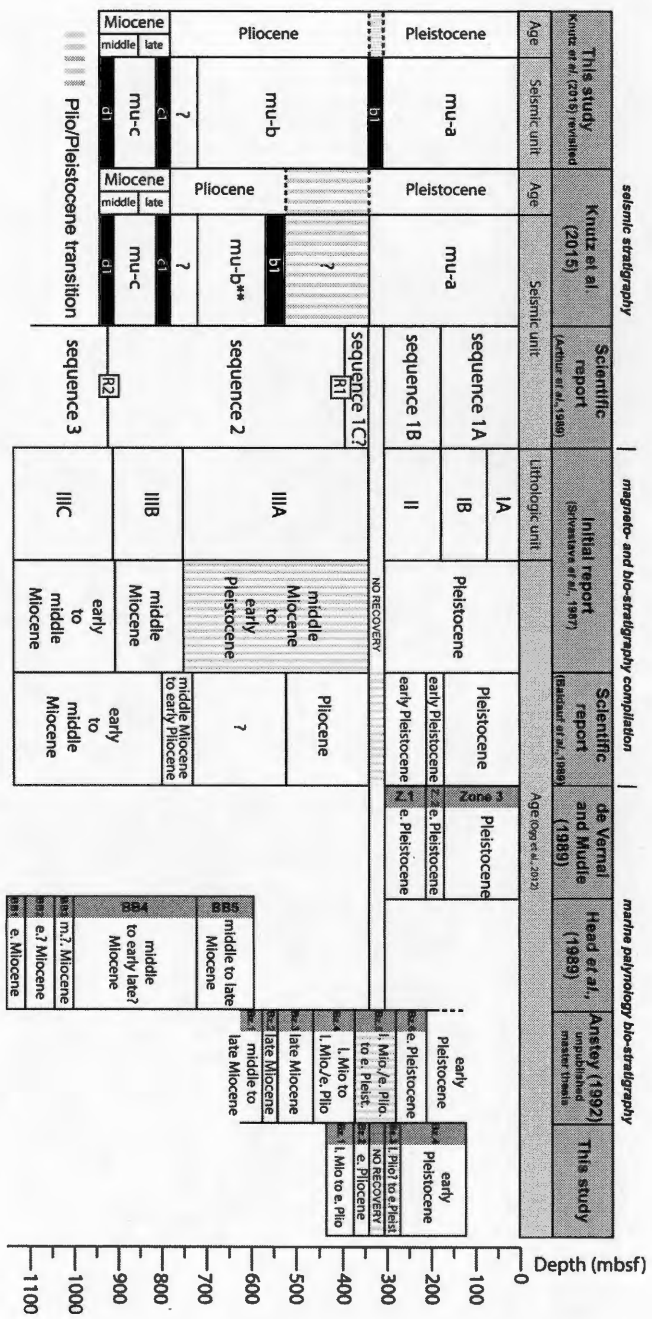


Figure 3.2 Overview of the chronological schemes proposed at ODP Site 645 based on seismic stratigraphy, lithostratigraphical units and palynostratigraphy.

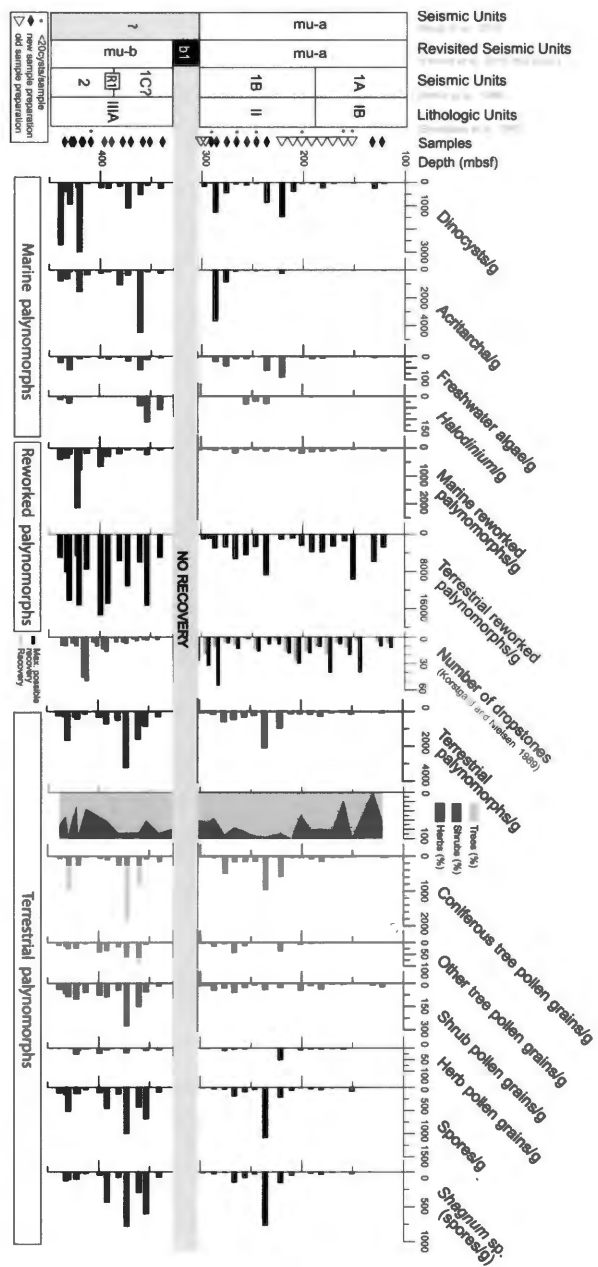


Figure 3.3 Concentrations of marine and detailed terrestrial palynomorphs. Number of dropstones from Korstgård and Nielsen (1989).

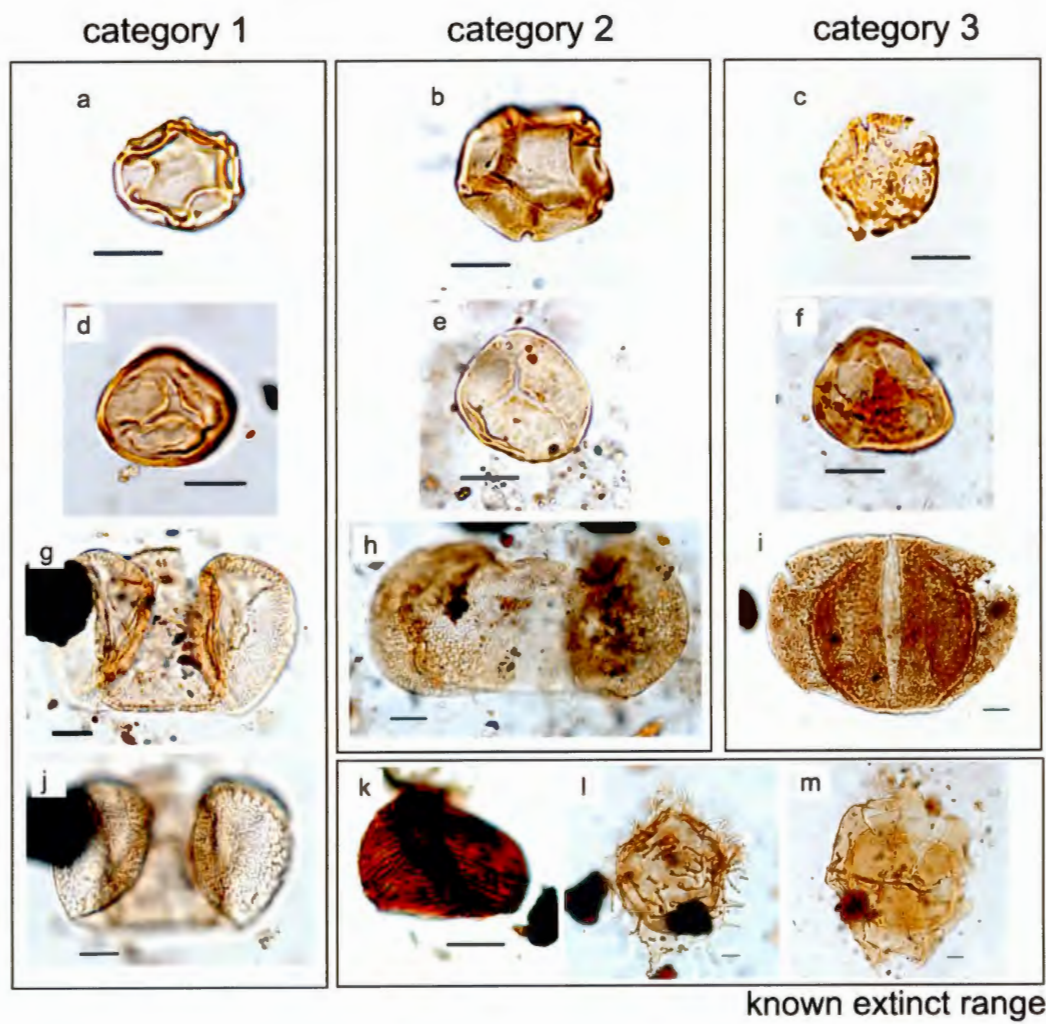


Figure 3.4 Pollen grains and preservation categories (as in Table 1). Scale bars are 10 μm .

a. Well preserved specimen of *Alnus rugosa*. ODP 645D-10R-1,90-91 cm, R31/4, slide 3305-5. Equatorial view. **b.** Moderately preserved specimen of *Alnus* cf. *rugosa*. ODP 645D-10R-1,90-91 cm, V20/0, slide 3305-5. Equatorial view. **c.** Poorly preserved specimen of *Alnus* sp. ODP 645D-10R-1,90-91 cm, V20/1, slide 3305-5. Equatorial view. **d.** Well preserved specimen of *Shagnum* sp. ODP 645D-17R-4,30-

31 cm, Z61/1, slide 3350-3. Equatorial view. **e.** Moderately preserved specimen of *Shagnum* sp. ODP 645B-26X-1,40-41 cm, Y41/0, slide 3497-3. Equatorial view. **f.** Poorly preserved specimen of trilete spore. ODP 645B-26X-1,40-41 cm, V63/0, slide 3497-3. Equatorial view. **g, j.** Well preserved specimen of *Pinus* sp. ODP 645B-26X-1,40-41 cm, Z55/3, slide 3497-3. High (g) and low (j) focus in proximal view. **h.** Moderately preserved specimen of *Picea* sp. ODP 645B-26X-1,40-41 cm, S30/1, slide 3497-3. Proximal view. **i.** Poorly preserved specimen of Gymnosperm. ODP 645D-17R-4,30-31 cm, X71/4, slide 3350-3. Proximal view. **k.** Spore of Cicatricosisporites (pre-Neogene). ODP 645D-16R-2,130-132 cm, M22/0, slide 3341-4. **l.** Cyst of *Wetzelia* sp. (pre-Neogene). ODP 645D-17R-6,19-21 cm, U42/0, slide 3351-5. Dorsal view. **m.** Cyst of *Chatangiella* sp. (pre-Neogene) ODP 645D-17R-6,19-21 cm, X28/1, slide 3351-5. Dorsal view.

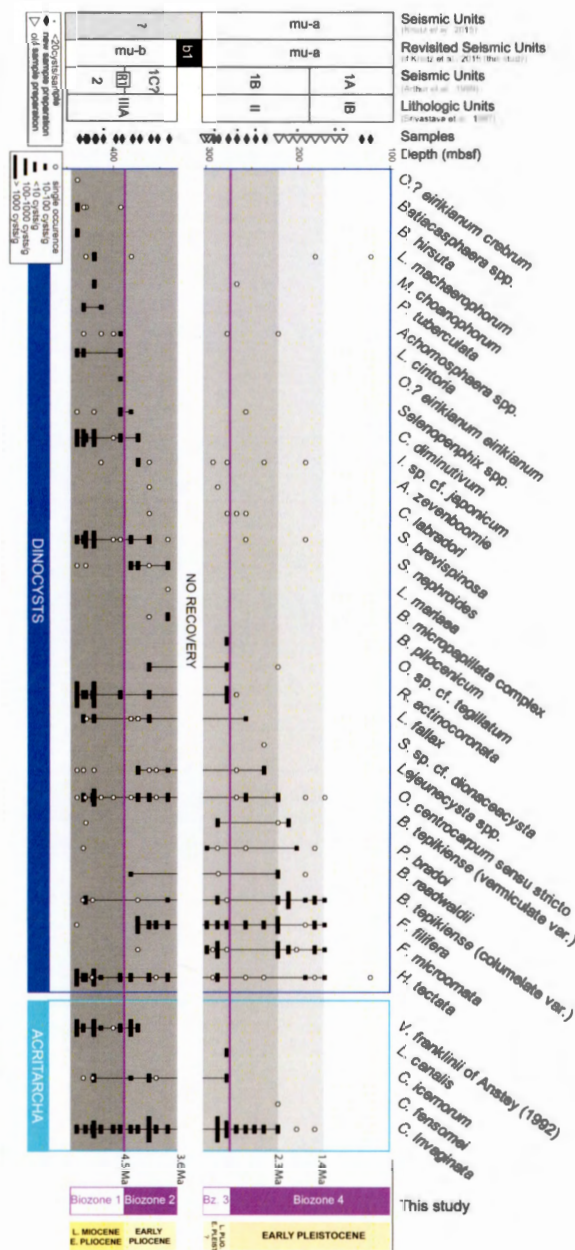


Figure 3.5 Biostratigraphical zonation based on dinocysts and acritarchs at ODP Site 645. Results with less than 20 cysts counted per sample (see* in the sample column) were not used

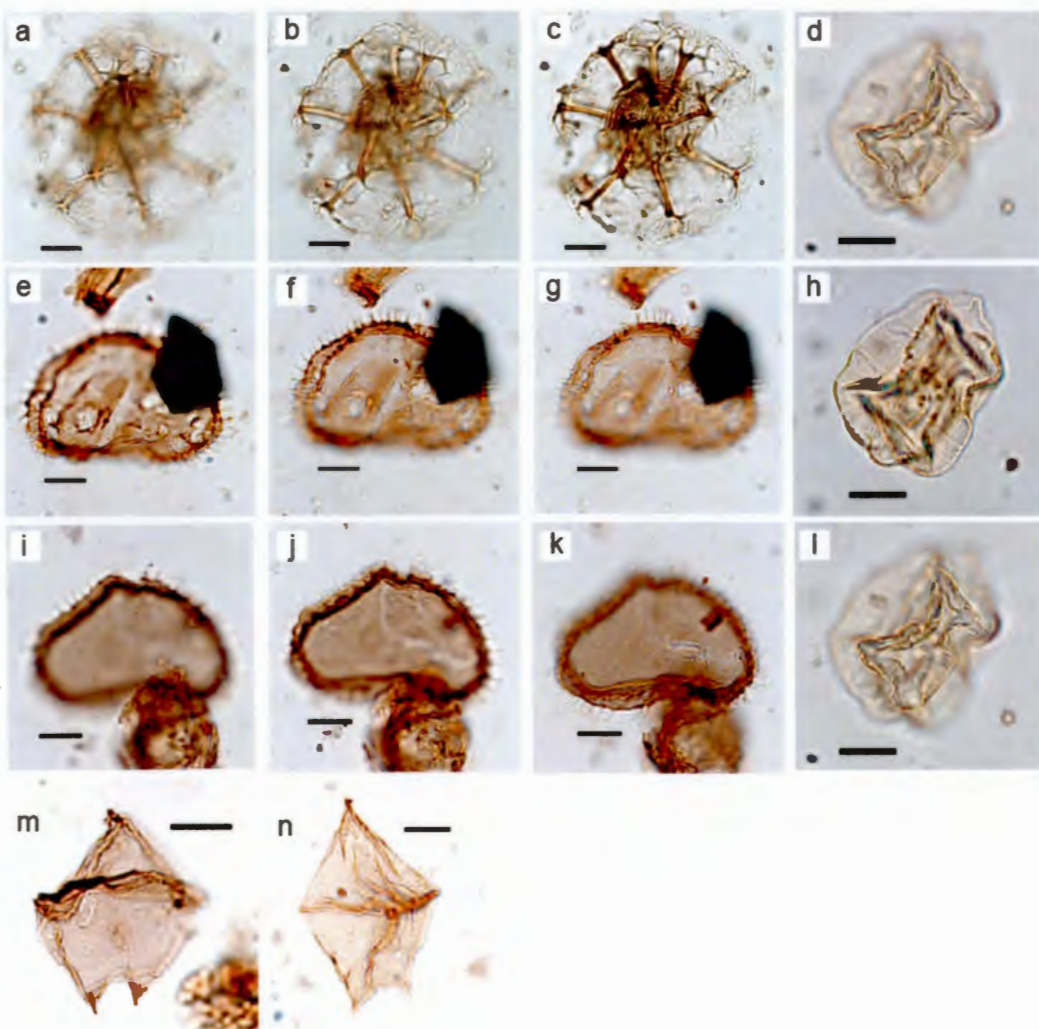


Figure 3.6 Photographs of the most biostratigraphically important dinocyst and acritarch taxa recovered in sediments from ODP Site n645. Scale bars are 10 μm .

a-c. *Reticulatosphaera actinocoronata*, ODP 645D-16R-2, 130-132 cm, Q44/3, slide 3341-4. **d, h, l.** “*Veriplicidium franklinii*” of Anstey (1992), ODP 645D-16R-2, 130-132 cm, L20/1, slide 3341-4. **e, f, g.** *Selenopemphix brevispinosa*, ODP 645D-16R-2, 130-132 cm, V54/0, slide 3341-4. **i, j, k.** *Selenopemphix brevispinosa*, ODP 645D-

16R-2, 130-132 cm, V57/4, slide 3341-4. **m, n.** *Cristadinium diminutivum*, ODP 645D-
17R-4, 30-31 cm, Z70/0, slide 3350-3.

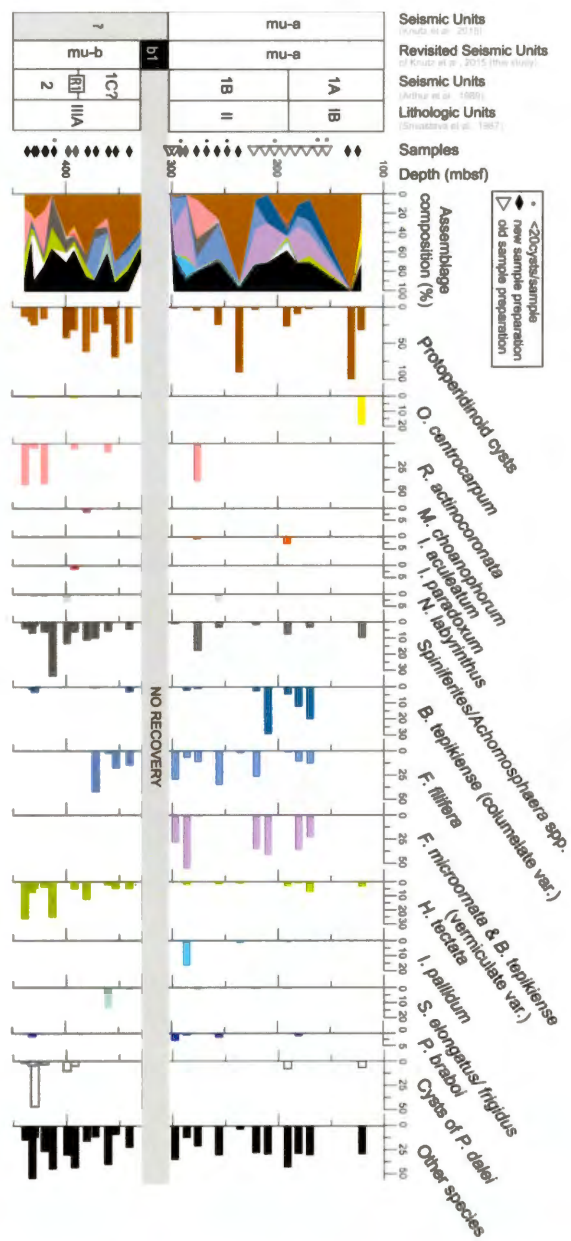


Figure 3.7 Relative abundances (percentages) of selected dinocysts. “Other species” includes: *A. zevenboomii*, *Batiacasphaera* spp., *B. hirsuta*, *B. micropapillata* complex, *Bitectatodinium* spp., *Bitectatodinium/Filisphaera* spp., *B. raedwaldii*,

Cordosphaerodinium spp., *C. labradori*, *Corrudinium* spp., *C. diminutivum*, *Filisphaera* spp., *Habibacysta* of Head 94, *Habibacysta* spp., *Impagidinium* sp. A of De Schepper and Head (2009), *Impagidinium* spp., brown *Impagidinium* spp., *L. machaerophorum*, *Lingulodinium* spp., *Nematosphaeropsis* spp., *O. centrocarpum*, *O.? eirikianum* *eirikianum*, *O.? eirikianum* *crebrum*, *O. tegillatum*, *Operculodinium* spp., *Palaeocystidium* spp., *P. tuberculata*, *Pyxidinopsis* spp., indet. Results with less than 20 cysts counted per sample (see * in the sample column) are not presented.

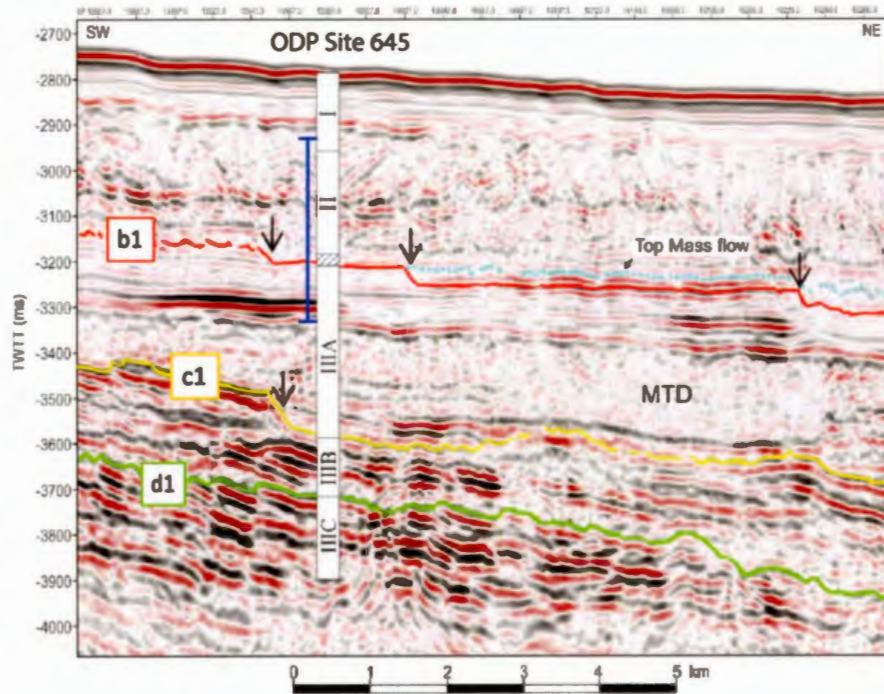


Figure 3.8 Revised correlation of the seismic profile of Knutz *et al.* (2015) with the upper part of the ODP Site 645 sequence. The lithological units at ODP Site 645 follow the new stratigraphical interpretation oh horizons and mega-units from this study. The vertical axis shows two-way travel-time (twtt). The vertical blue bar correspond to the interval of the present biostratigraphy study. Mass transport deposit associated to slide scars (black arrows) are highlighted with the pale blue line.

Tables

Categories	Identification	Preservation	Comments
1.Well-preserved	Very good, genus and species	No signs of deterioration	
2.Damaged	Medium, genus	Sporoderm alteration but exite visible and flattening	
3.Reworked	Poor (gymnosperm, spores or «other pollen grains»)	Flattened and/or very altered sproroderm, brocken, deteriorated	Know extinct range

Table 3.1 Pollen grain preservation state categories

Norwegian Sea	Iceland Sea	Western North Atlantic	Eastern North Atlantic	Other
ODP Site 642B <i>a, b</i>	ODP Site 907 <i>c, d</i>	DSDP Hole 603C ^e	DSDP Site 610 ^{f,g} IODP 1308	
DINOCYSTS				
<i>A. zevenboomii</i>	LO: 5.3 Ma			
<i>B. pliocenicum/graminosum</i>	HO: <3 Ma	HO: 4.5 Ma	HO : 2.74 Ma	HO: 2.1- 1.95 Ma in England ^h HO: 3.6 to 2.6-2.4 Ma in Denmark ⁱ
<i>B. hirsuta</i>	HO: 4.98 Ma HPO/HCP: 5.53 Ma	HO: 8.4 Ma		
<i>B. micropapillata</i> complex	HO: 4.64 Ma	HO: 3.4 Ma HCO: 4.5 Ma	HCO: 4.0 Ma	HO: 3.83 Ma
<i>C. labradori</i>	HO: 3.27 Ma	HO: 4.5 Ma		Lower Pleistocene in Labrador Sea ^j
<i>C. diminutivum</i>	HO: 4.91 Ma	HO: 5.81 Ma		HO: 5.3 Ma in Nordic seas ^k HO: 5.5 Ma in Labrador sea ^l
<i>F. filifera</i>	LO: 5.18 Ma (subsp. <i>filifera</i>)		HO/HPO: 1.44 Ma	Acme:~1.8 Ma ^m and references therein
<i>H. tectata</i>		LO: 14.2 Ma	HPO: 1.7 Ma HO: 0.8 Ma HPO: 2.07 Ma	HPO : Pleistocene ⁿ and references therein
<i>L. cinctoria</i>		HO: 5.31 Ma		
<i>M. choanophorum</i>	HO: 3.27 Ma	HO: 4.5 Ma HPO: 8.4 Ma		
<i>O.? eirikianum</i>		HO: 4.5 Ma LO: 13.0 Ma	HPO: 3.59 Ma HO: 2.62 Ma LO: 14.0 Ma	HO: 2.34 Ma ["]
<i>O.? eirikianum</i> <i>eirikianum</i>	LO: ≤ 3 Ma	HO: 4.5 Ma	HO: 2.62 Ma	HO: 2.34 Ma ["]
<i>O.? eirikianum</i> <i>cerbrum</i>	HO: 3.45 Ma LO: 4.23 Ma		LO: 3.33 Ma	
<i>O. tegillatum</i>	HO: 4.49 Ma LO: 5.29 Ma	HO: 4.5 Ma LO: 8.9 Ma	HCO: 4 Ma LO: 5.02 Ma	HO: 3.71 Ma
<i>P. tuberculata</i>				
<i>R. actinocoronata</i>	HO: 4.64 Ma	HO: 4.5 Ma	HO: 4 Ma ["] HCO: 4.5 Ma ["]	HO: 4.4 Ma in Belgium ^o HO: Lower Pliocene ^j in Labrador Sea and Davis Strait ^q HO: 4.8 Ma in Greenland Sea ^r
<i>S. brevispinosa</i>	HO: 4.64 Ma	HO: 8.4 Ma HPO: 10.4 Ma		Late Pliocene in Belgium ^p
<i>S. nephroides</i>		HPO: 8.5 Ma		Lower Pliocene
ACRITARCS				

<i>C.? icernorum</i>	HO: 1.71 Ma LO: 3.69 Ma	HO: 2.14 – 2.53 Ma HPO: 2.7-2.74 Ma LO: 3.74-3.35 Ma
<i>C.? invaginata</i>		HO: 1.82 Ma HPO: 2.74 Ma
<i>L. crista</i>	HO: ≤ 3 Ma	HO: 2.67 Ma HCO: 3.00 Ma
<i>L. canalis</i>		HO: 2.75 Ma LO: 2.84 Ma
<i>V. franklinii</i> of Anstey (1992)	HO: 5.29 Ma LO: 5.9 Ma	HO: 4.5 Ma
		HO: 2.9-3.0 Ma ^{s,q} HO: 2.60 Ma LO: 2.81 Ma at IODP 1308
		HO: 5.3 Ma LO: 8.2 Ma ^r

Table 3.2 Stratigraphic range of selected dinocyst and acritarch markers. Modified from De Schepper and Mangerud (2017).^a De Schepper *et al.* (2017); ^b De Schepper *et al.* (2015); ^c Schreck *et al.* (2012); ^d Schreck *et al.* (2013); ^e Head and Norris (2003); ^f De Schepper and Head (2008b); ^g De Schepper and Head (2009); ^h Head (1997); ⁱ Dybkjaer and Piasecki (2010); ^j de Vernal and Mudie (1989b); ^k Mudge and Bujak (1996); ^l Head *et al.* (1989); ^m Mattheissen *et al.* (2018); ⁿ Versteegh (1997); ^o Louwye *et al.* (2004); ^p Louwye and De Schepper (2010); ^q De Schepper and Head (2014); ^r Van Ranst (2015); ^s Piasecki *et al.* (2002); ^t Channell *et al.* (1999); ^u Canninga *et al.* (1987). HO: highest occurrence, LO: lowest occurrence, HPO: highest persistent occurrence, HCP: highest common occurrence.

Mio-Pliocene	Exi	N	O	Oli	Paleoecology ^a	Comments
Dinocysts						
<i>R. actinocoronata</i>	x	x	x		warm water, subtropical/tropical cold intolerant	cosmopolitan sporadic occurrence temperate/subarctic
<i>Batiascasphaera</i> spp.	x	x	x		warm water - cool tolerant	cosmopolitan
<i>O. centrocarpum</i> sensu stricto	x				warm water	
<i>O.? eirikianum</i>	x				cold intolerant	
<i>N. labyrinthus</i>		x	x		subpolar to temperate region	cosmopolitan
<i>L. machaerophorum</i>					warm water, temperate to tropical	similar to modern ^{b,c} endemic to the Gulf of Mexico (modern) ^d
<i>S. elongatus</i>		x	x		cool water - cold tolerant	
<i>I. pallidum</i>		x			warmer waters than modern distribution	cold water affinity (modern) ^{b,c}
<i>H. tectata</i>	x	x			subtropical/tropical	wider temperature distribution than Plio/Pleistocene ^{e,f}
Acritharchs						
<i>C.? invaginata</i>					cool water - cold tolerance	
Plio/Pleistocene	Exi	N	O	Oli	Paleoecology ^{e,f}	Comments
Dinocysts						
Protoperidinale cyst	x				temperate regions	abundant in coastal regions
<i>O. centrocarpum</i> sensu Wall and Dale (1966)	x	x			cosmopolitan	North Atlantic Current indicator
<i>I. aculeatum</i>	x	x			warm water	
<i>I. paradoxum</i>	x	x			warm water	optimum lower than <i>I. aculeatum</i>
<i>N. labyrinthus</i>	x	x			subpolar to temperate region	
<i>Spiniferites</i> spp.	x				cosmopolitan (modern) ^{b,c}	
<i>B. tepikiense</i> (columellate var.)		x	x		cool water tolerant	high seasonality, low salinity
<i>F. filifera</i>	x				cool water/moderate cold tolerant	
<i>B. tepikiense</i> (vermiculate var.) + <i>F. microornata</i> group		(x)	(x)		cool water tolerant	high seasonality, low salinity
<i>H. tectata</i>	x	x			cool water affinities to cold- tolerant	cool transitional character
<i>I. pallidum</i>		x			polar to subpolar water	but tolerance for warmer waters than modern
<i>S. elongatus</i>					cool-temperate to subpolar (modern) ^{b,c,g}	

<i>P. braboi</i>	x		cool-cold polar water	associated with Arctic Front and polar waters
cyst of <i>P. dalei</i>	x	x	cool-cold water tolerant	ice cover, low salinity (modern) ^{b,g}

Table 3.3 Paleoecological affinities of selected Mio-Pliocene and Plio-Pleistocene dinocyst and acritarch taxa based on the literature.^a Schreck *et al.* (2017), ^b de Vernal *et al.* (2013), ^c Zonneveld *et al.* (2013), ^d Limoges *et al.* (2013), ^e De Schepper *et al.* (2011), ^f Hennissen *et al.* (2017), and ^g Rochon *et al.* (1999). Exi: extinct, N: neritic, O: oceanic, Oli: oligotrophic.

CONCLUSION

Cette thèse avait pour but de documenter la transition Plio-Pléistocène aux hautes latitudes du nord-ouest de l'Atlantique Nord (Mer du Labrador et Baie de Baffin) dans l'optique de mieux comprendre l'enjeu des variations du climat et des conditions océaniques de surface dans le contexte de l'englaciation du Groenland. En effet, la transition Plio-Pléistocène, située autour de 2,58 Ma, est marquée par une intensification des grandes glaciations de l'Hémisphère Nord menant notamment au développement de la calotte groenlandaise. La zone d'intérêt, la Mer du Labrador et la Baie de Baffin, constitue un corridor qui mérite plus d'attention à la fois (1) pour son rôle dans les échanges d'eaux froides et peu salées de l'Océan Arctique avec les eaux relativement chaudes et salées de l'Océan Nord Atlantique, (2) mais également pour sa position entre le Canada et le Groenland en constituant un bassin de déversement des apports fluviatiles et atmosphériques des deux continents. L'originalité de ce travail repose sur le couplage entre des indicateurs marins et terrestres. J'ai choisi d'exploiter les dinokystes et les acritarches, qui sont sensibles aux conditions océanographiques de surface. Pour caractériser l'évolution du couvert de glace continentale, j'ai également utilisé les grains de pollen et les spores qui donnent une image de la végétation du continent adjacent, et les débris de vêlage de radeaux de glace (*ice rafted debris - IRD*) qui se déposent lors du passage d'icebergs ou de glace de mer.

Les seules études de palynologie marine concernant la Mer du Labrador et la Baie de Baffin au Pliocène datent de 30 ans (de Vernal et Mudie, 1989a, 1989b ; Head *et al.*, 1989 ; Anstey, 1992). Depuis lors, la taxonomie des dinokystes et acritarches du Néogène de l'Atlantique Nord a fait l'objet de nombreux travaux de révisions et

réajustements (Head, 1993, 1996, 1997 ; Versteegh et Zevenboom, 1995 ; Head et Norris, 2003 ; De Schepper *et al.*, 2004 ; De Schepper et Head, 2008a, 2014 ; Schreck *et al.*, 2012 ; Verhoeven *et al.*, 2013). De plus, la faible résolution temporelle des travaux réalisés par de Vernal et Mudie (1989a-b) et Head *et al.* (1989) ne permettait ni de définir précisément la position de la transition Plio-Pléistocène, ni d'effectuer des corrélations avec les nouveaux schémas biostratigraphiques établis dans l'Atlantique Nord et les mers nordiques (De Schepper et Head 2008a, 2008b, 2009 ; De Schepper *et al.*, 2017 ; Schreck *et al.*, 2012 ; Mattingdal *et al.*, 2014 ; Matthiessen *et al.*, 2018). Or, de telles corrélations sont indispensables pour comprendre les relations entre les conditions paléocéanographiques de surface régionales avec le courant nord-atlantique (*North Atlantic Current*, NAC) qui semblent jouer un rôle très important dans la dynamique des changements climatiques et l'englaciation de l'Hémisphère Nord au Pliocène (e.g., de Schepper *et al.*, 2013 ; Hennissen *et al.*, 2014, 2015 ; Panitz *et al.*, 2017).

Cette thèse a permis, à partir de 180 échantillons de sédiments marins provenant du Site IODP U1307, d'établir la première palynostratigraphie détaillée du Pliocène supérieur au Pléistocène inférieur (3,2 -2,2 Ma) dans la Mer du Labrador. Basée sur des bio-événements (apparition ou disparition d'espèces de dinokystes et/ou acritarches), d'acmées calibrées et à partir d'un nouveau, et plus robuste modèle d'âge de Blake-Mizen *et al.* (2019), nous avons défini trois biozones (LS1, LS2 et LS3) qui peuvent servir de références pour des corrélations régionales et extra-régionales. Malgré l'expression d'un certain régionalisme par de nombreux bio-événements asynchrones entre la Mer du Labrador, l'Atlantique Nord et les mers nordiques, notre étude montre que les changements enregistrés dans la Mer du Labrador se corrèlent bien avec ceux du nord-est de l'Atlantique Nord. Les bio-événements marquant les limites des biozones que nous avons définies dans la Mer du Labrador (LS1, LS2, LS3) sont généralement uniques au vu des taxa qui les caractérisent. Toutefois, ils ont eu lieu

simultanément aux limites des biozones établies dans le centre de l'Atlantique Nord (RT4, RT5, RT6 et RT7) au site DSDP 610 (De Schepper et Head, 2009). Seules les biozones LS1 et RT5 ont des limites correspondantes aux disparitions synchrones d'*Invertocysta lacrymosa* et de *Barssidinium graminosum*. Les différences de la composition taxonomique des assemblages dans la Mer du Labrador sont dues à la faible abondance ou la très sporadique présence d'espèces ayant des affinités écologiques pour les eaux de surface chaudes mettant en évidence le caractère régional relativement froid en comparaison avec le reste de l'Atlantique Nord.

Le second chapitre de cette thèse répond aux objectifs visant les reconstitutions paléoécologiques des assemblages de dinokystes et acritarches et a également permis de retracer les conditions terrestres au sud du Groenland à partir des assemblages de grains de pollen et des spores. Il présente les assemblages de dinokystes comme traceurs qualitatifs des conditions paléocéanographiques de surface. Dans l'Atlantique Nord et les mers nordiques, l'étude des dinokystes a permis de documenter les variations des conditions des eaux de surface durant le Pliocène tardif et la transition Plio-Pléistocène (De Schepper *et al.*, 2009a, 2013, 2015, Hennissen, 2013 ; Hennissen *et al.*, 2014 ; Panitz *et al.*, 2017). Comme démontré par plusieurs travaux dans la dernière décennie (De Schepper *et al.*, 2013 ; Hennissen, 2013; Hennissen *et al.*, 2014, 2015 ; Panitz *et al.*, 2017), notre travail confirme que l'espèce *Operculodinium centrocarpum* s'est révélée utile pour caractériser l'intensité et la trajectoire du courant nord-atlantique durant le Pliocène. Cependant, bien que la Mer du Labrador soit présentement influencée par une branche occidentale du NAC, aucune étude paléocéanographique n'avait permis de faire des inférences à l'échelle du Pliocène.

Les tests statistiques des analyses en composantes principales réalisés sur les assemblages de dinokystes de nos échantillons ont permis d'identifier des espèces particulièrement plus sensibles aux changements environnementaux, menant à la

définition de deux écozones majeures qui peuvent être associées à des changements dans l'intensité de l'influence du NAC dans la Mer du Labrador. Cette étude montre que peu avant la limite Plio-Pléistocène, une transition très importante a eu lieu à une échelle régionale. Elle se caractérise par un changement abrupt des assemblages avec la diminution de l'abondance d'*Operculodinium centrocarpum* (~2,65 Ma) et l'acmée de *Pyxidinopsis braboi* (~2,65-2,55 Ma). Ces résultats permettent de mettre en évidence la connexion entre la Mer du Labrador et le nord-est de l'Atlantique Nord. En effet, des événements similaires se produisent presqu'au même moment au site DSDP 610 dans le nord-est de l'Atlantique Nord (Hennissen, 2013 ; Hennissen *et al.*, 2014), indiquant une modification de la trajectoire du NAC et une position plus méridionale du front arctique suite à une augmentation des apports d'eaux de surface polaires vers les basses latitudes. Le changement majeur de la composition des assemblages de dinokystes dans l'Atlantique Nord et la Mer du Labrador coïncide avec l'intensification des glaciations de l'Hémisphère Nord et du Groenland.

Avec le nouveau modèle d'âge de Blake-Mizen *et al.* (2019) au site U1307, nous avons également produit une palynostratigraphie de haute résolution temporelle du mPwP dans la Mer du Labrador. Cet intervalle est largement étudié comme un analogue du réchauffement climatique en cours. Notre étude apporte des informations supplémentaires permettant de mieux comprendre les relations entre les conditions paléocéanographiques et le volume des glaces sur le Groenland pendant cet intervalle. L'optimum climatique du Pliocène a été marqué, dans la Mer du Labrador, par des changements de large amplitude reliés à un changement dans l'intensité de la pénétration du NAC à ~ 3,11 Ma menant à un refroidissement des masses d'eaux superficielles, une augmentation des apports d'eau douce en provenance du Groenland, et à une expansion du volume des glaces sur le Groenland.

De plus, les assemblages polliniques ainsi que les IRD ont permis de mettre en relation les changements paléocéanographiques avec l'expansion de la calotte groenlandaise, et donc de répondre à l'un de nos objectifs spécifiques visant à documenter le lien entre les milieux marin et terrestre. D'après les exercices de modélisation de Smith *et al.* (2018) proposant des trajectoires atmosphériques au Pliocène, nous suggérons que les assemblages polliniques au site IODP U1307 résultent de la présence d'un couvert végétal sur le Groenland pendant le Pliocène tardif.

Ces assemblages polliniques fond état d'une végétation de type forêt boréale-tempérée composée de conifères comme le pin, l'épinette, la pruche et le sapin, mais aussi de noisetier et chêne et bouleau traduisant un climat plus doux et tempéré, sans doute localisée sur le sud du Groenland. Les grains de pollen d'arbustes sont également très présents et proviennent d'aulne, de saule et de la famille des plantes éricacées souvent associées à des conditions plus humides. Les quelques grains de pollen d'herbacées appartiennent majoritairement à la famille des astéracées. La très forte concentration de spores de ptéridophytes et de bryophytes, suggère un climat humide. Les assemblages ne montrent pas de changement significatif au cours de l'intervalle d'étude (3,2-2,2 Ma) ni pendant le mPwP ou la transition Plio-Pléistocène, mais ceci pourrait être due à un comptage insuffisant de palynomorphes. Cependant une diminution des concentrations des palynomorphes terrestres simultanée à une augmentation drastique des IRD indiquerait une diminution du couvert végétal et une augmentation de la superficie occupée par les glaciers sur le Groenland autour de 2,65 Ma, soit de façon synchrone avec le changement principal observé dans les assemblages de dinokystes.

Finalement, le seul site foré dans la Baie de Baffin et permettant de remonter jusqu'au Miocène (ODP 645) a également fait l'objet d'analyses dans le cadre de cette thèse. Des problèmes de discontinuité dans les enregistrements sédimentaires font que la

transition Plio-Pléistocène n'a jamais été clairement identifiée. Le troisième chapitre de la thèse exploite donc la taxonomie et les études biostratigraphiques basées sur les dinokystes et les acritarches de l'Atlantique Nord, et maintenant la Mer du Labrador, afin de caractériser la transition Plio-Pléistocène dans la Baie de Baffin.

C'est pourquoi, 32 échantillons correspondant au Pliocène et Pléistocène d'après De Vernal et Mudie (1989b) et Knutz *et al.* (2015) ont été analysés. Comme il n'existe pas de modèle d'âge probant pour le site ODP 645, la distribution stratigraphique des espèces a été utilisée pour attribuer un âge aux sédiments. Quatre zones biostratigraphiques ont pu être définies et nous avons proposé un âge pour leurs limites. Cependant, une de ces limites est associée à un hiatus sédimentaire et l'autre à une discontinuité dans la récupération des sédiments lors du forage. L'intervalle étudié correspond à des sédiments attribués à la toute fin du Miocène-début du Pliocène ($> 4,5$ Ma) jusqu'au milieu du Pléistocène ($> 1,4$ Ma). Malgré ce large intervalle temporel, aucun indice biostratigraphique n'a permis d'identifier de façon univoque la transition Plio-Pléistocène au site ODP 645 qui se situerait ainsi, d'après cette étude, dans le hiatus de recouvrement des sédiments.

Grâce à ce travail, nous pouvons proposer une réinterprétation des profils sismiques réalisés entre le site ODP 645 et ceux publiés par Knutz *et al.* en 2015, dont l'acquisition a été faite à 17 km de notre site et dans l'est de la Baie de Baffin le long des marges groenlandaises. De plus, nous avons démontré que les assemblages de dinokystes se sont déposés dans un environnement néritique avec une influence océanique très limitée traduisant une faible connexion avec la Mer du Labrador. Globalement, les conditions étaient plus chaudes à la fin du Miocène-début du Pliocène que pendant le Pléistocène, respectivement avant et après le hiatus de récupération des sédiments.

Nous avons établi une nouvelle biostratigraphie détaillée basée sur les dinokystes et acritarches au Site IODP U1307, et démontré que malgré des conditions régionales plus froides, la Mer du Labrador est fortement connectée avec l'Océan Atlantique Nord. Le mPwP a été marqué par des changements importants liés à l'intensité du courant nord-atlantique et à la fonte de glace sur le Groenland. Au-delà du simple développement de glace pérenne dans l'Hémisphère Nord, la transition Plio-Pléistocène s'est singularisée par une réorganisation des conditions paléocéanographiques dans l'Atlantique Nord. La mise en place du front arctique et la migration vers le sud du NAC se sont faites à partir de 2,65 Ma dans la Mer du Labrador, ce qui serait un peu antérieur à l'enregistrement dans le nord-est de l'Atlantique Nord et à la limite formelle entre le Pliocène et le Pléistocène. Les conditions en milieu terrestre montrent également une diminution du couvert végétal et une augmentation du couvert de glace à partir de 2,65 Ma.

Les résultats de ce travail établissent de solides bases pour de futurs travaux de palynologie marine et terrestre dans la Mer du Labrador et la Baie de Baffin tout en démontrant la pertinence de telles études le long des marges groenlandaises. En effet, il serait opportun de revisiter, d'un point de vue palynologique, le site ODP 646 qui a été foré en 1985 en même temps que le site 645, et qui est situé juste au sud du site IODP U1307. Bien que le modèle d'âge ne soit pas aussi précis qu'au Site IODP U1307, le Site 646 couvre un intervalle plus long allant du milieu du Miocène à l'actuel (Srivastava *et al.*, 1989). L'utilisation de la biostratigraphie de la transition Plio-Pléistocène que nous avons établie au site U1307 permettrait de raffiner le modèle d'âge initial basé sur les inversions magnétiques et la biostratigraphie des cocolithes et foraminifères planctoniques (Baldauf *et al.*, 1989). De plus, il serait possible d'identifier clairement la transition Plio-Pléistocène et d'établir une palynostratigraphie régionale couvrant l'ensemble du Pliocène. Les analyses des assemblages de dinokystes permettraient des reconstitutions paléocéanographiques

alors que les assemblages polliniques contribueraient à retracer les changements paléogéographiques et paléoclimatiques en milieu continental sur le long terme. Ainsi, il serait possible de préciser quelles sont les relations entre la Mer du Labrador et l'Atlantique Nord au moment de l'initiation des grandes glaciations de l'Hémisphère Nord vers environ 3,6 Ma (Mudelsee et Raymo, 2005).

En ce qui concerne la Baie de Baffin, il paraît nécessaire de réaliser de nouveaux forages continus afin de documenter les conditions paléocéanographiques, paléogéographiques et paléoclimatiques au Néogène et au moment de l'intensification des glaciations de l'Hémisphère Nord. En effet, la compilation des données effectuée par Matthiessen *et al.* (2008) et les efforts de modélisation de PlioMIP (Dowsett *et al.*, 2016) laissent supposer que la connexion entre la Baie de Baffin et l'Océan Arctique n'existe pas pendant le Pliocène.

Enfin, cette thèse souligne l'importance de la proposition de mission de forage IODP 909 par Knutz *et al.* (2018). Les sites proposés permettraient de documenter l'évolution de la calotte groenlandaise du début du Néogène à l'Holocène et, ainsi, de démontrer comment l'expansion de la calotte groenlandaise est liée à l'intensification des glaciations de l'Hémisphère Nord, notamment lors de la transition Plio-Pléistocène.

ANNEXE A

SUPPLEMENTARY INFORMATION A DU CHAPITRE I

List of taxonomic names and their full authorial citations of dinocysts and acritarcha from the late Pliocene-early Pleistocene of IODP Site U1307

Dinocysts

- Achomosphaera* Evitt, 1963
Amiculatosphaera umbraculum Harlan, 1970
Ataxiodinium Reid, 1974
Ataxiodinium choane Reid, 1974
Ataxiodinium confusum Versteegh and Zevenboom, 1995
Barssidinium Lentin, Fensome and Williams, 1994
Barssidinium graminosum Lentin, Fensome and Williams, 1994
Barssidinium pliocenicum Head, 1994 emend. De Schepper and Head, 2004
Batiacasphaera Drugg, 1970 emend. Morgan, 1975
Batiacasphaera minuta (Matsuoka, 1983) Matsuoka and Head, 1992 emend. Matsuoka and Head, 1992
Bitectatodinium Wilson, 1973
Bitectatodinium raedwaldii Head, 1997
Bitectatodinium tepikiense Wilson, 1973
Bitectatodinium sp.A of De Schepper *et al.*, 2017
Brigantedinium Reid, 1977 ex Lentin and Williams, 1993
Brigantedinium auranteum Reid, 1977 ex Lentin and Williams, 1993
Brigantedinium cariacense (Wall, 1967) Lentin and Williams, 1993
Brigantedinium majusculum Reid, 1977 ex Lentin and Williams, 1993
Brigantedinium simplex Wall, 1965 ex Lentin and Williams, 1993
Cerebrocysta Bujak in Bujak *et al.*, 1980

- cf. *Cerebrocysts*? *namocensis* Head, Norris and Mudie, 1989
Cordosphaeridium minimum (Morgenroth, 1966) Benedek, 1972
Corrudinium Stover and Evitt, 1978
Corrudinium harlandii Matuoka, 1983
Corrudinium labradori Head, Norris and Mudie, 1989
Cyst of *Pentaspharodinium dalei* Indelicato and Loeblich III, 1989
Cyst of *Scrippsiella trifida* Lewis, 1991 ex Head 1996
Cysts type I de de Vernal and Mudie, 1989
Dubridinium Reid, 1977
Echinidinium Zonneveld 1997 ex Head, Harland and Matthiessen, 2001
Echinidinium zonneveldiae Head, 2003
Filisphaera Bujak, 1984
Filisphaera filifera Bujak, 1984
Filisphaera microornata (Head Norris and Mudie, 1989) Head, 1994
Habibacysta Head *et al.*, 1989
Habibacysta sp. of Head *et al.*, 1994
Habibacysta sp. A
Habibacysta tectata Head Norris and Mudie, 1989
Heteraulacacysta sp. of Costa and Downie, 1979
Impagidinium Stover and Evitt, 1978
Impagidinium aculeatum (Wall, 1967) Lentin and Williams, 1981
Impagidinium cantabrigiense De Schepper and Head, 2008
Impagidinium cf. *velorum* of Bujak 1984
Impagidinium pallidum Bujak, 1984
Impagidinium paradoxum (Wall, 1967) Stover and Evitt, 1978
Impagidinium patulum (Wall, 1967) Stover and Evitt, 1978
Impagidinium plicatum Versteegh and Zevenboom 1995
Impagidinium solidum Versteegh and Zevenboom in Versteegh, 1995
Impagidinium sphaericum (Wall, 1967) Lentin and Williams, 1981
Impagidinium striatum (Wall, 1967) Stover and Evitt, 1978
Impagidinium cf. *velorum* Bujak, 1984
Impagidinium sp. 2 of De Schepper and Head, 2009
Invertocysta Edwards, 1984
Invertocysta lacrymosa Edwards, 1984
Invertocysta tabulata Edwards, 1984
Islandinium? *cezare* (de Vernal *et al.*, 1989 ex de Vernal in Rochon *et al.* 1999) Head *et al.*, 2001
Islandinium brevispinosa Pospelova and Head, 2002

- Islandinium minutum* (Harland and Reid in Harland *et al.*, 1980) Head *et al.*, 2001
Lejeuneocysta Artzner and Dörhöfer, 1978 emend. Lentin and Williams, 1976 and Bujak in Bujak *et al.*, 1980
Lejeuneocysta catomus? Harland *et al.*, 1991
Lejeuneocysta hatterasensis Head and Norris, 2003
Lejeuneocysta marieae (Harland in Harland *et al.*, 1991) Lentin and Williams, 1993
Lejeuneocysta sp. A
Lingumodinium machaerophorum (Deflandre and Cookson 1955) Wall, 1967
Melitasphaeridium choanophorum (Deflandre and Cookson 1955) Wall, 1967
Nematosphaeropsis labyrinthus (Ostenfeld 1903) Reid, 1974
Nematosphaeropsis lativittata Wrenn, 1988
Operculodinium Wall, 1967 emend. Matsuoka, McMinn and Wrenn, 1997
Operculodinium ? *eirikianum cerebrum* Head *et al.*, 1989 emend. Head, 1997
Operculodinium ? *eirikianum eirikianum* (Head *et al.*, 1989) De Schepper and Head, 2008
Operculodinium centrocarpum sensu Wall and Dale (1966)
Operculodinium centrocarpum sensu stricto (Deflandre and Cookson, 1995) Wall, 1967
Operculodinium piaseckii Strauss and Lund, 1992 emend. de Verteuil and Norris, 1996
Piccoladinium Versteegh and Zevenboom, 1995
Polykrikos Bütschli, 1873
Pyxidinopsis Habib, 1976
Pyxidinopsis braboi De Schepper, Head and Louwye, 2004
Pyxidinopsis psilata (Wall and Dale, 1973) Head, 1994
Pyxidinopsis reticulata McMinn and Sun Xuekun, 1994 emend. Marret and de Vernal, 1997
Pyxidinopsis tuberculata Versteegh and Zevenboom, 1995
Reticulatosphaera actinocoronata (Benedel, 1972) Bujak and Matsuoka 1986 emend. Bujak and Matsuoka, 1986
Round brown cysts
Selenopemphix Benedek, 1972 emend. Head 1993
Selenopemphix brevispinosa Head, 1989
Selenopemphix dionaeacysta Head, Norris and Mudie, 1989
Selenopemphix nephroides Benedek 1972 emend. Bujak in Bujak *et al.*, 1980
Spiniferites Mantell, 1850 emend. Sarjeant, 1970/*Achromosphaera* Evitt, 1963
Spiniferites elongatus Reid, 1974
Spiniferites hyperacanthus (Deflandre and Cookson 1955) Cookson and Eisenack 1974
Spiniferites membranaceus (Rossignol, 1964) Sarjeant, 1970
Spiniferites mirabilis (Rossignol 1964) Sarjeant 1970
Spiniferites ramosus (Ehrenberg, 1828) Mantell, 1854
Spiniferites rubinus (Rossignol, 1962 ex Rossignol, 1964) Sarjeant, 1970

Spiniferites sp. A*Tectatodinium pellitum* (Wall, 1967) Head, 1994*Tectatodinium* sp. A*Trinovantedinium* Reid, 1977 emend. de Verteuil and Norris, 1992*Trinovantedinium glorianum* (Head, Norris and Mudie, 1989) de Verteuil and Norris, 1992*Trinovantedinium variabile* (Bujak, 1984) de Verteuil and Norris, 1992

Dinocyst sp. A

Dinocyst sp. B

Dinocyst spp.

Acritarchs*Cymatiosphaera* Wetzel, 1933 ex Deflandre, 1954*Cymatiosphaera? aegirii* De Schepper and Head, 2014*Cymatiosphaera? fensomei* De Schepper and Head, 2014*Cymatiosphaera? icernorum* De Schepper and Head, 2014*Cymatiosphaera? invaginata* Head, Norris and Mudie, 1989*Cymatiosphaera. latisepta* De Schepper and Head, 2008*Cymatiosphaera* sp.1 of Schreck, 2013*Cymatiosphaera* sp.2 of Schreck, 2013*Lavradosphaera* spp. De Schepper and Head, 2008*Lavradosphaera canalis* De Schepper and Head, 2014*Lavradosphaera crista* De Schepper and Head, 2008*Lavradosphaera lucifer* De Schepper and Head, 2008*Leiosphaeridia rockhallensis* Head and Norris, 2002*Leiosphaeridia* spp. Eisenack, 1985 emend. Downie, Evitt and Sarjeant, 1963*Micrystridium* spp.*Cystidiopsis certa* Nagy, 1965*Nannobarbophora walldalei* Head, 1996*Pterospermella* spp. Eisenack, 1972

Cyst 1 of de Vernal and Mudie, 1989

Acritarch sp. 1 of Hennissen, 2013

Acritarch sp. 6 of Hennissen, 2013

Acritarch sp. 9 of Hennissen, 2013

Acritarch spp. indet.

ANNEXE B

SUPPLEMENTARY INFORMATION B DU CHAPITRE II

**Concentration comparison for 4 Samples prepared and analyzed in Norway (S.
De Schepper) and Canada (A. Aubry)**

	Hole	B		B		B		B	
	Core	13		14		15		15	
	Section	04 W		06 W		01 W		04 W	
	Intervalle	30 - 32 cm		30-32 cm		30-32 cm		30-32 cm	
	Depth (mbsf)	114,1		126,6		128,6		133,1	
	Lab number	13C316	3287-1	13D62	3147-6	13D63	3148-3	13D65	3285-3
	Dry weight (g)	16,17	5,77	10,49	9,0383	16,95	4,7264	22,78	7,4
	Tablets added	1							
	Batch number	483216							
	Number of <i>Lycopodium clavatum</i> grains added	18583							
DINOCYSTS	Standard deviation	1708							
	Coefficient of variation (%)	9,19							
	Number of <i>Lycopodium clavatum</i> counted	334	1516	687	1274	819	1920	1203	1293
	SDS:Stijn De Schepper; AA=Aurélie Aubry	SDS	AA	SDS	AA	SDS	AA	SDS	AA
	Total dinocysts counted	321	189	311	139	357	90	295	126
	Number of species	14	14	18	13	18	10	17	12
	Dinocyst concentration (cyst/g)	1104	402	802	224	478	184	200	245
	Total of acritarcha counted	1	19	410	1651	27	98	1	429
	Number of species	1	6	6	10	5	8	1	6
	Acritarch concentration (cyct/g)	3	40	1057	2664	36	201	1	833
FRESH WATER ALGAE	Total of algae counted	0	0	0	0	0	1	1	0
	Number of species	0	0	0	0	0	1	1	0
	Fresh water algae concentration (algae/g)	0	0	0	0	0	2	1	0
POLLEN GRAINS	total of pollen grains counted	15	2	36	29	43	11	36	10
	Pollen grain concentration (grain/g)	52	4	93	47	58	23	24	19
SPORES	total of spores counted	0	2	3	18	13	2	8	4
	Spore concentration (spore/g)	0	4	8	29	17	4	5	8
REWORKING	Total of marine reworked palynomorphs counted	4	6	0	6	3	4	2	9
	Total of terrestrial reworked palynomorphs counted	9	44	1	258	8	109	4	373
	Reworked palynomorph concentration (palynomorph/g)	45	106	3	426	15	231	4	742

ANNEXE C

SUPPLEMENTARY INFORMATION B DU CHAPITRE I ET A DU CHAPITRE II

**Palynomorph counts, including pollen, spores, dinocysts and acritarcha, from
3.2 to 2.2 Ma in sediment samples from IODP Site U1307**

Étant trop volumineux, le fichier est disponible au format tableur excel dans le lien suivant. Après acceptation des articles des chapitres I et II, le fichier sera accessible en ligne via le site des revues.

<https://www.dropbox.com/s/zahdvd76rnzkf10/Annexe%20C%20Aubry%20PhD%202019.xlsx?dl=0>

ANNEXE D

SUPPLEMENTARY INFORMATION S2 DU CHAPITRE III

List of taxonomic names and their full authorial citations of dinocysts and acritarcha from the late Miocene to early Pleistocene of ODP Site 645

Dinocysts

- Achomosphaera* Evitt, 1963
Ataxiodinium zevenboomii Head, 1997
Barssidinium pliocenicum (Head, 1993) Head, 1994 emend. De Schepper and Head, 2004
Batiacasphaera Drugg, 1970 emend. Morgan, 1975
Batiacasphaera hirsuta Stover 1977
Batiacasphaera micropapillata complex (Stover 1977) Schreck and Matthiessen (2013)
Bitectatodinium Wilson, 1973
Bitectatodinium raedwaldii Head, 1997
Bitectatodinium tepikense Wilson, 1973
Brown cysts spp.
Brown spiny cysts spp.
Cordosphaeridium Eisenack, 1963 emend. Morgenroth, 1968; Davey, 1969; Sarjeant, 1981; Chengquan, 1991
Corrudinium Stover and Evitt, 1978
Corrudinium labradori Head *et al.*, 1989
Cyst of *Pentaspharodinium dalei* Indelicato and Loeblich III, 1989
Cristadinium diminutivum Head *et al.*, 1989
Echinidinium Zonneveld, 1997 ex Head *et al.*, 2001
Filisphaera Bujak, 1984
Filisphaera filifera Bujak, 1984
Filisphaera microornata (Head *et al.*, 1989) Head, 1994
Habibacysta Head *et al.*, 1989
Habibacysta tectata Head *et al.*, 1989
Impagidinium Stover and Evitt, 1978

- Impagidinium aculeatum* (Wall, 1967) Lentin and Williams, 1981
Impagidinium pallidum Bujak, 1984
Impagidinium paradoxum (Wall, 1967) Stover and Evitt, 1981
Impagidinium sp. 2 of De Schepper and Head, 1999
Lejeuneacysta Artzner and Dörhöfer, 1978 emend. Kjellström, 1972; Lentin and Williams, 1976 and Bujak in Bujak *et al.*, 1980
Lejeuneacysta marieae (Harland in Harland *et al.*, 1991) Lentin and Williams, 1993
Lejeuneacysra fallax (Morgenroth 1966) Artzner and Dörhöfer, 1978 emend. Biffi and Grignani, 1983
Lejeuneacysta cinctoria (Bujak in Bujak *et al.*, 1980) Lentin and Williams, 1981
Lingulodinium Wall, 1967 emend. Wall *et al.*, 1973
Lingumodinium machaerophorum (Deflandre and Cookson, 1955) Wall, 1967
Melitasphaeridium choanophorum (Deflandre and Cookson, 1955) Wall, 1967
Nematosphaeropsis Deflandre and Cookson, 1995 emend. Williams and Downie 1966, Wrenn 1988
Nematosphaeropsis labyrinthus (Ostenfeld, 1903) Reid, 1974
Operculodinium Wall 1967 emend. Matsuoka *et al.*, 1997
Operculodinium ? *eirikianum cerebrum* Head *et al.*, 1989 emend. Head, 1997
Operculodinium ? *eirikianum eirikianum* Head *et al.*, 1989 emend. Head, 1997
Operculodinium centrocarpum sensu Wall and Dale 1966 (Deflandre and Cookson, 1995) Wall, 1967, *sensu* Wall and Dale, 1966
Operculodinium centrocarpum sensu stricto Deflandre and Cookson, 1995
Operculodinium sp. cf. *tegillatum*
Pyxidinopsis Häbib, 1976
Pyxidinopsis braboi De Schepper, Head and Louwey, 2004
Pyxidinopsis tuberculata Versteegh and Zevenboom, 1995
Reticulatosphaera actinocoronata (Benedek, 1972) Bujak and Matsuoka, 1986 emend. Bujak and Matsuoka, 1986
 Round brown cysts = *Brigantedinium* Reid, 1977 ex Lentin and Williams, 1993
Selenopemphix Benedek, 1972 emend. Bujak in Bujak *et al.*, 1980
Selenopemphix brevispinosa Head, 1989
Selenopemphix dionaeacysta Head, Norris and Mudie, 1989
Selenopemphix nephroides (Benedek, 1972) Bujak in Bujak *et al.*, 1980
Spiniferites Mantell, 1850 emend. Sarjeant, 1970
Spiniferites elongatus Reid, 1974
Spiniferites ramosus (Ehrenberg, 1828) Mantel, 1854
 Dinocyst spp.

Acritarcha

- Cymatiosphaera* (Wetzel, 1933) Deflandre, 1954
Cymatiosphaera? *aegirii* De Schepper and Head 2014
Cymatiosphaera? *fensomei* De Schepper and Head 2014
Cymatiosphaera? *icernorum* De Schepper and Head 2014
Cymatiosphaera? *invaginata* Head, Norris and Mudie 1989

- Cymatiosphaera latisepta* De Schepper and Head 2008
Cymatiosphaera sp. 1 of Schreck
Cystidiopsis certa Nagy, 1965
Lavradosphaera De Schepper and Head, 2008
Lavradosphaera canalis De Schepper and Head 2014
Leiosphaeridia rockhallensis Head and Norris, 2003
Leiosphere spp. = Sphaeromorphitic acritarch of Schreck *et al.*, 2013
Ornamented Leiosphaera = Sphaeromorphitic acritarch of Schreck *et al.*, 2013
Micrystridium (Deflandre, 1973) Sarjeant, 1963
Nannobarbophora walldalei Head, 1996
Veryhachium Deunff, 1954
Veriplicidium franklinii of Anstey, 1992
Acritarch sp. 6 of Hennissen 2013
Acritarch spp.

ANNEXE E

SUPPLEMENTARY INFORMATION S1 DU CHAPITRE III

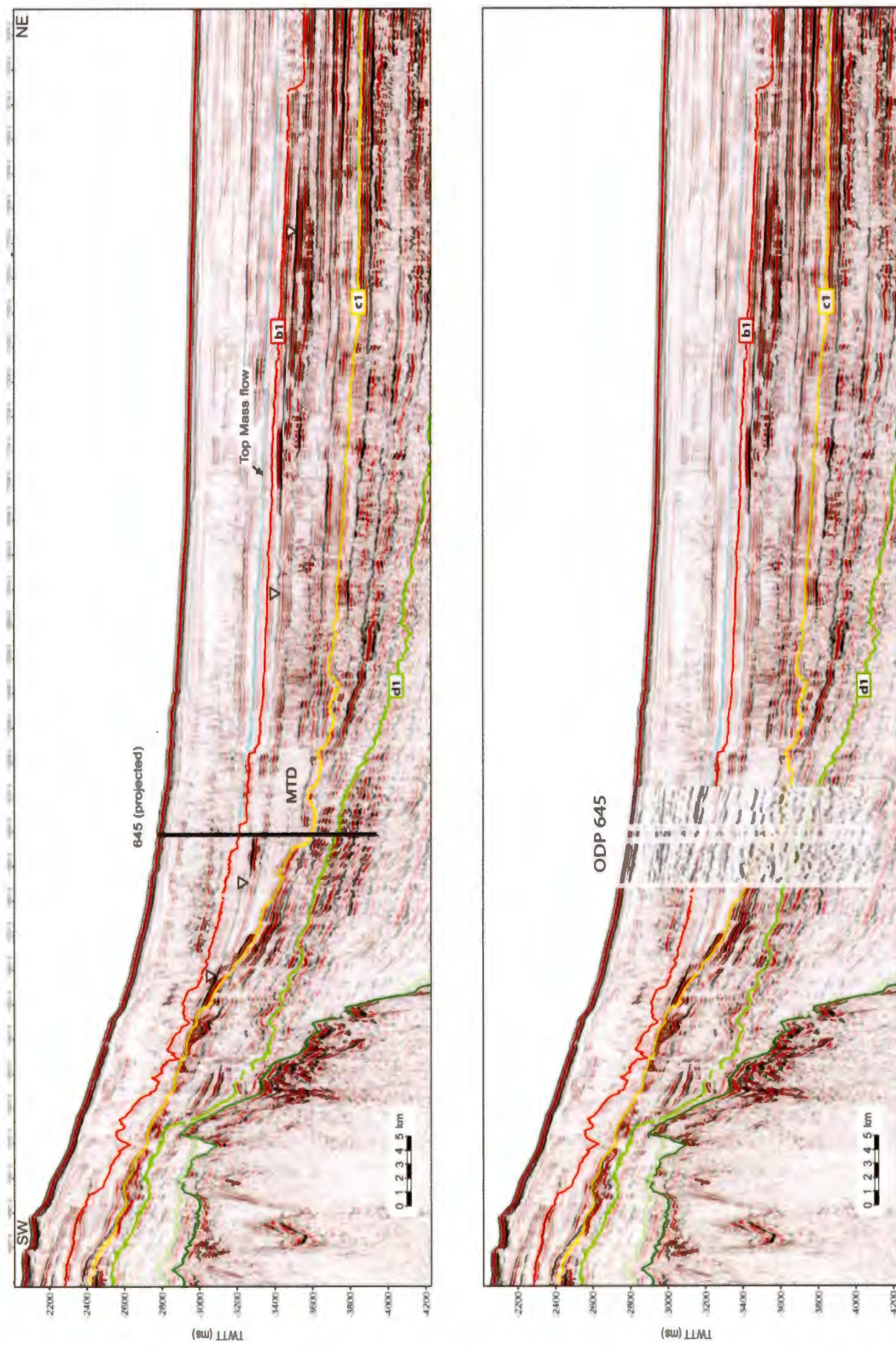
**Full marine and terrestrial palynomorph counts in ODP Hole 645B between
438.6 and 120.56 mbsf**

	mbf (m)	120.56	130	150.68	158.9	170	180.89	191.05	200.98	209.89	220.94	236	246.39	256	266.4	276	286.42	293.69	297.25	302.05	302.05	310.6	317.6	320.65	322	329.2	410.4	421.94	422.6	432	438.6			
<i>Sphagnum elongatum/ffigulus</i>																																		
<i>Sphagnum fuscum</i>																																		
<i>Sphagnum sp.</i>	3	1	5	1	1	2	1	2	1	16	1	1	3	1	4	22	5	2	3	2	19	2	2	2	4	4	8							
round brown spts	10	62	1	9	6	5	4	4	1	1	1	12	1	10	12	10	5	12	10	5	16	3	1	2	17									
brown cyst. spts																																		
brown spm/cysts sp.																																		
Dioon top index	4	1	10	1	2	1	8	1	1	1	1	1	1	1	1	1	7	3	6	3	28	1	1	2	3									
TOTAL	151.56	182	151.68	165.9	200	211.98	221.98	231.89	236.94	231	240.39	241	246.47	249.60	258.45	260.6	268.4	270.6	274.6	282.6	288.65	292.2	297.4	302.6	306	342.6								
Number of species	9	2	2	13	13	18	6	6	15	9	3	15	11	1	15	0	22	18	12	16	12	7	19	11	20	21	22							
Acrithoch. concentration (cps/m³)	213	179	182.8	210	252	685	589	565	4280	3222	2465	564	1332	2708	3018	338	462	2225.51	437	1723	2383	2398	1331	1485	3023	1395	6932	2372	5024	2564	8389			
ACRITHOCH. CONCENTRATION (cps/m³)																																		
ACRITHOCH. CONCENTRATION (cps/m³)																																		
<i>Cyanophora, Imugnophora</i>																																		
<i>Omniosphaera, Eustomel</i>																																		
<i>Omniosphaera, Eustomum</i>																																		
<i>Omniosphaera sp. of Shiret</i>																																		
<i>Cyanosphaera spp.</i>	1																																	
<i>Cyanocephala zetra</i>																																		
<i>Lamprocephala conidis</i>																																		
<i>Lamprocephala, conidis</i>																																		
<i>Leptosphaera sp.</i>	1																																	
<i>Leptosphaera prokochensis</i>	4																																	
oriented leiosphere																																		
<i>Leiosphaera</i> spp.	1																																	
<i>Micromidium</i> spp.																																		
<i>Nemobionphora wolderi</i>																																		
<i>Velidium kantolini</i>																																		
<i>Veronica</i> spp.	1																																	
ACRITHOCH. CONCENTRATION (cps/m³)	5	11	2	1	3	1	4	2	3	14	1	0	10	2	5	91	206	2	0	29	12	389	337	169	16	14	51	92	9	6	60	28		
ACRITHOCH. CONCENTRATION (cps/m³)	3	12	5	2	1	3	6	1	0	3	1	1	4	1	7	1	2	0	0	2	3	4	3	3	4	3	3	4	4	4	4	4		
ACRITHOCH. CONCENTRATION (cps/m³)	37	5	12	20	3	0	37	20	30	30	37	20	30	16	24	418	1832	2	0	0	0	55	2239	182	529	58	99	169	773	57	57	304	365	
POLLEN GRAMS																																		
Category 1																																		
Trees																																		
Abies	9	1	5	12	35	4	1	15	49	5	35	11	26	39	10	48	19	58	3	12	9	30	10	96	255	51	19	5	6	63	4	4		
Picea	12	1	19	50	67	11	2	26	39	10	48	19	58	3	12	9	30	10	96	255	51	19	5	6	63	4	4	4	4	4				
Rhus																																		
Tilia																																		
Tuta peruviana																																		
Gymno.																																		
Acer																																		
Betula																																		
Carpinus/Ostrya																																		
Corylus	1		4	1	3																													
Fraxinus																																		
Hedera																																		
Quercus																																		
Liriodendron																																		
TOTAL	22	0	1	2	28	64	118	18	3	49	96	15	96	42	86	10	23	15	3	48	21	161	392	93	41	15	10	26	7	108	13	7		
tree cone extract/gram (g)	34	0	12	3	35	157	82	50	47	622	954	148	204	52	54	26	24	23	169	96	927	193	148	106	33	264	44	1034	66	91				
Shrubs																																		
Betula																																		
Alnus spp.	6		2																															
Eriaceous	6	3																																
Hedysarum	2																																	
Salix	2	0	5	4	15	20	16	0	2	4	1	15	32	5	8	2	6	2	9	13	55	150	275	44	87	77	60	9	101	25	66	39		
TOTAL	14	3	0	6	5	4	15	20	16	0	2	4	1	15	32	5	8	2	6	2	9	13	55	150	275	44	87	77	60	9	101	25	66	39

ANNEXE F

SUPPLEMENTARY FIGURE S1 DU CHAPITRE III

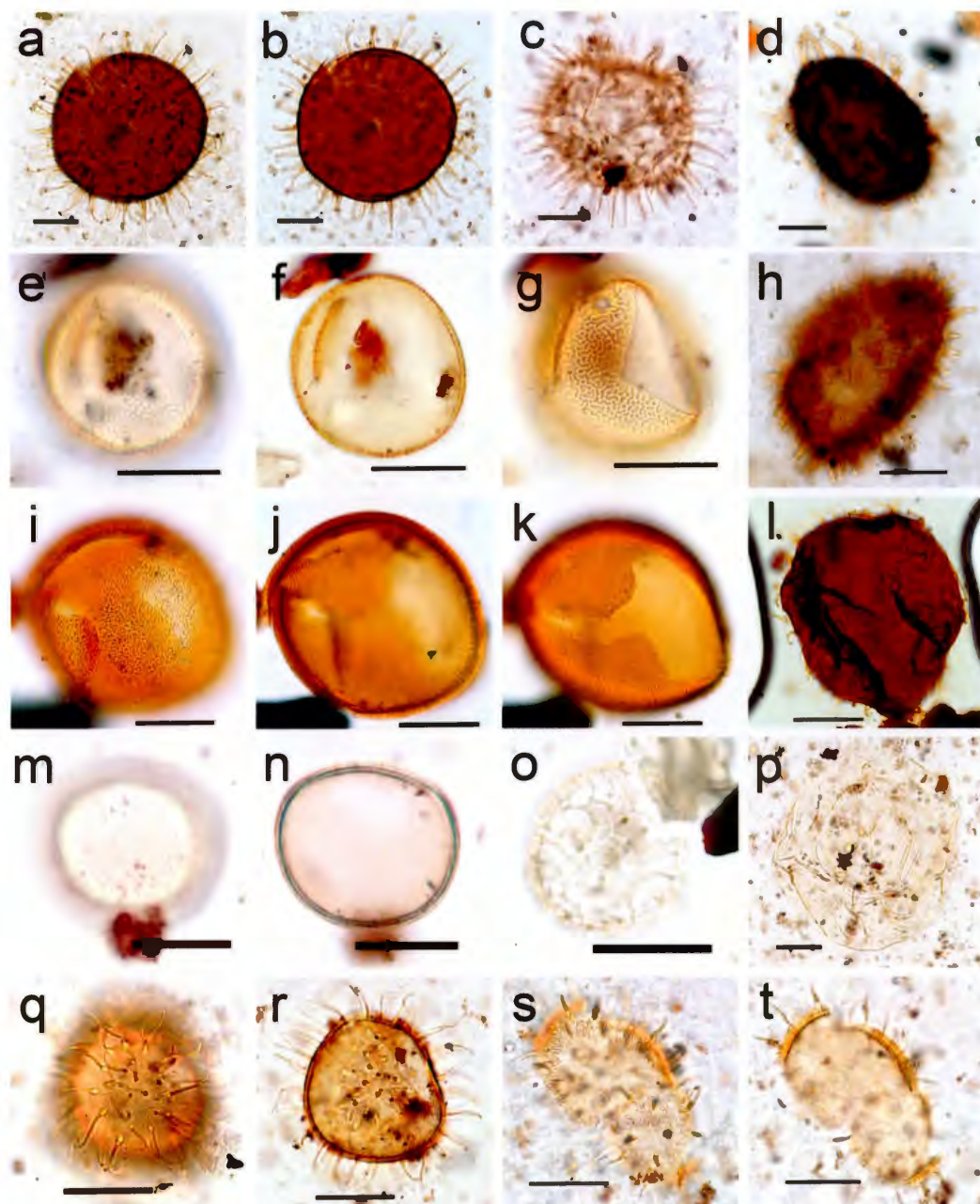
Overview of the seismic transect in southwest Baffin Bay (line TGS 2008) from Knutz *et al.* (2015) and correlation with ODP Site 645 displaying our new horizon and mega-unit interpretations. Vertical axis is in two-way traveltime (twtt). Original site survey lines and drilling site from the Shipboard Scientific Party (1987). Previous position of the b1 horizon is indicated by white triangles



ANNEXE G

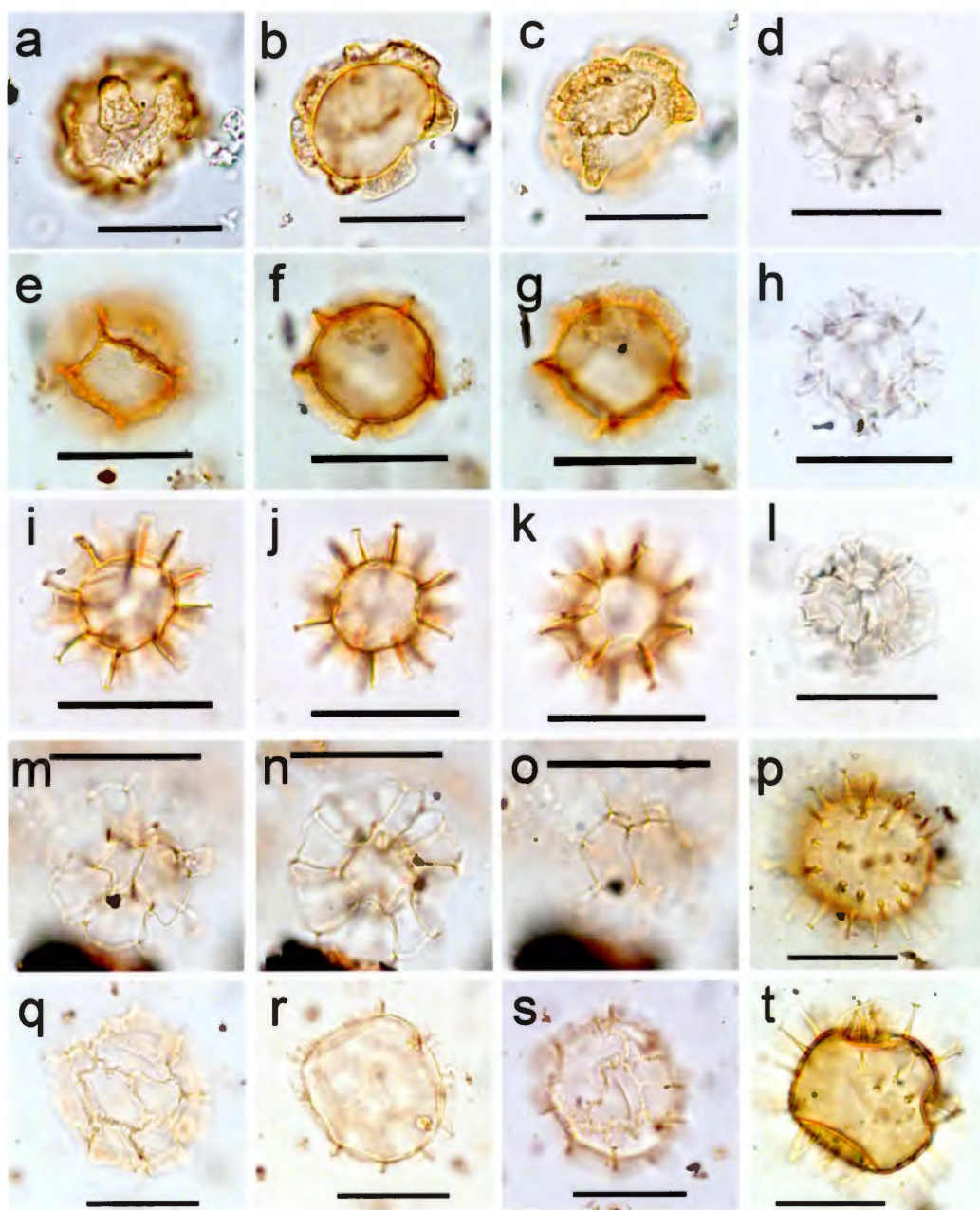
SUPPLEMENTARY PLATES DU CHAPITRE I

Plate 1.



Supplementary Plate 1. Photographs of the most biostratigraphically important dinocyst taxa recovered in sediments from IODP Site U1307. Scale bars are 10 µm.

- a-d.** *Barssidinium graminosum*, **a, b.** IODP U1307A-19H-4, 30-32 cm, U25/3, slide 3181-4. **c.** IODP U1307A-19H-4, 30-32 cm, U48/2, slide 3181-4. **d.** IODP U1307B-15H-5, 30-32 cm, AA39/0, slide 3285-1.
- e, f, g.** *Pyxidinopsis braboi*, IODP U1307A-14H-3, 140-142 cm, Z33/4, slide 3550-2.
- h, i, l.** *Barssidinium pliocenicum*, **h.** IODP U1307A-19H-4, 30-32 cm, AA38/4, slide 3181-4. **i.** IODP U1307B-15H-3, 80-82 cm, Z19/4, slide 3285-5.
- i, j, k.** *Filisphaera filifera*, IODP U1307B-15H-3, 130-132 cm, L33/2, slide 3285-4.
- m, n.** *Habibacysta tectata*, IODP U1307A-14H-3, 120-122 cm, Z52/3, slide 3550-1.
- o.** *Corrudinium harlandii*, IODP U1307B-15H-1, 30-32 cm, W39/0, slide 3148-3.
- p.** *Invertocysta lacrymosa*, IODP U1307B-16H-2, 88-90 cm, U23/0, slide 3255-5.
- q, r.** *Operculodinium? eirikianum* var. *eirikianum*, IODP U1307A-19H-2, 130-132 cm; G50/0, slide 3181-2.
- s, t.** *Operculodinium? eirikianum* var. *crebrum*, IODP U1307A-19h-6, 80-82 cm, AA46/1, slide 3182-4.

Plate 2.

Supplementary Plate 2. Photographs of the most abundant acritarch taxa (and one dinocysts) recovered in sediments from IODP Site U1307. Scale bars are 10 µm.

a, b, c. *Lavradosphaera canalis*, IODP U1307B-14H-3, 130-132 cm, V21/4, slide 3053-1

d, h, l. *Cymatiosphaera? invaginata*, IODP U1307B-14H-3, 130-132 cm, Z45/3, slide 3053-1

e, f, g. *Lavradosphaera crista*, IODP U1307B-15H-5, 30-32 cm, W46/1, slide 3285-1.

i, j, k. *Cymatiosphaera? icenorum*, IODP U1307B-15H-3, 80-82 cm, Q39/3, slide 3285-5.

m, n, o. *Cymatiosphaera? aegirii*, IODP U1307B-13H-4, 52-54 cm, L41/3, slide 3550-5.

p, t. *Operculodinium centrocarpum* sensu Wall and Dale (1966), IODP U1307A-14H-3, 120-122 cm, AA24/0, slide 3550-1.

q, r, s. *Cymatiosphaera? fensomei*, IODP U1307B-14H-5, 80-82 cm, X57/4, slide 3147-4

APPENDICE A

THE « WARM » MARINE ISOTOPE STAGE 31 IN THE LABRADOR SEA: LOW SURFACE SALINITIES AND COLD SUBSURFACE WATERS PREVENTED WINTER CONVECTION

Aubry, A. M. R., de Vernal, A., and Hillaire-Marcel, C. (2016). The “warm” Marine Isotope Stage 31 in the Labrador Sea: Low surface salinities and cold subsurface waters prevented winter convection. *Paleoceanography*, 31(9), 1206-1224. doi:10.1002/2015PA002903.



Paleoceanography

RESEARCH ARTICLE

10.1002/2015PA002903

Key Points:

- Warmer and generally low salinity in upper water layer in Labrador Sea during MIS 31 than present
- Cool subsurface waters in the inner Labrador Sea during MIS 31
- Strong stratification of the water column and no convection in the Labrador Sea during MIS 31

Correspondence to:
A. M. R. Aubry,
aubraumr@gmail.com

Citation:
Aubry, A. M. R., A. de Vernal, and C. Hillaire-Marcel (2016), The "warm" Marine Isotope Stage 31 in the Labrador Sea: Low surface salinities and cold subsurface waters prevented winter convection, *Paleoceanography*, 31, doi:10.1002/2015PA002903.

Received 18 NOV 2015
Accepted 14 AUG 2016
Accepted article online 22 AUG 2016

The "warm" Marine Isotope Stage 31 in the Labrador Sea: Low surface salinities and cold subsurface waters prevented winter convection

A. M. R. Aubry¹, A. de Vernal¹, and C. Hillaire-Marcel¹

¹GÉTOP, Université du Québec à Montréal, Montréal, Québec, Canada

Abstract Surface and subsurface conditions in the Labrador Sea during Marine Isotope Stage (MIS) 31 at the Integrated Ocean Drilling Program Site U1305 off southwest Greenland are reconstructed based on dinocyst and foraminifer assemblages. Isotopic compositions of planktonic (*Neogloboquadrina pachyderma*, Np) and benthic (*Cibicides wuellerstorff*, Cw, and *Ostreaforam umbonata*, Ou) foraminifers provide further information about water properties in the mesopelagic layer as well as at the seafloor. Dinocyst proxy reconstructions indicate low salinities (32–34.5), cool winters (3–6°C), and mild summers (10–15°C) in the surface water layer during the MIS 31 "optimum". However, planktonic foraminifer assemblages largely dominated by Np suggest relatively cold subsurface conditions in winter and summer (<4°C). Lower $\delta^{13}\text{C}$ values in Np versus Cw further suggest either a less-ventilated mesopelagic layer than the bottom one or high organic matter oxidation rates at Np habitat depth. The dinocyst and planktonic foraminifer records together suggest a strong stratification between the surface and subsurface water layers. Isotopic and micropaleontological data thus converge toward paleoceanographical conditions unsuitable for convection and intermediate or deep water formation in the Labrador Sea during the warm MIS 31 interglacial, a situation comparable to the one that prevailed during the warm MIS 5e.

1. Introduction

Marine Isotope Stage (MIS) 31 is dated between 1.081 Ma and 1.062 Ma and occurs at the base of the Jaramillo magnetic reversal [Lisiecki and Raymo, 2005; Villa et al., 2008; Scher et al., 2008]. It is often described as a "super interglacial" in both the Northern and Southern Hemispheres because of extreme warm conditions to which it has been associated [De Conto et al., 2012; Melles et al., 2012]. For example, in northeast Russia, pollen data suggest regional summer air temperatures of about 4–5°C higher than at present [Melles et al., 2012]. As another example, south of the Antarctic Circle, Mg/Ca ratios in planktonic foraminifera indicate sea surface temperatures 5–9°C higher than the modern temperatures [Dunbar, 2012]. The configuration of orbital parameters responsible for particularly high insolation in the Northern Hemisphere was used to explain the high temperatures and lower volume of continental ice sheets during MIS 31 [Laskar et al., 2004; Melles et al., 2012]. The interglacial of MIS 31 therefore deserves some attention as it may serve as a reference to investigate the response of ocean circulation and deep water formation under a warm climate regime.

In this study, we have paid special attention to the Labrador Sea, where winter convection [Marshall and Schott, 1999] presently accounts for a large part of the Atlantic Meridional Overturning Circulation (AMOC) [Wedder et al., 1999; Yashayaev, 2007; Yashayaev et al., 2007]. In this basin, convection has been recorded to be variable at interannual time scale [Lazier et al., 2002]. Paleoceanographical studies further suggest that it might have been mostly ineffective prior to the middle to late Holocene interval, and quite variable when effective [e.g., Hillaire-Marcel and Blouet, 2000]. Reconstruction of sea surface parameters in Holocene sediment cores from the Labrador Sea illustrate millennial scale changes in temperature and salinity and, thus, in density, indicating that the onset of conditions favorable to vertical convection and Labrador Sea Water (LSW) formation occurred only after circa 7.5 ka [de Vernal and Hillaire-Marcel, 2006; Gibb et al., 2014, 2015]. The analyses of older sedimentary sequences yielded so far no evidence of convection, notably during the last interglacial (MIS 5e, 128–117 ka) [Hillaire-Marcel et al., 2001, 2011].

The main objective of this study is to document the surface and subsurface conditions in the Labrador Sea and to assess vertical convection during the MIS 31 optimum. To meet these objectives, we have analyzed the micropaleontological content of sediments from the Integrated Ocean Drilling Program (IODP) Site

©2016. American Geophysical Union.
All Rights Reserved.

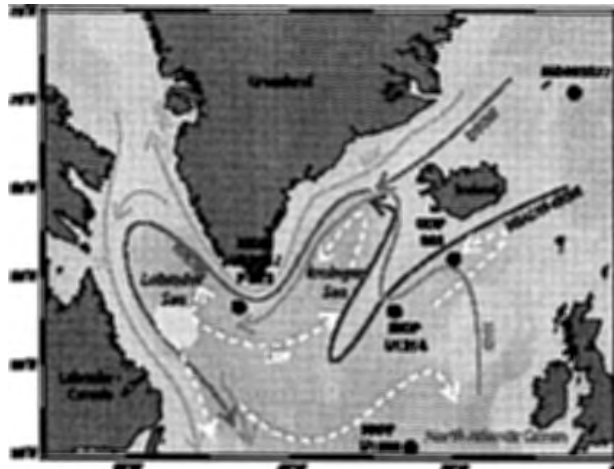


Figure 1. Schematic illustration of ocean circulation in the North Atlantic and location of the study site. Surface currents (green and yellow arrows) include the West Greenland Current (WGC), the East Greenland current (EGC), the Labrador Current (LC), and the North Atlantic Drift (NAD). The deep currents (blue arrows) include the North Atlantic Deep Current (NADC), the North East Atlantic Deep Water (NEADW), the Iceland-Scotland Overflow Water (ISOW), and the Denmark Strait Overflow Water (DSOW). The location of the Labrador Sea Water (LSW) formation is indicated by the white ellipse, and the circulation path of the LSW is figured by white-dashed arrows. IODP Site U1305, 57°28.5'N, 48°31.8'W, 3459 m; Other sites cited in the text are as follows: core HU-90-013-013 (P-013), 58°12.5'N, 47°22.40'W, 3380 m; core MD952277, 69°15'N 6°19'W, 2800 m; IODP Site U1314, 56°21'N, 27°53'W, 2799.4 m; IODP Site U1308, 49°52'N, 24°14'W, 3871 m; ODP Site 980, 55°29'N, 14°42'W, 2171.2 m; ODP Site 983: 60°24'N, 23°3.8'W, 1983 m.

U1305, which was drilled during the Expedition 303 [Channell et al., 2006] (Figure 1). We have used two main microfossil tracers, the planktonic foraminifer assemblages and the dinoflagellate cyst assemblages, in addition to stable isotopes ($\delta^{18}\text{O}$ and $\delta^{13}\text{C}$) measurements in planktonic and benthic foraminifer shells.

2. Regional Setting

Two main currents characterize the Labrador Sea surface waters. Along Canadian margins, the Labrador Current (LC) flows on the shelf and brings cool and fresh waters from the Arctic to the South. On the eastern side of the basin, the West Greenland Current (WGC) is the main source of low salinity water in the Labrador Sea [Schmidt and Send, 2007]. The WGC carries northwestward cold and fresh polar waters of the East Greenland Current (EGC, temperature <0°C, salinity 32.5–34) that mixes with the underlying warmer and saltier Irminger waters partly fed by the Atlantic Intermediate Water (34.8–35) [Aagaard and Coachman, 1968; Fratantoni and Pickart, 2007] (Figure 1).

The study site IODP U1305 is under the influence of the WGC, with sea surface temperatures (SSTs) of $8.2 \pm 1.7^\circ\text{C}$ in summer (July–September, SSTs), $3.5 \pm 0.7^\circ\text{C}$ in winter (January–March, SSTw), and salinity ranging 34.6–34.9 in summer and winter, respectively [National Oceanographic Data Center, <https://www.nodc.noaa.gov>]. Winter cooling leads to vertical convection from 1500 m to 1000–2500 m [Marshall and Schott, 1999; Lazier et al., 2002] and to the formation of Labrador Sea Water (LSW) that occupies the water column above the North East Atlantic Deep Water (NEADW, -3°C and 34.92), which is found between 2500 and 3000 m, and the Denmark Strait Overflow Water (DSOW, -1.78°C and 34.90, and > 3000 m; Figures 1 and 2) [Lucotte and Hilbre-Marcel, 1994; Yashayaev et al., 2007].

3. Stratigraphy of the Core

IODP Site U1305 is located off Southwest Greenland (57°28.5'N, 48°31.8'W) at a water depth of 3459 m [Channell et al., 2006]. The composite sedimentary sequence of 314 m encompasses the last 1.9 Ma, based

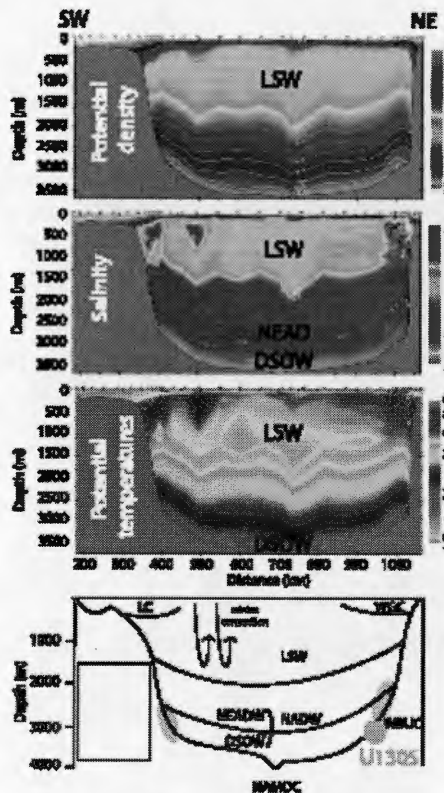


Figure 2. Transect across the Labrador Sea (AR7W section in the upper panel); the density, salinity, and potential temperature (in °C) profiles are from Yashayaev et al. (2014) based on measurements made in 2012; the scheme of the main water masses and currents and location of study Site U1305 is modified from Hillaire-Marcel and Blodéau (2000). LC = Labrador Current; WGC = West Greenland Current; LSW = Labrador Sea Water; MEADW = North East Atlantic Deep Water; DSOW = Denmark Strait Overflow Water; NADW = North Atlantic Deep Water; NAMOC = North Atlantic Mid-Ocean Channel. In the lower panel, the gray zones correspond to the maximum velocity depth of the Western Boundary Under Current (WBUC).

procedures [cf. de Vernal et al., 1999]. Lycopodium spore markers were added before treatment for calculating concentrations of palynomorphs [Matthews, 1969; Mertens et al., 2009]. Samples of 5 cm² were wet sieved on 10 and 105 µm mesh sieves. In order to follow the standard protocol of most studies, we counted foraminifera and the ice rafted debris (IRD) in the fraction greater than 150 µm after a second dry sieving. Concentrations were expressed in tests or grains per cm³ of wet bulk sediment. Planispheric foraminifera were identified according to the nomenclature of Hemleben et al. [1989], Kennett and Srinivasan [1983], and Kuva [2007] for *N. pachyderma* and *N. incisa*. Among benthic foraminifera, we have identified *Oridorsalis umbonata* (Ou) and *Gibicides wuellestorffii* (Cw) in reference to Jones and Brady [1994], Loeblich and Tappan [1988], and the web database *World Register of Marine Species Editorial Board* [2014]. These two benthic species are living on/in deep ocean sediment [Rathburn and Codiss, 1994].

on the calcareous nannofossil biostratigraphy [Charnell et al., 2006]. The most common lithology consists of silty clays, nannofossil oozes, or sandy clays [Charnell et al., 2006].

The isotope stratigraphy for the upper 184 m spanning MIS 33-1 was established by Hillaire-Marcel et al. [2011] from oxygen isotope measurements in *Neogloboquadrina pachyderma* (Rp). It was correlated with the benthic stack of Lisicki and Raymo [2005] for age boundary assignments, thus leading to potential offsets of up to a few 1000 years [Lisicki and Raymo, 2005, 2009]. The chronostratigraphy was further constrained from the paleomagnetic record (Table 1) [Charnell et al., 2006]. The base of the Jaramillo chronozone dated of 1.075 Ma is situated at 168.35 meters composite depth (mcd) [Charnell et al., 2006]. MIS 31 spans from 170.80 mcd (MIS 31/32, 1.081 Ma) to 165.91 mcd (MIS 30/31, 1.053 Ma) [Hillaire-Marcel et al., 2011]. Straightforward interpolation between these two transitions suggests a mean sedimentation rate of 25 cm yr⁻¹ for MIS 31, whereas upper and lower isotopic transitions suggest values of 22.27 cm yr⁻¹ and 30.5 cm yr⁻¹ below and above the Jaramillo interval, respectively (Figure 3).

4. Methods

A total of 82 sediment samples were analyzed at every 10 or 5 cm intervals between 165.91 and 170.75 mcd. This corresponds to a time resolution ranging between 7 and 3 1000 years (Figure 3). The samples were prepared for paleontological and micropaleontological analyses according to standard laboratory

Table 1. Chronostratigraphical Boundaries at IODP Site U1305

Depth (mcd)	Isotope Stage Transition	Paleomagnetic Datum From Channell et al. (2006)	Age (Ma) From Lisicki and Raymo (2005)
165.91	30/31		1.052
168.35		Jaramillo (bottom)	1.070
170.80	31/32		1.081
	32/33		1.104

Stable isotope measurements of *Neogloboquadrina pachyderma* were reported in Hillaire-Marcel et al. [2011]. Shells that were picked up in the 150–250 size range for stable isotope measurements were the most abundant and belong to the square-shaped morphotype. Here we add new measurements on the two-benthic foraminifer taxa (Cw and Ou). For stable isotope measurements, 100–120 µg of carbonate were analyzed. This corresponds to ~3 (Cw) to up to 36 (Ou) specimens. Before their isotopic analysis, benthic tests were baked at 250°C to oxidize their inner organic linings. Geochemical analyses were done at the Center for Research in Isotopic Geochemistry and Geochronology (GEOTOP) using a Multicarb™ preparation device on line with an IsoPrime™ isotope ratio mass spectrometer, through 100% orthophosphoric acidification method [Wendeborg et al., 2011]. Results are expressed in delta (δ) values against the international reference Vienna Pee Dee Belemnite. The home carbonate standard (UQ6) [Hillaire-Marcel et al., 1994] was calibrated using the Carrara marble National Bureau of Standards (NBS)-19 reference for $\delta^{13}\text{C}$ and $\delta^{18}\text{O}$. The overall analytical reproducibility is within $\pm 0.05\text{‰}$ ($\pm 1\sigma$) for both $\delta^{18}\text{O}$ and $\delta^{13}\text{C}$. The Cw $\delta^{18}\text{O}$ values must be corrected to account for specific vital effects and comparison with other benthic isotope records. A large array of offset values can be found in the literature [e.g., Costa et al., 2006], but for reason of consistency with most published records, we used the +0.6‰ correction proposed by Shackleton and Opdyke [1973].

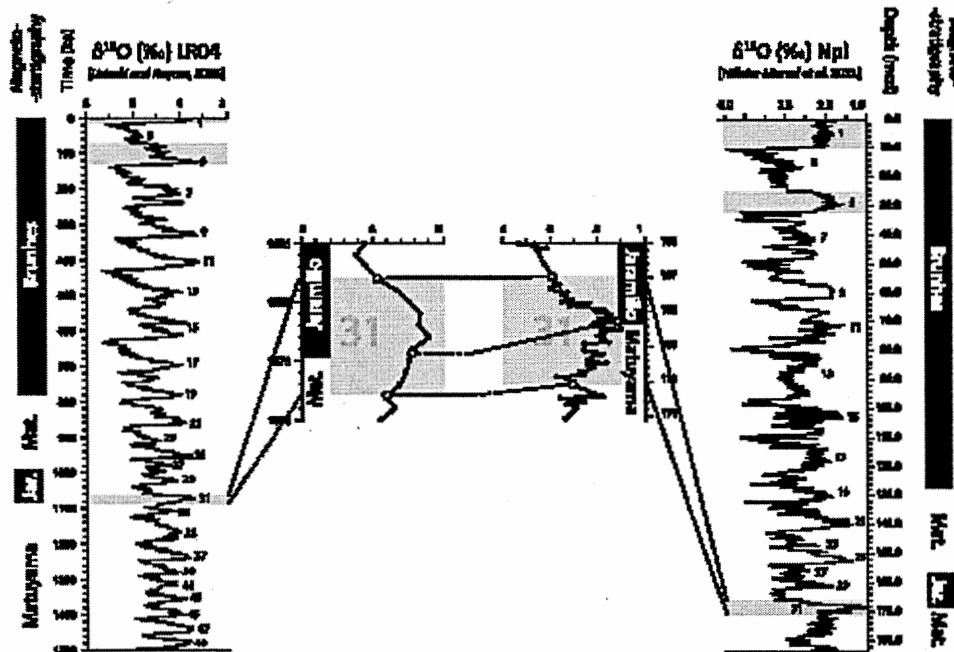


Figure 3. Stratigraphy at site IODP U1305 based on paleomagnetism [Channell et al., 2006] and correlation of the $\delta^{18}\text{O}$ in *Neogloboquadrina pachyderma* [Hillaire-Marcel et al., 2011] with the LR04 benthic stack of Lisicki and Raymo [2005].



The 10–106 µm fraction was treated for palynology with hydrochloric acid (HCl, 10%) to dissolve calcium carbonates and with hydrofluoric acid (HF, 48%) to remove silicates, then centrifuged and rinsed with distilled water. The residue was mounted between glass slides in glycerin jelly for microscopic observation. The identification of dinocysts at species or genus level was done at 400X or 1000X magnification, according to the nomenclature of Rochon *et al.* [1999] and De Schepper and Head [2008a, 2008b, 2009]. For each sediment sample, one or two slides were analyzed in order to obtain a minimum count of 300 specimens. Spores, pollen grains, benthic foraminifer linings, and reworked palynomorphs were also identified and counted at this unconstrained category level. Concentrations were expressed in terms of specimens per cm³ of wet sediment. According to de Vernal *et al.* [1987] and Mertens *et al.* [2009], this approach yields results with an accuracy of ± 10% for a confidence interval of 0.95.

Dinocysts are produced during the life cycle of dinoflagellates and are composed of resistant organic matter. They occur in relatively high numbers in polar and subpolar basins, where their assemblages include species related to both phototrophic and heterotrophic production [e.g., de Vernal and Maret, 2007]. Hence, dinocyst assemblages are routinely used to reconstruct environmental parameters such as sea surface salinity and temperature in winter and summer [de Vernal *et al.*, 1997, 2001, 2005a] in addition to mean annual primary productivity (PP) [Radi and de Vernal, 2008; Bonnet *et al.*, 2012]. They are found through a wide range of conditions from the tropics to the Arctic and from estuaries to open ocean [e.g., de Vernal *et al.*, 2001, 2005a, 2005b, 2013b; Radi and de Vernal, 2008; Bonnet *et al.*, 2012]. Multivariate analyses performed with the Canoco software [Ter Braak and Smilauer, 2002] on modern dinocyst assemblages, and surface ocean data demonstrate that SST, sea surface salinity (SSS), seasonality (seasonal contrast of temperature), sea ice cover, and productivity are all playing a determinant role on the distribution of dinocyst assemblages [Rochon *et al.*, 1999; Radi and de Vernal, 2008; Bonnet *et al.*, 2012; de Vernal *et al.*, 2013b]. Multivariate analyses were also performed on dinocyst assemblages of the study interval in order to identify the main changes in assemblages.

The modern analogue technique (MAT) using the software "R" (<http://cran.r-project.org>) with the script provided by J. Guiot (<https://www.ecorev.fr/sipiphp/article389>) has then been applied to obtain proxy estimates of the above parameters, following a procedure described in de Vernal *et al.* [2005a, 2013b]. The modern Northern Hemisphere dinocyst database of GEOTOP that includes 1492 sites and 66 taxa [de Vernal *et al.*, 2013b] has been used as reference. The modern hydrographic data were compiled from the 2001 version of the World Ocean Atlas. The modern sea ice distribution was compiled from data provided by the National Snow and Ice Data Center, based on observations spanning from 1953 to 2003; they show a large interannual variability that averages about 1 month yr⁻¹ [cf. de Vernal *et al.*, 2013b]. The modern PP was compiled from monthly values obtained from 2002 to 2005 using the Moderate Resolution Imaging Spectroradiometer (MODIS) program of the NASA (<http://daac.gsfc.nasa.gov>). Comparison with other productivity data sets also derived from satellite observations indicates a large uncertainty, on the order of 15%, which can be due to data acquisition techniques and/or inherent variability of productivity [cf. Radi and de Vernal, 2008].

Modern analogues of fossil assemblages were searched after log (for dinocysts) or square root (for planktonic foraminifera) transformations of taxa occurrences, in order to increase the weight of accompanying species, which often have narrower ecological affinities than dominant taxa. Reconstructions were made from the five best modern analogues, with the most probable values being calculated as a mean weighted inversely to the distance between the analogue and the fossil assemblage. A threshold value, defined from the mean distance minus standard deviation of randomly selected analogues in the database, was used to identify poor analogues. Assemblages with analogue distances beyond this threshold were excluded from reconstructions. The predictive ability of the approach was estimated from validation tests comparing observations and reconstructions using subsets of the reference data bases [Guiot, 2011; Guiot and de Vernal, 2007] (see Table 2). The error of reconstructions or Root-Mean-Square Error of Prediction (RMSEP), which is the standard deviation of the difference between observed and reconstructed values, provides a metric for the uncertainty of estimates.

The reconstruction of subsurface temperatures was made based on planktonic foraminifer assemblages using the Multiproxy Approach for the Reconstruction of the Glacial Ocean surface (MARGO) data [Kucera *et al.*, 2005a]. This data set includes 862 sites from the North Atlantic Ocean and 40 taxa [Kucera *et al.*, 2005b]. Validation tests performed for different depths in the water column indicate that the best reconstructed

Table 2. Correlation Coefficient (R^2) and Root Mean Square Error of Prediction (RMSEP) or Uncertainties of Sea Surface Reconstructions as Calculated From Validation Exercises for MAT Applied to Dinocyst Assemblages and Planktonic Foraminifer Assemblages

Parameters	R^2	RMSEP
Dinocysts		
SSTw (°C)	0.942	1.8
SSTs (°C)	0.944	1.9
SSSw (>30)	0.699	1.6
SSSs (>30)	0.693	1.5
PP (g C m ⁻²)	0.749	67
Sea ice (month/year)	0.858	1.4
Planktonic foraminifera		
T _w (°C) ≥ 50 m	0.906	0.98
T _s (°C) ≥ 50 m	0.905	1

parameter is the temperature at 50 m below the surface [cf. also Telford et al., 2013]. However, due to the presence of a thicker low-salinity surface layer in subarctic basins, stenohaline planktic foraminifers such as *Np* might develop deeper along the halocline with subsurface waters (e.g., Hillaire-Marcel and Blodeau, 2000). Hence, herein, we report foraminifer-based estimates of subsurface temperatures at a depth ≥ 50 m depth.

A "reliability code" of reconstruction has been calculated for each sample (both for foraminifer- and dinocyst-based estimates) using the criteria

proposed by de Vernal et al. [2013b]. A score ranging from 4 (excellent) to 1 (poor) was attributed to each sample depending upon (1) the total dinocyst or planktonic foraminifera, (2) the dissimilarity between the fossil sample and the best modern analogue, (3) the dissimilarity between the fossil sample and the last best modern analogue used for reconstruction, and (4) the number of modern analogues based on reconstruction with five close modern analogues. On these bases, reliability codes were given according to these scores: code A for scores of 14–16, code B for scores of 12–13, code C for scores of 10–11, and code D for scores < 10. Code A indicates reliable reconstructions from similar modern analogues and high dinocyst or planktonic foraminifer sums, whereas code D indicates reconstruction from distant analogues and/or lower counts that should be considered with caution.

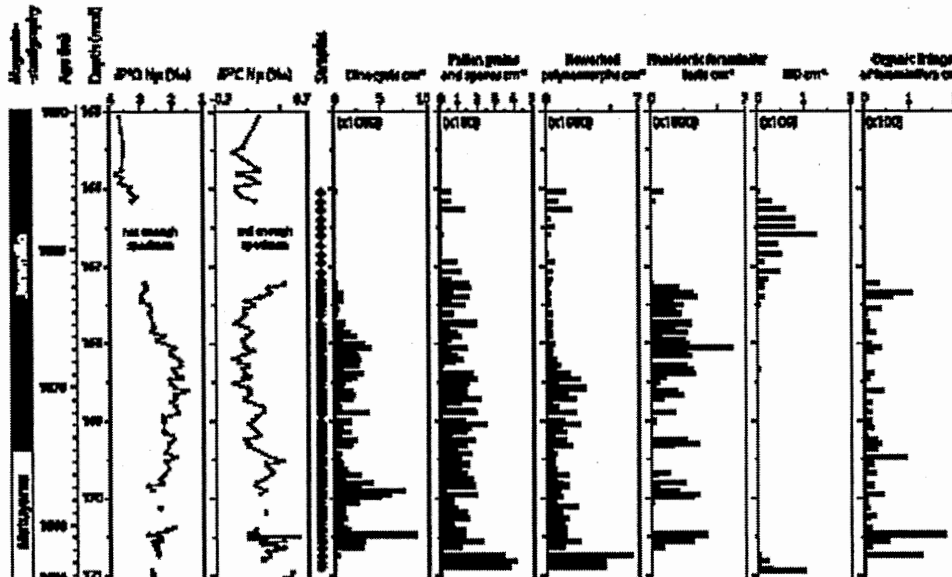


Figure 4. Concentration of dinocysts, pollen, and spores; reworked palynomorphs (dinocysts, pollen, spores, and acritarchs); planktonic foraminifera; and OM expressed in number of specimen per cm^3 .

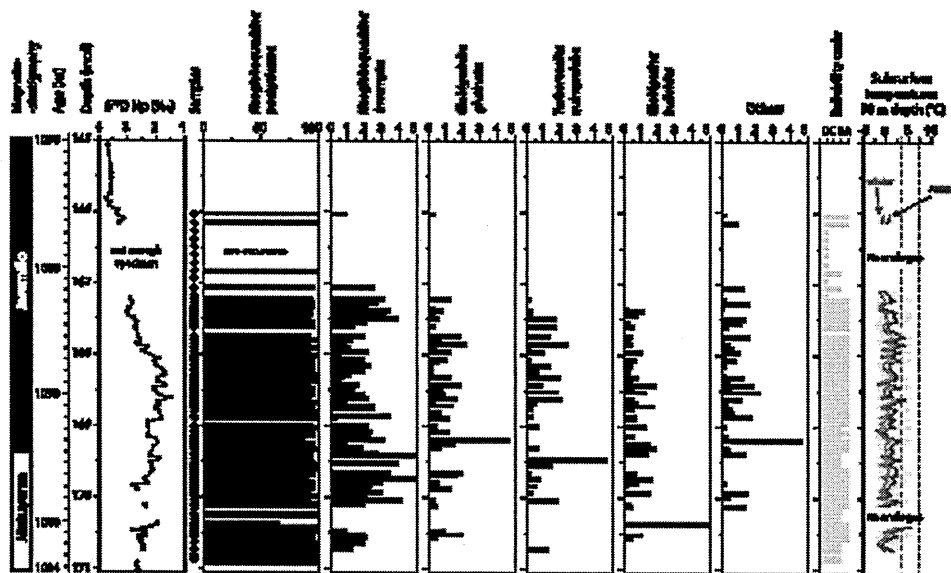


Figure 5. Magnetostratigraphy, isotopic stratigraphy, and relative abundance (percentages) of the main planktonic foraminifer taxa. Others include *Globorotalia truncatulinoides*, *Globorotalia hirsuta*, *Globorotalia theyeri*, and undetermined species. The reliability code for quantitative reconstructions and subsurface (≥ 50 m) temperature estimates from MAT are shown in the right. The most probable values are indicated by the lines, and the shaded areas correspond to the range between maximum and minimum values according to the set of selected analogues. The vertical dashed blue and red lines respectively correspond to modern winter and summer temperature at 50 m.

5. Results

5.1. Microfossil Concentration and Stratigraphy

Planktonic and benthic foraminifera occur in most samples between 166.96 mcd and 170.55 mcd (Figure 4), and their concentrations range between 1 and 6065 tests cm^{-3} . Samples above 166.71 mcd and below 170.55 mcd are generally barren of foraminifera (< 3 tests cm^{-3}). Conversely, a larger proportion of IRD are observed in these intervals.

Dinocysts occur in all samples below 170.55 mcd, but with very low concentrations above 166.96 mcd (< 140 cysts cm^{-3}). Between 166.96 mcd and 170.55 mcd, they reach concentrations as high as 8740 cysts cm^{-3} . Maximum and minimum concentrations of both foraminifera and dinocysts are observed simultaneously.

Concentration of other palynomorphs such as pollen grains, spores, and reworked palynomorphs are relatively high at the bottom of the study interval, between 170.55 mcd and 170.75 mcd, with counts up to 6389 reworked palynomorphs cm^{-3} and 470 pollen grain and spores cm^{-3} . Between 168 mcd and 170.55 mcd, concentrations average 1234 palynomorphs cm^{-3} and 126 pollen grains and spores cm^{-3} . At the top of the study interval, pollen and spore concentrations are decreasing with a mean value of 88 cm^{-3} . They almost disappear between 166.21 mcd and 166.61 mcd.

At the bottom of the study interval (below 170.55 mcd), low biogenic content, abundant terrigenous inputs and reworked palynomorphs were observed. The uppermost section of the study interval (above of 166.96 mcd) was barren in benthic and planktonic foraminifer, as well as in pollen and spores, but contained abundant IRD. In these intervals, dissolution of calcium carbonate could explain the low concentration of planktonic and benthic foraminifera, but there is no evidence for dissolution of the carbonate shells as their organic linings were also rare. Hence, low productivity and/or dilution with abundant detrital input can be invoked.

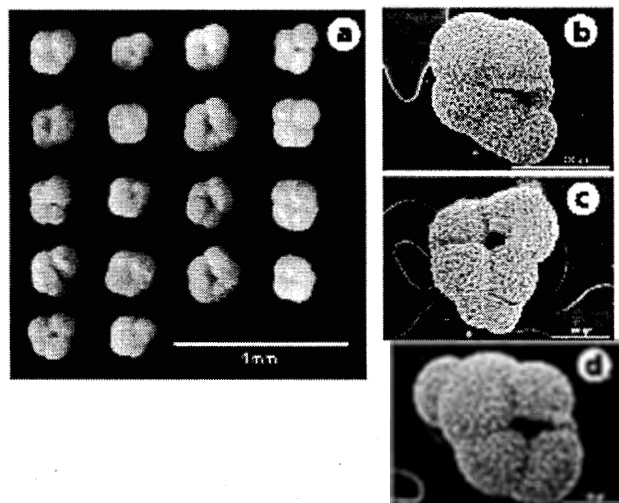


Figure 6. Photographs illustrating the morphological variations of *Neogloboquadrina pachyderma*. (a) Morphotypes from the optical microscope, scale 1 mm; (b–d) Aberrant forms from the scanning electron microscope, scales 200 μm and 100 μm , U130SA-16H-5 70-72 cm (UQP 3093-1).

Based on microfossil abundances and IRD occurrence, the onset and end of the MIS 31 optimum were set at 170.55 (1.82 Ma) and 166.96 mcd (1.06 Ma), respectively.

5.2. Planktonic Foraminifer Assemblages and Subsurface Conditions

Neogloboquadrina pachyderma (Np) is the most abundant species in all samples (>90%, Figure 5). Other species occur in low percentages: *Neogloboquadrina incompta* (<6%), *Globigerina glutinata*, *Turborotalita quinqueloba*, *Globigerinoides bulloides*, and *Globorotalia inflata* (<1%) (Figure 5). Such an assemblage is characteristic of subpolar waters, with mean annual sea surface temperature below 7°C [Kucera, 2007; Cronin et al., 2008; Carstens et al., 1997].

In all sample examined, Np presents various morphologies with regard to encrustation, thickness of the shell, number of chambers (4, 4.5, and 5 chambers), suture depth, and occurrence of an apertural lip (Figure 6). The range of the morphological variations in our samples is similar to what was described by Synaud et al. [2009] and Synaud [2011] from late Quaternary sediment of the Arctic Ocean. The morphological dissimilarities could be related to different depth habitats, ontogeny, and/or environmental stress [Kenett, 1968; Hernández-Almeida et al., 2013a; Synaud et al., 2009]. Generally, the incremental calcification related to ontogenetic stages of Np are characterized by thin and less encrusted shells for young specimens and by thick, more encrusted shells for the adult forms [e.g., Berberich, 1996; Kohfeld et al., 1996]. Morphological variation could also be associated with the occurrence of cryptic species [Daling et al., 2004, 2006]. Despite the differences morphology and test encrustation, all the counted individuals were grouped together as Np. Aside the above mentioned Np morphological variations we noticed the presence of specimens with aberrant morphologies in almost all samples. Some show two final chambers and two apertures, while others have additional chambers on the second, third, or last chamber in ventral view (Figure 6). This type of aberrant morphology was previously reported by Spindler and Deckmann [1986] and Hommers [1998] in circum-Antarctic sediments and generally attributed to Np growth within sea ice. Specimens with aberrant morphology were not included in the planktonic foraminifer assemblages and were not picked up for isotopic composition measurements.

As could be expected from the large dominance of Np, the application of the MAT yielded cold conditions with mean winter and summer subsurface temperatures of -0°C (-17°C to 3.7°C) and 1.3°C (-1.8° to 5.8°C).

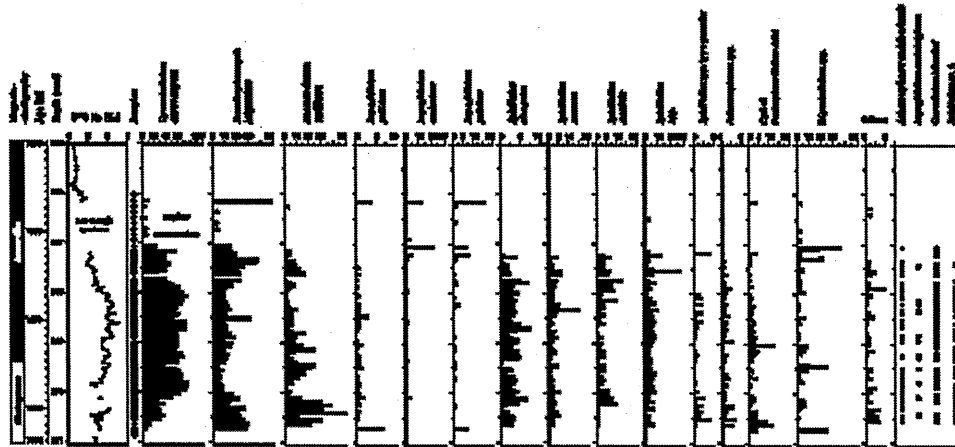


Figure 7. Magnetostratigraphy, isotope stratigraphy, relative abundance (percentaged) of the main dinocyst taxa in samples with very low concentrations, between 16.3 and 167 mcd, the dinocyst counts were not high enough to calculate percentages. In these samples, the presence is reported by small circles. Similarly, we did not include the extinct taxa into the sum for percentage calculation, and only their presence is reported. Others include *Impagidinium paradoxum*, *Impagidinium sphaericum*, *Impagidinium stolatum*, *Spiniferites membranaceus*, *Spiniferites delicatus*, *Spiniferites biferius*, *Spiniferites bentoni*, *Spiniferites polydermus*, and *Bleekerdinium minutum*.

respectively, at ≥ 50 m (Figure 5). Such estimates characterized by very little differences between summer and winter temperatures indicate that the planktonic foraminifera recorded the conditions below the mixed layer at the top of the thermocline, which was possibly shallow in the Labrador Sea during MIS 31.

5.3. Dinocyst Assemblages and Sea Surface Conditions

The dinocyst assemblages are dominated by two cosmopolitan temperate–subarctic species: *Oculodinium centrocarpum* (up to 100% in some samples) and *Nematospheeropsis labyrinthitus* (<50%). A third species, *Bleekerdinium tepicense* (<50%), is also abundant and even dominant in the lower part of the record (Figure 7). The significant occurrence of *Bleekerdinium tepicense* is interesting as this species presently characterizes environments marked by low surface salinity, strong stratification, and large winter to summer temperature contrasts [e.g., Rochon et al., 1999; de Vernal et al., 2001, 2005a]. Despite dominance of three main taxa, the overall assemblages are characterized by relatively high species diversity with occurrence of both thermophilic taxa (*Spiniferites mirabilis*, *Impagidinium patulum*, and *Laculleum*), and cool temperate to subarctic taxa (*Spiniferites elongatus*, *Impagidinium pallidum*, *Pentapharsodinium datei*) [e.g., Rochon et al., 1999; de Vernal et al., 2001, 2013b; Zonneveld et al., 2013]. The mixed character of the assemblage suggests large seasonal contrast of temperature in the upper photic layer.

At the beginning and the end of MIS 31, *Nematospheeropsis labyrinthitus* and *Bleekerdinium tepicense* dominate the assemblages, whereas *Oculodinium centrocarpum* is the most abundant taxa in the middle of MIS 31. At about 1.075 Ma, a decrease of *Oculodinium centrocarpum*, *Nematospheeropsis labyrinthitus*, and *Bleekerdinium tepicense* is recorded whereas *Brigantedinium* spp. is relatively abundant, which might relate to an important but short-lived change in upper water masses. At the very end of MIS 31, the dinocyst assemblages change with the disappearance of *Bleekerdinium tepicense* and the increase of *Brigantedinium* spp. (Figure 7).

Some extinct dinocyst species occur in samples from MIS 31 (see Figure 8). They include *Corindinium labrador* [Head et al., 1989], which disappeared during the lower Pleistocene [de Vernal and Mudie, 1989], *Impagidinium cantabrigense*, which has a late Pliocene to middle-Pleistocene age [De Schepper and Head, 2008a] and *Achomosphaera andalouensis*, the last occurrence of which is found within MIS 7 [de Vernal and Mudie,

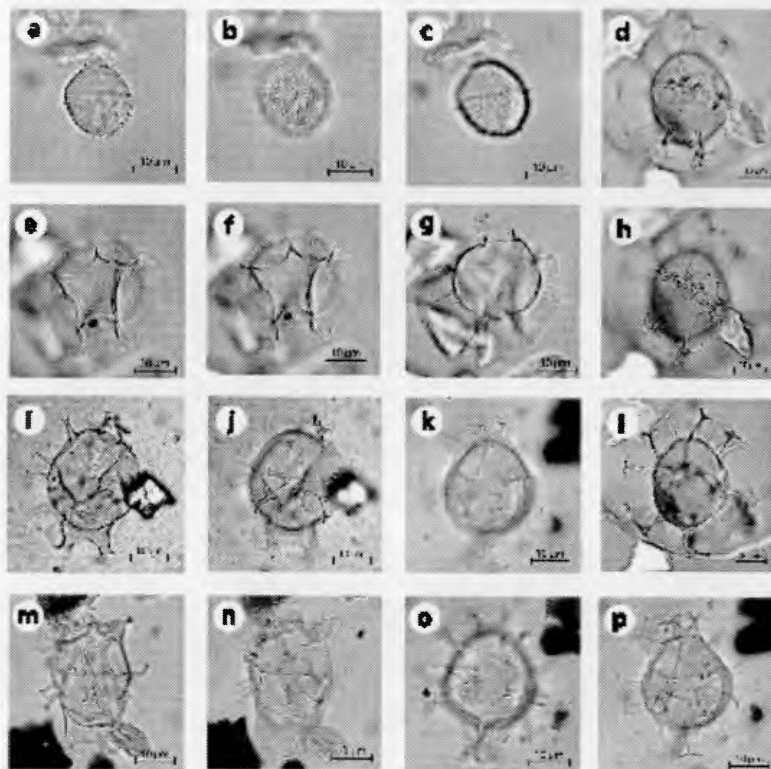


Figure 8. (a–c) *Coradinium labradori*; sample U1305A-16H5 65 cm (UQP 2266-5). (d, h, and i) *Achomosphaera andalousiensis*; sample U1305A-16H 5 115 cm (UQP 2267-4). (e–g) *Impagidium cantabrigiense*; sample U1305A-16H5 115 cm (UQP 2267-4). (f) *Leptodiscus* sp.; (g) *Spiniferites* sp. A of Louwey and De Schepper [2010]. (l, l) Sample U1305A-16H5 65 cm (UQP 2266-5). (k, o, and p) Sample, U1305A-16H7 35 cm (UQP 2273-1). (m, n) Sample U1305A-16H 6 145 cm (UQP 2272-3).

1992). We also noticed the occurrence of *Spiniferites* sp. A, a taxon described by Louwey and De Schepper [2010] from Miocene-Pliocene sediments. These extinct taxa occurred in most analyzed samples of MIS 31 but in low proportion with a few specimens per slide and maximum percentages as follows: *Coradinium labradori* < 7.2%, *Impagidium cantabrigiense* < 1%, *Achomosphaera andalousiensis* < 4%, and *Spiniferites* sp. A < 5.6%. These extinct taxa were not included in the sum for percentage calculation and were not taken into account for reconstruction.

The quantitative reconstructions of sea surface conditions based on dinocyst assemblages indicate relatively warm conditions during the optimum of MIS 31 (Figure 9). Estimated SST averages 12.2°C in summer and 5.3°C in winter. Winter SST fluctuates around the modern average in the lower part of MIS 31, but is slightly higher in the upper part, from 1.068 to 1.062 Ma, where it reaches about 1°C above the present one. Summer SST shows warmer than present conditions by about 1°C on average. However, it also suggests large amplitude variations with one important cooling pulse around 1.075 Ma, which is an interval also marked by winter sea ice cover. With the exception of this cooling event and the transitional interval prior and after MIS 31, sea ice occurrence is estimated to have been very rare throughout the study interval. SSS in August varied between 31 and 35.5 and was generally lower than at present, which is compatible with strong stratification of the upper water

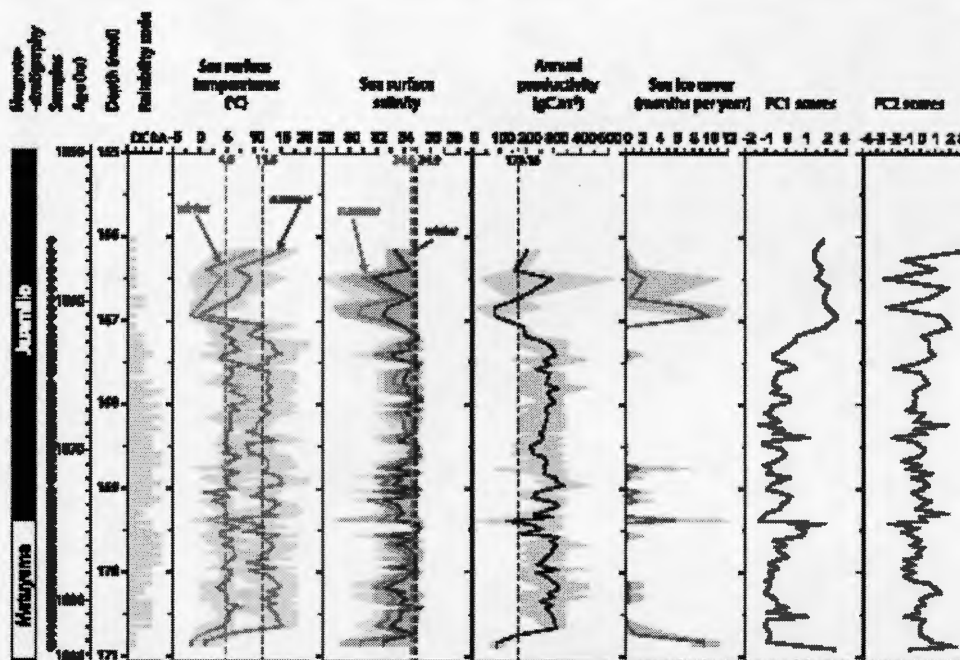


Figure 9. Magnetostratigraphy, reliability index, reconstruction of sea surface conditions from MAT applied to dinocyst assemblages and scores of principal components 1 and 2 derived from dinocyst assemblages at IODP site U1305. In samples with low dinocyst counts (see Figure 7), the uncertainty of reconstruction is high and the values are shown by dots. Sea surface temperature (SST) estimates are illustrated in blue and red for winter and summer respectively. Sea surface salinity curves are in yellow and purple for summer and winter, respectively. Annual productivity is represented in black and sea ice cover in deep blue. Most probable values are indicated by lines and the shaded areas correspond to the range between maximum and minimum possible values according to the set of selected analogues. Modern values of sea surface conditions are indicated by the vertical dashed lines. The first component (PC1), which explains 35% of the variance, opposes *Argamtinium*, to all the other taxa; it corresponds to cooler and less saline environments. The second component (PC2) explains 12% of the variance and opposes most *Impagidinium* species and *Opeicuspidinium centrocarpum* to other taxa. As *Impagidinium* often corresponds to oligotrophic environments [e.g., Radt and de Vernal, 2008], PC2 possibly captures a productivity signal.

mass and large amplitude of temperature from winter to summer. The estimated annual productivity of MIS 31 was about 270 g C m^{-2} , which is higher than at present at the study site by about 90 g C m^{-2} (Figure 9).

S.A. Isotopic Composition of Benthic and Planktonic Foraminifera

Most samples recovered between 167 mcd and 169.7 mcd contained benthic foraminifera, notably *Cw* and *Ov*. When *Cw* values are corrected, both taxa depict nearly similar $\delta^{18}\text{O}$ values around 3.4‰ and no particular variations throughout the MIS 31 interval.

Planktonic $\delta^{18}\text{O-Np}$ values are significantly lighter than those of benthic species. They average 2.2‰ and reached a minimum of 1.48‰ at 168.31 mcd (Figure 10). Three plateaus are observed. A first one is observed in the 170.55–169.66 mcd interval. It shows a mean value of 2.53‰, i.e., close to the late Holocene Np- $\delta^{18}\text{O}$ value of 2.6‰ in the Labrador Sea [Hillaire-Marcel et al., 2011]. Between 169.66 and 168.71 mcd, a second plateau, with values around 2.15‰, follows. At last, a third plateau, with an isotopically light average composition of 1.86‰, follows between 168.71 and 167.71 mcd. Then, Np- $\delta^{18}\text{O}$ values decrease toward glacial values above 167.71 mcd.

Planktonic Np- $\delta^{13}\text{C}$ values (ranging -0.4 to -0.4‰ ; Figure 10) are significantly lower than those observed during the middle and late Holocene ($+0.7\text{‰}$) at the site [de Vernal and Hillaire-Marcel, 2006; Hillaire-Marcel

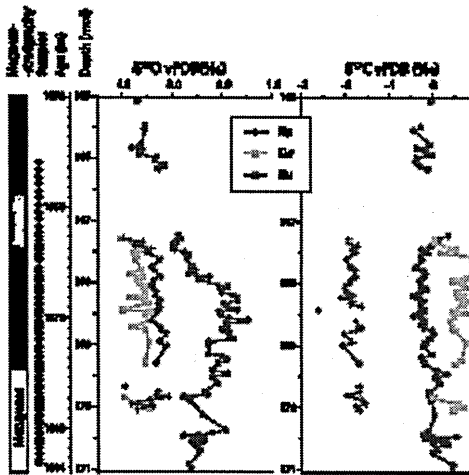


Figure 10. Stable isotope ($\delta^{18}\text{O}$ and $\delta^{13}\text{C}$) data in *Neogloboquadrina pachyderma* (Np) [cf. Hillaire-Marcel et al., 2011] and the benthic species *Cibicides wuellerstorffii* (Cw) and *Orbitolina umbonata* (Ou).

occurrences of extinct species increase the uncertainties about the ecological affinities of taxa; thus, the confidence in precise relationships between dinocyst assemblages and environmental conditions decreases [Guillet and de Vernal, 2007]. The assemblages of MIS 31 yielded specimens of four species that are now extinct: *Corrudinium Labradori* [Head et al., 1989], *Impagidinium cantabrigiense* [De Schepper and Head, 2008a], *Achromosphera andalusiensis* [de Vernal and Mude, 1992], and *Spiniferites* sp. A [Lourye and De Schepper, 2010]. However, these taxa were not an important component of the assemblages. They were not included in the search of analogues. Hence, in most samples, modern analogues were found with a suitable reliability (Figure 9).

The quantitative reconstructions of temperature based on planktonic foraminifer assemblages must be further examined. First, the assemblages are mostly monospecific with the quasi-exclusive occurrence of *Neogloboquadrina pachyderma*. Second, the populations contain specimens with a large array of morphotypes including aberrant forms [Hommers, 1998] (Figure 6). Hence, while the quasi-exclusive occurrence of *Neogloboquadrina pachyderma* suggests cold conditions, the morphological characteristics of individuals in the populations may reflect phenotypic adaptation and/or non-analogue situations.

Regardless of the accuracy of temperature estimates from the two proxies, their respective assemblages display distinct affinities. The planktonic foraminifer assemblages dominated by *Neogloboquadrina pachyderma* are typical of the polar environment and salinity higher than 34 [Hilbrecht, 1997; Kucera, 2007; Bergami et al., 2009] whereas dinocyst assemblages are composed of species having affinities for temperate-subpolar conditions [de Vernal and Marret, 2007]. Accordingly, the reconstructions of temperature show distinct values from the two proxies, with slightly warmer and much less saline conditions according to dinocyst assemblages, but colder conditions with planktonic foraminifer assemblages. The differences could relate to the ecology and habitat of the proxies and to the parameters that are recorded by the assemblages. Most dinocysts relate to phototrophic productivity and live in surface waters whereas planktonic foraminifera are heterotrophic, stenohaline, and live in mesopelagic waters along the pycnocline or halocline where they find suitable life conditions [Kucera, 2007; Ravelo and Hillaire-Marcel, 2007]. This explains why it is suitable to calibrate planktonic foraminifera for reconstruction of subsurface temperature, at $\geq 50\text{ m}$ of water depth, instead of the surface [cf. Telford et al., 2013; Hillaire-Marcel and Bilodeau, 2000]. Nevertheless, even if we accept that the two proxies relate to different water layers, one has to admit distinct anomalies when compared to the present, with slightly warmer surface waters and

et al., 2011] and depict relatively large-amplitude oscillations in comparison to the Holocene or MIS 5e records. Cw depicts similarly low $\delta^{13}\text{C}$ values when compared to the middle- and late Holocene records ($\leq 1\text{‰}$ versus $\geq 1\text{‰}$, respectively; Figure 11).

Noteworthy is the fact that Cw, which records deep water carbon isotope properties, shows heavier $\delta^{13}\text{C}$ values than Np, in contradiction to their nearly similar isotopic composition observed during the Holocene (Figure 11).

6. Discussion

6.1. Reconstruction of Surface and Subsurface Conditions

Quantitative reconstructions of sea surface conditions from MAT applied to dinocysts were previously done in late Pleistocene and Holocene assemblages [e.g., de Vernal et al., 2001, 2005a]. When going back in time, the

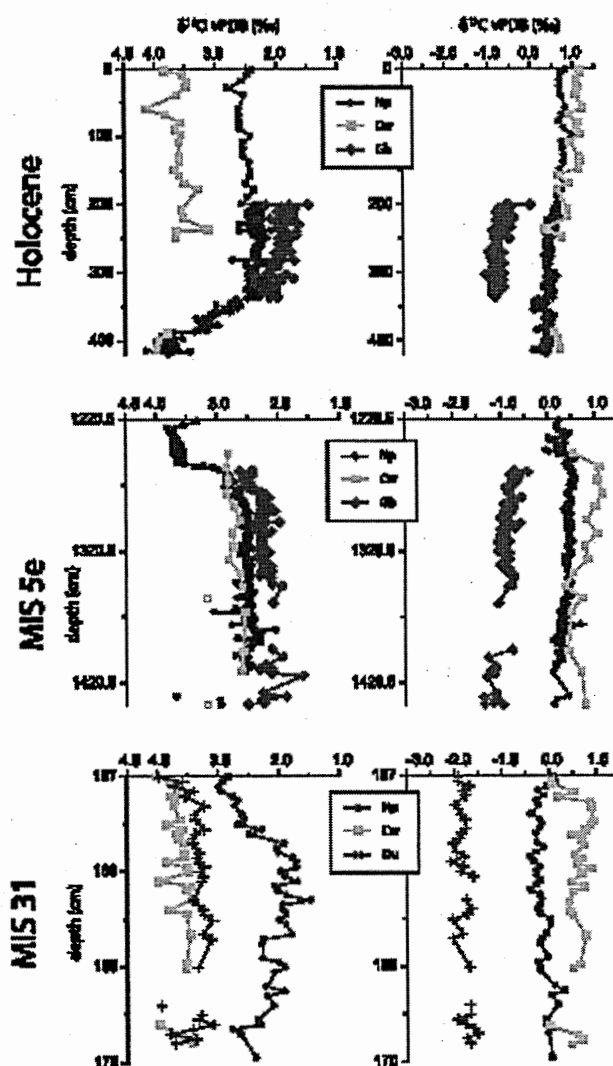


Figure 11. Oxygen and carbon isotopic composition of epipelagic (*Globigerinoides glutinosa* = Gg), mesopelagic (*Neogloboquadrina pachyderma* = Np), endobenthic (*Orbuloides umbonatus* = Ou), and epibenthic (*Ostrea nucleostriata* = Os) foraminifera. Holocene and MIS 5e data are from HU90-013-013 [Maire et al., 2001, 2011].

cooler conditions in subsurface water masses during MIS 31. This would indicate a much stronger stratification than at present, likely due to lower salinity at the surface. Such a decoupling of the paleoceanographic records from planktonic foraminifera and dinocysts is a feature that has been reported to occur during the late Quaternary in the North Atlantic and the Arctic Ocean, where it has been interpreted as the result of a strong stratification between a low-salinity surface water layer and subsurface waters where foraminifera

find higher-salinity conditions [e.g., Hillaire-Marcel *et al.*, 2001; de Vernal *et al.*, 2005b, 2006]. During MIS 31, the above scenario seems to fit data from IODP Site U1305. Thus, it implies a very strong stratification in the upper water column with surface water characterized by overall low-salinity and large thermal variations from summer to winter (as recorded by dinocysts) overlying a more saline and colder subsurface water mass, where foraminifer populations developed.

At Site U1305, under present day conditions, the ~100 m deep seasonal pycnocline between the surface and the underlying water mass constitutes the major Np habitat [Kohfeld *et al.*, 1996; Volkmann and Mensch, 2001; Simstich *et al.*, 2003] (Figure 2), but the subpolar-temperate planktonic species *Globigerina bulloides* (Gb) blooms in the shallow surface water layer where it finds suitable temperature and salinity conditions. This was apparently rarely the case during MIS 31 based on the low abundance of Gb in the planktonic foraminifer assemblages.

6.2. $\delta^{18}\text{O}$ Record in Benthic and Planktonic Foraminifera

Stable oxygen isotope composition of foraminifera illustrates contrasting situations during MIS 1, MIS 5e, and MIS 31 (Figure 11). Distinct values in the shells of benthic and planktonic species suggest stratified water masses during MIS 31 and the Holocene (MIS 1). This contrast with the similar values in all species during MIS 5e, suggesting the presence of a more homogeneous subsurface to bottom water mass [Hillaire-Marcel *et al.*, 2001, 2011].

The isotopic compositions of planktonic foraminifera, in particular $\delta^{18}\text{O}$ of Np, depict some change throughout the MIS 31, with a gradual decrease from the base of the interval toward minimum values at about 168 mcd and then a relatively steep increase near the top of the layer. This behavior suggests changes in the intermediate water mass distinct from those recorded in the surface water layer by the dinocyst assemblages (Figure 9) and also from those recorded in the bottom water by the isotopic composition of benthic foraminifera (Figure 10).

The $\delta^{18}\text{O}$ plateau depicted by Np during the early Jaramillo interval (Figure 10) seems incompatible with the salinity requirement of the species (≥ 34) and the mean temperature of less than 4°C as indicated by planktonic foraminifer assemblages (Figure 5). Indeed, by using the paleotemperature equation [O'Neil *et al.*, 1969; Shackleton, 1974] with this temperature and the mean isotopic composition of Np in the light isotopic plateau, we estimate an isotopic composition of approximately -18.2‰ versus SMOW for the ambient water. This value seems much too low for the salinity of an interglacial not too far from that of the modern ocean. One explanation could be the addition of isotopically light brines in the subsurface water mass at its production site, a situation similar to present day in the Arctic Ocean [e.g., Simstich *et al.*, 2003; Hillaire-Marcel and de Vernal, 2008]. Given the relatively warm SST estimates from MIS 31 at IODP Site U1305, a distal sea ice production site, in the Greenland Sea, for example, could be evoked. An alternative explanation for the low $\delta^{18}\text{O}$ values in planktonic foraminifera is a more local signal related to isotopically light meltwaters from the Greenland ice sheet either from outlets south of the Denmark Strait or carried from northern Greenland through the EGC. Considering that even the most coastal ice of Greenland have $\delta^{18}\text{O}$ values as low as -25 to -20‰ during the present and last interglacials [Johnsen *et al.*, 2001], enhanced continental ice melt would necessarily impact the isotopic composition of seawater [cf. Cox et al., 2010]. Thus, the very high summer temperatures in the Arctic as recorded at the Lake El'gygytgyn during MIS 31 [Melles *et al.*, 2012] could well have fostered accelerated melt of Greenland ice resulting in low-isotopic composition of the EGC and the Labrador Sea.

During MIS 31, the high $\delta^{13}\text{C}$ values in Cw suggest the presence of ventilated water mass at the sea floor, thus relatively young waters, which would have resulted from convection in areas at the origin of deep waters in the Labrador Sea. Potential production sites are the Nordic Seas, the Irminger and/or Iceland basins. Overflowing waters from Baffin Bay to the Labrador Sea can also be hypothesized as it was apparently the case during the early phase of the present interglacial as suggested from very low $\delta^{18}\text{O}$ values in deep corals of the Orphan Knoll area in the southern Labrador Sea [Ménard-Bézot *et al.*, 2015].

The benthic-planktonic $\delta^{18}\text{O}$ offset, not unlike the modern one in the Labrador Sea (LS) [e.g., de Vernal and Hillaire-Marcel, 2006], points to distinct production of intermediate and deep water masses, outside the Labrador Sea, as no convection can be inferred due to the large density difference between surface and subsurface waters. Assuming that Np corresponds to a relatively high salinity (≥ 34), the most important

Table 3. Summarized Information About MIS 31 Paleceanographical Data From Northern North Atlantic Sites as Discussed in the Text^a

Site	Latitude, Longitude	Water Depth (m)	Indicator and Proxy Approach	Paleceanographical Reconstructions	References
U1305	57°28.5'N, 48°31.8'W	3459	Planktonic foraminifera—MAT	Cool subsurface conditions (50 m depth; $T_w = 0^\circ\text{C}$ and $T_s = 13^\circ\text{C}$) $\Delta T_{winter} = -3.4^\circ\text{C}$ $\Delta T_{summer} = -4.5^\circ\text{C}$	This study
			Dinocysts—MAT	Warmer surface conditions ($\text{SST}_w = 5.3^\circ\text{C}$ and $\text{SST}_s = 12.2^\circ\text{C}$) $\Delta \text{SST}_{winter} = +0.4^\circ\text{C}$ $\Delta \text{SST}_{summer} = +0.6^\circ\text{C}$	
ODP 607	41°0.68'N, 32°57.4'W	3427	Planktonic foraminifera—Transfer function AOF13XS	Sea surface temperatures similar to modern ones in summer and winter	Ruddiman et al. [1989]
U1314 (late MIS 31 only)	56°21.9'N, 27°53.3'W	2820	RD	Sea ice and/or iceberg input at the end of MIS 31	Hemínder-Almeida et al. [2013a]
			Planktonic foraminifera MAT	Colder than modern at the end of MIS 31 at 10 m depth ($T_s = 8^\circ\text{C}$) $\Delta T_{summer} = -12^\circ\text{C}$ Temperate conditions Warm water from the North Atlantic Current (NAC)	Hemínder-Almeida et al. [2012]
			Radiolarian	Cooler (-6°C) subsurface conditions	Hemínder-Almeida et al. [2013b]
ODP 983	60°24'N, 23°38'W	1985	Mg/Ca on Np	Cooler (-6°C) subsurface conditions	Hemínder-Almeida et al. [2015]
MD992277	69°15'N, 6°19'W	2800	Akenones (%C _{37.4} and U ₃₇)	Mean annual SST (10 m depth) similar to modern	McLennan et al. [2008]
			RD	Similar conditions than present	Helmke et al. [2003]
			Bulk carbonate content	Higher carbonate productivity	

^aThe location of sites is illustrated in Figure 1.

difference between the deep and the intermediate water masses might have been temperature, with a gradient probably lower than 4°C . A slightly negative temperature in the deep water mass during MIS 31 cannot be discarded.

6.3. Primary Productivity and Winter Convective Regime

The large carbon isotope offset between the foraminifer species throughout the MIS 31 interval suggests stratified water masses but relatively stable conditions in the habitats of respective species. Highly depleted values in Cw are linked to its endobenthic habitat and may also suggest relatively high organic carbon fluxes at the sea floor in relation with the high primary productivity inferred for the interval (Figure 9). Surprisingly, the epibenthic species Cw shows heavier carbon isotope values than Np. This might indicate high oxidation rates of sinking organic matter at the depth of Np habitat and/or a poor ventilation of the intermediate water mass in comparison with the bottom one. Low Np $\delta^{13}\text{C}$ values are observed during MIS 31 by comparison with MIS 1 and MIS 5e (Figure 11), whereas Cw depicts nearly similar values during the three intervals, thus pointing to some specificity of the subsurface water mass or of organic carbon mineralization rates during MIS 31.

Another factor that should be mentioned is the possibility that the intermediate waters were less ventilated than the deep water mass. In such hypothesis, the low $\delta^{13}\text{C}$ values of Np during MIS 31 indicate that convection in the Labrador Sea was unlikely. In a stratified surface water layer, without convection, $\delta^{13}\text{C}$ values of dissolved inorganic carbon decrease with depth in contrast to a convective regime where surface water are characterized by higher $\delta^{13}\text{C}$ values [Ravelo and Hillaire-Marcel, 2007]. From this viewpoint, MIS 31 differs significantly from the Holocene [Marshall and Schout, 1999], which was characterized by Np and Cw displaying both high and nearly similar $\delta^{13}\text{C}$ values ($\sim +1\text{‰}$; Figure 11).

6.4. Comparison With Other Records From the North Atlantic Subpolar Gyre

The benthic carbon isotope composition of Cw in MIS 31 sediments from IODP Site U1305 averages 0.58‰ . This value is comparable to other sites from the North Atlantic subpolar gyre during this time interval, notably IODP Site U1308 (Figure 1) where values of about 0.66‰ are recorded in Cw [Hadell et al., 2008] and Deep Sea Drilling Project Site (DSDP) 607 where values of 0.62‰ are recorded in *Uvigerina* sp. and *Glyptidiscus* sp.

[Ruddiman et al., 1989]. Hence, the overall data from the northern North Atlantic tend to suggest relatively uniform conditions in deep water masses in the area (Table 3). Moreover, the similarities between planktonic foraminifer assemblages of MIS 31 at IODP Site U1305 and U1314 (Figure 1), which are both characterized by dominant Np [cf. Hernández-Almeida et al., 2013a], suggest uniform conditions in subsurface waters at the scale of the North Atlantic subpolar gyre during this interval.

The available records that document sea surface conditions in the North Atlantic subpolar gyre during MIS 31 indicate slightly warmer conditions than at present (Table 3). This is consistent with our data from IODP Site U1305. High carbonate productivity has been proposed from geochemical and sedimentological data of core MD99-2277 in the Nordic Seas [Helmke et al., 2003]. Higher species diversity and warm-water radiolarian species allow for the interpretation of temperate conditions at IODP Site U1314 [Hernández-Almeida et al., 2013b]. Alkenone data from Ocean Drilling Program (ODP) Site 983, south of Iceland indicate temperature of $\sim 12^{\circ}\text{C}$ in the photic zone during MIS 31, similar to the modern condition [McClintock et al., 2008].

The results from IODP Site U1314 are particularly interesting as they include data from different proxies that may document gradients in the upper water column [Hernández-Almeida et al., 2015]. At this site, Mg/Ca in Np indicates subsurface temperatures of about 6°C during MIS 31 despite microfossil assemblages suggesting warmer than present surface waters. A quite similar offset is here shown from MAT results based on dinocyst and planktonic foraminifer assemblages at Site U1305 (Figures 5 and 9).

The paleoceanographical information therefore suggests a decoupling between surface and subsurface waters in the subpolar gyre. In the inner Labrador Sea, the decoupling may relate to the southward penetration of subsurface Arctic water masses, possibly linked to a stronger Greenland Current at the surface contrasting with a weaker western boundary undercurrent (WBUC) along the deep slope, thus a weaker production of NEADW and DSOW as it was suggested by Soare [2010] from clay assemblages and Lamoureaux [2008] from radiogenic isotope (Sm-Nd and Pb) studies in the same interval of IODP Site U1305.

7. Conclusion

The data presented herein indicate that MIS 31, which is often described as a super interglacial in both the Northern and Southern Hemispheres, was characterized by warm conditions in surface waters in the Labrador Sea, northwest North Atlantic, with sea surface temperatures higher than at present by about 2°C in both the summers and winters. However, MIS 31 differed significantly from the present interglacial, notably because of strong stratification in the upper water column. Above the pycnocline, there was a temperate water mass with low salinity and a large seasonal gradient of temperature (dinocysts) and below the pycnocline, the water mass was colder with high salinity and very low seasonal amplitude of temperature (planktonic foraminifera). Such conditions were unsuitable for vertical convection and intermediate or deep water formation in the Labrador Sea. A weaker and more southern position of the convection center of the AMOC possibly led to the presence, in the subsurface, of cold waters, despite relatively warm surface conditions.

References

- Aagaard, K., and L. K. Coachman (1968), The East Greenland Current north of Denmark Strait: Part I, Arctic, 181–200, doi:10.14410/arctic3262.
- Borchert, D. (1990), Die planktischen Foraminiferen Neoglobigerinoides pacificensis (Ehrenberg) im Weddellmeer, Antarktis, Bericht zur Polarforschung (Reports on Polar Research), 785, p. 193.
- Borgene, C., L. Caporaso, L. Langone, F. Giglio, and M. Ravello (2009), Distribution of living planktonic foraminifera in the Ross Sea and the Pacific sector of the Southern Ocean (Antarctica), *Mar. Micropaleontol.*, 73, 37–48, doi:10.1016/j.micropal.2009.06.007.
- Bonatti, S., A. de Vernal, R. Gersonde, and L. Lambek (June 2012), Modern distribution of dinocysts from the North Pacific Ocean (37° – 64° N, 144° – 148° W) relative to hydrographic conditions, seaice and productivity, *Mar. Micropaleontol.*, 84, 87–113, doi:10.1016/j.micropal.2011.11.005.
- Carrasco, J., D. Habermann, and G. Wefer (1997), Distribution of planktic foraminifera at the ice margin in the Arctic (Fram Strait), *Mar. Micropaleontol.*, 28(3), 257–269, doi:10.1016/S0377-8398(96)00014X.
- Chambers, J. E. T., T. Kanamatsu, T. Sato, R. Shiraishi, C. A. Alvarez-Zarza, M. J. Malone, and the Expedition 303/306 Scientists (2009), Proc. IODP, 303/306: College Station TX (Integrated Ocean Drilling Program Management International, Inc.), doi:10.2204/iodp.proc.30306.105.2006.
- Costa, K. B., F. A. L. Toledo, M. A. G. Pivell, A. Y. C. Moura, and F. Chemale Jr. (2009), Evaluation of two genera of benthic foraminifera for downcore paleotemperature studies in the western South Atlantic, *Braz. J. Oceanogr.*, 57(1), 75–84, doi:10.1590/S1679-62762008000100027.
- Cox, K. A., J. D. Stanford, A. J. McVicar, E. J. Rohling, K. J. Heywood, S. Bacon, R. Bushnall, P. A. Dodd, S. D. de Rosa, and D. Wilkinson (2010), Interannual variability of Arctic sea ice export into the East Greenland Current, *J. Geophys. Res.*, 115, C12063, doi:10.1029/2010JC006227.
- Cronin, T. M., S. A. Smith, F. Lyman, M. O'Regan, and J. King (2002), Quaternary paleoceanography of the central Arctic based on integrated Ocean Drilling Program Arctic Coring Expedition 302 foraminiferal assemblages, *Paleoceanography*, 17, PA1029, doi:10.1029/2007PA001484.

Acknowledgments
This research used samples provided by the Integrated Ocean Drilling Program (IODP, 2003–2013). Funding was granted from the Natural Sciences and Engineering Research Council of Canada (Discovery grants to A. de Vernal and C. Hillaire-Marcel) and the Fondation Québécoise de la Recherche sur la Nature et les Technologies (team awards to de Vernal et al.). We are grateful to Michel Racine for providing the MARGO data and the corresponding temperatures at different water depths in the water column. We acknowledge the help of Jean-François Hillaire (GEOTOP-UQAM) for isotopic measurements in foraminifera. All the data set for this paper are available through the GEOTOP database <http://www.geotop.ca/cadesbase/donnees/paleoceanographiques.html>. For any questions or requests about the data set, please contact me at aurelia.aubry@geotop.ca. We thank Anne Voilley and the anonymous reviewers for their helpful and constructive comments on the manuscript.



- Dading, K. F., M. Kuway, C. J. Pusack, and C. M. Wade (2004), Molecular evidence links cryptic diversification in polar planktonic protists to Quaternary climate dynamics, *Proc. Natl. Acad. Sci. U.S.A.*, **101**(20), 7657–7662, doi:10.1073/pnas.0402401101.
- Dading, K. F., M. Kuway, D. Kroon, and C. M. Wade (2006), A resolution for the colling direction paradox in Neogloboquadrina pachystoma, *Paleoceanography*, **21**, PA2011, doi:10.1029/2005PA001189.
- De Schaefer, S., and M. J. Head (2003a), New dinoflagellate cyst and acitarch taxa from the Pliocene and Pleistocene of the eastern North Atlantic (DSDP Site 610), *J. Syst. Palaeontology*, **60**(1), 101–117, doi:10.1075/j.1477-2092.907012167.
- De Schaefer, S., and M. J. Head (2003b), Age calibration of dinoflagellate cyst and acitarch taxa in the Risorane-Pliocene of the eastern North Atlantic (DSDP Hole 610A), *Sedimentology*, **50**(1), 137–161.
- De Schaefer, S., and M. J. Head (2008), Pliocene and Pleistocene dinoflagellate cyst and acitarch zonation of DSDP Hole 610A, eastern North Atlantic, *Palaeontology*, **51**(3), 179–216, doi:10.1080/083605908022009908673.
- de Vernal, A., and C. Hillaire-Marcel (2006), Provenance in trends and high frequency changes in the northeast North Atlantic during the Holocene, *Global Planet. Change*, **54**, 263–290, doi:10.1016/j.gloplacha.2006.06.023.
- de Vernal, A., and F. Muret (2007), Organic-walled dinoflagellate cysts: Tracers of sea-surface conditions, in *Development in Marine Geology*, vol. 1, edited by C. Hillaire-Marcel, and A. de Vernal, pp. 37–408, doi:10.1016/S1573-5480(07)0104-7.
- de Vernal, A., and P. J. Mude (1998), Pliocene and Pleistocene palynostigraphy at ODP Sites 646 and 647, eastern and southern Labrador Sea, in *Proceedings of the Ocean Drilling Program, Scientific Results*, vol. 105, edited by Ocean Drilling Program College Station, pp. 401–422, Publications Distribution Center, Ocean Drilling Program, Texas, doi:10.2973/odp.proc.105.134.1899.
- de Vernal, A., and P. J. Mude (1992), Pliocene and Quaternary dinoflagellate cyst stratigraphy in the Labrador Sea: Paleoenvironmental implications, in *Holocene and Quaternary Dinoflagellate Cysts and Acitarchs*, edited by M. J. Head and J. H. Warren, pp. 329–346, American Association of Stratigraphic Palynologists Foundation, Dallas, Tex.
- de Vernal, A., A. Laruelle, and P. J. H. Richard (1997), Evaluation of polymorphomorph concentrations: Do the aliquot and the marker grain methods yield comparable results?, *Pollen et spores*, **29**(2–3), 291–304.
- de Vernal, A., A. Rochon, J. L. Turon, and J. Matthesiusen (1997), Organic-walled dinoflagellate cysts: Palynological tracers of sea-surface conditions in middle to high-latitude marine environments, *Globulus*, **36**(7), 905–920, doi:10.1016/S0016-6995(97)80215-X.
- de Vernal, A., M. Henry, and G. Blédeau (1999), Techniques de préparation et d'analyse en micropaléontologie, *Le cahier du GEOTOP*, **3**, 41.
- de Vernal, A., et al. (2001), Dinoflagellate cyst assemblages as tracers of sea-surface conditions in the northern North Atlantic, Arctic and sub-Arctic seas: The new “n = 67” data base and its application for quantitative paleoceanographic reconstruction, *J. Quaternary Sci.*, **16**(7), 681–698, doi:10.1002/jqs.659.
- de Vernal, A., et al. (2005a), Reconstruction of sea surface conditions at middle to high latitudes of the Northern Hemisphere during the Last Glacial Maximum (LGM) based on dinoflagellate cyst assemblage, *Quat. Sci. Rev.*, **24**(7), 897–924, doi:10.1016/j.quascirev.2004.06.014.
- de Vernal, A., C. Hillaire-Marcel, and D. Darby (2005b), Variability of sea ice cover in the Chukchi Sea (western Arctic Ocean) during the Holocene, *Paleoceanography*, **20**, PA4018, doi:10.1029/2005PA001157.
- de Vernal, A., A. Rosell-Marié, M. Kuway, C. Hillaire-Marcel, F. Eynaud, M. Weiland, T. Dokken, and M. Kugayama (2006), Comparing proxies for the reconstruction of LGM sea-surface conditions in the northeast North Atlantic, *Quat. Sci. Rev.*, **25**(10), 2830–2844, doi:10.1016/j.quascirev.2006.06.022.
- de Vernal, A., A. Rochon, B. Fréchette, M. Henry, T. Radj, and S. Solignac (2013a), Reconstructing past sea ice cover of the Northern Hemisphere from dinocyst assemblages: Status of the approach, *Quat. Sci. Rev.*, **79**, 122–134, doi:10.1016/j.quascirev.2013.06.022.
- de Vernal, A., C. Hillaire-Marcel, A. Rochon, B. Fréchette, M. Henry, S. Solignac, and S. Bonatti (2013b), Dinocyst-based reconstructions of sea ice cover concentration during the Holocene in the Arctic Ocean, the northern North Atlantic Ocean and its adjacent seas, *Quat. Sci. Rev.*, **79**, 111–121, doi:10.1016/j.quascirev.2013.07.006.
- DeConto, R. M., D. Pollard, and D. Kowalewski (2012), Modeling Antarctic ice sheet and climate variations during Marine Isotope Stage 31, *Global Planet. Change*, **85**, 45–52, doi:10.1016/j.gloplacha.2012.03.008.
- Dubar, G. B. (2012), Mg/Ca sea surface temperature during the Marine Isotope Stage 31 collapse of the Ross Ice Shelf, *Eur. Geosci. Union, Gen. Assem. Conf. Abstr.*, **14**, 14473.
- Eynaud, F. (2011), Planktonic foraminifera in the Arctic: Potentials and issues regarding modern and Quaternary populations, *DP Conf. Ser.: Earth Environ. Sci.*, **14**(1), doi:10.1088/1755-1315/14/1/012005.
- Eynaud, F., T. M. Conin, S. A. Smith, S. Zanoghi, J. Mavel, Y. Mary, V. Mas, and C. Pujol (2009), Morphological variability of the planktonic foraminifer *Neogloboquadrina pachystoma* from ACEX cores: Implications for late Pliocene circulation in the Arctic Ocean, *Microbeam Analysis*, **18**(2–3), 101–116.
- Finstrom, P. S., and R. S. Pickart (2007), The western North Atlantic shelfbreak current system in summer, *J. Phys. Oceanogr.*, **37**(10), 2509–2533, doi:10.1175/JPO3123.1.
- Gibb, D. T., C. Hillaire-Marcel, and A. de Vernal (2014), Oceanographic regimes in the northeast Labrador Sea since Marine Isotope Stage 3 based on dinocyst and stable isotope proxy records, *Quat. Sci. Rev.*, **92**, 269–279, doi:10.1016/j.quascirev.2013.12.010.
- Gibb, D. T., S. Stainthorpe, B. Fréchette, A. de Vernal, and C. Hillaire-Marcel (2015), Diachronous evolution of sea surface conditions in the Labrador Sea and Bath Bay since the last deglaciation, Holocene, doi:10.1177/0959683615599352.
- Güler, J., and A. de Vernal (2007), Transfer functions: Methods for quantitative paleoceanography based on microfossils, in *Development in Marine Geology*, vol. 1, edited by C. Hillaire-Marcel, and A. de Vernal, pp. 523–563, doi:10.1016/S1573-5480(07)01018-4.
- Head, M. J., G. Horke, and P. J. Mude (1999), New species of dinocysts and a new species of acitarch from the upper Miocene and lowermost Pliocene, ODP Leg 105, Site 646, Labrador Sea, *Proc. Ocean Dril. Program, Sci. Results*, **105**, 453–466.
- Heldmaier, J.P., H. A. Bauch, and H. Ehrenkaufer (2003), Development of glacial and interglacial conditions in the Nordic seas between 1.5 and 0.35 Ma, *Quat. Sci. Rev.*, **22**(5), 1717–1728, doi:10.1016/j.quascirev.2002.37.910 (03001264).
- Hemleben, C., M. Spindler, and O. R. Egan (1998), *Modern Planctonic Foraminifera*, Springer, Berlin.
- Hernández-Almeida, I., F. J. Sierra, J. Cacho, and J. A. Flores (2012), Impact of suborbital climate changes in the North Atlantic on ice sheet dynamics at the mid-Pliocene transition, *Paleoceanography*, **27**, PA3214, doi:10.1029/2011PA002209.
- Hernández-Almeida, I., F. J. Sierra, J. A. Flores, J. Cacho, and G. M. Flippai (2013a), Paleoclimatic changes in the North Atlantic during the mid-Pliocene transition (MIS 31–19) as inferred from planktonic foraminiferal and calcium carbonate records, *Bioscience*, **63**(1), 140–159, doi:10.1111/j.1365-313X.2012.00283.x.
- Hernández-Almeida, I., K. R. Björklund, F. J. Sierra, G. M. Flippai, J. Cacho, and J. A. Flores (2013b), A high resolution opal and radiolarian record from the subtropical North Atlantic during the mid-Pliocene transition (1608–779 ka): Paleoclimatic implications, *Paleogeogr., Paleoclimatol., Paleoecol.*, **391**, 40–70, doi:10.1016/j.palaeo.2011.05.040.



- Hemondes-Almeida, I., F. J. Somo, I. Cacho, and J. A. Flores (2015), Subsurface North Atlantic warming as a trigger of rapid cooling events: Evidence from the early Holocene (MIS 31–19), *Geol. Pers.*, 43(4), 687–696, doi:10.1130/G36442.1, p. 11–687–2015.
- Hildebrand, H. (1997), Morphologic gradation and ecology in *Nucibiquadrina pachyderma* and *N. duorima* (glandic foraminifera) from core-top sediments, *Mar. Micropaleontol.*, 31(1), 31–43, doi:10.1016/S0377-8398(96)00254-0.
- Hillaire-Marcel, C., and G. Blödau (2000), Instability in the Labrador Seawater mass structure during the last climatic cycle, *Can. J. Earth Sci.*, 37(5), 795–809, doi:10.1139/A99-108.
- Hillaire-Marcel, C., and A. de Vernal (2008), Stable isotopes due to episodic sea-ice formation in the glacial North Atlantic, *Earth Planet. Sci. Lett.*, 268, 143–150, doi:10.1016/j.epsl.2008.01.012.
- Hillaire-Marcel, C., A. de Vernal, G. Blödau, and G. Wu (1994), Isotope stratigraphy, sedimentation rates, deep circulation, and carbonate events in the Labrador Sea during the last ~200 ka, *Geol. J. Earth Sci.*, 31(1), 63–80, doi:10.1130/0362-9400-94-007.
- Hillaire-Marcel, C., A. de Vernal, G. Blödau, and A. J. Weaver (2001), Absence of deep-water formation in the Labrador Sea during the last interglacial period, *Nature*, 406(6832), 1072–1077, doi:10.1038/35074609.
- Hillaire-Marcel, C., A. de Vernal, and J. McDay (2011), Foraminiferal isotope study of the Pleistocene Labrador Sea, northwest North Atlantic (ODP sites 1302/03 and 1305), with emphasis on paleoceanographical differences between the "inner" and "outer" basins, *Mar. Geol.*, 279(1), 188–198, doi:10.1016/j.margeo.2010.11.001.
- Hodell, D. A., J. E. T. Charnay, J. H. Curtis, O. E. Roman, and U. Röhl (2008), Onset of "Hudson Strait" Heinrich events in the eastern North Atlantic at the end of the middle Pleistocene transition (64°0'N), *Paleoceanography*, 23, PM4216, doi:10.1029/2008PA001591.
- Hommersommer, H. (1998), Gehäusessortierungen an planktonischen Foraminiferen höher Südländer: Hinweise auf Umweltveränderungen während der letzten 140.000 Jahre – Analyse von planktonischen foraminiferalen taxa aus hoch intrudierenden Indikatoren: Indicators of climate change during the last 140,000 years, *Berichte zur Polarforschung (Reports on Polar Research)*, 295.
- Johnsen, S. J., D. Dahl-Jensen, N. Gundestrup, J. P. Staff, N. H. Clausen, H. Miller, V. Masson-Delmotte, A. E. Steinenbrenner, and J. White (2001), Oxygen isotope and paleotemperature records from six Greenland ice-core stations: Camp Century, Dye 3, GRIP, GISP2, Renland and NorthGRIP, *J. Quaternary Sci.*, 16(4), 299–307, doi:10.1002/jqs.622.
- Jones, R. W., and H. B. Brady (1994), *The Challenger Foraminifera*, vol. 140, Oxford University Press, Oxford, UK, doi:10.1046/j.1470-9110.1996.9010124.x.
- Kanneworf, J.P. (1968), Latitudinal variation in *Globigerina pachyderma* (Ehrenberg) in surface sediments of the southwest Pacific Ocean, *Micropaleontology*, 14(3), 305–318, doi:10.2307/1484691.
- Kanneworf, J.P., and M. S. Sankaran (1983), Neogene Planktonic Foraminifera: A Phylogenetic Atlas, vol. 265, Hutchinson Ross Publ. Co., Stroudsburg, Pennsylvania, USA.
- Kohfeld, K.E., R. G. Fairbanks, S. L. Smith, and L.D. Walsh (1996), *Neogloboquadrina pachyderma* (sinistral coiling) as paleoceanographic tracers in polar oceans: Evidence from northeast Water Polynya plankton tow, sediment traps, and surface sediments, *Paleoceanography*, 11, 679–698, doi:10.1029/95PA02617.
- Kuiper, M. (2007), Planktonic foraminifera as tracers of past oceanic environment, in *Development in Marine Geology*, vol. 1, edited by C. Hillaire-Marcel and A. de Vernal, pp. 213–262, doi:10.1016/S1572-5480(07)80101-1.
- Kuiper, M., A. Rosati-Malù, R. Schneider, C. Veldhuis, and M. Walneit (2005a), Multiproxy approach for the reconstruction of the glacial ocean surface (MARGO), *Quat. Sci. Rev.*, 24(7), 813–819, doi:10.1016/j.quascirev.2004.07.017.
- Kuiper, M., et al. (2005b), Reconstruction of sea-surface temperatures from assemblages of planktonic foraminifera: Multi-technique approach based on geographically constrained calibration data sets and its application to glacial Arctic and Pacific Oceans, *Quat. Sci. Rev.*, 24(7), 951–968, doi:10.1016/j.quascirev.2004.07.014.
- Lamontagne, R. (2008), Millet PD comme traceur isotopique du Pliocène récent : circulation thermohaline dans l'Atlantique du Nord-Ouest [sic] (ICDP-1305), M.S. thesis, Department of Earth Sciences, Université du Québec à Montréal, Montréal, Québec, Canada.
- Laskar, J., P. Robutel, F. Joura, M. Gaiducou, A. C. M. Correia, and B. Levrard (2004), A long-term numerical solution for the motion of the Earth, *Astron. Astrophys.*, 42(4), 261–285, doi:10.1051/0004-6361:20041335.
- Lazar, J., R. Handley, A. Calkin, I. Yoshimura, and P. Rhines (2002), Convection and restratification in the Labrador Sea, 1990–2000, *Deep Sea Res., Part I*, 49, 1819–1835, doi:10.1016/S0896-0843(02)00054-X.
- Leisell, L.E., and E. M. Raymo (2005), A Pliocene–Pleistocene stack of 57 globally distributed benthic $\delta^{18}\text{O}$ records, *Paleoceanography*, 20, PA1003, doi:10.1029/2004PA001071.
- Leisell, L.E., and E. M. Raymo (2009), Dynchronous benthic $\delta^{18}\text{O}$ responses during late Holocene terminations, *Paleoceanography*, 24, PA3216, doi:10.1029/2009PA001732.
- Loeblich, A. R., and H. Tappan (1988), *Foraminiferal Genera and Their Classification*, vol. 2, Van Nostrand Reinhold, New York.
- Louwey, S., and S. de Schepper (2010), The Macrone-Rioense fauna in the southern North Sea Basin (northern Belgium) revealed by dinoflagellate cysts, *Geol. Mag.*, 147(5), 760–776, doi:10.1017/S0016756810000191.
- Lucotte, M., and C. Hillaire-Marcel (1994), Identification et distribution des grands masses d'eau dans les mers du Labrador et d'Amérique, *Can. J. Earth Sci.*, 31, 5–13, doi:10.1139/b94-002.
- Marshall, J., and F. Schout (1999), Open-ocean convection: Observations, theory, and models, *Rev. Geophys.*, 37, 1–64, doi:10.1029/98RG002739.
- Matthews, J. (1968), The assessment of a method for the determination of absolute pollen frequencies, *New Phytol.*, 61(3), 161–166, doi:10.1111/j.1469-8137.1968.tb0643x.
- McClymont, E. L., A. Rosati-Malù, G. H. Haug, and J. M. Lloyd (2008), Expansion of subarctic water masses in the North Atlantic and Pacific Oceans and implications for mid-Pleistocene ice sheet growth, *Paleoceanography*, 23, PM4214, doi:10.1029/2008PA001632.
- Meller, M., et al. (2012), 2.8 million years of Arctic climate change from Lake Elgygytgyn, NE Russia, *Science*, 337(6092), 315–320, doi:10.1126/science.1222135.
- Méndez, L., J. Meccari, A. Blanck, A. Poirier, B. Ghaleb, E. Edinger, and C. Hillaire-Marcel (2015), Neodymium isotopic composition of deep-sea corals from the Labrador Sea: Implications for NW Atlantic deep-water mass/mass circulation during the Holocene, *Boring-Afghan MS 55c and 77a, Goldschmidt Conference Abstracts*, p. 2101.
- Mariotti, K. N., et al. (2008), Determining the absolute abundance of dinoflagellate cysts in recent marine sediments: The "Lyngvigum" marker-grain method put to the test, *Rev. Palaeobot. Palynol.*, 157(3), 238–252, doi:10.1016/j.revpalbo.2008.05.024.
- O’Neil, J. R., R. N. Clayton, and T. K. Mayeda (1969), Oxygen isotope fractionation in divalent metal carbonates, *J. Chem. Phys.*, doi:10.1063/1.1671982.
- Rao, T., and A. de Vernal (2008), Dinocysts as proxy of primary productivity in mid-high latitudes of the Northern Hemisphere, *Mar. Micropaleontol.*, 68(1), 84–114, doi:10.1016/j.micromicron.2008.01.012.
- Rathburn, A. E., and B. H. Codling (1994), The ecology of living (stained) deep-sea benthic foraminifera from the Sulu Sea, *Paleoceanography*, 9, 87–150, doi:10.1029/93PA02327.

- Ravelo, A.C., and C. Hilberts-Marcot (2007), The use of oxygen and carbon isotopes of foraminifera in paleoceanography, In: *Development in Marine Geology*, vol. 1, edited by C. Hilberts-Marcot, and A. de Vernal, pp. 735–764, doi:10.1016/S1573-4480(07)01023-4.
- Rochon, A., A. de Vernal, J.-L. Tison, J. Mathewes, and M.J. Head (1999), Distribution of recent dinoflagellite cysts in surface sediments from the North Atlantic Ocean and adjacent seas: In relation to sea-surface parameters, *Am. Assoc. Stratigraphic Palynologists Contrib. Ser.*, 35, 1–46.
- Ruddiman, W. F., M. Raymo, D. G. Martinson, B. M. Clemens, and J. Backman (1980), Pleistocene evolution: Northern Hemisphere ice sheets and North Atlantic Ocean, *Paleoceanography*, 4, 353–412, doi:10.1029/PA004004p00351.
- Sano, Y. (2010), Assemblages microfongiques arctiques et circulation thermohaline d'Atlantique Nord pendant les stades isotropiques 27 à 31, MS thesis, Département of Earth Sciences, Université du Québec à Montréal (Montréal, Québec, Canada).
- Schmitz, R. P., S. M. Bohaty, R. B. Durbar, Q. Esper, J. A. House, R. Gascoigne, D. M. Harwood, A. P. Roberts, and M. Taviani (2008), Antarctic records of precession-paced isolation of iron warming during early Pleistocene Marine Isotope Stage 31, *Geophys. Res. Lett.*, 35, L03505, doi:10.1029/2007GL032254.
- Schmidt, S., and U. Sieg (2007), Origin and composition of seasonal Labrador Sea freshwater, *J. Phys. Oceanogr.*, 37(9), 1445–1454, doi:10.1175/JPO3065.1.
- Shackleton, N.J. (1974), Attainment of isotopic equilibrium between ocean water and the benthonic foraminifera genus *Uvigerina*: Isotopic changes in the ocean during the last glacial, *Cahiers Internationaux de Géologie*, 219, 203–208.
- Shackleton, N.J., and N. D. Opdyke (1973), Oxygen isotopes and paleomagnetic stratigraphy of Equatorial Pacific core V28-23B: Oxygen isotope temperatures and ice volumes on a 10³ year scale, *Quat. Res.*, 3(1), 30–55, doi:10.1016/0033-5897(73)90052-5.
- Sinitsch, L., M. Samain, and H. Erkensius (2003), Paired ^{87}Sr /Neogloboquadrina pachymelina (S) and Turborotalita quinquelobata show thermal stratification structure in Nordic Seas, *Nat. Microbiol.*, 4(1), 107–115, doi:10.1038/nm0303-107-115.
- Spindler, M., and G.S. Dieckmann (1986), Distribution and abundance of the planktonic foraminifera *Neogloboquadrina pachymelina* in sea ice of the Weddell Sea (Antarctica), *Polar Biol.*, 5, 185–191, doi:10.1007/BF00414169.
- Talbot, R.J., C. Li, and M. Nuccio (2013), Mismatch between the depth habitat of planktonic foraminifera and the calibration depth of SST transfer functions may bias reconstructions, *Clim. Past*, 9, 859–870, doi:10.5194/cp-9-859-2013.
- Tur Book, C. F., and P. Smilauer (2002), *Canoco for Windows Version 4.5*, Biometris Plant Research International, Wageningen, The Netherlands.
- Vita, G., C. Lupi, M. Cobbin, N. F. Flisende, and S.F. Polar (2008), A Pleistocene warming event at Ma In Pyda Bay, East Antarctica: evidence from ODP site 1165, *Paleogeogr. Paleoclimatol. Palaeoecol.*, 262(1), 230–244, doi:10.1016/j.palaeo.2007.08.017.
- Volkmann, R., and M. Mersch (2001), Stable isotope composition ($\delta^{13}\text{C}$, $\delta^{18}\text{O}$) of living planktic foraminifera in the outer Laptev Sea and the Fram Strait, *Mar. Micropaleontol.*, 42, 161–188, doi:10.1016/S0377-8398(01)00018-4.
- Weaver, A.J., C.M. Bitz, A.F. Faure, and M.M. Holland (1998), Thermohaline circulation: High-latitude phenomena and the difference between the Pacific and Atlantic, *Annu. Rev. Earth Planet. Sci.*, 27(1), 231–265, doi:10.1146/annurev.earth.27.1.231.
- Wendeborg, M., J.M. Richter, M. Roth, and W.A. Brand (2011), ^{18}O anchoring to VPDB: Calcite digestion with ^{18}O -depleted orthophosphoric acid, *Rapid Commun. Mass Spectrom.*, 25(7), 851–860, doi:10.1002/rcm.4933.
- World Register of Marine Species Editorial Board (2014), World Register of Marine Species. [Available from <http://www.marinespecies.org>, at VUZ. Accessed 2014-09-30]
- Yashayaev, I., E.H. Head, K. Anslow-Scott, Z. Wang, W.K. W. Li, B.J.W. Gruarion, J. Anning, and S. Pandion (2014), Oceanographic and environmental conditions in the Labrador Sea during 2012, *DFO Can. Sci. Advic. Ser. Rep. Doc.*, 2014/D46, v + p.24.
- Yashayaev, I. (2007), Hydrographic changes in the Labrador Sea, 1963–2005, *Prog. Oceanogr.*, 73, 242–276, doi:10.1016/j.pocean.2007.04.015.
- Yashayaev, I., M. Boisefort, M. Handorf, and M. van Aken (2007), Spreading of the Labrador Sea Water to the Irminger and Island basins, *Geophys. Res. Lett.*, 34, L11602, doi:10.1029/2006GL028998.
- Zonneveld, K.A., et al. (2013), Atlas of modern dinoflagellate cyst distribution based on 2405 data points, *Rev. Palaeobot. Palynol.*, 191, 1–17, doi:10.1016/j.revpalbo.2013.08.003.

APPENDICE B

RÉSULTATS BRUTS DE LA COMPOSITION MINÉRALOGIQUE DES IRD AU SITE IODP U1307 À PARTIR D'ANALYSES PAR DIFFRACTION À RAYONS X

Hole	Core	Section	Interval	Depth (mbsf)	Depth (rmcd)	Age (ka)	albite	microcline	anorthite	goethite	chlorite	mica	amphibole	calcite	dolomite?	pyroxene	gypsum	quartz	pyrite	quartz	talc	kaolinite?	clinoptilolite?
B	13	01 W	60-62 cm	109,9	116,43	2235,6	37,3	1,1	3,6	0,1	5,3	2,7	10,8	1,6	0,5	2,1	1,5	0,7	32,7	0	0	0	
B	13	01 W	130-132 cm	109,9	117,13	2245,4	33,1	0,9	3,2	0,1	8,6	5,3	15,3	5,6	10,4	3,7	0,6	0,3	12,9	0	0	0	
B	13	02 W	30-32 cm	111,1	117,63	2253,8	38	0,7	1,6	0,1	6,6	3,8	3,5	0,5	0,7	4,3	0,7	0	39,5	0	0	0	
B	13	02 W	130-132 cm	112,1	118,63	2271,7	47,5	1,6	2,1	0,1	0,2	5,8	1,3	0,4	0,2	0,1	0,1	0,4	40,2	0	0	0	
B	13	03 W	12-14 cm	112,42	118,95	2279,8	13,1	8,9	0	0	2,1	3,1	2,1	0,8	0,6	trace	0,2	68,2	0	0,3	0		
B	13	03 W	30-32 cm	112,6	119,13	2284,3	40,1	2,1	4,8	0,1	0,3	3,3	4,8	1	0,2	0,1	0,2	0,5	42,5	0	0	0	
B	13	03 W	55-57 cm	112,85	119,38	2290,6	23,1	11,1	0	0	2,9	6,3	3,1	0,9	1,2	0,7	0,9	1,1	48,3	0	0,4	0	
B	13	03 W	80-82 cm	113,1	119,63	2296,9	36,6	1,8	3,3	0,1	0,2	0,9	0,8	0,6	0,1	0	0,1	0,3	55,2	0	0	0	
B	13	04 W	30-32 cm	114,1	120,63	2322,3	39,5	2,5	1,4	0,1	0,2	2,8	1,2	6,8	0,1	0,1	1,2	0,3	43,8	0	0	0	
B	13	04 W	52-54 cm	114,32	120,85	2328,2	17,4	11,5	0	0	2,2	3,8	2,5	5,7	0,9	0,4	2,8	1	49,4	0	0,9	1,5	
B	13	04 W	80-82 cm	114,6	121,13	2335,7	3,8	0,5	0,6	0,1	0,2	2,9	1,3	84	0,1	0,1	1,2	0,3	4,8	0	0	0	
B	13	04 W	130-132 cm	115,1	121,63	2354,4	7,7	1	1,7	0,2	0,4	28,3	2,6	47,7	0,2	0,2	2,5	0,7	6,8	0	0	0	
B	13	05 W	6-8 cm	115,36	121,89	2365,2	3,6	4,3	0	0	0,4	0,9	0,6	0,4	0,5	0,3	trace	0,2	88,6	0	0,2	0	
B	13	05 W	30-32 cm	115,6	122,13	2372,7	8,4	0,4	0,7	0,1	0,2	5,1	1,1	77,9	0,1	0,1	1,9	0,4	3,6	0	0	0	
B	13	05 W	47-49 cm	115,77	122,3	2377,5	10,5	7	0	0	2,1	4,1	3,3	2	1,2	0,4	1,2	0,7	67,3	0	0,2	0	
A	14	05 W	62-64 cm	114,52	122,43	2382,3	3,7	5,1	0	0	1,2	2,8	1,8	0,2	0,5	0,3	0,6	0,3	83,3	0	0,2	0	
B	13	05 W	67-69 cm	115,97	122,57	2392	9,6	6,5	0	0	1,8	2,1	1,3	0,3	0,4	0,3	1,9	0,2	75,2	0	0,4	0	
B	13	05 W	80-82 cm	116,1	122,76	2405,1	15,9	1,1	1	0,1	0,7	1,5	0,7	0,3	0,2	0,2	1,8	0,3	76,2	0	0	0	
B	13	05 W	84-86 cm	116,14	122,82	2409,2	19,9	11,7	0	0	3,2	3,8	1,7	0,8	2,4	0,5	1,3	0,7	53,3	0	0,7	0	
B	13	05 W	88-90 cm	116,18	122,88	2413,3	10,5	5,7	0	0	3,1	3,7	1,6	0,6	1,2	0,5	0,7	0,4	71,5	0	0,5	0	
B	13	05 W	92-94 cm	116,22	122,93	2416,8	13,4	7,3	0	0	3,9	4,8	1,9	0,7	0,8	0,5	0,6	0,2	65,4	0	0,5	0	
A	14	02 W	113-115 cm	115,03	122,94	2417,5	11,9	7,1	0	0	1,7	2,4	1,1	0,6	0,5	0,4	trace	0,2	73,9	0	0,2	0	
B	13	05 W	96-98 cm	116,26	122,99	2420,9	17,9	9,7	0	0	2,4	4,3	0,9	1,1	0,9	0,9	0,8	0,3	60,5	0	0,3	0	
B	13	05 W	112-114 cm	116,42	123,23	2439,2	14,7	7,9	0	0	2,1	4,6	3,5	0,7	0,5	0,5	0,5	0,8	63,9	0	0,3	0	
A	14	03 W	2-4 cm	115,42	123,33	2447,6	36,7	7,8	0	0	3,3	6,8	3,7	0,3	0,2	0,2	trace	1,2	39,2	0	0,6	0	
A	14	03 W	12-14 cm	115,52	123,43	2456	19,7	10,7	0	0	2,6	4,7	1	0,8	2,3	0,7	0,7	0,3	56,2	0	0,3	0	
B	13	05 W	130-132 cm	116,6	123,49	2461	8,1	0,4	0,7	0,1	0,1	1,5	0,5	74,3	0,1	0,1	5,4	0,4	8,3	0	0	0	
A	14	03 W	28-30 cm	115,68	123,59	2472,3	22,1	11,1	0	0	2,7	4,8	1,1	0,6	2	0,7	0,9	0,3	53,3	0	0,4	0	
A	14	03 W	32-34 cm	115,72	123,63	2477,6	35,6	7,4	0	0	2,7	3,7	1,9	0,9	0,3	0,2	0,2	trace	1,2	46,5	0	0,5	0
A	14	03 W	40-42 cm	115,8	123,71	2488,2	22,9	10,6	0	0	2,4	4,4	2,1	0,4	1,5	0,4	trace	1,6	53,2	0	0,5	0	
A	14	03 W	48-50 cm	115,88	123,79	2498,9	34,7	9,1	0	0	3,3	3,1	2,3	0,3	0,3	0,3	trace	0,9	45,3	0	0,4	0	
A	14	03 W	56-58 cm	115,96	123,87	2509,5	19,5	9,1	0	0	2,2	4	2,1	0,5	1,2	0,6	1,3	2,1	57,1	0	0,3	0	
A	14	03 W	66-68 cm	116,06	123,97	2522,2	30,4	10	0	0	3,4	5,1	2,6	0,3	0,3	0,3	trace	0,9	46,3	0	0,4	0	
A	14	03 W	78-80 cm	116,18	124,09	2531,8	27,3	9	0	0	1,8	4,6	2,3	0,3	0,8	0,3	5,8	0,8	42,7	0	0,4	3,9	
B	13	06 W	30-32 cm	117,1	124,22	2542,2	26,1	1,2	2,2	0,2	0,5	1,4	1,5	0,1	0,3	0,3	38,2	1,2	26,8	0	0	0	
A	14	03 W	100-102 cm	116,40	124,31	2549,4	9,3	8,2	0	0	2	2,8	1,7	12,1	0,8	0,5	4,4	1,2	56,7	0	0,3	0	
A	14	03 W	112-114 cm	116,52	124,43	2559	25,3	15,7	0	0	3,8	5,4	3,3	1,9	1,7	1	trace	0,5	40,9	0	0,5	0	
A	14	03 W	120-122 cm	116,6	124,51	2565,4	16,5	8,5	0	0	2,3	5	2,1	0,7	1	0,5	trace	0,8	62,3	0	0,3	0	
A	14	03 W	140-142 cm	116,8	124,71	2581,4	18,7	11	0	0	2,4	5,6	2,8	0,5	0,9	0,3	3,7	1,2	50,7	0	0,5	1,7	
A	14	03 W	148-150 cm	116,88	124,79	2587,8	23,1	11,4	0	0	3,2	2,4	0,9	0,8	1,2	0,4	0	1,1	55,2	0	0,3	0	
B	13	06 W	100-102 cm	117,8	125,24	2623,8	30,3	1,4	2,3	0,1	0,2	2,3	10	0,3	8	1,4	1,3	0,5	41,9	0	0	0	
B	13	06 W	130-132 cm	118,1	125,68	2617,8	43,7	1,1	2,2	0,2	0,6	4,1	1,4	2,3	0,6	0	0,4	0,8	42,6	0	0	0	
B	13	06 W	145-147 cm	118,25	125,9	2624	19,3	1,6	1,2	0,2	0,3	1,2	2,1	0,6	0,4	2,4	0,2	0,2	70,3	0	0	0	
B	13	07 W	10-12 cm	118,4	126,12	2630,3	36,5	1,4	3,5	0,2	0,1	1,9	1,9	0,6	0,5	4,8	0,3	0,5	47,8	0	0	0	
B	13	07 W	25-27 cm	118,55	126,34	2636,6	34,1	1,5	3	0,1	0,1	1,2	4	0,6	0,4	3	0,3	0,3	51,4	0	0	0	
B	13	07 W	40-42 cm	118,7	126,55	2642,5	39,6	1,9	3,9	0,1	0,1	1,4	3,3	3,9	0,3	2,9	0,3	0,2	42,1	trace	0	0	0
B	13	07 W	55-57 cm	118,85	126,75	2648,2	23,1	10,7	0	0	2,1	5,4	2,8	0,7	0,8	0,3	2,2	1	50,1	0	0,8	0	
B	14	01 W	20-22 cm	119	126,9	2652,5	26	1,9	1,7	0,1	0,1	1,4	1,8	4	0,3	6,8	0,3	0,2	55,4	0	0	0	
B	14	01 W	30-32 cm	119,1	127	2653,3	31,7	1,1	2,5	0,1	0,4	2,3	1	1	0,4	0	0,3	0,2	59	0	0	0	
A	14	05 W	96-98 cm	119,36	127,27	2663	7,9	6,9	0	0	1,7	2,4	1,4	0,3	0,7	0,4	1,1	0,1	76,9	0	0,2	0	
B	14	01 W	80-82 cm	119,6	127,5	2671,2	32,3	1,1	2,5	0,1	0,4	1	1	0,5	0,4	0	0,3	0,3	60,1	0	0	0	
B	14	01 W	130-132 cm	120,1	128	2689,8	43,2	1,5	3,4	0,2	0,5	1,3	1,4	0,5	0,3	0	0,4	0,4	46,9	0	0	0	
A	14	06 W	60-62 cm	120,50	128,41	2705,1	14,5	6,9	0	0	1,7	3	2,4	0,4	0,4	0,4	1	0,9	68,2	0	0,2	0	
B	14	02 W	46-48 cm	120,76	128,66	2714,4	15,9	11,2	0	0	3,4	6,3	5,2	0,7	1,2	0,7	0,9	1,5	52,6	0	0,4	0	
B	14	02 W	80-82 cm	121,1	129	2727	63,7	1,7	4,7	0,1	1	0,5	8,6	0,7	0,2	0	0,2	0,3	18,3	0	0	0	
B	14	02 W	130-132 cm	121,6	129,5	2741,6	37	2,5	1,5	0,1	0,7	5,3	0,7	0,3	0,2	0,2	1,9	0,4	49,2	0	0	0	

B	14	02 W	148-150 cm	121,78	129,68	2747,2	20,5	11,8	0	0	1,6	4,9	2	0,9	1,1	0,7	1,2	1,8	52,8	0	0,7	0
B	14	03 W	30-32 cm	122,1	130	2751,2	35,1	3,3	5,2	0,2	3,2	1,5	5,9	1,1	0,8	0	0,5	0,6	42,6	0	0	0
B	14	03 W	66-68 cm	122,46	130,36	2755,7	19,6	11,5	0	0	2,5	4,8	3,4	1,4	1,5	0,4	2,9	1,2	50,2	0	0,6	0
B	14	03 W	80-82 cm	122,6	130,5	2757,4	40,1	2,5	4	0,2	2,2	2,6	2,6	0,9	0,6	0	0,4	0,5	43,4	0	0	0
B	14	03 W	96-98 cm	122,76	130,66	2759,4	22,5	10,8	0	0	1,6	4,9	3,4	0,9	1,1	0,7	0,9	1,3	51,2	0	0,7	0

Hole	Core	Section	Interval	Depth (mbf)	Depth (rmcd)	Age (ka)	stibite	microcline	anorthite	goethite	clinoite	mica	amphibole	calcite	dolomite?	pyroxene	Gypse	Pyrite	quartz	talc	kaolinite?	clinozoilite?
B	14	03 W	130-132 cm	123,1	131	2763,6	34,8	1,7	1,8	0,3	0,8	4,5	1,3	22,8	1,4	0,4	3,4	2,1	24,7	0	0	0
B	14	04 W	30-32 cm	123,6	131,5	2769,9	10,5	0,7	0	10,3	0	2,8	0,9	15,4	0	0	51,2	1,8	6,4	0	0	0
B	14	04 W	80-82 cm	124,1	132	2776,1	7,6	0,6	0	2,8	0	1,6	0,4	5,2	0	0	75,2	0,5	6,1	0	0	0
B	14	04 W	130-132 cm	124,6	132,51	2780,9	24,2	0,8	0	1,1	0	6,2	0,6	29,3	0	0	5,3	0,8	31,7	0	0	0
B	14	05 W	30-32 cm	125,1	133,01	2785,5	6,5	0,8	0	0,8	0	4,1	3,4	19,5	0	0	49,9	0,5	14,5	0	0	0
B	14	05W	80-82 cm	125,6	133,51	2790,2	16,7	0,7	0	1,3	0	6,6	10,4	31,6	0	0	7,1	2,1	23,5	0	0	0
B	14	05 W	130-132 cm	126,1	134,01	2794,8	50,3	2,1	3,3	0,2	1,5	1,8	2,1	0,7	0,5	0	0,3	1,1	36,1	0	0	0
B	14	06 W	30-32 cm	126,6	134,51	2799,5	32,1	0,9	0	1,5	0	6,7	3,3	17,2	0	0	14,6	0,9	22,8	0	0	0
B	14	06 W	80-82 cm	127,1	135,01	2804,3	10,6	1,3	0	1	0	5,2	2,6	57	0	0	5,3	1,2	15,8	0	0	0
B	14	06 W	130-132 cm	127,6	135,44	2815	41,9	0,5	0	0,4	0	39,7	0,9	0	0	0	0,7	0,2	15,7	0	0	0
B	14	07 W	30-32 cm	128,1	135,84	2824,9	39,7	3,3	3,3	0,3	1,6	5,2	1,5	0,6	0,4	0,4	1,5	2,6	39,6	0	0	0
B	15	01 W	30-32 cm	128,6	136,3	2835,2	43,6	1	0	0,8	0	0	3,2	1,1	0	0	12,1	2,5	35,7	0	0	0
B	15	01 W	80-82 cm	129,1	136,8	2845,5	35,9	1,1	0	0,9	0	6,7	3,5	13,2	0	0	3,9	0,7	34,1	0	0	0
B	15	01 W	130-132 cm	129,6	137,3	2870,8	55,1	1,7	0	0,2	0	1,8	1,1	0,5	0	0	23,8	0,1	15,7	0	0	0
B	15	02 W	30-32 cm	130,1	137,8	2887,4	30,7	3,9	0	1,7	0	3,2	2,6	0,6	0	0	33,2	1	23,1	0	0	0
B	15	02 W	80-82 cm	130,6	138,3	2900,4	63,5	0,9	1,6	0,2	0,4	1,9	0,7	3,1	0,8	0,2	2,2	2,8	21,7	0	0	0
B	15	02 W	130-132 cm	131,1	138,8	2930,1	36,1	1,1	2,2	0,2	0,4	0,8	1,3	0,2	0,4	0,3	0,4	1	55,6	0	0	0
B	15	03 W	30-32 cm	131,6	139,3	2939,9	21,9	0,9	1,4	0,2	0,4	11,7	1,2	0,2	0,3	0,2	0,4	0,4	60,8	0	0	0
B	15	03 W	80-82 cm	132,1	140,07	2951,3	41,8	2,5	2,2	0,2	0,3	1	1,5	0,1	0,4	0,9	0,3	0,3	48,5	0	0	0
B	15	03 W	130-132 cm	132,6	140,9	2963,4	43,2	1,4	4	0,1	0,3	1,6	1,4	0,1	0,5	4,3	0,9	0,5	41,7	0	0	0
B	15	04 W	30-32 cm	133,1	141,74	2974,6	44,5	1,5	2,8	0,1	0,3	2,3	1,4	0,1	0,5	4,5	1	0,5	40,5	0	0	0
B	15	04 W	80-82 cm	133,6	142,57	2985,2	20,6	1,2	0,7	0,2	0,4	2	0,8	43,1	0,2	0,2	13,5	0,7	16,4	0	0	0
B	15	04 W	130-132 cm	134,1	143,41	2995,9	43,4	1,5	4,6	0,1	0,2	2,4	1,4	0,1	0,2	4,3	1,3	1	39,5	0	0	0
B	15	05 W	30-32 cm	134,6	144,24	3003,7	40,7	1,4	4,3	0,2	0,3	1,5	2	0,1	0,5	0	14,7	1,5	32,8	0	0	0
B	15	05 W	80-82 cm	135,1	145,07	3009,3	41,1	4,3	8,5	trace	0	1,8	8,5	1,8	2,7	0	3,7	2,8	24,8	0	0	0
B	15	05 W	130-132 cm	135,6	145,91	3015	38,1	3,2	6,2	trace	0	1,3	4,8	6,8	1,1	0	13,9	2,1	22,5	0	0	0
B	15	06 W	10-12 cm	135,9	146,41	3018,4	24,1	1,8	2,8	0,3	0,2	7,6	2,6	25,8	1	2	1,1	9,1	21,6	0	0	0
B	15	06 W	30-32 cm	136,1	146,74	3020,6	37,1	3,1	6,1	trace	0	1,3	4,6	2,2	1	0	0,6	1,7	42,3	0	0	0
B	15	06 W	47-48,5 cm	136,65	147,02	3022,5	49,9	2,8	4,3	0,1	0,1	2	4,5	0,6	0,8	1	0,6	0,9	32,4	0	0	0
B	15	06 W	64-65 cm	136,44	147,31	3024,5	39,3	2,2	3,3	0,1	0,1	1,5	3,6	0,5	0,6	0,8	0,4	0,7	46,9	0	0	0
B	15	06 W	80-82 cm	136,6	147,58	3026,4	33,6	11,2	14,6	trace	0	0,9	3,3	3,8	0,7	0	0,4	1,2	30,3	0	0	0
B	15	06 W	97-98,5 cm	136,765	147,85	3028,2	31,6	1,8	2,7	0,1	0,1	1,2	2,9	0,8	0,5	0,6	0,3	0,6	56,8	0	0	0
B	15	06 W	113-115 cm	136,93	148,13	3030,6	41,7	2,4	3,6	0,1	0,1	1,6	3,8	1	1,7	0,9	0,5	0,8	41,8	0	0	0
B	15	06 W	128-130 cm	137,08	148,38	3033,1	38,2	2,2	3,3	0,1	0,1	1,5	1,6	0,9	1,6	0,8	0,4	0,8	48,5	0	0	0
B	15	06 W	130-132 cm	137,1	148,41	3033,4	44,9	3,6	6	trace	0	0,6	2,3	2,7	0,5	0	0,3	0,4	38,7	0	0	0
B	15	06 W	146-148 cm	137,26	148,68	3036,1	37,5	2,1	3,2	0,1	0,1	1,5	1,5	0,9	19,6	0,8	0,5	0,5	31,7	trace	0	0
B	15	07 W	13-14,5 cm	137,425	148,95	3038,8	46,7	1,9	3,8	0,1	0,1	1,3	1,3	1,1	0,1	0,7	0,4	0,5	42	0	0	0
B	15	07 W	28-30 cm	137,6	149,25	3041,8	38,9	2,3	0,9	0,1	0,1	1,1	0,1	0,9	0,1	0,9	0,3	1	52,3	0	0	0
B	15	07 W	46-47,5 cm	137,755	149,5	3044,3	38,8	2,3	0,9	0,1	0,1	1,1	0,1	1,1	0,1	0,9	1,3	1	52,2	0	0	0
B	15	07 W	62-64 cm	137,92	149,7	3046,3	42,8	2,6	4	0,1	0,1	8	2,1	1,4	0,1	1,7	3,4	1,1	28,9	3,7	0	0
B	16	01 W	14-15,5 cm	137,935	149,71	3046,4	44,4	0,9	0,8	0,1	0,1	6,2	11,1	4,1	0,1	1,1	17,5	1,1	12,6	0	0	0
B	16	01 W	30-32 cm	138,1	149,88	3048,1	58,4	1,2	1	0,1	0,1	5,4	0,3	10,7	0,1	1,5	1,4	0	19,9	0	0	0
B	16	01 W	47-48,5 cm	138,265	150,04	3049,7	30,7	2,3	1,2	0,1	0,1	1,3	0,4	1,1	0,1	0,4	38,2	0,5	23,6	0	0	0
B	16	01 W	63-65 cm	138,43	150,21	3051,4	39,1	3,9	1	0,1	0,1	1	0,3	0,9	0,1	0,3	38,5	0,6	14,1	0	0	0
B	16	01 W	80-82 cm	138,6	150,38	3053,1	48,8	1,8	3,2	trace	0	0,7	2,5	6,5	0,6	0	17,8	0,5	17,6	0	0	0
B	16	01 W	92,5-94,5 cm	138,725	150,51	3054,4	22,6	3,4	1,2	0,1	0,1	1,3	0,4	1,2	0,1	0,4	50	0,8	18,3	0	0	0
B	16	01 W	105-107 cm	138,85	150,63	3055,6	50,2	3,5	1,3	0,1	0,1	1,9	0,4	5,9	0,1	0,4	15,1	2,3	18,7	0	0	0
B	16	01 W	118-120 cm	138,975	150,76	3056,9	12,1	1,3	1	0,2	0,2	2,3	0,5	2,3	0,1	0,4	63,3	2,8	13,5	0	0	0
B	16	01 W	130-132 cm	139,1	150,88	3058,1	38,1	2,9	4,5	trace	0	3,6	5,2	2,2	0,9	0	12,3	0,6	29,7	0	0	0
B	16	02 W	30-32 cm	139,6	151,38	3062,3	36,5	2,8	4,3	trace	0	3,5	5	2,2	0,8	0	11,9	4,7	2			

B	16	02 W	35-37 cm	139,65	151,43	3062,7	28,9	3,3	1,9	0,5	0,3	8,8	1	18	0,4	0,8	0,9	19,7	15,5	0	0	0
B	16	02 W	42-44 cm	139,72	151,5	3063,3	32,2	1,6	2,1	0,5	0,3	13,9	1,5	20,1	0,6	1	1,5	13,1	11,6	0	0	0
B	16	02 W	49-50,5 cm	139,785	151,57	3063,8	28,6	1,5	1,8	0,5	0,3	12,3	2,3	30,7	0,6	1,2	2,2	7,7	10,3	0	0	0
B	16	02 W	55-56,5	139,845	151,63	3064,3	13,9	0,9	1,1	0,3	0,2	4,3	1,4	18,9	0,6	1,4	32,2	3,1	21,7	0	0	0
B	16	02 W	62-63,5 cm	139,915	151,69	3064,8	30,2	1	2,9	0,3	0,2	5,1	3	25,3	0,9	3,2	7,4	3,6	16,9	0	0	0
B	16	02 W	67-69 cm	139,97	151,75	3065,2	27,8	1,8	3,6	0,8	0,2	5,9	2,3	27,5	1,2	4,4	3,8	4,2	16,5	0	0	0
B	16	02 W	73-75 cm	140,03	151,81	3065,7	26,4	1,5	2,7	0,6	0,1	5,6	1,8	38,3	1,3	3,8	4,3	2,5	11,1	0	0	0
B	16	02 W	80-82 cm	140,1	151,88	3066,3	27,8	2,2	3,3	0,1	0	2,7	3,8	4,3	0,7	0	15,8	2,1	37,2	0	0	0
B	14	03 W	96-98 cm	122,76	130,66	2759,4	22,5	10,8	0	0	1,6	4,9	3,4	0,9	1,1	0,7	0,9	1,3	51,2	0	0,7	0

Hole	Core	Section	Interval	Depth (mbsf)	Depth (rmcd)	Age (ka)	albite	microcline	anorthite	goethite	chlorite	mica	amphibole	calcite	dolomite?	pyroxene	epste	pyrite	quartz	talc	kaolinite?	clinozoilite?
B	16	02 W	97-98,5 cm	140,265	152,04	3067,5	29,4	1	2,4	0,4	0,1	1,7	2	14,4	0,5	3,7	24,5	5,2	14,7	0	0	0
B	16	02 W	105-107 cm	140,35	152,13	3068,2	18,7	0,9	2,3	0,4	0,1	1,6	0,2	13,7	0,5	3,5	40,2	1	16,9	0	0	0
B	16	02 W	113-115 cm	140,43	152,21	3068,8	25,2	1,8	3,7	0,6	0,2	2,8	0,3	16,5	1	7,1	16,1	1,9	22,8	0	0	0
B	16	02 W	121-123 cm	140,51	152,29	3069,5	45,9	2,1	4,3	0,5	0,1	6,2	0,3	11,6	0,8	3,9	2,2	3,1	19	0	0	0
B	16	02 W	130-132 cm	140,6	152,38	3070,2	37,3	3,7	5,6	0,1	0	10,1	6,5	4,6	0,9	0	6,7	4,7	19,8	0	0	0
B	16	03 W	5-7 cm	140,85	152,63	3072,1	30,4	2,8	3,4	0,8	0,2	3,2	0,5	20,2	0,9	10,5	3,9	3,6	19,6	0	0	0
B	16	03 W	30-32 cm	141,1	152,88	3074,1	28,5	1,2	1,8	0,2	0,6	3,1	0,9	0,4	0,4	0,3	32,7	6	23,9	0	0	0
B	16	03 W	55-57 cm	141,35	153,13	3076,1	16,1	1,8	2,1	0,8	0,2	4	0,5	50,5	0,8	0	4,8	6,1	12,3	0	0	0
B	16	03 W	80-82 cm	141,6	153,38	3078	26,1	1,3	1,5	0,3	0,6	8,9	1,3	31,6	0,3	0,3	1,7	7,6	18,5	0	0	0
B	16	03 W	105-107 cm	141,85	153,63	3080	13,8	1,5	1,8	0,6	0,2	16,4	0,4	27,3	0,8	0	12,2	11,7	13,3	0	0	0
B	16	03 W	130-132 cm	142,1	153,88	3082	38,6	1,6	3,4	0,1	0	11,1	6,7	16,1	0,6	0	3,2	3,3	15,3	0	0	0
B	16	04 W	5-7 cm	142,35	154,13	3083,9	15,6	1,7	2,1	0,7	0,2	15,6	0,5	35,2	0,9	0	2,7	5,9	18,9	0	0	0
B	16	04 W	30-32 cm	142,6	154,38	3085,9	37,8	1,5	3,3	0,1	0	16,2	6,6	15,7	0,8	0	1,6	1,7	14,7	0	0	0
B	16	04 W	55-57 cm	142,85	154,63	3087,9	18,1	1,7	2	0,7	0,2	15,1	0,5	40,9	3	0	3,5	2,1	12,2	0	0	0
B	16	04 W	80-82 cm	143,1	154,88	3089,8	31,3	1,5	3,3	0,1	0	16,1	6,5	15,6	0,5	0	1,5	8,7	14,9	0	0	0
B	16	04 W	105-107 cm	143,35	155,13	3091,8	7,5	0,8	1,1	0,3	0	34,7	0,5	27,8	2,3	0	4,3	3,8	16,7	0	0	0
B	16	04 W	130-132 cm	143,6	155,38	3093,8	18,2	0,8	1,2	0,2	0,4	9,1	0,6	28,1	0,4	2,2	21	2,4	15,4	0	0	0
B	16	05 W	30-32 cm	144,1	155,88	3099,4	24,1	0,7	1,5	0,1	0	2,8	5,1	3,6	0,6	0	18,2	0,9	42,4	0	0	0
B	16	05 W	80-82 cm	144,6	156,38	3105,1	24,3	0,7	1,5	0,1	0	2	4,2	3,6	0,6	0	18,3	0,9	43,8	0	0	0
B	16	05 W	130-132 cm	145,1	156,88	3114,4	21,9	1,2	2,5	0,1	0	4,4	1,8	5,9	1	0	30,2	2,9	28,1	0	0	0
A	19	02 W	80-82 cm	155,4	168,13	3161,3	41,1	2,2	4,7	0,3	0	3,7	1,3	16,8	1,3	0	2,8	5,5	20,3	0	0	0
A	19	02 W	130-132 cm	155,9	168,63	3164,9	24,2	2,4	5,1	0,3	0	13,4	1,8	18,2	1,4	0	6,7	8,9	17,6	0	0	0
A	19	03 W	80-82 cm	156,9	169,63	3175,2	44	2,3	4,9	0,3	0	3,8	1,4	11	1,3	0	2,7	2,5	25,8	0	0	0
A	19	04 W	30-32 cm	157,9	170,63	3186,9	44,5	1,8	5,9	0,2	0	3	1,1	1,6	1	0	18,2	2,6	20,1	0	0	0
A	19	04 W	80-82 cm	158,4	171,13	3189,9	42,3	2,4	5,3	0,3	0	3,3	1	4,8	0,5	0	8,1	11,6	20,4	0	0	0
A	19	04 W	130-132 cm	158,9	171,63	3192,5	55,2	1,4	6,9	0,2	0	2,9	9	2,8	0,3	0	2,6	1,1	17,6	0	0	0
A	19	05 W	80-82 cm	159,9	172,63	3197,6	27,9	2,1	3,4	0,3	0	11,6	13,1	11,9	0,5	0	2,3	8,3	18,7	0	0	0
A	19	05 W	130-132 cm	160,4	173,13	3200,1	26,8	2	3,3	0,3	1,1	11,1	12,6	11,4	2	0	0,9	3,3	25,2	0	0	0
A	19	06 W	80-82 cm	161,4	174,13	3205,2	40,2	1,5	3,1	0,2	5,7	7,4	6,4	7,1	0,8	0	0,9	5,3	21,4	0	0	0
A	19	07 W	20-22 cm	162,3	175,03	3209,8	45	1,1	3,5	0,2	2,8	4,6	4,8	5,3	0,6	0	0,4	2,5	29,2	0	0	0
A	19	07 W	70-72 cm	162,8	175,53	3212,3	50	0,8	4,9	0,3	3,3	1,6	5,9	7,5	0,8	0	0,5	5,6	18,8	0	0	0

RÉFÉRENCES

- Aksu, A. E., et Kaminski, M. A. (1989). Neogene and Quaternary planktonic foraminifer biostratigraphy and biochronology in Baffin Bay and the Labrador Sea. In Proceedings of the Ocean Drilling Program: Scientific Results. Vol. 105, pp. 287-304. doi:10.2973/odp.proc.sr.105.122.1989
- Anstey, C.E. (1992). Biostratigraphic and paleoenvironmental interpretation of upper middle Miocene through lower Pleistocene dinoflagellate cyst, acritarch, and other algal palynomorph assemblages from Ocean Drilling Program Leg 105, Site 645, Baffin Bay. Mémoire de maîtrise, University of Toronto. 271 pp
- Baldauf, J.G., Clement, B.G., Aksu, A.E., de Vernal, A., Firth, J.V., Hall, F., Head, M.J., Jarrard, R.D., Kaminski, M.A., Lazarus, D., Monjanel, A.-L., Berggren, W.A., Gradstein, F.E., Knüttel, S., Mudie, P.J., et Russell, M.D. (1989). Magnetostratigraphic and biostratigraphic synthesis of Ocean Drilling Program Leg 105: Labrador Sea and Baffin Bay. In Srivastava, S.P., Arthur, M.A., Clement, B., et al., Proc. ODP, Sci. Results, 105: College Station, TX (Ocean Drilling Program), 935–956. doi:10.2973/odp.proc.sr.105.165.1989
- Bartoli, G., Sarnthein, M., Weinelt, M., Erlenkeuser, H., Garbe-Schönberg, D., et Lea, D. W. (2005). Final closure of Panama and the onset of Northern Hemisphere glaciation. *Earth and Planetary Science Letters*, 237(1-2), 33-44. 10.1016/j.epsl.2005.06.020
- Bartoli, G., Höönsch, B., et Zeebe, R. E. (2011). Atmospheric CO₂ decline during the Pliocene intensification of Northern Hemisphere glaciations. *Paleoceanography*, 26(4). doi:10.1029/2010PA002055
- Bennike, O., et Böcher, J. (1990). Forest-tundra neighbouring the North Pole: plant and insect remains from the Plio-Pleistocene Kap København formation, North Greenland. *Arctic*, 331-338. doi:10.14430/arctic1629

- Bennike, O., Abrahamsen, N., Bak, M., Israelson, C., Konradi, P., Matthiessen, J., et Witkowski, A. (2002). A multi-proxy study of Pliocene sediments from Île de France, North-East Greenland. *Palaeogeography, Palaeoclimatology, Palaeoecology*, 186(1-2), 1-23.
- Blake-Mizen, K., Hatfield, R., Stoner, J., Carlson, A., Xuan, C., Walczak, M., Lawrence, K.T., Channell, J.E.T., et Bailey, I. (2019). Southern Greenland glaciation and Western Boundary Undercurrent evolution recorded on Eirik Drift during the late Pliocene intensification of Northern Hemisphere glaciation. *Quaternary Science Reviews*, 209, 40-51. <https://doi.org/10.1016/j.quascirev.2019.01.015>
- Bogus, K., Mertens, K. N., Lauwaert, J., Harding, I. C., Vrielinck, H., Zonneveld, K. A., et Versteegh, G. J. (2014). Differences in the chemical composition of organic-walled dinoflagellate resting cysts from phototrophic and heterotrophic dinoflagellates. *Journal of Phycology*, 50(2), 254-266.
- Channell, J. E. T., Hodell, D. A., et Curtis, J. H. (2016). Relative paleointensity (RPI) and oxygen isotope stratigraphy at IODP Site U1308: North Atlantic RPI stack for 1.2–2.2 Ma (NARPI-2200) and age of the Olduvai Subchron. *Quaternary Science Reviews*, 131, 1-19. <https://doi.org/10.1016/j.quascirev.2015.10.011>
- Clement, B.M., Hall, F.J., et Jarrard, R.D. (1989). The magnetostratigraphy of Ocean Drilling Program Leg 105 sediments. In Srivastava, S.P., Arthur, M.A., Clement, B., et al., Proc. ODP, Sci. Results, 105: College Station, TX (Ocean Drilling Program). 583–595. doi:10.2973/odp.proc.sr.105.147.1989
- Clotten, C., Stein, R., Fahl, K., et De Schepper, S. (2018). Seasonal sea ice cover during the warm Pliocene: Evidence from the Iceland Sea (ODP Site 907). *Earth and Planetary Science Letters*, 481, 61-72. <https://doi.org/10.1016/j.epsl.2017.10.011>
- Contoux, C., Dumas, C., Ramstein, G., Jost, A., et Dolan, A. M. (2015). Modelling Greenland ice sheet inception and sustainability during the Late Pliocene. *Earth and Planetary Science Letters*, 424, 295-305. <https://doi.org/10.1016/j.epsl.2015.05.018>
- Cremer, M., et Legigan, P. (1989). Morphology and surface texture of quartz grains from ODP Site 645, Baffin Bay. In Proceedings of the Ocean Drilling Program, Scientific Results(Vol. 105, pp. 21-28). Ocean Drilling Program Texas A & M University, College Station, Texas
- Csank, A. Z., Fortier, D., et Leavitt, S. W. (2013). Annually resolved temperature reconstructions from a late Pliocene–early Pleistocene polar forest on Bylot Island,

- Canada. *Palaeogeography, palaeoclimatology, palaeoecology*, 369, 313-322.
doi:10.1016/j.palaeo.2012.10.040.
- DeConto, R. M., Pollard, D., Wilson, P. A., Pälike, H., Lear, C. H., et Pagani, M. (2008). Thresholds for Cenozoic bipolar glaciation. *Nature*, 455(7213), 652.
doi:10.1038/nature07337
- De Schepper, S., et Head, M. J. (2008a). Age calibration of dinoflagellate cyst and acritarch events in the Pliocene–Pleistocene of the eastern North Atlantic (DSDP Hole 610A). *Stratigraphy*, 5(2), 137-161.
- De Schepper, S., et Head, M. J. (2008b). New dinoflagellate cyst and acritarch taxa from the Pliocene and Pleistocene of the eastern North Atlantic (DSDP Site 610). *Journal of Systematic Palaeontology*, 6(1), 101-117. doi:10.1017/S1477201907002167
- De Schepper, S., et Head, M. J. (2009). Pliocene and Pleistocene dinoflagellate cyst and acritarch zonation of DSDP Hole 610A, eastern North Atlantic. *Palynology*, 33(1), 179-218. doi:10.1080/01916122.2009.9989673.
- De Schepper, S., et Head, M. J. (2014). New late Cenozoic acritarchs: evolution, palaeoecology and correlation potential in high latitude oceans. *Journal of Systematic Palaeontology*, 12(4), 493-519. doi:10.1080/14772019.2013.783883.
- De Schepper, S., Head, M. J., et Louwye, S. (2004). New dinoflagellate cyst and incertae sedis taxa from the Pliocene of northern Belgium, southern North Sea Basin. *Journal of Paleontology*, 78(4), 625-644. [https://doi.org/10.1666/0022-3360\(2004\)078<0625:NDCAIS>2.0.CO;2](https://doi.org/10.1666/0022-3360(2004)078<0625:NDCAIS>2.0.CO;2)
- De Schepper, S., Head, M. J., et Groeneveld, J. (2009a). North Atlantic Current variability through marine isotope stage M2 (circa 3.3 Ma) during the mid-Pliocene. *Paleoceanography and Paleoceanography*, 24(4). <https://doi.org/10.1029/2008PA001725>
- De Schepper, S., Head, M. J., et Louwye, S. (2009b). Pliocene dinoflagellate cyst stratigraphy, palaeoecology and sequence stratigraphy of the Tunnel-Canal Dock, Belgium. *Geological Magazine*, 146(1), 92-112. doi:10.1017/S0016756808005438
- De Schepper, S., Fischer, E. I., Groeneveld, J., Head, M. J., et Matthiessen, J. (2011). Deciphering the palaeoecology of Late Pliocene and Early Pleistocene dinoflagellate cysts. *Palaeogeography, Palaeoclimatology, Palaeoecology*, 309(1-2), 17-32.
doi:10.1016/j.palaeo.2011.04.020

- De Schepper, S., Groeneveld, J., Naafs, B. D. A., Van Renterghem, C., Hennissen, J., Head, M. J., Louwye, S., et Fabian, K. (2013). Northern Hemisphere glaciation during the globally warm early late Pliocene. *PLoS One*, 8(12), e81508. <https://doi.org/10.1371/journal.pone.0081508>
- De Schepper, S., Gibbard, P. L., Salzmann, U., et Ehlers, J. (2014). A global synthesis of the marine and terrestrial evidence for glaciation during the Pliocene Epoch. *Earth-Science Reviews*, 135, 83-102. DOI: 10.1016/j.earscirev.2014.04.003
- De Schepper, S., Schreck, M., Beck, K. M., Matthiessen, J., Fahl, K., et Mangerud, G. (2015). Early Pliocene onset of modern Nordic Seas circulation related to ocean gateway changes. *Nature Communications*, 6, 8659. DOI: 10.1038/ncomms9659
- De Schepper, S., Beck, K. M., et Mangerud, G. (2017). Late Neogene dinoflagellate cyst and acritarch biostratigraphy for Ocean Drilling Program Hole 642B, Norwegian Sea. *Review of Palaeobotany and Palynology*, 236, 12-32. <https://doi.org/10.1016/j.revpalbo.2016.08.005>
- de Vernal, A., et Mudie, P. J. (1989a). Pliocene and Pleistocene palynostratigraphy at ODP Sites 646 and 647, eastern and southern Labrador Sea. In Proceedings of the Ocean Drilling Program, Scientific Results (Vol. 105, pp. 401-422). Ocean Drilling Program Texas A & M University, College Station, Texas. doi:10.2973/odp.proc.sr.105.134.1989
- de Vernal, A., et Mudie, P.J. (1989b). Late Pliocene to Holocene palynostratigraphy at ODP Site 645, Baffin Bay. In Proceedings of the Ocean Drilling Program, Scientific Results (Vol. 105, pp. 387-399). Ocean Drilling Program Texas A & M University, College Station, Texas doi:10.2973/odp.proc.sr.105.133.1989
- de Vernal, A., et Marret, F. (2007). Chapter nine organic-walled dinoflagellate cysts: tracers of sea-surface conditions. *Developments in marine geology*, 1, 371-408. [https://doi.org/10.1016/S1572-5480\(07\)01014-7](https://doi.org/10.1016/S1572-5480(07)01014-7)
- de Vernal, A., et Hillaire-Marcel, C. (2008). Natural variability of Greenland climate, vegetation, and ice volume during the past million years. *Science*, 320(5883), 1622-1625. DOI: 10.1126/science.1153929
- de Vernal, A., Henry, M., et Bilodeau, G. (1999). Techniques de préparation et d'analyse en micropaléontologie. *Les cahiers du GEOTOP*, 3, 41
- de Vernal, A., Rochon, A., Fréchette, B., Henry, M., Radi, T., et Solignac, S. (2013). Reconstructing past sea ice cover of the Northern Hemisphere from dinocyst

- assemblages: status of the approach. *Quaternary Science Reviews*, 79, 122-134.
<https://doi.org/10.1016/j.quascirev.2013.06.022>
- Dolan, A. M., Hunter, S. J., Hill, D. J., Haywood, A. M., Koenig, S. J., Otto-Bliesner, B. L., Abe-Ouchi, A., Bragg, F., Chan, W.L., Chandler, M.A., Contoux, C., Jost, A., Kamae, Y., Lohmann, G., Lunt, D.J., Ramstein, G., Rosenbloom, N.A., Sohl, L., Stepanek., C., Ueda, H., Yan, Q., et Zhang, Z. (2015). Using results from the PlioMIP ensemble to investigate the Greenland Ice Sheet during the mid-Pliocene Warm Period. *Climate of the Past Discussions*, 11(3), 403-424. doi: 10.5194/cp-11-403-2015
- Dowsett, H. J., Robinson, M. M., et Foley, K. M. (2009). Pliocene three-dimensional global ocean temperature reconstruction. *Climate of the Past*, 5(4), 769-783.
- Dowsett, H., Robinson, M., Haywood, A. M., Salzmann, U., Hill, D., Sohl, L. E., Chandler, M., Williams, M., Foley, K., et Stoll, D. K. (2010a). The PRISM3D paleoenvironmental reconstruction. *Stratigraphy*, 7(2-3), 123-139.
- Dowsett, H. J., Robinson, M. M., Foley, K. M., et Stoll, D. K. (2010b). Mid-Piacenzian mean annual sea surface temperature: an analysis for data-model comparisons. *Stratigraphy*, 7(2-3), 189-198.
- Dowsett, H., Dolan, A., Rowley, D., Pound, M., Salzmann, U., Robinson, M., Chandler, M., Foley, K., et Haywood, A. (2016). The PRISM4 (mid-Piacenzian) palaeoenvironmental reconstruction. *Climate of the Past Discussions*, 12, 1519-1538. doi:10.5194/cp-12-1519-2016.
- Driscoll, N. W., et Haug, G. H. (1998). A short circuit in thermohaline circulation: a cause for Northern Hemisphere glaciation?. *Science*, 282(5388), 436-438. DOI: 10.1126/science.282.5388.436
- Evitt, W. R. (1963). A discussion and proposals concerning fossil dinoflagellates, hystrichospheres, and acritarchs, I. *Proceedings of the National Academy of Sciences of the United States of America*, 49(2), 158.
- Flesche Kleiven, H. F., Jansen, E., Fronval, T., et Smith, T. M. (2002). Intensification of Northern Hemisphere glaciations in the circum Atlantic region (3.5–2.4 Ma)—ice rafted detritus evidence. *Palaeogeography, Palaeoclimatology, Palaeoecology*, 184(3-4), 213-223.doi:10.1016/S0031-0182(01)00407-2
- Funder, S., Abrahamsen, N., Bennike, O., et Feyling-Hanssen, R. W. (1985). Forested arctic: evidence from North Greenland. *Geology*, 13(8), 542-546.

- Funder, S.V., Bennike, O., Böcher, J., Israelson, C., Petersen, K.S., et Símonarson, L. A. (2001). Late Pliocene Greenland–The Kap København Formation in North Greenland. *Bulletin of the Geological Society of Denmark*, 48, 117-134.
- Gibb, O. T., Steinhauer, S., Fréchette, B., de Vernal, A., et Hillaire-Marcel, C. (2015). Diachronous evolution of sea surface conditions in the Labrador Sea and Baffin Bay since the last deglaciation. *The Holocene*, 25(12), 1882-1897.
doi:10.1177/0959683615591352
- Hanna, E., et Cappelen, J. (2002). Recent climate of southern Greenland. *Weather*, 57(9), 320-328. <https://doi.org/10.1256/00431650260283497>
- Haug, G. H., et Tiedemann, R. (1998). Effect of the formation of the Isthmus of Panama on Atlantic Ocean thermohaline circulation. *Nature*, 393(6686), 673.
- Haug, G. H., Ganopolski, A., Sigman, D. M., Rosell-Mele, A., Swann, G. E., Tiedemann, R., Jaccard, S.L., Bollmann, J., Maslin, M.A., Leng, M.J. et Eglinton, G. (2005). North Pacific seasonality and the glaciation of North America 2.7 million years ago. *Nature*, 433(7028), 821.
- Haywood, A., Dowsett, H., Otto-Bliesner, B., Chandler, M., Dolan, A., Hill, D., Lunt, D.J., Robinson, M.M., Rosenbloom, N., Salzmann, U., et Sohl, L. (2010). Pliocene model intercomparison project (PlioMIP): experimental design and boundary conditions (experiment 1). *Geoscientific Model Development*, 3(1), 227-242.
- Haywood, A. M., Dowsett, H. J., Robinson, M. M., Stoll, D. K., Dolan, A. M., Lunt, D. J., Otto-Bliesner, B., et Chandler, M. A. (2011). Pliocene Model Intercomparison Project (PlioMIP): experimental design and boundary conditions (experiment 2). <https://doi.org/10.5194/gmd-4-571-2011>
- Head, M. J. (1993). Dinoflagellates, sporomorphs, and other palynomorphs from the Upper Pliocene St. Erth Beds of Cornwall, southwestern England. Memoir (The Paleontological Society), 1-62.
- Head, M. J. (1996). Late Cenozoic dinoflagellates from the Royal Society borehole at Ludham, Norfolk, eastern England. *Journal of Paleontology*, 70(4), 543-570.
- Head, M. J. (1997). Thermophilic dinoflagellate assemblages from the mid Pliocene of eastern England. *Journal of Paleontology*, 165-193.
- Head, M. J., et Norris, G. (2003). New species of dinoflagellate cysts and other palynomorphs from the latest Miocene and Pliocene of DSDP Hole 603C, western

- North Atlantic. *Journal of Paleontology*, 77(1), 1-15. [https://doi.org/10.1666/0022-3360\(2003\)077<0001:NSODCA>2.0.CO;2](https://doi.org/10.1666/0022-3360(2003)077<0001:NSODCA>2.0.CO;2)
- Head, M.J., Norris, G., et Mudie, P.J. (1989). Palynology and dinocyst stratigraphy of the Miocene in ODP Leg 105, Hole 645E, Baffin Bay. In Srivastava, S.P., Arthur, M.A., Clement, B., *et al.*, Proc. ODP, Sci. Results, 105: College Station, TX (Ocean Drilling Program), 467–514. doi:10.2973/odp.proc.sr.105.137.1989
- Hennissen, J.A. (2013) Late Pliocene–Early Pleistocene North Atlantic circulation: integrating dinocyst assemblages and foraminiferal geochemistry. Thèse doctorale, University of Toronto, 243 p.
- Hennissen, J. A., Head, M. J., De Schepper, S., et Groeneveld, J. (2014). Palynological evidence for a southward shift of the North Atlantic Current at~ 2.6 Ma during the intensification of late Cenozoic Northern Hemisphere glaciation. *Paleoceanography and Paleoclimatology*, 29(6), 564-580. 10.1002/2013PA002543
- Hennissen, J. A., Head, M. J., De Schepper, S., et Groeneveld, J. (2015). Increased seasonality during the intensification of Northern Hemisphere glaciation at the Pliocene–Pleistocene boundary~ 2.6 Ma. *Quaternary Science Reviews*, 129, 321-332. <https://doi.org/10.1016/j.quascirev.2015.10.010>
- Hennissen, J. A., Head, M. J., De Schepper, S., et Groeneveld, J. (2017). Dinoflagellate cyst paleoecology during the Pliocene–Pleistocene climatic transition in the North Atlantic. *Palaeogeography, palaeoclimatology, palaeoecology*, 470, 81-108. <http://dx.doi.org/10.1016/j.palaeo.2016.12.023>
- Hiscott, R. N., Aksu, A. E., et Nielsen, O. B. (1989). Provenance and dispersal patterns, Pliocene-Pleistocene section at Site 645, Baffin Bay. In Proceedings of the Ocean Drilling Program, Scientific Results (Vol. 105, pp. 31-52). Ocean Drilling Program Texas A & M University, College Station, Texas
- IPCC, (2013). Climate Change 2013: The Physical Science Basis. Contribution of Working Group I to the Fifth Assessment Report of the Intergovernmental Panel on Climate Change [Stocker, T.F., D. Qin, G.-K. Plattner, M. Tignor, S.K. Allen, J. Boschung, A. Nauels, Y. Xia, V. Bex et P.M. Midgley (eds.)]. Cambridge University Press, Cambridge, United Kingdom and New York, NY, USA: 1535. doi:10.1017/CBO9781107415324.

- Klocker, A., Prange, M., et Schulz, M. (2005). Testing the influence of the Central American Seaway on orbitally forced Northern Hemisphere glaciation. *Geophysical Research Letters*, 32(3). DOI: 10.1029/2004GL021564
- Knies, J., Matthießen, J., Vogt, C., et Stein, R. (2002). Evidence of 'Mid-Pliocene (~ 3 Ma) global warmth' in the eastern Arctic Ocean and implications for the Svalbard/Barents Sea ice sheet during the late Pliocene and early Pleistocene (~ 3–1.7 Ma). *Boreas*, 31(1), 82–93.
- Knüttel, S., Russell, M.D., Jr., et Firth, J.V. (1989). Neogene calcareous nannofossils from ODP Leg 105: implications for Pleistocene paleoceanographic trends. In Srivastava, S.P., Arthur, M.A., Clement, B., et al., Proc. ODP, Sci. Results, 105: College Station, TX (Ocean Drilling Program), 245–262. doi:10.2973/odp.proc.sr.105.130.1989
- Knutz, P. C., Sicre, M. A., Ebbesen, H., Christiansen, S., et Kuijpers, A. (2011). Multiple-stage deglacial retreat of the southern Greenland Ice Sheet linked with Irminger Current warm water transport. *Paleoceanography and Paleoclimatology*, 26(3).
- Knutz, P. C., Hopper, J. R., Gregersen, U., Nielsen, T., et Japsen, P. (2015). A contourite drift system on the Baffin Bay–West Greenland margin linking Pliocene Arctic warming to poleward ocean circulation. *Geology*, 43(10), 907–910. <https://doi.org/10.1130/G36927.1>
- Knutz, P., Campbell, C., Bierman, P., de Vernal, A., Huuse, M., Jennings, A., Cox, D., DeConto, R., Gohl, K., Hogan, K., Hopper, J., Keisling, B., Newton, A., Perez, L., Rebschläger, J., Sliwinska, K., Thomas, E., Willerslev, E., Xuan, C., et Stoner, J. (2018). Cenozoic evolution of the northern Greenland Ice Sheet exposed by transect drilling in northeast Baffin Bay (CENICE). IODP proposal Cover Sheet 909-Full 2https://docs.iodp.org/Proposal_Cover_Sheets/909-Full2_Knutz_cover.pdf
- Koenig, S. J., Dolan, A. M., De Boer, B., Stone, E. J., Hill, D. J., DeConto, R. M., Abe-Ouchi, A., Lunt, D. J., Pollard, D., Quiquet, A., Saito, F., Savage, J., et van de Wal, R. (2015). Ice sheet model dependency of the simulated Greenland Ice Sheet in the mid-Pliocene. *Climate of the Past*, 11(3), 369–381. doi:10.5194/cp-11-369-2015
- Korstgård, J. A., et Nielsen, O. B. (1989). Provenance of dropstones in Baffin Bay and Labrador Sea, Leg 105. In Proceedings of the Ocean Drilling Program, Scientific Results (Vol. 105, pp. 65–69). Ocean Drilling Program Texas A & M University, College Station, Texas

- Kürschner, W. M., van der Burgh, J., Visscher, H., et Dilcher, D. L. (1996). Oak leaves as biosensors of late Neogene and early Pleistocene paleoatmospheric CO₂ concentrations. *Marine Micropaleontology*, 27(1-4), 299-312.
- Kuijpers, A., Knutz, P., et Moros, M. (2016). Ice-raftered Debris (IRD). 10.1007/978-94-007-6238-1_182.
- Lazarus, D., et Pallant, A. (1989). Oligocene and Neogene radiolarians from the Labrador Sea: ODP Leg 105. In Srivastava, S.P., Arthur, M.A., Clement, B., *et al.*, Proc. ODP, Sci. Results, 105: College Station, TX (Ocean Drilling Program), 349–380. doi:10.2973/odp.proc.sr.105.125.1989
- Lazier, J., Hendry, R., Clarke, A., Yashayaev, I., et Rhines, P. (2002). Convection and restratification in the Labrador Sea, 1990–2000. Deep Sea Research Part I: Oceanographic Research Papers, 49(10), 1819-1835. doi:10.1016/S0967-0637(02)00064-X
- Lunt, D. J., Foster, G. L., Haywood, A. M., et Stone, E. J. (2008a). Late Pliocene Greenland glaciation controlled by a decline in atmospheric CO₂ levels. *Nature*, 454(7208), 1102. doi:10.1038/nature07223
- Lunt, D. J., Valdes, P. J., Haywood, A., et Rutt, I. C. (2008b). Closure of the Panama Seaway during the Pliocene: implications for climate and Northern Hemisphere glaciation. *Climate Dynamics*, 30(1), 1-18. doi: 10.1007/s00382-007-0265-6
- Marshall, J., et Schott, F. (1999). Open-ocean convection: Observations, theory, and models. *Reviews of Geophysics*, 37(1), 1-64.
- Martínez-Botí, M. A., Foster, G. L., Chalk, T. B., Rohling, E. J., Sexton, P. F., Lunt, D. J., Pancost, R.D., Badger, M.P.S., et Schmidt, D. N. (2015). Plio-Pleistocene climate sensitivity evaluated using high-resolution CO₂ records. *Nature*, 518(7537), 49.
- Matthews, J. (1969). The assessment of a method for the determination of absolute pollen frequencies. *New Phytologist*, 68(1), 161-166.
- Matthiessen, J., Knies, J., Vogt, C., et Stein, R. (2008). Pliocene palaeoceanography of the Arctic Ocean and subarctic seas. *Philosophical Transactions of the Royal Society A: Mathematical, Physical and Engineering Sciences*, 367(1886), 21-48. doi:10.1098/rsta.2008.0203
- Matthiessen, J., Schreck, M., De Schepper, S., Zorzi, C., et de Vernal, A. (2018). Quaternary dinoflagellate cysts in the Arctic Ocean: Potential and limitations for

- stratigraphy and paleoenvironmental reconstructions. *Quaternary Science Reviews*, 192, 1-26. <https://doi.org/10.1016/j.quascirev.2017.12.020>
- Mattingsdal, R., Knies, J., Andreassen, K., Fabian, K., Husum, K., Grøsfjeld, K., et De Schepper, S. (2014). A new 6 Myr stratigraphic framework for the Atlantic–Arctic Gateway. *Quaternary Science Reviews*, 92, 170-178. <http://dx.doi.org/10.1016/j.quascirev.2013.08.022>
- Mertens, K. N., Verhoeven, K., Verleye, T., Louwye, S., Amorim, A., Ribeiro, S., Deaf, A.S., Harding, I.C., De Schepper, S., Gonzalez, C., Kodrans-Nsiah, M., de Vernal, A., Henry, M., Radi, T., Dybkjaer, K., Poulsen, N.E., Feist-Burkhardt, S., Chitolie, J., Heilmann-Clausen, C., Londeix, L., Turon, J-L., Marret, F., Matthiessen, J., McCarthy, F.M.G., Prasad, V., Pospelova, V., Kyffin Highes, J.E., Riding, J.B., Rochon, A., Sangiorgo, F., Welters, N., Sinclair, N., Thun, C., Soliman, A., Van Nieuwenhove, N., Vink, Annemiek, et Young, M . (2009). Determining the absolute abundance of dinoflagellate cysts in recent marine sediments: the Lycopodium marker-grain method put to the test. *Review of Palaeobotany and Palynology*, 157(3-4), 238-252. <https://doi.org/10.1016/j.revpalbo.2009.05.004>
- Miller, K. G., Wright, J. D., Browning, J. V., Kulpecz, A., Kominz, M., Naish, T. R., Cramer, B., S., Rosenthal, Y., Peltier, W., R., et Sosdian, S. (2012). High tide of the warm Pliocene: Implications of global sea level for Antarctic deglaciation. *Geology*, 40(5), 407-410. doi:10.1130/G32869.1.
- Monjanel, A.-L., et Baldauf, J.G. (1989). Miocene to Holocene diatom biostratigraphy from Baffin Bay and Labrador Sea, Ocean Drilling Program Sites 645 and 646. In Srivastava, S.P., Arthur, M.A., Clement, B., et al., Proc. ODP, Sci. Results, 105: College Station, TX (Ocean Drilling Program), 305–322. doi:10.2973/odp.proc.sr.105.127.1989
- Moore, P.D., Webb, J.A. et Collison, M.E. (1991). Pollen analysis. Blackwell scientific publications, Oxford. pp. viii+216
- Mudelsee, M., et Raymo, M. E. (2005). Slow dynamics of the Northern Hemisphere glaciation. *Paleoceanography*, 20(4). doi:10.1029/2005PA001153
- Munsterman, D., et Kerstholt, S. (1996). Sodium polytungstate, a new non-toxic alternative to bromoform in heavy liquid separation. *Review of Palaeobotany and Palynology*, 91(1-4), 417-422. [https://doi.org/10.1016/0034-6667\(95\)00093-3](https://doi.org/10.1016/0034-6667(95)00093-3)

- Naafs, B. D. A., Stein, R., Hester, J., Khélifi, N., De Schepper, S., et Haug, G. H. (2010). Late Pliocene changes in the North Atlantic current. *Earth and Planetary Science Letters*, 298(3-4), 434-442. <https://doi.org/10.1016/j.epsl.2010.08.023>
- Pagani, M., Liu, Z., LaRiviere, J., et Ravelo, A. C. (2010). High Earth-system climate sensitivity determined from Pliocene carbon dioxide concentrations. *Nature Geoscience*, 3(1), 27. doi:10.1038/ngeo724
- Panitz, S., De Schepper, S., Salzmann, U., Bächem, P. E., Risebrobakken, B., Clotten, C., et Hocking, E. P. (2017). Mid-Piacenzian Variability of Nordic Seas Surface Circulation Linked to Terrestrial Climatic Change in Norway. *Paleoceanography*, 32(12), 1336-1351. DOI: 10.1002/2017PA003166
- Polyak, L., Alley, R. B., Andrews, J. T., Brigham-Grette, J., Cronin, T. M., Darby, D. A., Dyke, A.S., Fitzpatrick, J.J., Funder, S., Holland, M., Jennings, A.E., Miller, G.H., O'Regan, M., Savelle, J., Serreze, M., St. John, K., White, J.C.W.C et Wolff, E. (2010). History of sea ice in the Arctic. *Quaternary Science Reviews*, 29(15-16), 1757-1778. doi:10.1016/j.quascirev.2010.02.010.
- Pound, M. J., Tindall, J., Pickering, S. J., Haywood, A. M., Dowsett, H. J., et Salzmann, U. (2014). Late Pliocene lakes and soils: a global data set for the analysis of climate feedbacks in a warmer world. *Climate of the Past*, 10(1), 167-180.doi: 10.5194/cp-10-167-2014
- Ravelo, A. C., Andreasen, D. H., Lyle, M., Lyle, A. O., et Wara, M. W. (2004). Regional climate shifts caused by gradual global cooling in the Pliocene epoch. *Nature*, 429(6989), 263.doi:10.1038/nature02567
- Raymo, M. E., Grant, B., Horowitz, M., et Rau, G. H. (1996). Mid-Pliocene warmth: stronger greenhouse and stronger conveyor. *Marine Micropaleontology*, 27(1-4), 313-326. doi:10.1016/0377-8398(95)00048-8.
- Rochon, A., et Vernal, A. D. (1994). Palynomorph distribution in recent sediments from the Labrador Sea. *Canadian Journal of Earth Sciences*, 31(1), 115-127. doi:10.1139/e94-010
- Rochon, A., Vernal, A. D., Turon, J. L., Matthießen, J., et Head, M. J. (1999). Distribution of recent dinoflagellate cysts in surface sediments from the North Atlantic Ocean and adjacent seas in relation to sea-surface parameters. *American Association of Stratigraphic Palynologists Contribution Series*, 35, 1-146.

- Rudels, B. (1986). The outflow of polar water through the Arctic Archipelago and the oceanographic conditions in Baffin Bay. *Polar Research*, 4(2), 161-180. doi:10.3402/polar.v4i2.6929
- Sánchez Goñi, M. F., Desprat, S., Fletcher, W. J., Morales-Molino, C., Naughton, F., Oliveira, D., Urrego, D. H., et Zorzi, C. (2018). Pollen from the deep-sea: a breakthrough in the mystery of the Ice Ages. *Frontiers in plant science*, 9, 38. <https://doi.org/10.3389/fpls.2018.00038>
- Salzmann, U., Haywood, A. M., Lunt, D. J., Valdes, P. J., et Hill, D. J. (2008). A new global biome reconstruction and data-model comparison for the middle Pliocene. *Global Ecology and Biogeography*, 17(3), 432-447. doi:10.1111/j.1466-8238.2008.00381.x
- Salzmann, U., Williams, M., Haywood, A. M., Johnson, A. L., Kender, S., et Zalasiewicz, J. (2011). Climate and environment of a Pliocene warm world. *Palaeogeography, Palaeoclimatology, Palaeoecology*, 309(1-2), 1-8. doi:10.1016/j.palaeo.2011.05.044
- Schlitzer, R. (2018). Ocean Data View, odv.awi.de
- Seki, O., Foster, G. L., Schmidt, D. N., Mackensen, A., Kawamura, K., et Pancost, R. D. (2010). Alkenone and boron-based Pliocene pCO₂ records. *Earth and Planetary Science Letters*, 292(1-2), 201-211. doi:10.1016/j.epsl.2010.01.037
- Shackleton, N. J., Backman, J., Zimmerman, H., Kent, D. V., Hall, M. A., Roberts, D. G., Scnitker, D., Baldauf, J.G, Desprairies, A., Homrighausen, R., Huddleston, P., Keene, J.B., Kaltenback, A.J., Krumsiek, K.A.O., Morton, A.C., Murray, J.W., et Westberg-Smith, J. (1984). Oxygen isotope calibration of the onset of ice-rafting and history of glaciation in the North Atlantic region. *Nature*, 307(5952), 620.
- Schneider, B., et Schneider, R. (2010). Palaeoclimate: Global warmth with little extra CO₂. *Nature Geoscience*, 3(1), 6. DOI 10.1038/ngeo736.
- Schreck, M., et Matthiessen, J. (2014). *Batiacasphaera bergenensis* and *Lavradosphaera elongata*—New dinoflagellate cyst and acritarch species from the Miocene of the Iceland Sea (ODP Hole 907A). *Review of palaeobotany and palynology*, 211, 97-106. doi:10.1016/j.revpalbo.2014.07.002
- Schreck, M., Matthiessen, J., et Head, M. J. (2012). A magnetostratigraphic calibration of Middle Miocene through Pliocene dinoflagellate cyst and acritarch events in the Iceland Sea (Ocean Drilling Program Hole 907A). *Review of Palaeobotany and Palynology*, 187, 66-94. <http://dx.doi.org/10.1016/j.revpalbo.2012.08.006>

- Schreck, M., Meheust, M., Stein, R., et Matthiessen, J. (2013). Response of marine palynomorphs to Neogene climate cooling in the Iceland Sea (ODP Hole 907A). *Marine Micropaleontology*, 101, 49-67. doi:10.1016/j.marmicro.2013.03.003
- Schreck, M., Nam, S. I., Clotten, C., Fahl, K., De Schepper, S., Forwick, M., et Matthiessen, J. (2017). Neogene dinoflagellate cysts and acritarchs from the high northern latitudes and their relation to sea surface temperature. *Marine Micropaleontology*, 136, 51-65. https://doi.org/10.1016/j.marmicro.2017.09.003
- Smith, Y. M., Hill, D. J., Dolan, A. M., Haywood, A. M., Dowsett, H. J., et Risebrobakken, B. (2018). Icebergs in the Nordic seas throughout the Late Pliocene. *Paleoceanography and Paleoclimatology*, 33(3), 318-335. https://doi.org/10.1002/2017PA003240
- St. John, K. E. S., et Krissek, L. A. (2002). The late Miocene to Pleistocene ice-rafting history of southeast Greenland. *Boreas*, 31(1), 28-35.
- Tang, C. C., Ross, C. K., Yao, T., Petrie, B., DeTracey, B. M., et Dunlap, E. (2004). The circulation, water masses and sea-ice of Baffin Bay. *Progress in Oceanography*, 63(4), 183-228. doi:10.1016/j.pocean.2004.09.005
- Thiede, J., Jessen, C., Knutz, P., Kuipers, A., Mikkelsen, N., Nørgaard-Pedersen, N., et Spielhagen, R. F. (2011). Millions of years of Greenland Ice Sheet history recorded in ocean sediments. *Polarforschung*, 80(3), 141-159.
- Tripathi, A. K., Eagle, R. A., Morton, A., Dowdeswell, J. A., Atkinson, K. L., Bahé, Y., Dawber, C.F., Khadun, E., Shaw, R.M.H., Shorttle, O., et Thanabalanandaram, L. (2008). Evidence for glaciation in the Northern Hemisphere back to 44 Ma from ice rafted debris in the Greenland Sea. *Earth and Planetary Science Letters*, 265(1-2), 112-122. doi:10.1016/j.epsl.2007.09.045
- Van Nieuwenhove, N., Bauch, H. A., et Matthiessen, J. (2008). Last interglacial surface water conditions in the eastern Nordic Seas inferred from dinocyst and foraminiferal assemblages. *Marine Micropaleontology*, 66(3-4), 247-263. DOI: 10.1016/j.marmicro.2007.10.004
- Verhoeven, K., et Louwye, S. (2013). Palaeoenvironmental reconstruction and biostratigraphy with marine palynomorphs of the Plio-Pleistocene in Tjörnes, Northern Iceland. *Palaeogeography, Palaeoclimatology, Palaeoecology*, 376, 224-243. https://doi.org/10.1016/j.palaeo.2013.03.002

- Versteegh, G. J. M., et Zevenboom, D. (1995). New genera and species of dinoflagellate cysts from the Mediterranean Neogene. *Review of Palaeobotany and Palynology*, 85(3-4), 213-229. DOI: 10.1016/0034-6667(94)00127-6
- Yashayaev, I. (2007). Hydrographic changes in the Labrador Sea, 1960–2005. *Progress in Oceanography*, 73(3-4), 242-276. doi:10.1016/j.pocean.2007.04.015
- Yashayaev, I., Bersch, M., et van Aken, H. M. (2007). Spreading of the Labrador Sea Water to the Irminger and Iceland basins. *Geophysical Research Letters*, 34(10). doi:10.1029/2006GL028999
- Weaver, A. J., Bitz, C. M., Fanning, A. F., et Holland, M. M. (1999). Thermohaline circulation: High-latitude phenomena and the difference between the Pacific and Atlantic. *Annual Review of Earth and Planetary Sciences*, 27(1), 231-285. doi:10.1146/annurev.earth.27.1.231
- Winkler, A., Wolf-Welling, T., Stattegger, K., et Thiede, J. (2002). Clay mineral sedimentation in high northern latitude deep-sea basins since the Middle Miocene (ODP Leg 151, NAAG). *International Journal of Earth Sciences*, 91(1), 133-148. doi: 10.1007/s005310100199
- Zachos, J., Pagani, M., Sloan, L., Thomas, E., et Billups, K. (2001). Trends, rhythms, and aberrations in global climate 65 Ma to present. *Science*, 292(5517), 686-693. doi:10.1126/science.1059412.
- Zweng, M. M., et Münchow, A. (2006). Warming and freshening of Baffin Bay, 1916–2003. *Journal of Geophysical Research: Oceans*, 111(C7). doi:10.1029/2005JC003

